Environmental Effects on the Application of Spring Load Restrictions on Low Volume Roads in Northern Ontario

by

Jeffrey Chapin

A Thesis
Submitted to the Faculty of Graduate Studies
in Partial Fulfillment of the Requirements
for the Degree of

Masters of Science in Environmental Engineering

Faculty of Engineering
Lakehead University
Thunder Bay, Ontario
June, 2010

Your file Votre référence
ISBN: 978-0-494-71747-9
Our file Notre référence
ISBN: 978-0-494-71747-9

Abstract

Many jurisdictions throughout Canada and the United States utilize Spring Load Restriction (SLRs) on low volume roads to minimize the damage during spring thaw. The main objective of this research is to develop a SLR method for use in northern Ontario (the Lakehead University (LU) method). In order to achieve this objective a detailed review and assessment was conducted on three potential SLR methods for their use on low volume roads in northern Ontario. The three methods assessed were an empirically based approach developed by the Minnesota Department of Transportation (Mn/DOT), a semi-empirical approach developed by the University of Waterloo and a thermal numerically based method using the finite element code TEMP/W.

Each of the methods was calibrated for two study sites, Highway 569 in northeastern Ontario and Highway 527 in northwestern Ontario. These methods were calibrated using historical data collected from these study sites including air temperature data and observed frost and thaw depths determined from thermistor measurements. The Highway 569 study site was calibrated for the 2005/2006, 2007/2008 and 2008/2009 seasons while the Highway 527 study site was calibrated for the 2008/2009 season only. The calibrated methods were then used to predict the application and removal dates for SLRs for the two sites for the 2009/2010 season.

Pavement stiffness testing was conducted during the freezing and thawing seasons at the two sites using a Light Weight Deflectometer (LWD). The purpose of LWD testing was to examine the changes in pavement stiffness resulting from progressive freezing and thawing of the pavement structure. The results of the LWD testing indicate a significant decrease in pavement stiffness during pavement structure thawing between depths of 0.2 and 0.4 m. Based on these results and an extensive literature review, a 0.3 m threshold thawing depth was selected to trigger SLR application. LWD testing also indicated a slight increase in pavement stiffness within 2 weeks of complete pavement structure thawing. Using these results it was decided that, for this research, SLRs could be removed 7 days after complete pavement structure thawing.

During the calibration of the three SLR methods it was discovered that the Waterloo method requires significant adjustments to the frost and thaw depth algorithm coefficients at the onset of the thawing period. It was also determined that the accuracy of the thermal numerical modelling simulation is strongly associated with the boundary conditions used for the model.

The assessment of the three methods indicates that the Mn/DOT method can closely predict the SLR application date (within 1 to 2 days) and was less accurate in predicting the SLR removal date (within 6 to 9 days). The Waterloo and TEMP/W methods did not display the same degree of accuracy as the Mn/DOT method when used in a predictive mode.

Based on the LWD test results and the SLR calibration and prediction results, it was decided that the LU method should follow the Mn/DOT method and use threshold Cumulative Thawing Index (CTI) values representative of northern Ontario conditions as a trigger for application of the SLRs. In this method air temperatures are adjusted by reference temperatures which are then used to calculate a CTI. When the CTI exceeds a value corresponding to a 0.3 m pavement structure thawing depth, SLRs will be implemented. SLR removal will be based on average pavement structure thawing duration. Furthermore, LWD testing during the predicted thawing season will be used to further develop the method by qualifying pavement stiffness reductions during the onset of thaw and stiffness rebound after complete pavement structure thawing. Also, the TEMP/W thermal numerical model will be used as a tool to further refine the LU method through assessment of other pavement structures and environmental conditions.

Acknowledgements

I would like to acknowledge and sincerely thank my thesis supervisor Dr. Bruce Kjartanson for the tremendous amount of support and guidance that he provided to me throughout the development of this thesis. Drawing from his experiences and knowledge was invaluable to both the development of this thesis and to the growth of my academic career.

I would also like to thank and acknowledge Dr. Juan Pernia for providing me the opportunity to work with him on this project. The guidance and feedback that he supplied was extremely valuable and greatly appreciated.

I would like to also acknowledge Dr. Eltayeb Mohamedelhassan from Lakehead University and Dr. Myint Win Bo of DST Consulting Engineers for reviewing this thesis and providing valuable comments which increased the quality of this work.

I would like to thank NSERC, the Ministry of Transportation for Ontario for providing the funding for this research. I would also like to thank DST Consulting Engineers for their engineering scholarship award which aided in the financing of this research. I would specifically like to thank individuals from the MTO that were directly involved in the development of this thesis including: Mr. Max Perchanok, Mr. Ken Mossop, Mr. Dino Bagnariol, Ms. Fiona Leung, Mr. Justin White, Mr. Dino Leombruni, Mr. Don Petryna and Mr. Doug Flegel.

To the numerous graduate and undergraduate students that helped me directly with this research or provided unwavering support, I express my thanks and gratitude.

Finally I would like to thank my wife Trista, and the rest of my family for their unending support and encouragement throughout this whole process.

Table of Contents

List of Tables

Table of Figures

1.0 Introduction

1.1 Problem Statement

Approximately 20% (3, 715 centre line kilometers) of Ontario roadways are low volume roads which are subjected to infrequent but intense traffic loading. These roads are often built with minimal sub-base and surface treatments. During periods of spring thaw, melt water becomes trapped in the thawed sub-base soil between the pavement surface layer and the underlying still frozen subsurface. This increase in water content reduces base stiffness and the overall bearing capacity of the pavement structure. In order to reduce road damage during these weakened periods, jurisdictions typically implement Spring Load Restrictions (SLRs), often referred to as half loads, to all truck traffic that utilize these roadways. For this reason accurate implementation and subsequent removal of the SLRs is imperative to maximizing the life of the pavement structure and minimizing the economic hardships endured by the trucking industry during these periods.

The accurate application and removal of SLRs requires knowledge of pavement stiffness and strength and corresponding frost and thaw depths (Figure 1.1). An appropriate SLR method therefore, requires accurately determined implementation and removal dates based on pavement performance. Achieving acceptable accuracy is a difficult task due to the variability of pavement structures, roadway locations, weather conditions and the relationships between weather conditions and heat transfer into and out of the pavement structure that need to be encompassed in an SLR method. Further to this, freezing and frost action and subsequent thawing have an effect on pavement conditions and corresponding stiffness and strength that can be observed through changes in the pavement deflection measured with, for example, a falling weight deflectometer. It is therefore essential that a SLR implementation and

removal program correlate frost and thaw depth estimates with corresponding pavement deflections to confirm pavement structure behavior.

Methods for applying SLRs may be grouped into empirical, semi-empirical or analytical numerical methods. Empirical methods rely on SLR application and removal dates from historical pavement observations, pavement observations made during the current spring thaw and/or correlation of historical air temperature indices, such as a freezing or thawing index, with frost and thaw depth and pavement stiffness and strength for specific sites. Semi-empirical methods go a step beyond the empirical methods in that algorithms based on correlations between historical air temperature indices and pavement structure frost and thaw depths are used to estimate frost and thawing front depths in a pavement structure for the current spring thaw conditions. For analytical/numerical methods, such as finite difference and finite element software codes, freezing and thawing front migration can be simulated for a given pavement structure with a given set of boundary conditions and pavement structure material properties and moisture conditions.

Currently in Ontario, SLR application and removal dates are based on historical pavement observations and corresponding application/removal dates and current spring thaw visual observations. There is a need to develop a more rational SLR method for Ontario. This rational method could be an empirical, semi-empirical or analytical/numerical-based method or a hybrid combination. Empirically based methods are easy to apply but are limited in that they are very site and climate/pavement structure condition dependent; i.e. they were developed from measurements and observations at specific sites and they must be recalibrated for different locations and conditions. The method used by the Minnesota Department of Transportation (Mn/DOT) is an example of an empirical method. Numerical-modelling based methods, on the other hand, allow simulation of freezing and thawing depths under various climate and pavement structure conditions but require the most input parameters of any of the methods for a given site. Quantifying the parameters and boundary conditions for a variety of site conditions can be difficult and expensive.

The challenge, therefore, and the subject of this research is to develop a rational SLR method for Ontario that accounts for variations in pavement structure and climate conditions

throughout the province, accounts for pavement stiffness and strength issues as related to freezing and thawing depths and yet can be readily implemented by the transportation authority.

1.2 Objectives and Scope of Research

The following objectives have been developed to assess current SLR methods used in northern jurisdictions as well as to develop an SLR method for Northern Ontario.

1. Compare and assess current SLR practices including empirical and pavement strength based methods used throughout Canada and the United States. This assessment includes design details of low volume roads, freeze/thaw effects, material thermal properties and environmental conditions to examine their influence on the various SLR practices.
2. Assess and compare three SLR methods in terms of effectiveness, accuracy and ease of implementation. An empirical method developed by the Minnesota Department of Transportation (Mn/DOT), a semi-empirical method developed by the University of Waterloo that utilizes correlations between air temperatures, surface temperatures and measured frost and thaw depths and a finite-element-based thermal numerical model form the basis for this comparison and assessment.
3. Assess the role and application of a Light Weight Deflectometer (LWD) in the implementation of SLRs. Compare pavement deflections, corresponding surface deflection modulus and composite modulus values obtained from LWD measurements on low volume roads throughout the winter/spring season with Falling Weight Deflectometer (FWD) measurements and measured frost and thaw depths.
4. Develop the Lakehead University (LU) method for applying SLRs in northern Ontario.

To achieve these objectives a flow chart of tasks (Figure 1.2) was followed. Each of the three SLR methods will be calibrated at two specific sites for up to three winter/spring seasons. Using the available winter/spring season data, the methods will be calibrated so that each

method can be used to predict the application and removal dates for SLRs for a following winter/spring season using only measured and forecasted air temperatures. The results, accuracy of the methods in both the method calibrations and their use in a predictive manner will be assessed to determine the benefits and drawbacks of each method. Light Weight Deflectometer (LWD) testing will be conducted throughout the winter/spring season to observe the pavement stiffness and strength changes. The LU method will be developed using the method assessment and LWD results and will be implemented as indicated in Figure 1.3.

1.3 Organization of Thesis

The organization of this thesis is as follows. Chapter 2 provides a literature review including an examination of material and thermal properties, current SLR methods, thermal numerical modelling and pavement deflection analysis. Chapter 3 describes the study sites used for model calibration and predictions. Chapter 4 outlines development and calibration of the three SLR methods for northern Ontario conditions. Chapter 5 outlines the pavement stiffness data collection that was conducted at the two northern Ontario study sites. An examination of the three calibrated methods in a predictive manner will be provided in Chapter 6. Chapter 7 outlines the development of the LU method for SLR placement and removal using the method prediction and LWD results. Chapter 8 provides the conclusions of this research and recommendations for further work. The appendices include comprehensive details of model development and testing procedures.

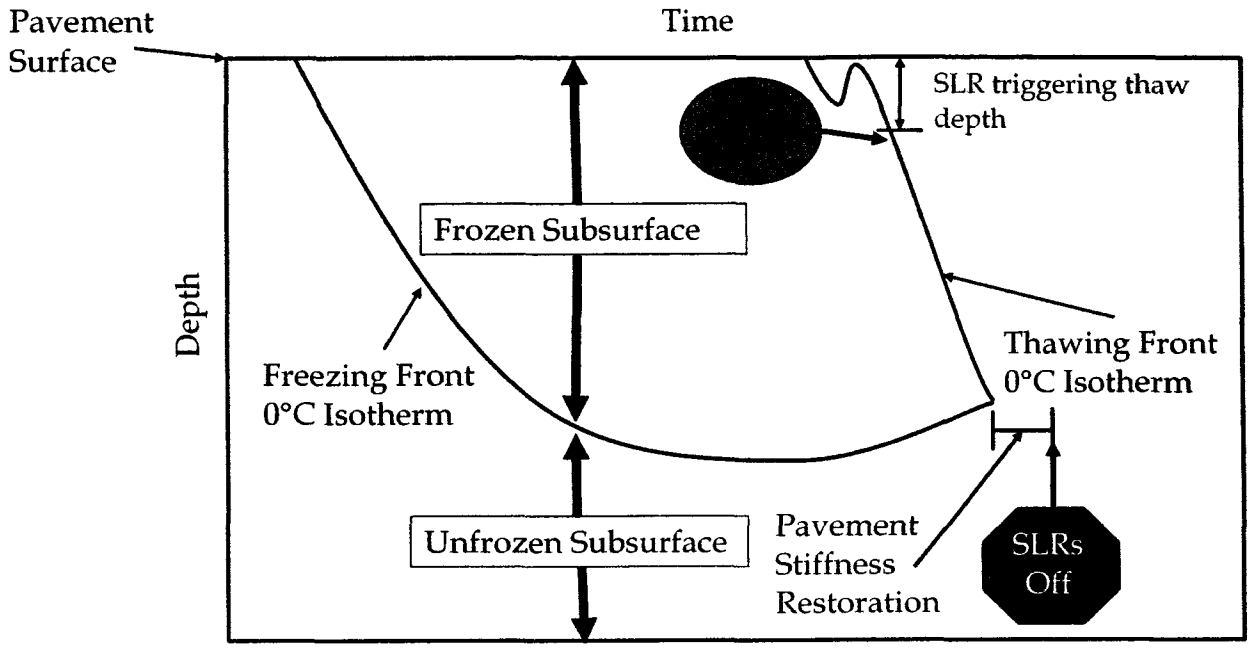

Figure 1.1 SLR Implementation and Removal Criteria

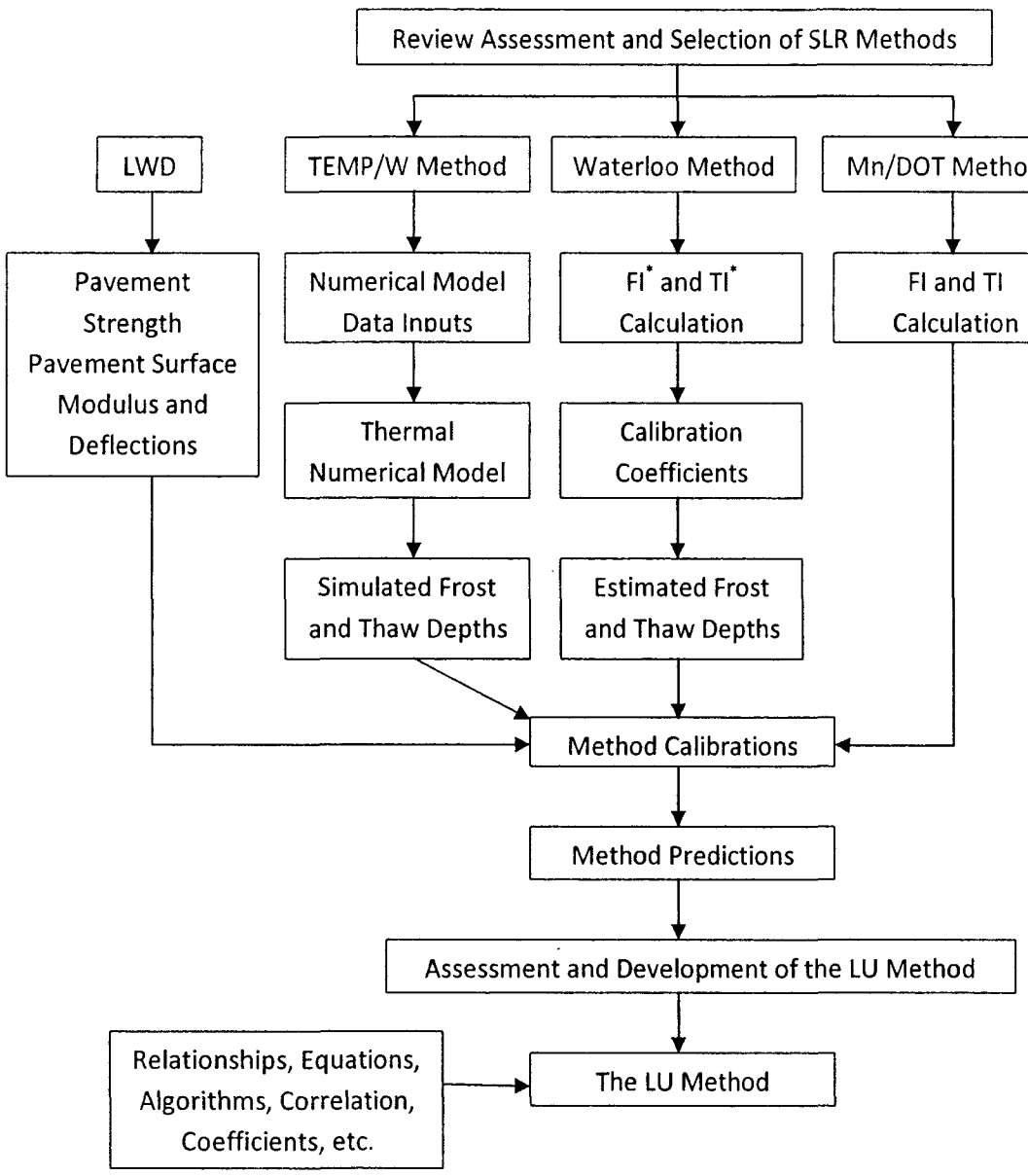

*FI: Freezing Index

*TI: Thawing Index

Figure 1.2 LU Method Development Flow Chart

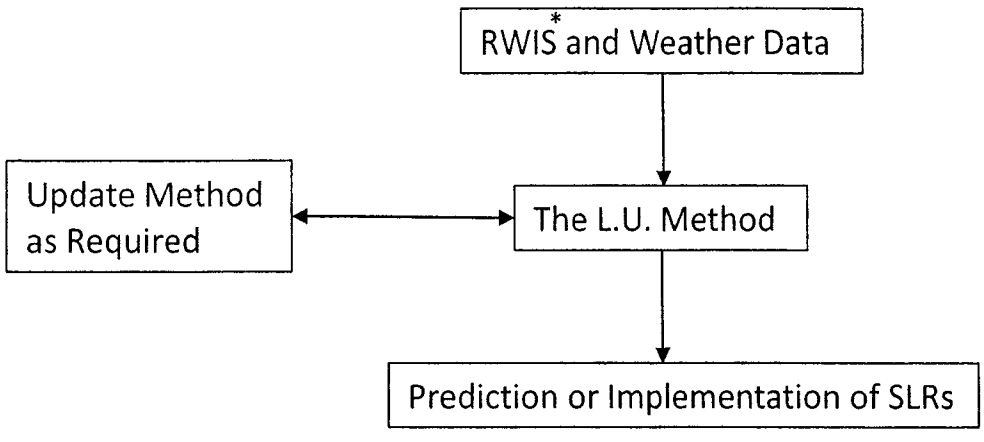

*RWIS: Road Weather Information Systems

Figure 1.3 LU Method Implementation Flow Chart

2.0 Literature Review

2.1 Low Volume Roads in Ontario

Low volume roads are classified as those roads which carry less than 1000 vehicles per day (Ningyuan et al., 2006). These roads are traditionally used by the transportation industry to access remote locations and are thus subjected to infrequent but intensive loading patterns. In Ontario, approximately 20% (3,715 centre-line km) of the roadway network consist of low volume roads (Ningyuan et al., 2006). The typical pavement structure for these roadways (Figure 2.1) consists of hot mix asphalt or a surface treatment as the pavement surface material and a base and sub-base consisting of granular material. In some instances a hot mix binder will be placed between the pavement surface material and the base material. The subgrade layer will vary with location and consist of materials native to the area ranging from organic matter to bedrock (Baiz et al., 2007). Roadways in these areas of low population and traffic levels are often built on a natural foundation with a minimal sub-base. Most of the low volume roads in Ontario consist of thin bituminous pavement surface layers which categorize the roads as flexible pavement structures. Flexible pavements typically transfer traffic loading from the pavement surface through the subsequent pavement layers in such a way that the whole pavement structure will bend without cracking or breaking (TAC, 1997). Most of these roads are designed to handle year round traffic; however, they are not designed for frost effects and are therefore susceptible to premature deterioration (Baiz et al., 2007).

2.2 Seasonal Freezing and Thawing of Roadways

Frost action is a complex process which involves frost heave during a freezing season followed by a loss of strength during the thawing season (Andersland and Ladanyi, 2004). A combination of unsteady heat flow near the ground surface for variations in air temperatures along with

crystal ice nucleation and growth, provide the necessary conditions for forming alternating bands of soil and ice. The formation of ice bands coupled with the segregation of ice during the freezing season results in an increase in volume of the soil/water system and/or soil consolidation (Andersland and Ladanyi, 2004). This increase in the volume of the soil/water system is the essential action involved in frost heaving.

During the freezing period a frozen subsurface layer exists bordered by an unfrozen layer below and subzero temperatures above. The frozen and unfrozen layers are separated by the 0°C interface temperature in which surface temperatures above this point are below 0°C, while temperatures below this point are above 0°C (Figure 2.2). Under these conditions energy is released from the frozen zone through the surface of the roadway and the thickness of the frozen zone increases. The freezing rate and amount are governed by the pavement structure frozen thermal properties.

During the onset of the spring thawing season the pavement structure will typically experience thawing from the top downward (from air temperature increases) and from the bottom upward (from the geothermal gradient). In the thawing period surface temperatures above 0°C in conjunction with warming of the bottom of the pavement structure by the geothermal gradient results in the creation of two 0°C interface temperature boundaries, one at the top of the frozen zone and the other at the bottom of the frozen zone (Figure 2.3). As a result of these conditions, energy is transferred into the frozen zone thereby thawing the frozen layer and thus reducing its thickness. The rate at which energy is transferred during the thawing period is a function of the subsurface unfrozen thermal properties.

This process results in melt water being trapped between the relatively impermeable pavement surface layer above and the still frozen soil below. In some instances, depending on the properties of the subgrade material, a second layer of trapped water overlain by the frozen soil and underlain by the low permeability subgrade may be present. The presence of trapped water results in decrease in the strength of the subgrade and sub-base and in turn reduces the material's ability to support the overlying pavement structure (Van Deusen, 1998).

Mean annual surface temperatures do not vary in a constant manner from corresponding mean annual air temperatures (Andersland and Ladanyi, 2004). Many factors

contribute to the difference between air and surface temperatures including (Anderland and Landayi, 2004):

- Net radiation
- Vegetation
- Snow cover
- Ground thermal properties
- Subsurface drainage

In order to estimate surface temperatures from air temperatures, empirically designed n-factor values are used. The n-factors can be determined for both the freezing and the thawing seasons. The n-factors are defined as the ratio of the surface temperature index to the air temperature index. A temperature index is calculated for both the freezing season and the thawing season. These indices utilize the degree-day concept to describe the intensity of the air and surface temperature variations. For example, a mean daily temperature of -4°C for 4 days equals an air freezing index of -16°C-days. The air and surface freezing indices represent the cumulative value of negative degree-days during the freezing season, while the air and surface thawing indices represent the cumulative positive degree-days during the thawing season. Table 2.1 indicates typical n-factor values for both the freezing and thawing seasons for various surface materials.

2.3 Thermal Properties of Soils

The greatest influences on the depth of frost and the length of time that the frost remains in the ground are the water content and the thermal properties of the soils in question, including the unfrozen water content, thermal conductivity, heat capacity, thermal diffusivity, and the latent heat of fusion. The thermal properties are greatly influenced by the material properties of the soil constituents, including:

- Grain size

- Plasticity index
- Liquid limit, and
- Quartz content.

2.3.1 Unfrozen Water Content

As not all water in a soil sample experiences phase change at a specific and exact temperature, different amounts of unfrozen water will be present in a soil at different freezing temperatures. This variance can be expressed as a function of unfrozen water content versus temperature, and varies based on many factors that contribute to the amount of unfrozen water present in a frozen soil sample. The main factors that influence unfrozen water content are: temperature, specific surface area of the solid phase, pressure, chemical and mineralogical composition of the soil, and other physio-chemical characteristics (especially ionic exchange capacity) and solute content and composition (Johnston, G.H, 1981). The thermal properties of ice and water are significantly different and the amount of each found within a soil sample will have an impact on the frozen soil behavior. For this reason it is important to understand the ice-water phase relationship within the subsurface materials to effectively determine the rate of frost development and amount of frost within the pavement structure. This relationship is related to grain size, with coarser grained materials having much lower unfrozen water contents compared with finer grained materials.

Tice et al. (1976) have developed a power curve using characteristic soil parameters (constants α and β that are empirically derived dimensionless constants that account for the change in units from °C to %) and temperature (θ expressed as a positive number in degrees Celsius below freezing) to express the unfrozen water content (w_u) of a sample (Equation 2.1).

$$w_u = \alpha\theta^{\beta} \tag{2.1}$$

For cohesive soils, the values of α and β can be calculated using empirical equations (Equations 2.2 and 2.3) that relate the closing of a standard groove in a liquid limit test using 25

($w_{N=25}$) and 100 ($w_{N=100}$) blows at temperatures of -1 and -2°C, respectively, and the corresponding water contents of the sample.

$$w_{u,\theta=1} = 0.346 w_{N=25} - 3.01 \tag{2.2}$$

$$w_{u,\theta=2} = 0.338 w_{N=100} - 3.72 \tag{2.3}$$

Then, taking the log of both sides of Equation 2.1 and substituting $w_{u,\theta=1}$ and $w_{u,\theta=2}$ in for w_u, it is possible to solve for both α and β using simultaneous equations.

Using the power curve (Equation 2.1) has provided excellent accuracy and consistency when compared to dilatometry, adiabatic and isothermal calorimetry, X-ray diffraction, heat capacity measurements, nuclear magnetic resonance, and differential thermal analysis tests reported by Anderson and Morgenstern (1973) on various soil types, provided that the soils being considered do not contain excessive amounts of soluble salts.

Solutes, such as salt, in the soil water will shift unfrozen water content versus temperature curves toward lower temperatures. Ladanyi (1989) found that an increase in salinity reduced the ice content within a frozen soil, thereby reducing the frozen soil strength and increasing its rate of creep at a given temperature.

If plasticity index values are available, the unfrozen water content can be estimated using a method developed in the Soviet Union (USSR 1969). This method utilizes a multiplication of the water content of the soil at the plastic limit, by a variable termed k_u (Table 2.2) that depends on the soil type and temperature.

2.3.2 Thermal Conductivity

The thermal conductivity of a soil is defined as the quantity of heat that will flow through a unit volume of a soil medium of unit thickness in unit time under a unit temperature gradient (Andersland and Ladanyi, 1994). The main factors that contribute to the thermal conductivity of a soil are the water content and dry density of the soil being tested. It has been observed that when the water content of the sample is kept constant and the dry density is varied, that

any increases in the dry density result in increases in thermal conductivity. Conversely, when the dry density is kept constant and the water content is varied, any increase in water content results in an increase in the thermal conductivity (Andersland and Ladanyi, 1994).

When examining the thermal conductivities of frozen and unfrozen soil it was observed that in most cases the thermal conductivity of a soil is greater when frozen than when it is unfrozen. The reason for the increase in the thermal conductivities of the frozen soil over an unfrozen soil is directly related to the higher thermal conductivity of ice compared to liquid water (Table 2.3). A major exception to this observation is a sandy soil with a moisture content less than about 7% which indicates a reverse in the thermal conductivity behavior, i.e. the thermal conductivity of the unfrozen soil is higher than the frozen soil (Andersland and Ladanyi, 1994).

There are several methods available to calculate the thermal conductivity of a soil, including approaches developed by Kersten (1949), Johansen (1975) and most recently Cotê and Konrad (2006), amongst others. Farouki (1982), while working for the U.S. Army Cold Regions Research and Engineering Laboratory, examined the available methods for calculating the thermal conductivity of soil, with the exception of the Cotê and Konrad method. Each method was tested using a variety of grain sizes, moisture contents, dry densities, and temperatures in order to establish the most accurate method to be used in calculating the thermal conductivity of a soil sample under specific conditions. Of the methods found to be applicable the Johansen method proved to be the most adaptable to varying conditions. The Kersten method provides an easily obtained approximation, however the results are not always accurate due to the reliance of this method on quartz content, while Cotê and Konrad's method expands upon the Johansen method. Kersten, Johansen, and Cotê and Konrad's methods are examined further.

2.3.2.1 Kersten's Method

The Kersten (1949) method utilizes Equations 2.4, 2.5, 2.6 and 2.7 along with soil moisture content and dry density to establish the thermal conductivity. The equations were developed through extensive testing on natural soils and crushed rock (Andersland and Ladanyi, 2004).

The equations are for both coarse-grained soils (silt-clay content < 20% and consisting of predominantly quartz) (Equations 2.4 and 2.5) and fine-grained soils (50% or more silty-clay) (Equations 2.6 and 2.7), for both frozen (-4°C) and unfrozen (+4°C) soils.

Unfrozen Coarse-grained: $k = 0.1442(0.7\log w + 0.4)(10)^{0.6243\rho_d}$ (2.4)

Frozen Coarse-Grained: $k = 0.01096(10)^{0.8116\rho_d} + [0.00461(10)^{0.9115\rho_d}]w$ (2.5)

Unfrozen Fine-Grained: $k = 0.1442(0.9\log w - 0.2)(10)^{0.6243\rho_d}$ (2.6)

Frozen Fine-Grained: $k = 0.001442(10)^{1.373\rho_d} + [0.01226(10)^{0.4994\rho_d}]w$ (2.7)

Where the following parameters with associated units must be used:

k = thermal conductivity (W/(m*K))

W = Watts, m = meters, K = °Kelvin

w = gravimetric water content of the soil sample (%)

ρ_d = the dry density of the soil (kg/m^3)

The thermal conductivity calculated using the above formulae differ from measured values by less than ±25%, which is sufficient for practical application due to the heterogeneity of natural soil properties in the field (Farouki, 1981). However, it should be noted that when applying the Kersten equation to high quartz content sands outside the ones used to fit the Kersten equation (e.g. Fairbanks sand, Lowell sand, standard and graded Ottawa sand) the Kersten equation underpredicts the thermal conductivity (Farouki, 1981). In summary, when Kerstens method is applied to coarse soils or soil materials it "overpredicts for those with a low quartz content while it underpredicts for those with a high quartz content". In either case the deviations are too large to be acceptable. Use of Kersten method when estimating thermal

conductivity of soils outside of the ones used to fit Kerstens equations should therefore be limited to coarse soils with intermediate quartz content" (quartz content of approximately 60%) (Farouki, 1981).

2.3.2.2 Johansen's Method

As mentioned above Johansen's Method is the most adaptable method to use with varying soil conditions. Johansen's Method utilizes both the dry (k_{dry}) and the saturated (k_{sat}) thermal conductivities of the mineral soil in question, as well as an empirically derived factor referred to as the Kersten number (K_e). The main equation (Equation 2.8) used in the computation of the thermal conductivity is:

$$k = (k_{sat} - k_{dry})K_e + k_{dry} \tag{2.8}$$

Where:

k = Thermal conductivity (W/(m*K))

k_{sat} = Saturated thermal conductivity (W/(m*K))

k_{dry} = Dry thermal conductivity (W/(m*K))

K_e = Kersten number

The Kersten number is calculated in one of three ways (Equations 2.9 through 2.11) depending on the grain size and degree of saturation (S_r).

Coarse-Grained Unfrozen Soil with $S_r > 5\%$: $K_e = 0.7 \log S_r + 1.0$ (2.9)

Fine-Grained Unfrozen Soil with $S_r > 10\%$: $K_e = \log S_r + 1.0$ (2.10)

Frozen medium and fine sands and fine-grained soils: $K_e = S_r$ (2.11)

The saturated thermal conductivity can be computed for either a soil that is frozen (Equation 2.12) or one that is unfrozen (Equation 2.13).

Saturated Unfrozen Soil: $k_{sat} = k_s^{1-n} k_w^n$ (2.12)

Saturated Frozen Soils Containing Some Unfrozen Water (w_u): $k_{sat} = k_s^{1-n} k_i^{n-Wu} k_w^{Wu}$ (2.13)

Where:

k_w = Thermal conductivity of water (0.57 W / (m*K))

k_i = Thermal conductivity of ice (2.2 W / (m*K))

k_s = Thermal conductivity of the soil constituents (W/(m*K))

n = Soil Porosity

w_u = Unfrozen water content (%)

The value of k_s is determined through the use of a geometric mean equation that utilizes the fraction of the quartz of the total solid contents (q), the thermal conductivity of quartz (k_q) and the thermal conductivity of the other mineral components (k_o), and can be computed using Equation 2.14, where A = 2.0 when q > 0.2 or A = 3.0 when q ≤ 0.2.

$$k_s = k_q^q A k_0^{1-q} \quad (2.14)$$

Johansen's method also requires the computation of the thermal conductivity of a soil in a dry condition, which is accomplished through the use of a semi-empirical equation (Equation 2.15) developed by Johansen (1975).

$$k_{dry}[W/(m*K)] = \frac{0.137\rho_d + 64.7}{2700\left(\frac{kg}{m^3}\right) - 0.947\rho_d} \pm 20\% \quad (2.15)$$

Where:

ρ_d = Dry density (kg/m^3)

If the degree of saturation is less than 5% for a coarse grained unfrozen soil and less than 10% for a fine grained unfrozen soil, use of another method should be considered. Farouki (1981) has found that unfrozen coarse grained soils that have a degree of saturation above 20% provide the best agreement between calculated and measured thermal conductivities when compared with other applicable methods. These agreements fall within the range of ±25%. When examining unsaturated frozen coarse soils Farouki found that again Johansen's method gives the closest estimates of thermal conductivity. He also suggested that due to the ease of calculations, Johansen's method should be used in calculating the thermal conductivity of coarse and fine soils with varied quartz contents and a degree of saturation above 20%. Similar conclusions were also made when a comparison of applicability to saturated soils was conducted, in which Farouki (1981) suggests the use of Johansen's method to calculate the thermal conductivity.

2.3.2.3 Cotê and Konrad Method

All of the other methods available to calculate the thermal conductivity of soils are quite inaccurate when used to estimate the values of base-course materials. Cotê and Konrad (2006) have modified the methods developed by Johansen in order to more accurately define the thermal conductivity of these materials. It was observed that when saturated soil freezes while in a hydraulically closed system the volume of the voids will increase by 9%. This in turn results in an increase in the porosity of the saturated frozen soil. With large pores the degree of saturation will increase consistent with the porosity of the soil, thus resulting in an increase in the degree of saturation of approximately 9%. Equations 2.16 and 2.18 were developed by Cotê and Konrad to account for the increases in both porosity and degree of saturation, respectively:

Porosity of Saturated soils freezing in a closed system: $$n_f = \frac{1.09n_u}{(1+0.09n_u)} \quad (2.16)$$

Where:

n_f = Porosity of saturated frozen soil

n_u = Porosity of an unfrozen soil as expressed by Equation (2.17)

Porosity of unfrozen soil: $n_u = 1 - \frac{\rho_d}{\rho_s}$ (2.17)

Where:

ρ_d = Dry density (kg/m^3)

ρ_s = Density of the solid particles (kg/m^3)

Degree of saturation for a frozen soil: $S_{rf} = \frac{1.09S_{ru}}{(1+0.09S_{ru})}$ (2.18)

Where:

S_{ru} = Degree of saturation for an unfrozen soil

In order to ensure that the effect of mineralogy of dry crushed rock be considered in the thermal conductivity they replaced the thermal conductivity of ice and water with thermal conductivity of air when using the geometric mean method. These modifications resulted in errors of less than 15% when examining unfrozen materials and less than 20% when examining frozen samples.

2.3.3 Heat Capacity

The heat capacity of a material represents the amount of heat that is required to raise the material's temperature by 1 degree (Andersland and Ladanyi, 2004). The units of heat capacity are (kJ / (kg °C)). When the heat capacity is defined as a ratio of the material's heat capacity to that of water, it is referred to as the specific heat capacity and is measured in the same units as heat capacity. Due to soils consisting of numerous materials, including solids, water/ice, and air the heat capacity of a soil in its entirety must be representative of every constituent present. In order to accomplish this, mass fractions of the materials (i.e. solids (m_s), water (m_w), ice (m_i) and air (m_{air})) are multiplied by their corresponding specific heat capacities (i.e. solids (c_s),

water (c_w), ice (c_i), and air (c_{air})), for a specified volume (Equation 2.19) in which "m" is equal to the total mass (Andersland and Ladanyi, 2004).

$$c\ [kJ/(kg\ °C)] = (1/m)*(c_s m_s + c_w m_w + c_i m_i + c_{air} m_{air}) \quad (2.19)$$

When the specific heat capacity of a soil is divided by the volume, while at the same time ignoring the negligible air term the volumetric heat capacity (c_v) of the soil is defined as follows (Equation 2.20).

$$c_v\ [kJ/(m^3 °C)] = c_m \rho_f = \rho_{df} (c_s + c_w w_u + c_i w_i) \quad (2.20)$$

Where:

ρ_f = the frozen bulk density (kg/m^3)

ρ_{df} = the frozen dry density (kg/m^3)

w_u = the unfrozen water content (%)

w_i = the frozen water content (%)

c_m = specific heat capacity of the total soil mass (kJ / (kg°C))

Heat capacity values for common surface and subsurface materials can be seen in Table 2.3.

2.3.4 Thermal Diffusivity

The ratio of thermal conductivity (k) over heat capacity (c) and bulk density (ρ) is defined as the soil thermal diffusivity (Andersland and Ladanyi, 2004). The thermal diffusivity essentially provides "an index of the rate at which a material will undergo a temperature change in response to external temperature changes" (Andersland and Ladanyi, 2004). This is represented in the following equation.

$$\alpha\left(\frac{m^2}{s}\right) = \frac{k}{c\rho}\left(\frac{{}^{W}/_{m*°C}}{{}^{J}/_{kg*°C}}\frac{1}{{}^{kg}/_{m^3}}\right) \tag{2.21}$$

The thermal diffusivity of ice (11.2 x 10^{-7} m^2/s) is much greater than that of water (1.4 x 10^{-7} m^2/s); therefore the thermal diffusivity of a frozen soil will be much larger than that of an equivalent thawed soil, which indicates that "the average temperature of a mass of saturated frozen soil will increase more quickly than that of a mass of unfrozen soil with equal dimensions at an equal difference between the initial temperature of the soil mass and that of the surrounding soil" (Andersland and Ladanyi, 2004).

2.3.5 Latent Heat

The latent heat of fusion indicates the amount of heat energy that is absorbed when a unit mass of ice is converted into a liquid at the melting point (Andersland and Ladanyi, 2004). The total energy involved with latent heat of fusion is reliant upon the total amount of water contained in the soil sample and can be calculated using Equation 2.22 (Andersland and Ladanyi, 2004).

$$L = \rho_d L' \frac{w - w_u}{100} \tag{2.22}$$

Where:

L = Volumetric latent heat of fusion (kJ/m^3)

ρ_d = Soil dry dendsity (kg/m^3)

L' = Mass latent heat of water (333.1 kJ/kg)

w = Total water content (%)

w_u = Unfrozen water content (percentage dry mass basis)

For coarse grained soils such as sands and gravels, the unfrozen water content (w_u) term will be quite small and for this reason will be considered zero in most practical problems. This

assumption has been found to provide acceptable latent heat of fusion values estimates (Andersland and Ladanyi, 2004).

2.4 Spring Load Restrictions

In order to minimize the damage to low volume roads, many jurisdictions throughout Canada and the United States implement SLRs during the spring-thaw weakened period. Ideally, SLRs should commence when thawing front migration exceeds a depth which results in significant pavement structure weakening. Studies such as Hein and Cole (2002) and Kestler et al. (1999), indicate that SLR implementation at the onset of thawing front migration into the pavement resulted in appropriate start dates, while others have found that a significant decrease in pavement stiffness does not occur until thawing reaches a specific depth within the pavement structure. In one such examination, Van Deusen (1998) studied the effect of air temperature on frost and thaw penetrations which indicated that there is a dramatic decrease in aggregate base stiffness at approximately the time that the thawing front passes through the base layer (shown as the Granular A base layer in Figure 2.1). Furthermore, Ovik et al. (2000) indicate that pavement deflections measured with a Falling Weight Deflectometer (FWD) at numerous test sections of varying composition at the Minnesota Road test site significantly increase when the pavement structure has thawed to between 300mm and 600mm. Rutherford (1989) found that the thickness of the asphalt concrete layer played a significant role in pavement strength. Thin pavements (2 in.) reached a critical condition at the time of base thaw, while thicker pavements (4 in.) did not reach this condition until some subgrade thawing had occurred. A significant issue regarding the implementation of SLRs is the effect that thawing followed by refreezing, which is common during most thawing seasons, has on the implementation date.

SLR removal is also a complicated process. Andersland and Ladanyi (2004) indicate that SLR removal should occur when the pavement structure has completely thawed, thus, allowing natural drainage conditions to be restored. Hein and Cole (2002) have found (through pavement deflection testing) that the duration of pavement structure weakness can be double that of the time required to achieve complete pavement structure thawing. Extensive falling weight deflectometer testing conducted in New Hampshire has found that pavement strength

is not fully restored until about a week after full pavement structure thawing is observed (Berg, 2010).

2.4.1 SLR Application and Removal

Historically, SLRs in Canada and the northern United States (US) have been implemented and removed using one or a combination of the following:

- Engineering judgement
- The use of prescheduled calendar dates
- Visual observations
- Pavement deflection testing
- Empirical model methods

SLR methods vary by jurisdiction. Table 2.4 indicates the various SLR methods used by each Canadian province(C-SHRP, 2002). Empirical correlation methods used in the US by states such as Minnesota and Wisconsin, provide a relationship between air temperatures and pavement conditions that can also be used to determine effective SLR implementation and removal times.

Many of the current methods (engineering judgement, visual observation and pavement deflection testing) require a 3 to 5 day lag time between observed pavement distress and SLR implementation. This lag time is needed to provide sufficient notice to the transportation industry which allows for companies to make appropriate arrangements. During this period the pavement structure is subjected to full loads, and potentially winter weight premium loads, while in a weakened state, resulting in damage to the roadway.

Visual observation techniques are beneficial when used in conjunction with other SLR methods. However, this method cannot be used to assess the depth or amount of thawed material present within the sub-grade and sub-base of the road structure. Because the implementation of SLRs in this method requires the observation of pavement distress, much roadway damage can occur in the early and most damage-susceptible thawing period.

The use of prescheduled dates effectively eliminates the problems that are associated with the lag period. However, this method can dramatically increase the length of time that SLRs are applied to a roadway as restrictions may be in place when the pavement structure is completely thawed or long after pavement strength has completely returned. This results in increased costs to the transportation industry. Conversely they may be applied too late if an unseasonably warm period occurs in late winter, which would result in damage to the roadway. As climatic changes become more prevalent it becomes more difficult to effectively establish appropriate prescheduled dates on a year-to-year basis.

Numerous SLR implementation methods have been developed to predict the pavement structure response to changes in air temperatures using empirical methods (e.g. Mn/DOT method) or to predict freezing and thawing trends using semi-empirical methods(e.g. Waterloo method described in Section 2.4.1.2) techniques. In many cases these methods are used in conjunction with pavement deflection testing conducted with a Benkelman Beam (BB), FWD, or Light Weight Deflectometer (LWD) to qualify their findings.

2.4.1.1 Mn/DOT Research

The concepts used in development of the Mn/DOT method (MN/DOT, 2004) were first researched by the Washington State Department of Transportation (Ws/DOT) (Ovik et al., 2000). The Mn/DOT method uses reference temperatures and measured air temperatures to calculate daily Freezing Index (FI) and daily Thawing Index (TI) values. The FI is defined by the Mn/DOT as the "positive cumulative deviation between a reference freezing temperature and the mean daily air temperature for successive days" (Ovik et al, 2000), and the TI is defined as the "positive cumulative deviation between the mean daily air temperature and a reference thawing temperature for successive days" (Ovik et al, 2000). These values are then used to calculate a Cumulative Thawing Index (CTI) which indicates the need for SLR implementation (Equation 2.23) (Mn/DOT, 2004).

$$\mathrm{CTI} = \sum_{i=1}^{n} (\text{Daily Thawing Index} - 0.5 \times \text{Daily Freezing Index}) \tag{2.23}$$

- When $\left(\frac{T_{maximum}+T_{minimum}}{2} - T_{reference}\right) > 0°C$

  Daily Thawing Index = $\left(\frac{T_{maximum}+T_{minimum}}{2} - T_{reference}\right)$ and

  Daily Freezing Index = 0°C

- When $\left(\frac{T_{maximum}+T_{minimum}}{2} - T_{reference}\right) < 0°C$

  Daily Thawing Index = 0°C and

  Daily Freezing Index = $0°C - \left(\frac{T_{maximum}+T_{minimum}}{2} - T_{reference}\right)$

Where:

CTI = Cumulative thawing index calculated over a period from 1 to n days (°C-days)

$T_{maximum}$ = Maximum daily air temperature (°C)

$T_{minimum}$ = Minimum daily air temperatures (°C), and

$T_{reference}$ = Reference air temperature (°C)

The Mn/DOT method uses a floating reference temperature to convert recorded air temperatures into corresponding surface temperatures. The negative reference temperatures are subtracted from the air temperatures (Equation 2.23) resulting in temperature increases, which account for the increases in solar energy during the spring thawing season. Beginning on February 1st the reference temperature is set at -1.5°C, and decreased weekly by 0.5°C, until it reaches -9.5°C during the week of May 24th – May 30th (Mn/DOT, 2004). Table 2.5 indicates the reference temperatures applied throughout the spring thaw season. The 0.5 factor applied to the FI in Equation 2.23 is a refreeze factor that is used to account for the partial phase change of water from a liquid to a semi-solid during periods of refreeze (Mn/DOT, 2004).

Numerous studies conducted by the Ws/DOT show that using a Cummulative Thawing Index (CTI) of 15°C-days corresponded to 150mm of thawing front penetration. The 15°C-day CTI

value is used to indicate when SLRs should be implemented to optimize SLR placement, while a 30°C-day CTI value is used to indicate when SLRs must be in place to avoid substantial amounts of pavement damage (Ovik et al., 2000). This method was adjusted to represent Minnesota conditions. For the Mn/DOT method the SLRs are implemented when a 3-day forecasted temperature period gives a cumulative thawing index (CTI) greater than 14°C-days, with predicted increases well in excess of 14°C days. For this method SLRs, will remain in effect until an examination of the following variables for several cities within each frost zone is considered (Mn/DOT, 2004):

1. Measured and forecast daily air temperatures (cumulative thawing index)
2. Cumulative spring precipitation
3. Accumulated fall precipitation measured during the preceding year
4. Maximum cumulative freezing index resulting from the preceding winter freeze period

A contingency plan also remains in place specifying a minimum duration of SLRs of 4 weeks, while the maximum duration will not exceed 8 weeks.

2.4.1.2 University of Waterloo Research

The Waterloo method (Baiz et al., 2007) also requires the use of reference temperatures. Unlike the Mn/DOT method which uses defined weekly reference temperatures, the Waterloo reference temperatures are calculated on a monthly basis using site specific data. The reference temperatures are determined from the intercept of a best fit line of measured air temperatures and corresponding pavement surface temperatures (Figure 2.4). The reference temperatures are subtracted from the average daily air temperatures and used in the calculation of daily FI and TI values and determination of the start of the thawing season (day i_0) (Figure 2.5). These FI and TI values are then input into the algorithms in Equations 2.24 and 2.25, to calculate freezing depth (FD) and thawing depth (TD) (Baiz et al., 2007).

$$0 \le i \le i_0 \Rightarrow \begin{cases} FD_i = a + b\sqrt{FI_i} + c\sqrt{TI_i}) \\ TD_i = d + e\sqrt{FI_i} + f\sqrt{TI_i}) \end{cases} \quad (2.24)$$

$$i \ge i_0 \Rightarrow \begin{cases} FD_i = g + h\sqrt{FI_i} + i\sqrt{TI_i}) \\ TD_i = j + k\sqrt{FI_i} + l\sqrt{TI_i}) \end{cases} \quad (2.25)$$

Where :

i = 0	Day on which T_{Air} first falls below 0°C
i	Number of days after the day indexed as day i = 0
i_0	Day after which the TI consistently rises above 0°C-days
FD_i	Depth of frost on day *i* (from the pavement surface, in negative cm)
TD_i	Depth of thaw on day *i* (from the pavement surface, in negative cm)
FI_i	Freezing Index value on day *i* (in °C-days)
TI_i	Thawing Index value on day *i* (in °C-days)
a,b,c,d,e,f	Calibration coefficients used during the freezing season
g,h,l,j,k,l	Calibration coefficients used during the thawing season

Following determination of the monthly reference temperatures, calibration coefficients are calculated with a best fit regression analysis of the FI, TI and the corresponding measured site specific frost and thaw depths with time. Equations 2.24 and 2.25 can then be used to simulate the frost and thaw depths with time within the pavement structure (Figure 2.6). With this method SLRs should be implemented on day i_0 which determines the beginning of the thawing season and removed when the algorithm indicates complete pavement structure thawing (Figure 2.6)(Baiz et al., 2007).

2.4.1.3 Alaska Research

SLRs in Alaska are implemented, amended and removed based on decisions of a regional maintenance engineer (ADOT&PF, 2007). These decisions are based on the following:

1. Historical Data
2. Thermistor Data
3. Weather forecasts
4. Field observations and photographs
5. Any other objective data which help forecast potential roadway damage

Historically, the SLRs have remained in effect for approximately 6 weeks and notification was given online in a public access forum and in local newspapers. Currently, a method is being developed by the ADOT&PF that uses a thermistor probe profile to issue fact-based weight restriction notice (TAT, 2006). The regional maintenance engineer monitors the thaw progression indicated by numerous thermistor instrumented sites across Alaska to ensure that SLRs are not unnecessarily in effect.

2.4.1.4 British Columbia Research

The province of British Columbia in conjunction with the Forest Engineers Research Institute of Canada (FERIC) have examined the effects of allowing transportation vehicles equipped with Tire Pressure Control Systems (TPCS) to resume full load hauling on thaw weakened pavement structures (Mabood et al., 2008). Results of this examination indicate that fully loaded logging trucks equipped with TPCS were able to use the thaw weakened roads three to five weeks prior to SLR removal without measureable pavement rutting or cracking (Mabood et al., 2008). In response to this study the province of British Columbia introduced legislation that exempts tucks equipped with TPCS from adhering to SLRs on approved roads throughout the province.

2.4.1.5 New Hampshire Research

The New Hampshire Department of Transportation (NH/DOT) developed a method that utilizes FI and TI values determined from an examination of air temperatures, surface temperatures and the sinusoidal air temperature amplitude (Eaton et al., 2009). This is accomplished through

first assuming a trial amplitude value and inputting it into an equation (Equation 2.26 below) developed by Sanger (1963).

$$|\mathrm{FI}| = (365 / \pi)\,[\sqrt{A^2 - V_0^2} - V_0 cos^{-1}(\tfrac{V_0}{A})] \qquad (2.26)$$

Where:

|FI| = The absolute value of the freezing index, °C-days

V_0 = Mean annual air temperature, °C

A = Amplitude of the sinusoidal variation, °C

Variation of the amplitude value is continued until the calculated FI is equal to the absolute value of the air freezing index determined from mean monthly air temperatures. N-factor values are applied to the air freezing index and air thawing index to determine pavement surface FI and TI values. This process is repeated until calculated values equal the value of the air freezing index multiplied by the freezing season's n-factor value. Next, daily air and pavement surface temperature values are determined using the mean monthly air temperatures and annual sinusoidal temperature amplitudes. Then, the difference between air temperatures and pavement surface temperatures between February 15th and May 30th are used in daily SLR calculations. The daily SLR calculations are conducted in a similar manner to that done in the Mn/DOT method; however the NH/DOT uses an initial reference temperature of 0°C instead of the -1.5°C that is used by the Mn/DOT.

These relationships were used in the development of the Enhanced Integrated Climactic Model (EICM) used by New Hampshire, which is a subprogram of the Mechanistic Empirical Design Guide (MEPDG) software. The EICM is a finite element based, coupled heat and mass flow program. This program requires that air temperature, precipitation, wind speed and estimated percent sunshine be input as upper boundary (i.e. pavement surface) conditions. This program utilizes a fixed temperature that is equal to the average annual air temperature at a depth of 9.1 m, as the bottom boundary condition. The pavement structure properties are determined through an interpretation of two input material properties, grain size and Atterberg limits. Using the EICM to predict freezing and thawing front depths, the NH/DOT will

implement SLRs when thawing first begins to penetrate the pavement surface and will be removed approximately one week after the subsurface has completely thawed (Berg, Personal Communication, 2010).

2.4.1.6 Thermal Numerical Modelling

Thermal numerical modelling used in this research is based on the principles of finite element analysis. A numerical model is used to mathematically simulate a real life process (TEMP/W, 2007). A thermal numerical model can simulate the physical process of heat flow through a fully or partially saturated, frozen or thawed subsurface. For this reason there are many advantages to using a numerical model over a physical model, such as (TEMP/W, 2007):

- The speed in which a numerical model can be developed relative to a physical model, where a numerical model may be constructed in minutes to hours while a physical model requires days to months.
- Physical models are typically constrained by a narrow set of conditions, while almost infinite scenarios can be developed and tested using a numerical model.
- Numerical models have no difficulty accounting for gravity while laboratory work typically requires the use of a centrifuge as gravity cannot be scaled.
- Numerical model results can be obtained for any location throughout the cross-section of the model, while a physical model will only provide external visual responses and data from specific instrumented points within the model.

The thermal model does have some limitations when compared with traditional physical modelling, however. The most significant of these limitations is that due to the extreme complexity that would be required in the mathematical equations certain conditions are not accounted for when the model is developed including (TEMP/W, 2007):

- Pore water pressure changes
- Volume changes, and

- Chemical reactions
- Complexity of the boundary conditions, particularly the upper pavement surface boundary condition

For the purposes of this research the thermal numerical modelling software, TEMP/W, developed by GEO-SLOPE International Ltd. was used to simulate subsurface freezing and thawing trends. This software is specifically designed to simulate thermal changes in the ground due to environmental changes or the construction of a facility and is described in more detail in Section 2.5 (TEMP/W, 2007).

2.4.1.7 Summary and Assessment of SLR Methods

All of the potential SLR methods provide advantages and limitations with respect to accuracy and/or potential ease of implementation. An examination of each method outlining the main advantages and limitations of each can be seen in Table 2.6.

With the exception of the British Columbia research, all of these methods can be largely grouped into empirical, semi-empirical or analytical/numerical methods. The Mn/DOT method is the most empirical of the methods using only air temperature values as inputs into an empirically-derived formula. The Waterloo and Alaska methods both utilize a semi-empirical method. However the difference between the two methods is that the Waterloo method uses an empirically-derived formula to determine the depths of frost and thaw from which SLR placement and removal is determined, while the Alaska method reinforces field observations using a combination of forecasted air temperatures and thermistor data to determine SLR placement and removal. The thermal numerical modelling method and the New Hampshire method are the most analytical of the methods, requiring numerous inputs. The analytical methods have the ability to be the most representative of a system, however require the largest amount of variable data.

This thesis will examine the Mn/DOT, Waterloo and thermal numerical modelling methods to determine which method provides the most appropriate indication of SLR placement and removal for two northern Ontario study sites. These methods were chosen for a

detailed assessment as they encompass a range of complexity and input requirements. The Mn/DOT method is the least complex requiring the fewest inputs, while the thermal numerical modelling method is the most complex requiring the most model inputs (thermal model). The Waterloo method lies between the Mn/DOT and thermal modelling method as it provides a balance between model inputs requirements and complexity.

2.5 TEMP/W Thermal Numerical Modelling

TEMP/W is a finite element software program that is used to model thermal changes through any type of porous or solid material using comprehensive formulae (TEMP/W, 2007). These formulae make it possible to simulate complex scenarios that encompass multiple regions and varying material properties, while applying a wide range of possible boundary conditions. In all TEMP/W analysis there is an inherent assumption that moisture content does not change during calculation of the solution. The phase change of water is accounted for with the summation of ice and water contents continuously equal to the total moisture content. If the effects of moving water on heat transfer are assumed to be an important parameter, TEMP/W can be coupled with SEEP/W (a groundwater flow finite element program available through GEO-SLOPE International Ltd.).

For TEMP/W to accurately simulate physical behavior numerous conditions and variables must be established and defined including:

- Analysis type (transient or steady state)
- Convergence criteria
- Time step
- Region development
- Mesh size and shape
- Material properties
- Boundary conditions

Once these variables have been defined and applied, the model will undergo numerous iterations per time step to establish temperatures at nodes throughout the model.

2.5.1 Model Development

Model development includes the definition of analysis type, convergence criteria, appropriate time step, regions and mesh size and shape. Material properties and boundary conditions are described in Sections 2.5.2 and 2.5.3, respectively.

There are three types of analysis available in TEMP/W. The first type is a steady state analysis in which temperature and heat flow rates are not changing with time. This type of analysis is required to establish the initial conditions of the model. A steady state analysis cannot be used to determine how long it takes to reach the final condition but instead will interpret what the subsurface will resemble given the specific set of initial boundary conditions. The second type of analysis is a transient analysis which by definition is one that is constantly changing. The initial conditions established with the steady state analysis must be provided along with current and future boundary conditions for the analysis to proceed in time. The third type of analysis is the convective heat transfer analysis, which is used to couple the TEMP/W software with the SEEP/W software.

The convergence criteria are divided into three categories. The first category allows for user determination of the maximum number of iterations and the tolerance applied to the model. The phase change region category allows the user to implement the number of Gauss regions per iteration. The final category allows the user to define the type of equation solver to be used. The user has the option of using a direct equation solver or a parallel direct equation solver which is typically used with a larger mesh size.

Determination of the appropriate time step is based on the described duration and frequency of simulation output during a specified freeze/thaw event. The step size increases can be set as either linear or exponential.

The mesh size and shape are automatically generated by TEMP/W based on the shape of the region and the size of the grid (Figure 2.7).

2.5.2 Thermal Modelling Material Inputs

The TEMP/W thermal numerical model requires that each region within the model be assigned a specific set of material and thermal properties. The material properties can be obtained through geotechnical characterization of the pavement structure, while the thermal properties can be estimated from the material properties using the equations presented earlier. The latent heat of water and the phase change temperature variables are assumed to remain constant throughout the duration of the model and are therefore set as constant values under the "Units and Scale" tab. All of the other thermal properties are defined under the "Materials" tab. The material properties can be defined using the functions in one of the following five material models (TEMP/W, 2007):

1. None (used to remove part of a region of the model in an analysis)
2. Full thermal:
    - Thermal conductivity vs. temperature function
    - Unfrozen water content function
    - Frozen and unfrozen volumetric heat capacities
    - In situ volumetric water content
3. Coupled convective thermal (with SEEP/W):
    - Thermal conductivity vs. water content function
    - Unfrozen water content function
    - Volumetric heat capacity vs. water content function
4. Simplified thermal:
    - Frozen and unfrozen volumetric heat capacities
    - Frozen and unfrozen thermal conductivity
    - In situ volumetric water content
5. Interface:
    - Thermal conductivity

Examples (screen captures) of the thermal conductivity and unfrozen water content functions can be seen in Figures 2.8 and 2.9, respectively.

The full thermal model is typically used in TEMP/W thermal analysis as it provides a comprehensive representation of the subsurface thermal behavior. All of the functions in the full thermal model are dependent on temperature only and are therefore only valid when there is a constant water content (i.e. although water is able to undergo a phase change, the overall amount of water/ice is fixed throughout the analysis).

The coupled convective thermal model requires that the thermal functions be dependent on both the water content and the temperature.

The simplified thermal model can be used in cases where the latent heat of phase change is not of particular importance. In the simplified model there is no release of latent heat and all phase change is to occur at the specified phase change temperature and not over a range of temperatures (TEMP/W, 2007).

2.5.3 Thermal Modelling Boundary Conditions

Accurate definition and application of boundary conditions are key components of a numerical analysis (TEMP/W, 2007). The finite element equations for a thermal analysis just prior to solving for the unknowns are represented in Equation 2.27.

$$[K]\{T\} = \{Q\} \tag{2.27}$$

Where:

[K] = A matrix of coefficients related to a model geometry and material properties

{T} = A vector of the temperature at the nodes, and

{Q} = A vector of the heat flow quantities at the nodes

The unknowns in any thermal model will be computed relative to T values specified at one node and either a T or Q value specified at another node (TEMP/W, 2007). These specified T and/or Q values are the boundary conditions of a model. Specifying either T or Q at a node is

the only option available when considering boundary condition specification; however, these conditions can be applied in a variety of ways. It should also be noted that if T values are specified the thermal numerical model will calculate corresponding Q values while alternatively if Q is specified, T will be computed.

In all TEMP/W modelling, boundary conditions can be applied directly to the following geometric items (TEMP/W, 2007):

- Region faces
- Region lines
- Free lines
- Free points

Temperature and climate boundary conditions are used to represent the specified temperature at a node. The following steps outline the process of establishing a temperature based boundary condition:

1. Determine the type of temperature boundary condition (thermal, total flux, or unit flux) based on known and unknown variables.
2. Determine from the following which method will be used to apply temperature data to the specified nodes:
    - Constant temperature: Temperature value will remain constant throughout the thermal numerical analysis
    - Temperature function: Temperature data will vary based on specified time step (example screen captures shown in Figure 2.10).
    - Thermosyphon: Used to remove heat from the model (an example is a cooled pipeline).
    - Convective surface: Used to introduce heat into the model (an example is a heated pipeline).

3. If required, create a modification function that will be applied to the temperature data in the temperature function (example screen captures shown in Figure 2.11).
4. Apply the temperature boundary condition to the desired nodes within the model.

The application of climate boundary conditions is more complex and requires far more data inputs than does the temperature boundary condition option (Figure 2.12). The following is a list of required climatic boundary condition inputs:

- Location latitude
- Solar energy data source
- Distribution pattern
- Start date
- Minimum and maximum temperatures
- Minimum and maximum relative humidity
- Wind speed
- Precipitation amount and duration

2.6 Pavement Deflection Testing

Non-destructive pavement deflection testing has long been used to establish the stiffness and strength of a pavement section. The most common mechanisms used to measure a pavement response from an applied load are the Benkelman Beam (BB) and the Falling Weight Deflectometer (FWD). The deflection measurements and corresponding interpreted pavement modulus values can be used to supplement a SLR program. A significant drawback to using these devices is the high cost and large size of the equipment used. Many studies have examined using a Light Weight Deflectometer (LWD) to determine pavement strength parameters as an alternative to using these other devices. Steinert et al. (2005) found that the LWD could be used as a suitable replacement to a FWD for the purposes of estimating composite modulus values of pavement sections for some pavement thicknesses. Dynatest (2006) indicates that the LWD is best suited for unbounded materials such as sand or gravel and

is not well suited for testing on asphalt as the device lacks the force necessary to obtain accurate measurements. It has also been noted however, that in general correlation coefficients tended to increase as the pavement thickness decreased (Steinert et al., 2005). To this end, the accuracy of the LWD is limited to thin pavement surfaces and substantially decreases as the pavement thickness and corresponding rigidity increase.

2.6.1 Light Weight Deflectometer

A LWD will create a non-destructive shock-wave through the subsurface as a result of the impact of a falling weight (Steinert et al., 2005). Steinert et al. (2005) found that for the best results the largest drop weight, largest plate diameter, and largest drop height should be used. Velocity transducers and accelerometers are used to measure the deflections resulting from applied load. Once deflections are determined and force is calculated (based on drop height and mass of weight) modulus values can be calculated.

2.6.1.1 Dynatest 3031 LWD

The Dynatest 3031 LWD is one type of device available for pavement deflection testing. This device has a maximum drop height of 850 mm which can easily be adjusted by moving the catch assembly up and down using the engraved scale along the guide rod (Figure 2.13). The drop weights can be adjusted from 10 kg to 20 kg by adding additional weights (Figure 2.14). The load is dropped onto buffer pads which protect the load cell. The load cell (Figure 2.15) measures the force of the impact and the velocity transducer, or geophone (Figure 2.16), measures the deflection. For this LWD loading plates of 150 mm, 200 mm or 300 mm can be used and two extra geophones can be added to measure deflections at specific distances from the centre of the device.

Force and deflection results from the LWD are transferred to a Personal Digital Assistant (PDA) via Bluetooth technology. Through software installed on the PDA, test results including force, deflection and surface deflection modulus values can be displayed graphically and numerically (Figure 2.17). The entire test results are saved in the PDA's internal memory and transferred into an accompanying program called LWDmod.

In LWDmod, collected data can be observed and quality assured. Using this program all erroneous results can be removed and further statistical analysis can be conducted. Using the pavement structure layer thicknesses and assumed seed values (LWDmod default values for modulus values at corresponding reference stress levels and exponents for nonlinearity) LWDmod can be used to estimate composite modulus values from the surface deflection modulus values obtained through testing. Surface deflection modulus values represent the modulus values calculated solely on the deflection values measured at the pavement surface, where as the composite modulus value is representative of the entire pavement structure. It is also possible to plot deflection data, deflection details, surface deflection moduli, and drop statistics for one or all of the test locations using LWDmod (example screen capture shown in Figure 2.18), which can then be imported into Microsoft Excel. LWDmod can also be used to create a comprehensive report which can include the following:

- Test results
    - Point number
    - Location
    - Drop number
    - Time
    - Plate size
    - Force
    - Stress
    - Distance of additional geophones
    - Deflection measured at each geophone
    - Surface deflection modulus
    - Temperature
    - Notes
- Analysis results
    - Location
    - Thickness

- Composite elastic modulus values

2.6.2 Pavement Deflection Data by Other Sources

Research comparing pavement deflections and stiffness with observed frost and thaw depth has been conducted at the Minnesota Road (MnROAD) testing site. The MnROAD test site is a section of roadway constructed with differing pavement structures which are exposed to varying and controlled traffic patterns. This test site is used for multiple studies to closely monitor pavement performance under varying environmental conditions. Using the MnROAD test site, Ovik et al. (2000) discovered that pavement surface deflections significantly increased when the pavement structure had thawed between 300 mm and 600 mm (Figure 2.19).

Steinert et al. (2005) researched the relationship between LWD composite modulus values and FWD composite modulus values. This research found that the correlation between LWD and FWD composite modulus values was strongly associated with the pavement thickness. Figure 2.20 shows the comparison between LWD and FWD composite modulus values when the pavement thickness is less than 127 mm. Figure 2.20 indicates that the two composite modulus values correspond well with an R^2 value of 0.87. Examination of Figure 2.21 provides a comparison of LWD and FWD composite modulus values when the pavement structure is equal to 152 mm. This correlation is not as good, with a reduction in the R^2 value to 0.56.

2.7 Road Weather Information Systems (RWIS) in Ontario

As of 2005, the Ontario Ministry of Transportation (MTO) had installed 113 Road Weather Information System (RWIS) stations throughout the province (Buchanan and Gwartz, 2005). The RWIS stations employ real-time pavement and atmospheric sensors to obtain current pavement and weather conditions. Data are stored in the RWIS data logger so that historical data can be observed and compared to the current data. RWIS stations in Ontario currently are capable of collecting and displaying (Figure 2.22) the following data (TWNCS, 2009):

- Current air temperature
- Minimum and maximum recorded air temperature over the previous 24 hour period

- Dew point temperature
- Relative humidity
- Forecasted wind chill factor
- Forecasted heat index
- Wind speed and direction
- Maximum wind speed (gusts) over an evaluation cycle
- Probability of precipitation
- Precipitation intensity, rate and accumulation
- Surface status (i.e. wet, dry, ice covered) and temperature
- Subsurface temperature and moisture content

Subsurface data are collected from thermistor probes installed within the pavement structure. These probes record the electrical resistance variations that occur with changing temperature. These variations are then converted into corresponding temperatures.

2.8 Environmental Considerations

The implementation of SLRs has both positive and negative environmental impacts both in the short term and the long term. As truck traffic increases during periods of SLR implementation numerous adverse environmental impacts are created including increases in road noise, heat generation and vehicular emissions. Furthermore, increases in distance that are incurred when making multiple trips increases wear on tires and transportation vehicles mechanical systems which require replacement.

Alternatively the placement of SLRs can have significant positive environmental impact. Ovik et al. (2000) found that for a typical low volume road application of SLRs will increase a pavement lifespan by approximately 10%. This increase in lifespan will reduce the amount of rehabilitation or replacement required on the roadway, thus, reducing the negative impacts of construction including those created during extraction, manufacturing, transportation and placement of materials (Ahmed et al., 2006). Further to this, Amos (2006) found that a 53%

increase in pavement smoothness resulted in a 2.46% increase in fuel efficiency, thus, illustrating that a well maintained road is an essential part of reduced vehicular emissions.

A further environmental condition to consider is that the forecasts for the Canadian climate indicate average annual temperature increases by 2 to 3°C by as late as 2069 and as early as 2040 (Stewart, 2003). These changing temperatures will in turn affect the start and duration of the freezing and thawing seasons. Climate changes have already begun to show more variability than they have in the past. These changes must be considered when examining future SLR programs.

Table 2.1 Typical n-factor Values (Andersland and Landayi, 2004)

Surface	Freezing, n_f	Thawing, n_t	Sources[a]
Snow	1.0	—	1, 2
Pavement free of snow and ice	0.9	—	2, 4
Sand and gravel	0.9	2.0	2, 4
Turf	0.5	1.0	2, 4
Spruce trees, brush, moss over peat soil	0.29 (under snow)	0.37	1, 3
Trees and brush cleared moss over peat soil	0.25 (under snow)	0.73	1, 3
Vegetation and 6-cm soil stripped, mineral soil surface	0.33	1.22	1, 3
Gravel	0.6–1.0	1.3–2	1, 3
(Probable range, northern conditions)	(0.9–0.95)		1
Asphalt pavement	0.29–1.0 or greater	1.4–2.3	1
(Probable range, northern conditions)	(0.9–0.95)	[b]	1
Concrete pavement	0.25–0.95	1.3–2.1	1
(Probable range, northern conditions)	(0.7–0.9)	[b]	1

[a] 1: Lunardini, 1978; 2: McRoberts, 1974; 3: Lunardini, 1985; 4: Department of the Army, 1966.

Table 2.2 k_u Coefficient Table (U.S.S.R. 1969)

		k_u Coefficients					
		Temperature (°C)					
Soil Type	Plasticity Index	-0.3	-0.5	-1	-2	-4	-10
Sands	< 1	0	0	0	0	0	0
Silty Sands	1 - 2	0	0	0	0	0	0
Sandy Silts	2 - 7	0.6	0.5	0.4	0.35	0.3	0.25
Clayey Silts	7 - 13	0.5	0.65	0.6	0.5	0.45	0.4
Silty Clays	13 - 17	*	0.75	0.65	0.55	0.5	0.45
Clays	> 17	*	0.95	0.9	0.65	0.6	0.55

* All pore water is unfrozen

Table 2.3 Typical Thermal Conductivity and Heat Capacity Values (After Andersland and Ladanyi, 2004)

Material	Heat Capacity kJ/(kg°C)	Thermal Conductivity W/(m°K)
Air 10 °C	1	0.026
Water 0 °C	4.22	0.56
Water 10 °C	4.19	0.58
Ice 0 °C	2.09	2.21
Snow Loose	2.09	0.08
Snow Compacted	2.09	0.7
Concrete		
Sand and Gravel Aggregate	0.89	1.3 - 1.7
Lightweight Aggregate		0.74
Concrete, Asphalt		1.05 - .152
Quartz	0.73	8.4
Granite	0.8	1.7 - 4.0
Limestone		1.3 - 5.0
Shale		1.5
Sandstone		1.8 - 4.2

Table 2.4 SLR Implementation and Removal Dates for Canadian Provinces (C-SHRP, 2002)

Province	Start/End Dates
British Columbia	**Start:** Mid-February **End:** Mid-June
Alberta	**Start:** 30cm thaw and a heat flow model **End:** FWD testing
Saskatchewan	**Start:** 2nd or 3rd week in March **End:** Maximum six weeks after start
Manitoba	**Start:** Southern Zone: March 23 Northern Zone: April 15 **End:** May 31
Ontario	**Start:** Variable, typically 1st Monday in March **End:** Variable, typically Mid-May
Quebec	**North:** March 24 - May 25 **Central:** March 6 - May 12 **South:** March 21 to May 19
New Brunswick	**Southern Zone:** 2nd week in March to mid-May **Northern Zone:** Third week in March to end of May
P.E.I	**Start:** March 1 **End:** April 30
Nova Scotia	**Southern Region:** March 2 - Arpil 24 **Central/Northern Region:** March 2 - April 27
Newfoundland	**Start:** February **End:** April

Table 2.5 Mn/DOT Reference Temperatures Used When Calculating the Cumulative Thawing Index (Mn/DOT, 2004)

Date	Reference Temperature (°F)	Reference Temperature (°C)
January 1 – January 31	32	0
February 1 – February 7	29.3	-1.5
February 8 – February 14	28.4	-2
February 15 – February 21	27.5	-2.5
February 22 – February 28	26.6	-3
March 1 – March 7	25.7	-3.5
March 8 – March 14	24.8	-4
March 15 – March 21	23.9	-4.5
March 22 – March 28	23	-5
March 29 – April 4	22.1	-5.5
April 5 – April 11	21.2	-6
April 12 – April 18	20.3	-6.5
April 19 – April 25	19.4	-7
April 26 – May 2	18.5	-7.5
May 3 – May 9	17.6	-8
May 10 – May 16	16.7	-8.5
May 17 – May 23	15.8	-9
May 24 – May 30	14.9	-9.5
June 1 – December 31	32	0

Table 2.6 SLR Methods for Canada and the Northern United States

SLA Method	Description	Inputs Required	Advantages	Limitations
Mn/DOT Method	- Weekly reference temperatures - Calculation of Freezing Index (FI) and Thawing Index (TI) - Implement SLRs when specified Cumulative Thawing Index (CTI) value reached	- Measured air temperature - 3 day air temperature forecast	Air temperature values are the only input making this method quick and easy to apply	The most empirical of the approaches. Does not account for site specific conditions such as subsurface properties
Waterloo Method	- Monthly reference temperatures - Calculate TI and FI - Develop algorithm coefficients - Calculation of frost and thaw depth based on measured freezing and thawing indices using algorithm	- Measured air temperatures - Pavement surface temperatures - Measured frost depth - Measured thaw depth	Uses database of reference temperatures and algorithm coefficients Frost/thaw depth prediction from air temperatures	Needs a database of reference temperatures and algorithm coefficients based on numerous sites. Does not directly account for site specific conditions such as subsurface properties
Alaska Method	- Historical and thermistor data collected along with weather forecasts and field observations - Regional maintenance engineer decides when to implement amend and remove SLRs	- Air and pavement structure data - Weather forecasts - Field observations	Use of thermistor data allows actual subsurface conditions to be observed	SLR Implementation largely based on pavement response to thawing. Limited predictive ability
British Columbia Method	- Transportation vehicles with reduced tire pressure allowed to haul fully loaded on thaw weakened pavement	- Not applicable	Reduced stress on the pavement structure due to larger tire surface area	Only available for vehicles equipped with appropriate tire deflation mechanisms
New Hampshire Method	- FI and TI values are collected - EICM program used to simulate frost and thaw depths which are used to guide implementation and removal of SLRs	- Numerous weather variables (i.e. temp., wind speed, % sunshine) - Pavement structure	Transferable to any pavement structure under any climactic condition	Numerous model inputs required including upper boundary condition and pavement structure variables
Thermal Numerical Modelling	- Utilizes a finite element approach - Requires input of specific upper and lower thermal boundary conditions, pavement structure and thermal properties of pavement structure materials - Transient analysis simulates freezing and thawing front movement	- Measured air temperatures - 3 day air temperature forecast - Pavement structure - Material thermal properties	Easily transferable to any pavement structure and/or climate conditions for which an analysis can be conducted	Modelling software requires numerous inputs and requires specific pavement structure information and definition of boundary conditions

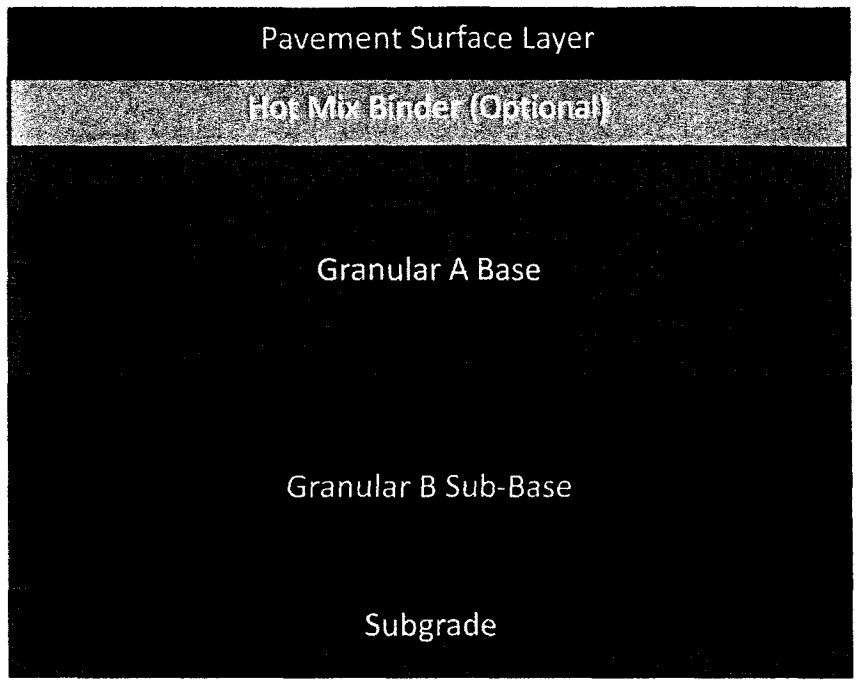

Figure 2.1 Typical Low Volume Road Pavement Structure

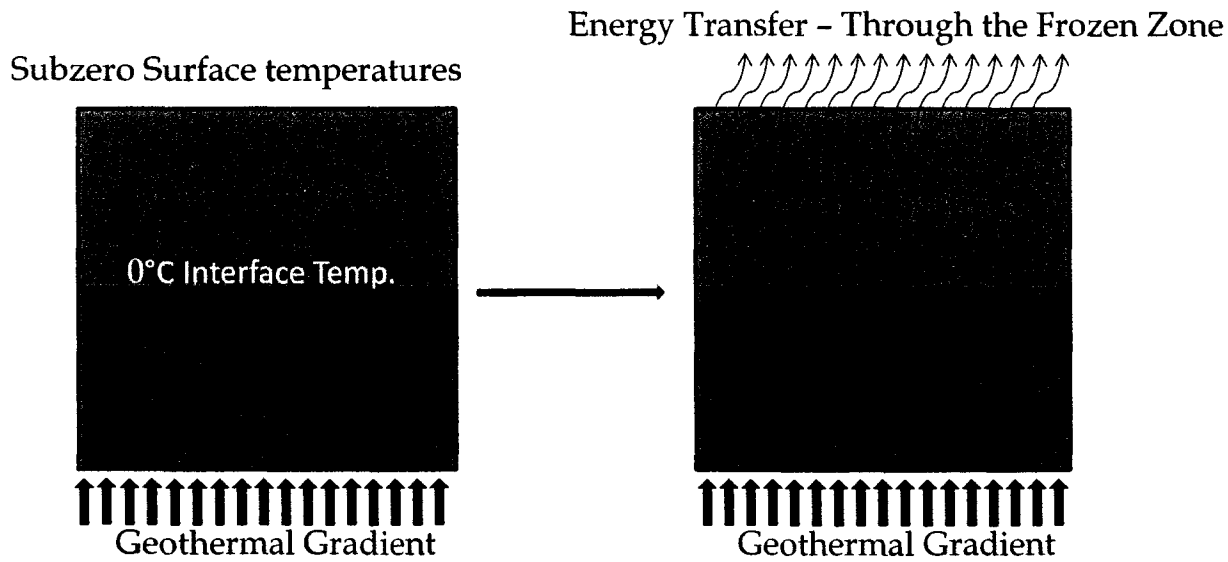

Figure 2.2 Freezing Season Energy Transfer

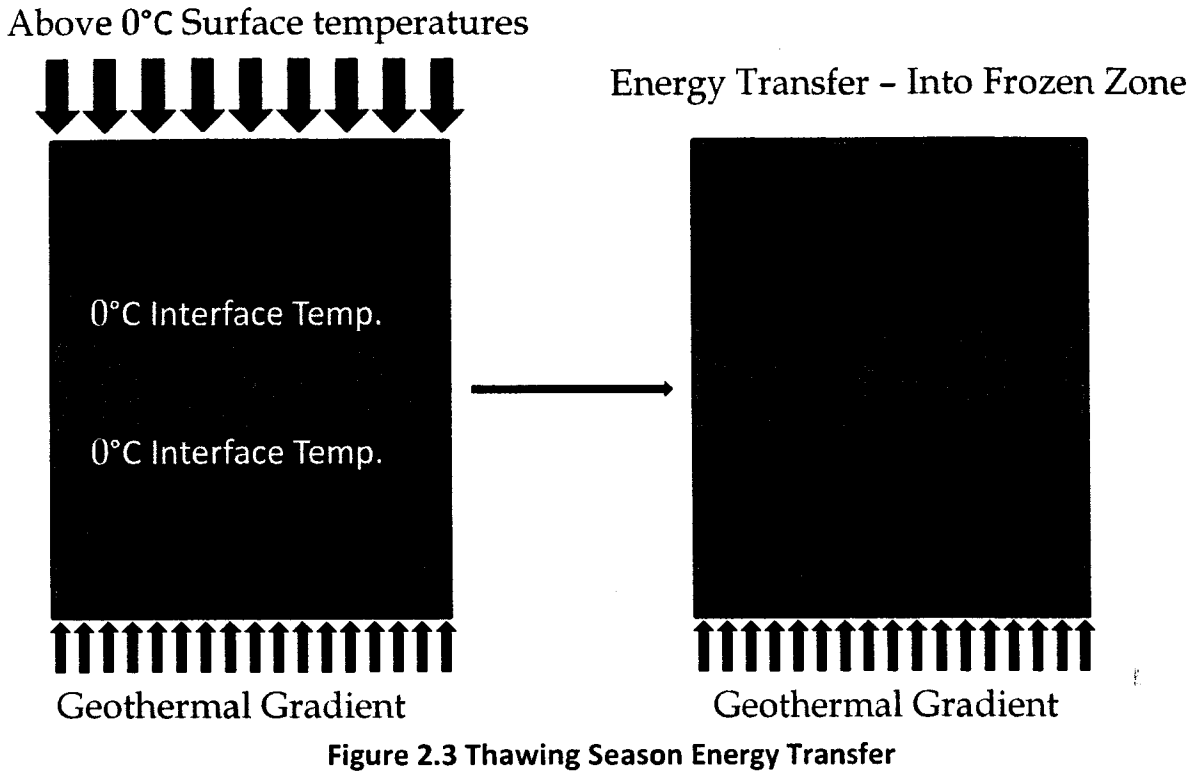

Figure 2.3 Thawing Season Energy Transfer

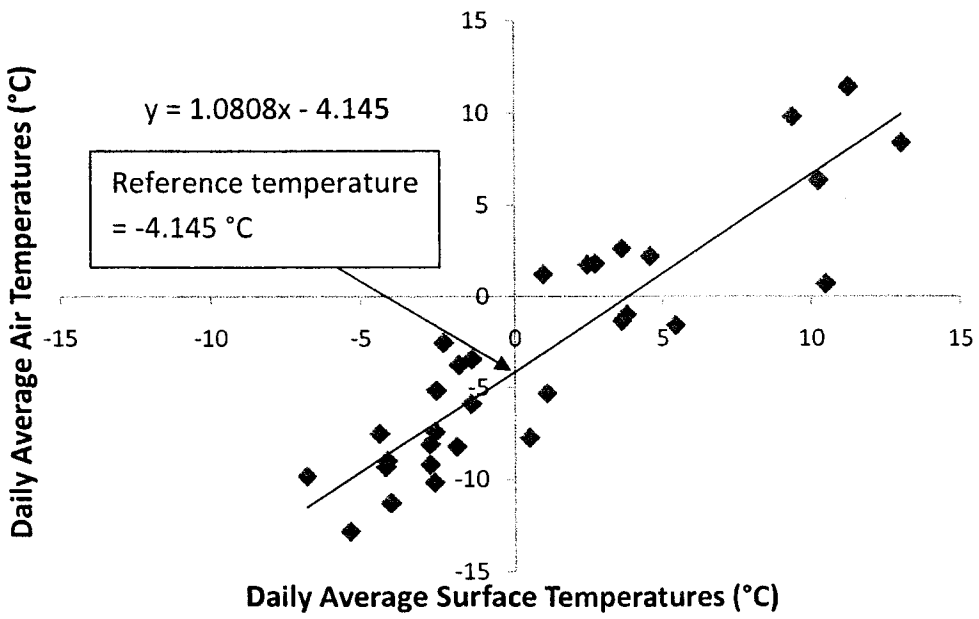

Figure 2.4 Waterloo Method Reference Temperature Determination for the Highway 569 Site (November 10, 2005 – December 10, 2005)

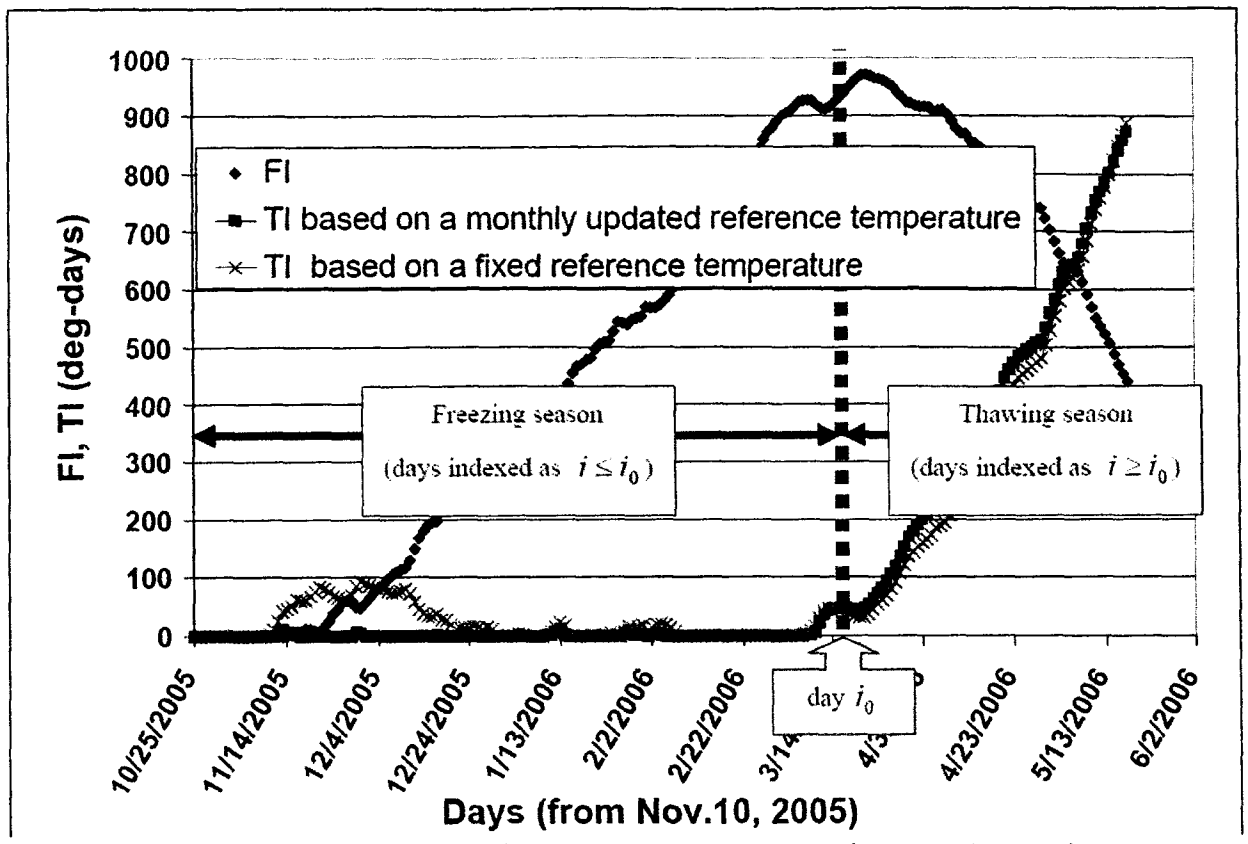

Figure 2.5 Waterloo Method Day i_0 Determination (Baiz et al., 2007)

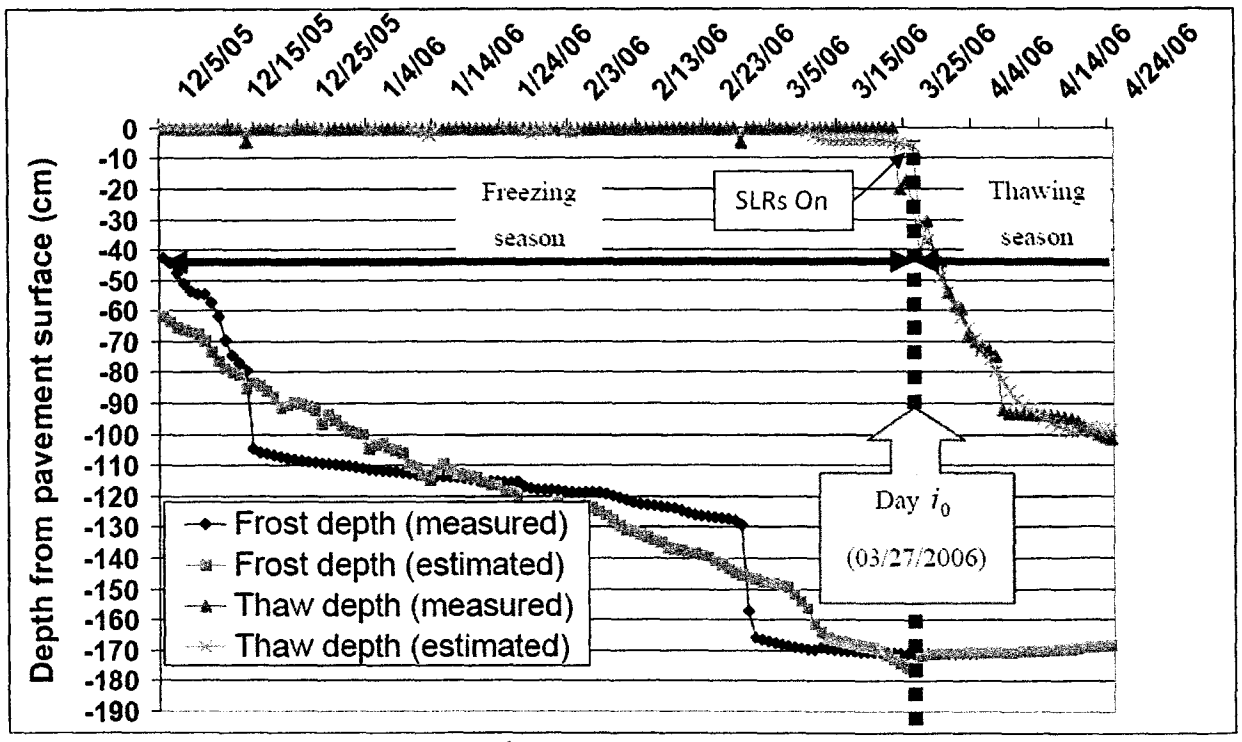

Figure 2.6 Waterloo Method Simulation Using Developed Algorithm (Baiz et al., 2007)

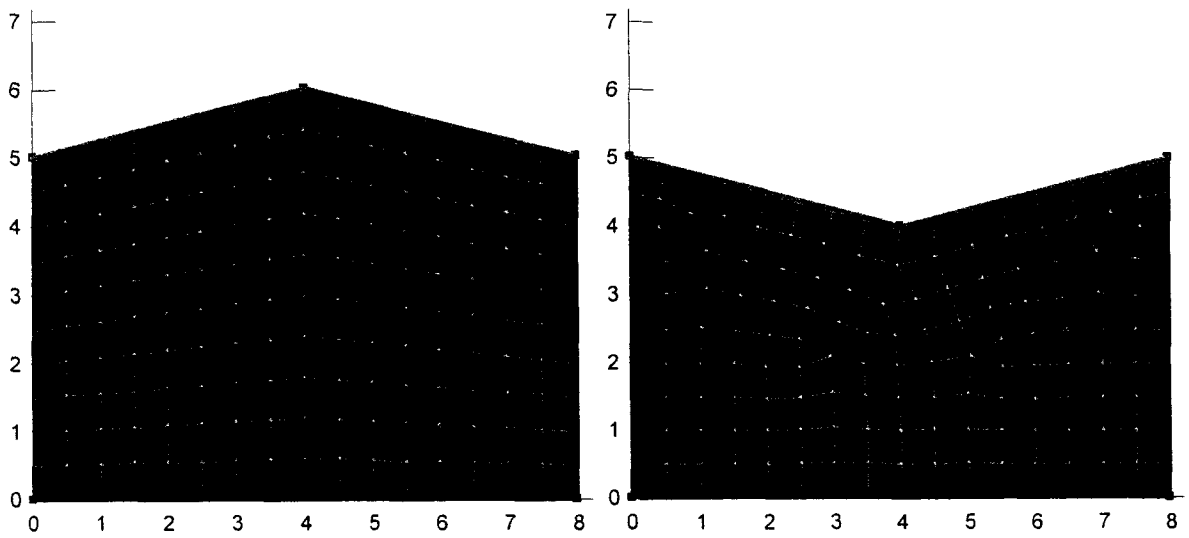

Figure 2.7 Mesh Changes Based on Region Shape

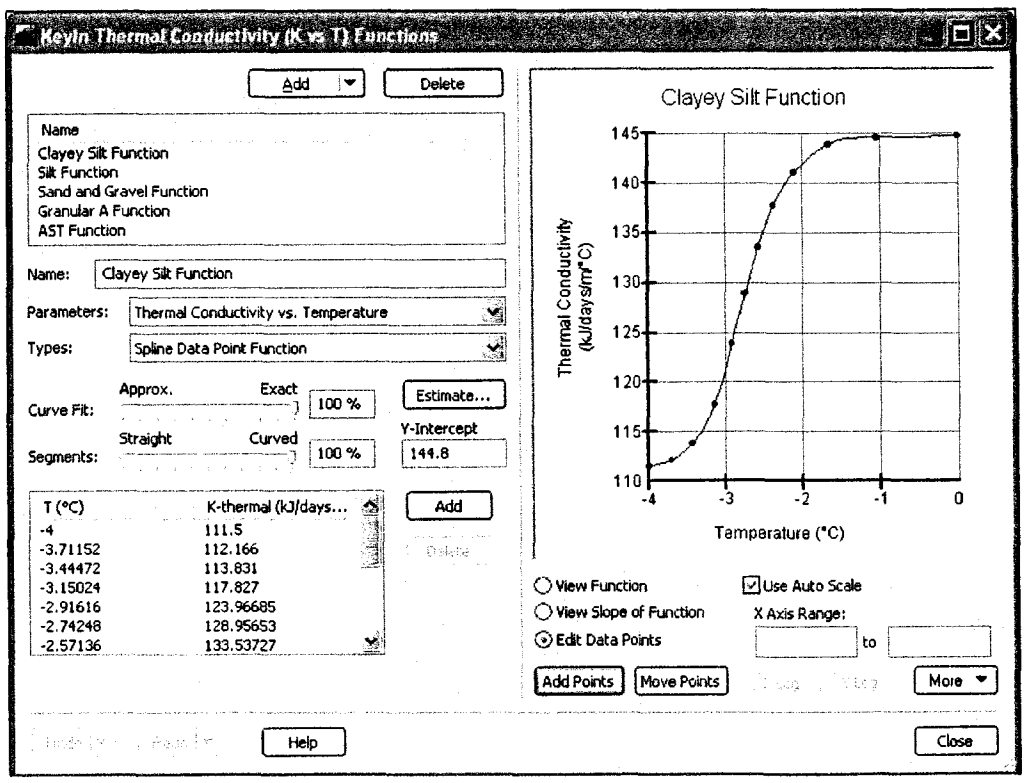

Figure 2.8 Thermal Conductivity Function Used in TEMP/W Model

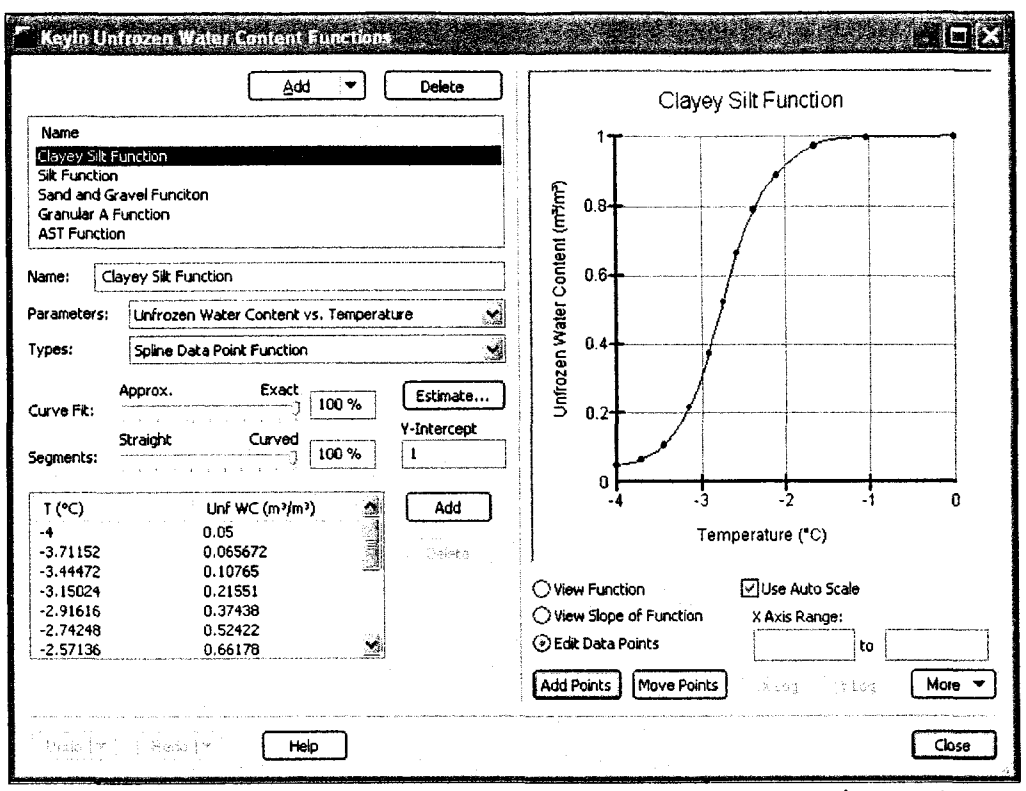

Figure 2.9 Unfrozen Water Content Function Used in TEMP/W Model

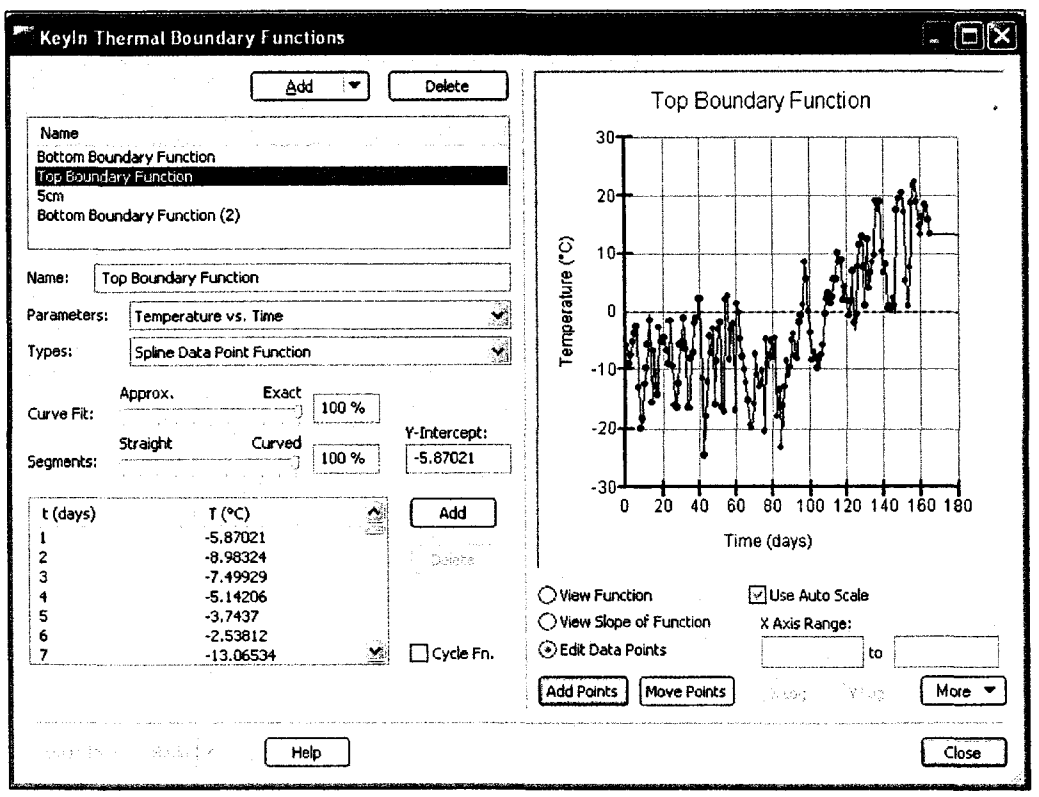

Figure 2.10 Thermal Function Used in TEMP/W Modelling

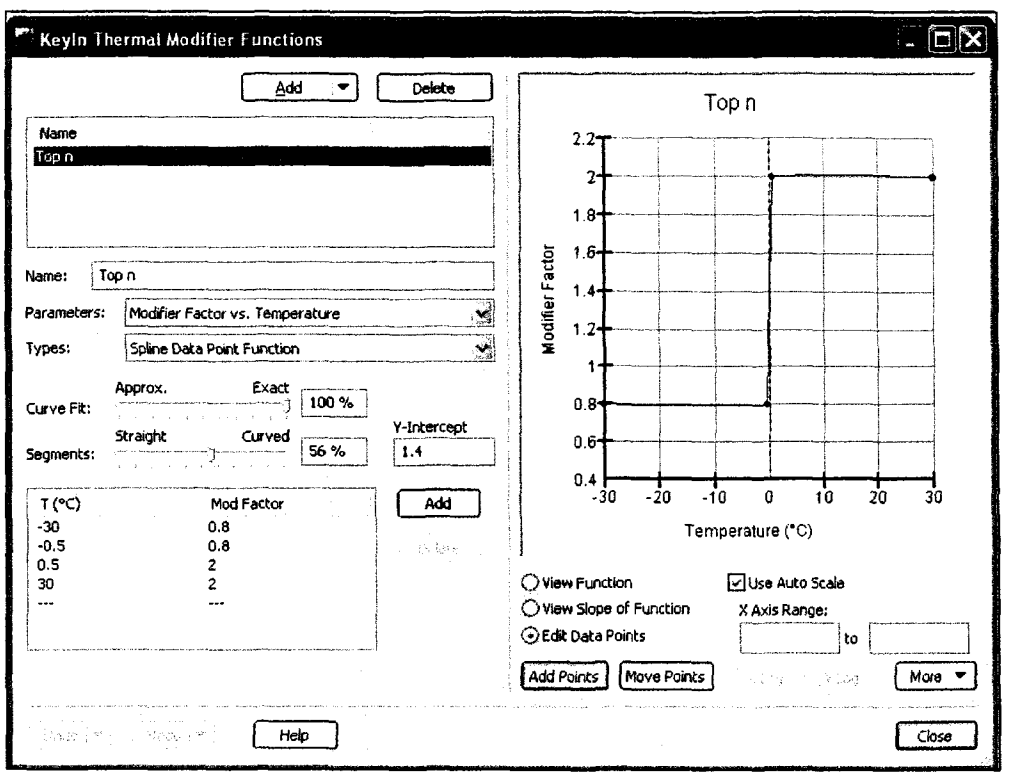

Figure 2.11 Temperature Modification Function Used in TEMP/W Modelling

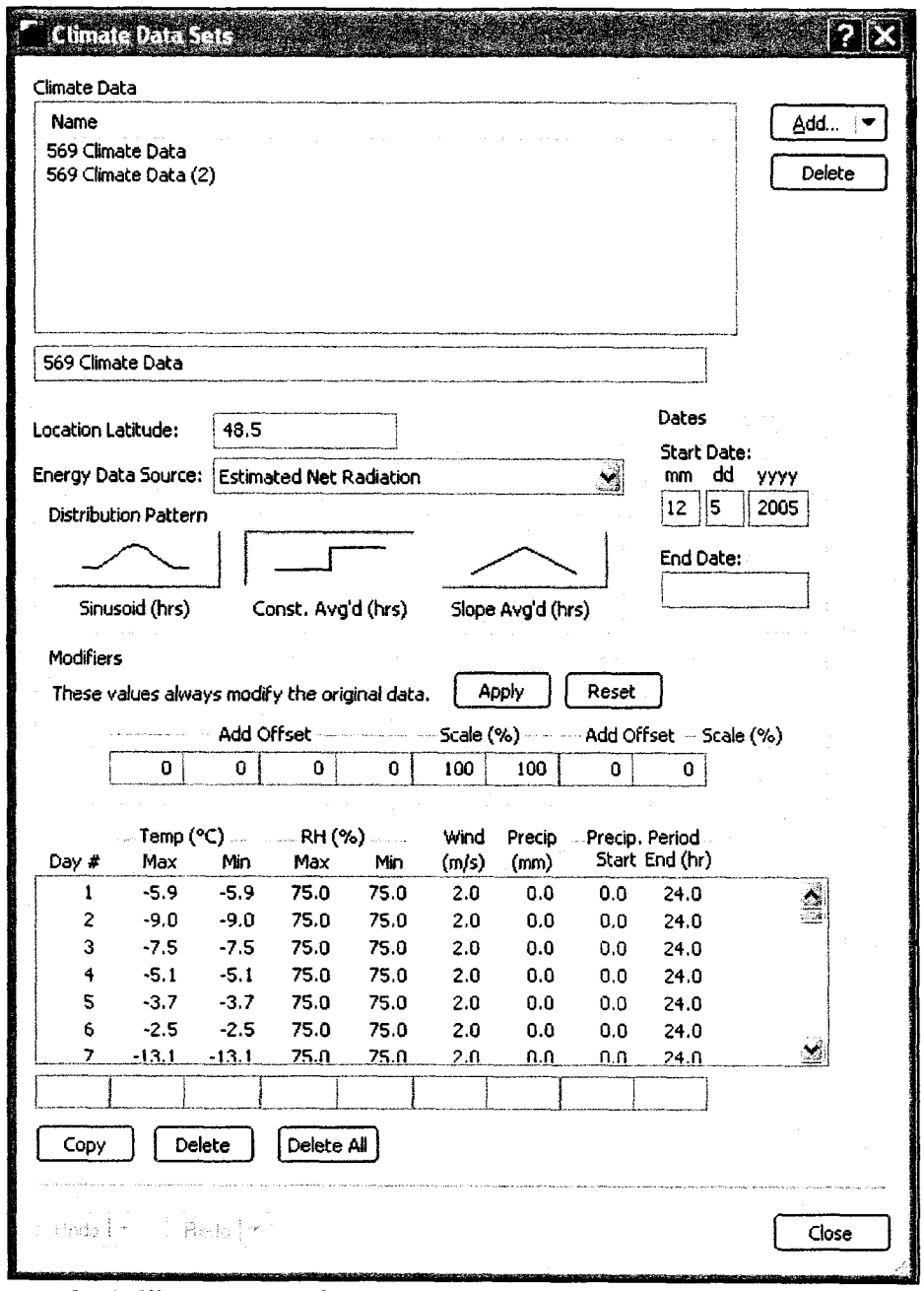

Figure 2.12 Climate Boundary Condition Function Used in TEMP/W Model

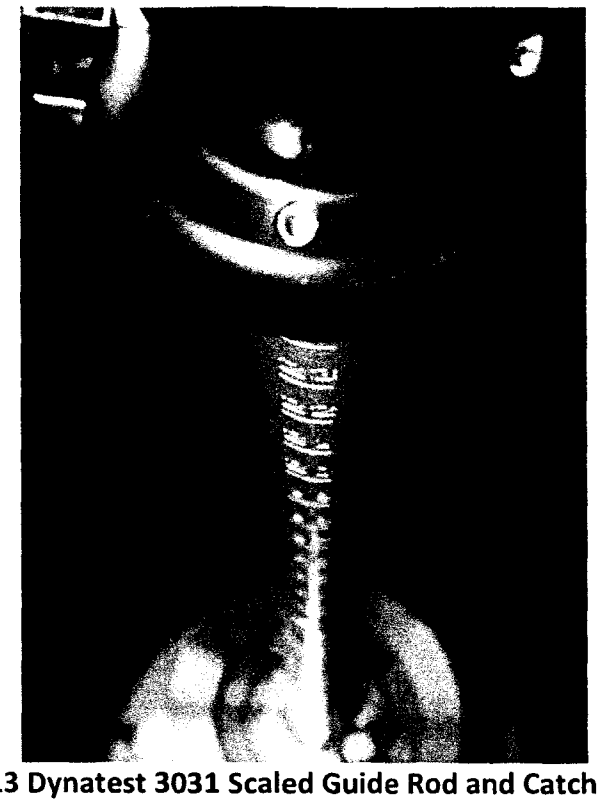

Figure 2.13 Dynatest 3031 Scaled Guide Rod and Catch Assembly

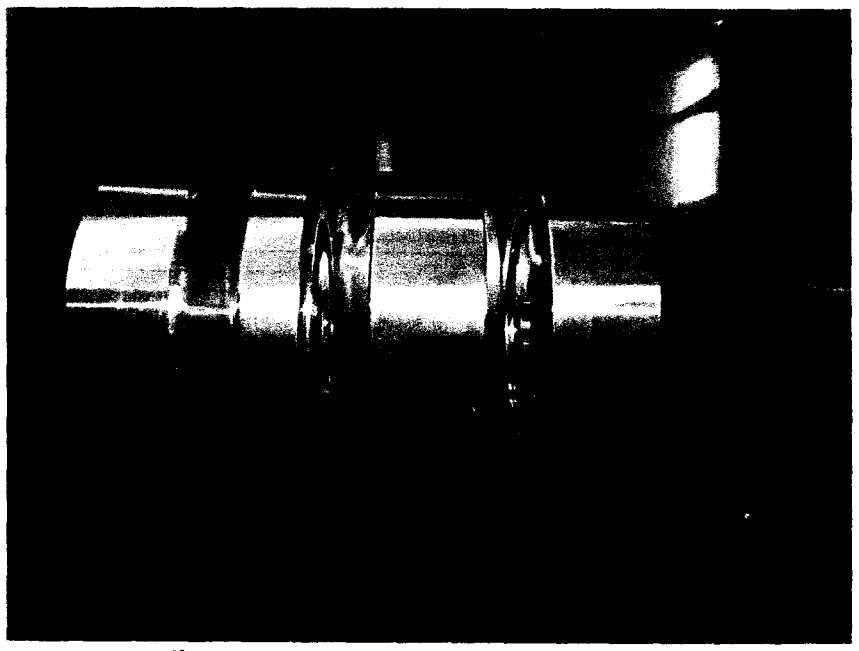

Figure 2.14 Drop Weight Configurations

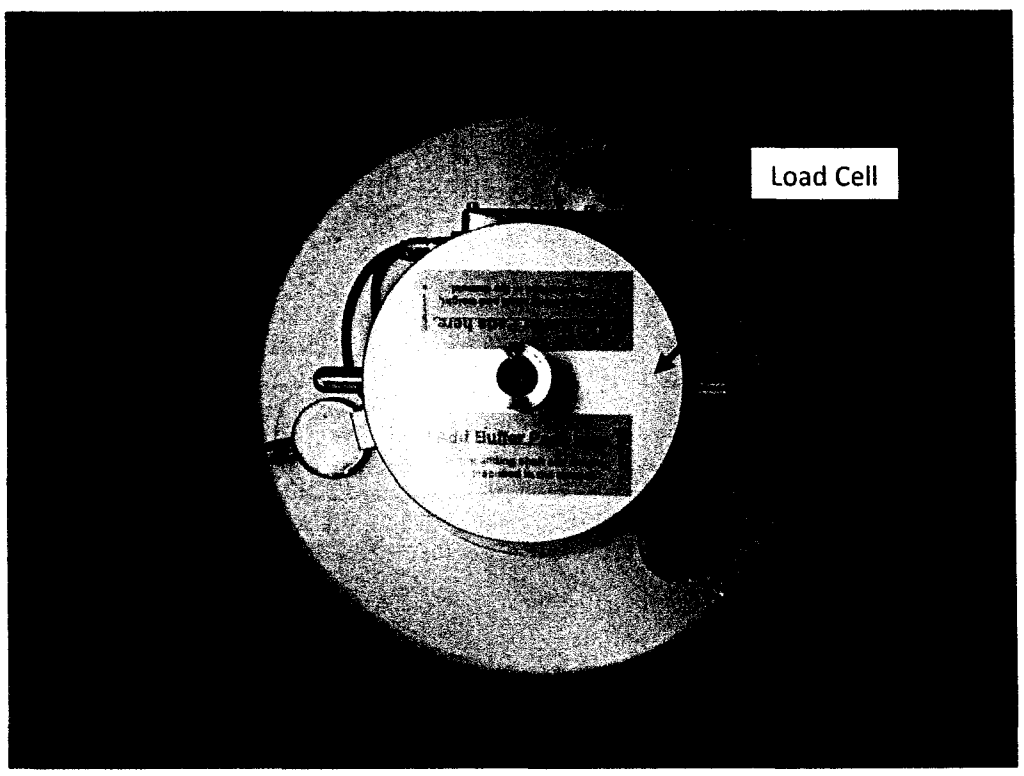

Figure 2.15 Dynatest 3031 LWD Load Cell

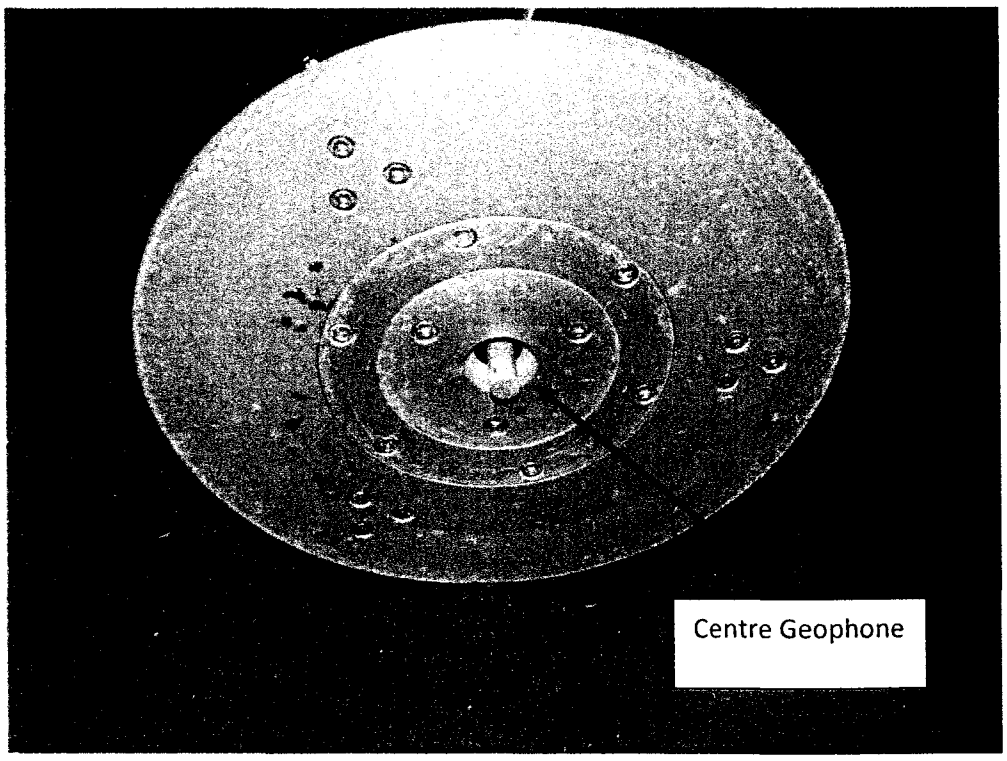

Figure 2.16 Dynatest 3031 LWD Centre Geophone and 300 mm Loading Plate

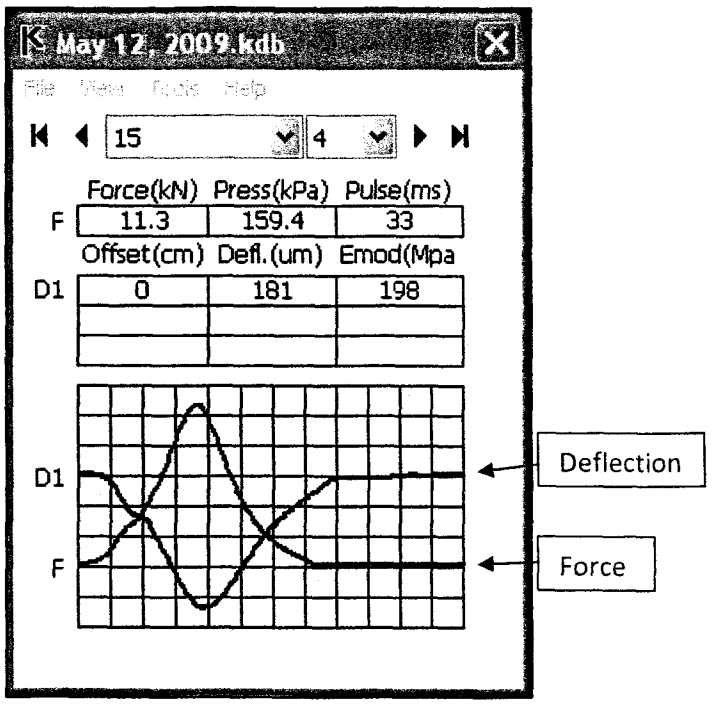

Figure 2.17 PDA Display for Dynatest 3031 LWD

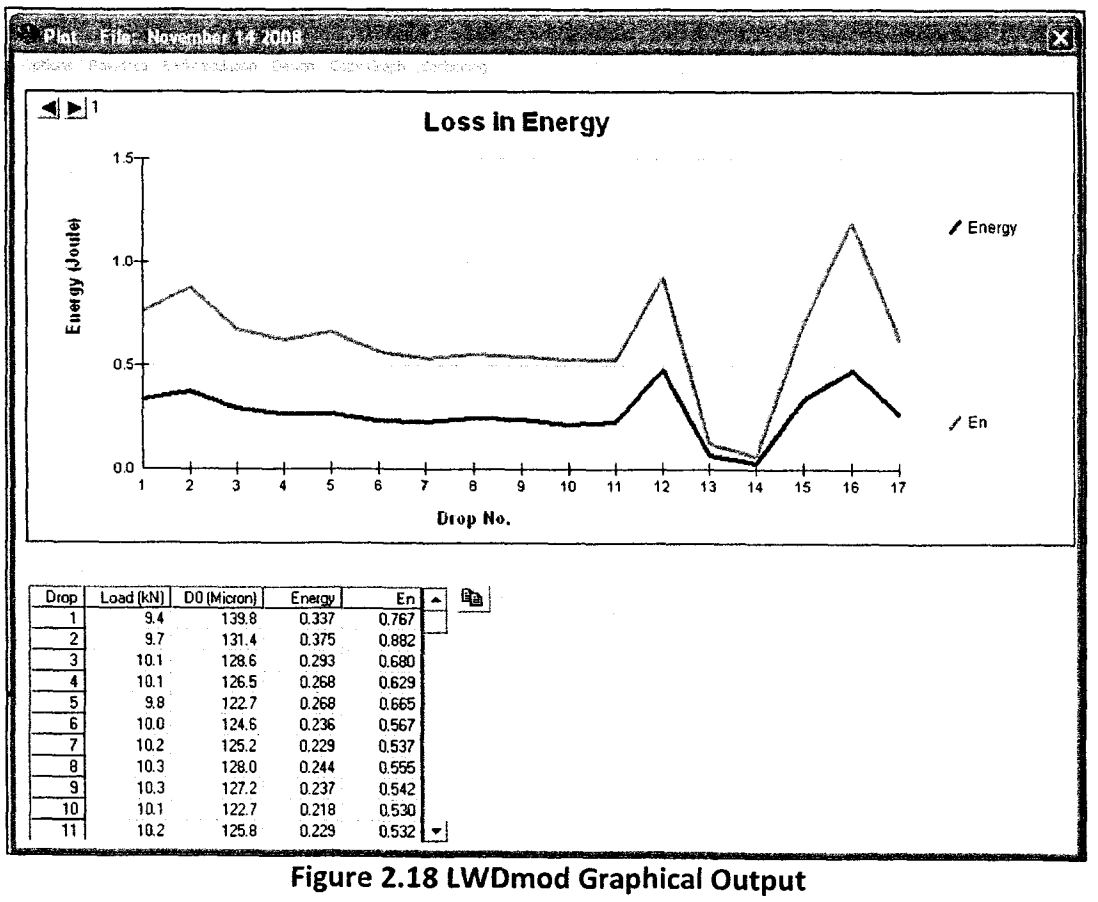

Drop	Load (kN)	D0 (Micron)	Energy	En
1	9.4	139.8	0.337	0.767
2	9.7	131.4	0.375	0.882
3	10.1	128.6	0.293	0.680
4	10.1	126.5	0.268	0.629
5	9.8	122.7	0.268	0.665
6	10.0	124.6	0.236	0.567
7	10.2	125.2	0.229	0.537
8	10.3	128.0	0.244	0.555
9	10.3	127.2	0.237	0.542
10	10.1	122.7	0.218	0.530
11	10.2	125.8	0.229	0.532

Figure 2.18 LWDmod Graphical Output

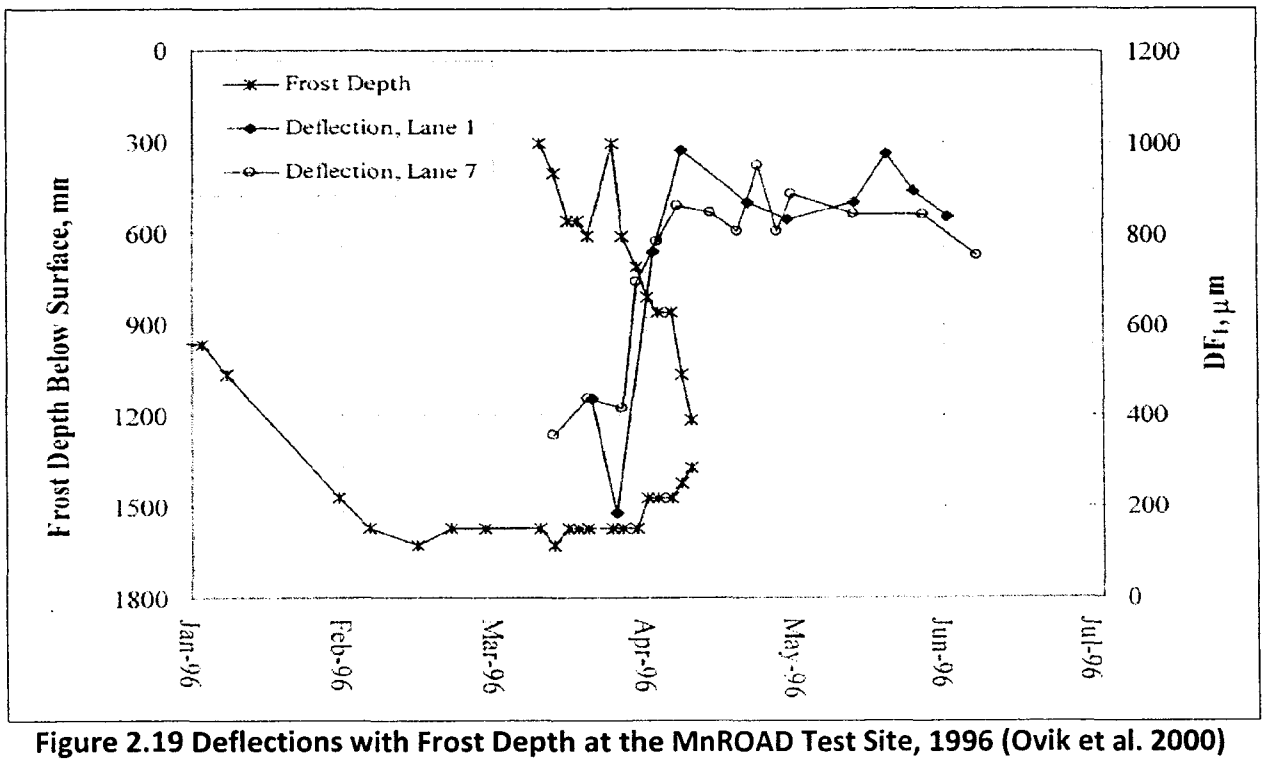

Figure 2.19 Deflections with Frost Depth at the MnROAD Test Site, 1996 (Ovik et al. 2000)

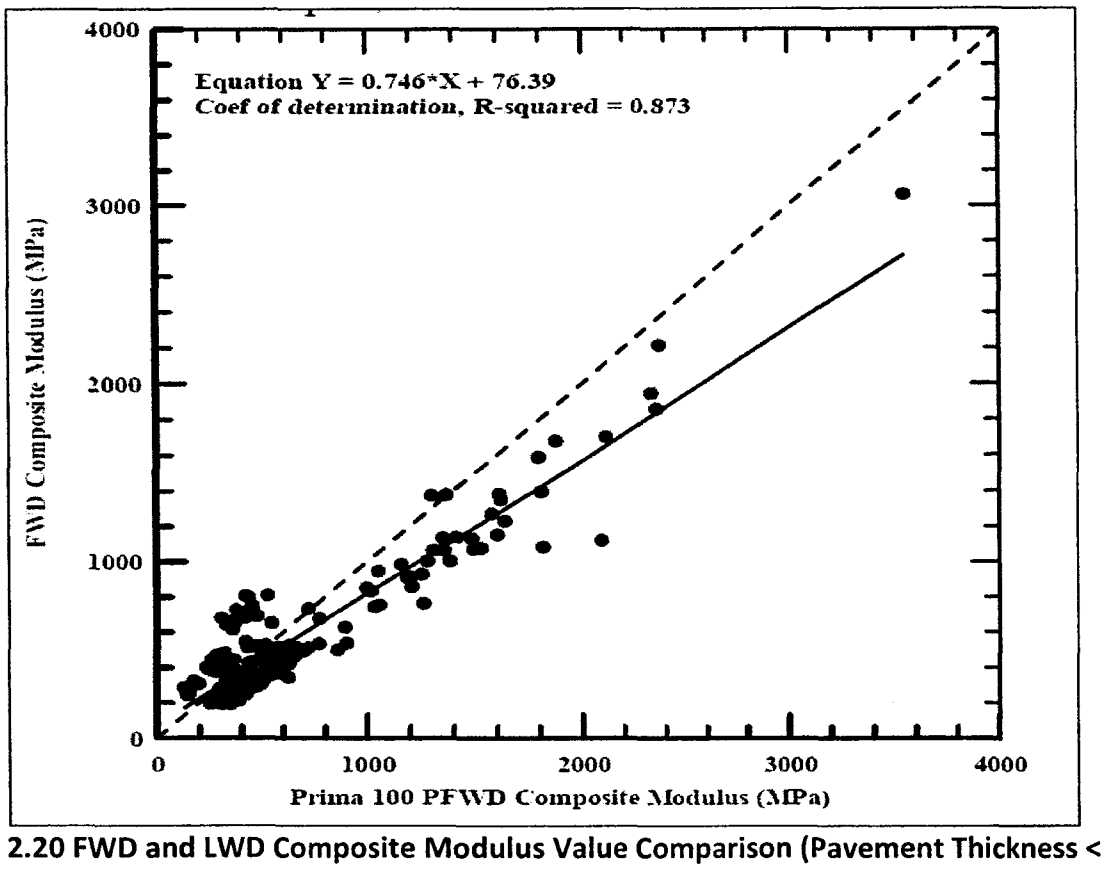

Figure 2.20 FWD and LWD Composite Modulus Value Comparison (Pavement Thickness < 127 mm) (Steinert et al., 2005)

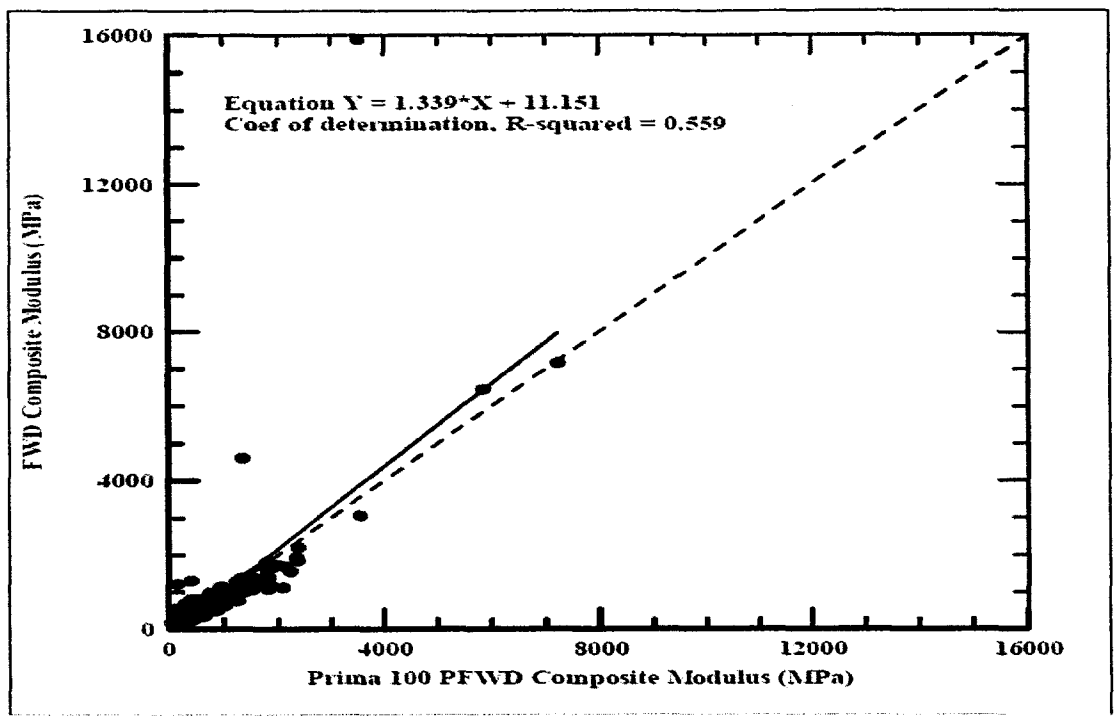

Figure 2.21 FWD and LWD Composite Modulus Value Comparison (Pavement Thickness = 152 mm) (Steinert et al., 2005)

Site Status
NR-10 Nagagami River (600010)
MTO NorthEast

Current Time: 8/18/2009 14:19 EDT

Data Time: 8/18/2009 14:12 EDT

Air Data						Wind Data			
Temp	RH	Dew	WtBlb	Min	Max	SpdAvg	SpdGst	DirAvg	DirGst
18C	61%	11C	14C	15C	25C	20 kph	32 kph	W	W

Precipitation			Last Precipitation Period		Accumulation					
Type	Intensity	Rate	Start Time	End Time	10 min.	1 hr.	3 hr.	6 hr.	12 hr.	24 hr.
None	None	0.0 cph	-	-	-	0.00 cm	0.00 cm	0.00 cm	0.22 cm	0.22 cm

Surface Data

Sensor	Status	Sfc	Sub	Frz	CF	Chem	Dpth	Ice	Cond	Salin	
Hwy 11 E/B (0)	Trace Moisture	34.0C	24C	0C	-	-	0 mm	-	0 mhos	0	History
Hwy 11 W/B (1)	Dry	35.1C	24C	0C	-	-	0 mm	-	0 mhos	0	History
Hwy 11 E/B - Bridge (2)	No Report	-	-	-	-	-	-	-	-	-	History

Subsurface Data

Sensor	Temp	
Hwy 11 E/B (40cm, Puck 1) (0)	24C	History
Hwy 11 E/B (150cm, Puck 1) (1)	22C	History

Figure 2.22 Road Weather Information Systems (RWIS) Data Display

3.0 SLR Northern Ontario Study Sites

3.1 Ontario Conditions

The province of Ontario covers 1,068,580km^2 of land and has a north/south span of 1730km (educationcanada.com). Due to the large size of the province conditions can vary significantly from locations in the southern parts of the province to locations in more northern sections. An examination of average annual daily air temperatures (climate.weatheroffice.ec.gc.ca) for two locations in Ontario, Toronto (more southern) and Thunder Bay (more central), for 2008 indicated large differences in temperature. The average annual air temperature for Toronto was 9.2°C, while the average annual air temperature for Thunder Bay was 2.5°C. This corresponds to a temperature difference of close to 7°C on an annual basis between the southern and the central regions of the province. This poses an issue with respect to development of a unique SLR method that would cover the entire province. For the purposes of this research two study sites are used to examine the difference between the conditions in the Northeastern (Highway 569) (Figure 3.1) and Northwestern (Highway 527) (Figure 3.2) sections of the province. The Highway 569 study site is located approximately 3 km east of Highway 11, while the Highway 527 study site is located approximately 8 km north of Highway 811 (see insets on Figures 3.1 and 3.2).

3.2 Thermistor Installations

At each of the study sites, a thermistor string was installed in a borehole drilled at the centre of the roadway (Figure 3.3) to monitor temperatures and allow interpretation of freezing and thawing front depths. The thermistor string was assembled with thermistors placed vertically at depths of 5 cm, 15 cm , 30 cm, 45 cm, 60 cm, 75 cm, 90 cm, 105 cm, 135 cm, 165 cm, 195 cm, 225 cm and 255 cm, from the top of the pavement surface (Figure 3.4). Thermistors are

sintered semiconductor sensors that measure resistance, and these resistance measurements are converted into corresponding temperatures (www.omega.ca). The signals from the thermistors are transferred through buried cables (Figure 3.5) to a datalogger which is housed at the side of the roadway. Data stored in this datalogger (Figure 3.6) can then be obtained through direct downloading of the information to a computer (Highway 527) or sent via telephone cable to a data collection location (Highway 569). Air temperatures are also measured at these sites.

Technical issues were encountered with respect to data collection from the thermistors. It was observed that many of the thermistors were either not recording data or that the data that were being recorded were incorrect. For this purpose, a criterion was developed (Appendix A) to ensure that erroneous thermistor readings were removed and that only reliable thermistor readings were used for analysis.

3.4 Frost and Thaw Depth Determination from Subsurface Thermistor Measurements

Frost and thaw depths were determined at each study site through the winter/spring seasons using an analysis of the thermistor measurements. Two Excel macros (Appendix B) (Baiz et al., 2007) were used to determine the depth of the freezing and thawing fronts respectively. These macros were used to interpolate the depths of the 0°C isotherm between two successive thermistors, one having a measured temperature above 0°C and the next having a measured temperature below 0°C. This interpolation was conducted on a daily basis from the freezing season through the thawing season to establish measured frost and thaw depth at each study site for each study period.

3.5 Highway 569 Study Site

The Highway 569 study site (Figure 3.7) was selected to observe the pavement surface and subsurface conditions during seasonal freeze/thaw cycles for a low volume road under environmental conditions present in northeastern Ontario. This Highway is a provincial secondary highway that is classified as a low volume road and subsequently subjected to SLRs.

This roadway is 28 km in length and forms a loop off of Highway 11, having both its northern and southern extents connecting with Highway 11. Sections 3.5.1 and 3.5.2 outline the Highway 569 study site pavement structure and the RWIS and thermistor data available, respectively.

3.5.1 Highway 569 Pavement Structure

The pavement structure cross section for the Highway 569 study site was determined through an examination of data obtained from two probe holes (PH#5 and PH#6) drilled at the site. The material type observations recorded during the drilling of these probe holes (Table 3.1 and 3.2) provide guidance with respect to layer thicknesses and layer compositions. PH#5 was drilled in the eastbound lane approximately 5 m east of the thermistor installation, while PH#6 was drilled in the westbound lane approximately 18 m west of the thermistor string. Both probe holes were drilled in the outer wheel path of the roadway. The logs of these probe holes indicate a clayey silt layer beginning at a depth of between 1.23 m and 1.32 m. This layer persists to the bottom of the probe holes, depths of between 1.69 m and 1.85 m. As no other information is provided from the probe holes, it is assumed that this layer continues to a depth of 2.55 m at the thermistor string location; this is the depth of the lowest thermistor on the thermistor string. The logs of these probe holes did not indicate a water table depth at these locations.

The Highway 569 test site pavement structure (Figure 3.8) consists of an asphalt concrete surface layer, followed by a Granular A (specifications in Appendix C) sub-base layer, a second asphalt concrete layer, a silty fine sand layer, sand and gravel, silt and finally a clayey silt layer. The thicknesses of each of these layers are indicated in Table 3.3.

3.5.2 Highway 569 RWIS and Thermistor Data

The Highway 569 Road Weather Information System (RWIS) stations did not record air or pavement surface temperature values from 2005 to 2006. For this reason thermal model calibrations conducted during this time frame required these values to be obtained through triangulation of the three closest working RWIS stations (Baiz et al., 2007). The proximity of

each station to the Highway 569 site was used to weight the temperature values provided. That is, the closer the RWIS station, the greater the emphasis that was placed on the temperature values provided. Thus, a weighted average of the three stations was used to estimate the air and pavements surface temperatures at the study site location.

As a result of thermistor error at the Highway 569 study site, the 2006/2007 season was not used for calibration. Thermistor repairs were conducted and during this repair time, air temperature recording equipment was installed on site. This made it possible to conduct thermal model calibrations using RWIS data gathered directly at the site, which was done from 2007 to the present. Figures 3.9 to 3.11 indicate the average daily air temperatures and measured frost and thaw depths for the Highway 569 study site for the 2005/2006, 2007/2008 and 2008/2009 periods, respectively. It must be noted that the thermistor installation at the Highway 569 study site occurred after pavement structure freezing had begun in 2005. It was for this reason that no frost and thaw data are available at the beginning of the freezing season indicated in Figure 3.9.

Thermistor readings from three depths were removed using the thermistor removal criteria outlined in Appendix A. The thermistor values at the 105 cm, 135 cm, and 165 cm depths showed inconsistent temperature readings that fluctuated unrealistically between positive and negative temperatures during the 2005/2006 study period. Figure 3.12 indicates the difference between measured frost and thaw depths with and without the removal of the erroneous thermistors. During the 2006/2007 period all of the thermistor readings at all of the depths indicated error and could not be used in analysis. At this point repairs were conducted on the thermistor string.

The repairs to the thermistor string enabled readings to be taken during the 2007/2008 winter/spring season; however these readings were not without error. During the 2007/2008 period the 30 cm and 135 cm depth thermistor readings were shown to be erroneous and subsequently removed using the established thermistor removal criteria. Furthermore, the thermistor readings between February 12, 2008 and March 15, 2008 at all depths indicated erratic readings which were excluded from further analysis. As a result of the erratic readings, thermistor data between these dates were determined through linear interpolation.

The thermistor problems persisted into the 2008/2009 period where again using the established criteria the 30 cm, 135 cm and 165 cm depth thermistor reading were removed from analysis.

Table 3.4 outlines the data available for analysis for each study period at the Highway 569 study site.

3.6 Highway 527 Study Site

Highway 527 (Figure 3.13) is a secondary highway, 242 km in length, stretching from just north of Thunder Bay, Ontario to the town of Armstrong, Ontario. Sections of this highway receive different levels of maintenance service depending on their locations, with service levels increased on the section of the highway south of Highway 811 and decreased on the section north of Highway 811 (Petryna, 2010). Sections 3.6.1 and 3.6.2 outline the Highway 527 pavement structure, RWIS data and thermistor readings available, respectively.

3.6.1 Highway 527 Pavement Structure

The pavement structure of low volume roads in Ontario not only changes from highway to highway but also alters along the length of the highway based on numerous factors including underlying subgrade and availability of construction materials. For these reasons low volume roads in northern Ontario often do not follow the typical design structure outlined in Section 2.1 (Figure 2.1). As with Highway 569, this non-typical pavement structure was observed at the Highway 527 study site (Figure 3.14).

The Highway 527 study site is not constructed to the typical low volume road structure. The pavement structure consists of far fewer layers than that of the Highway 569 study site. Due to the inability to drill a full depth borehole and install the thermistor string in a pavement structure that contains a large amount of boulders, the Highway 527 study site was located within a section of sand and gravel fill where a borehole could more easily be advanced. For this reason the pavement structure profile consists of only a thin pavement surface layer (50mm) overlying a thick layer of sand and gravel fill (Figure 3.14). This pavement structure was

defined by observations made during the drilling of the borehole for the thermistor installations.

3.6.2 Highway 527 RWIS and Thermistor Data

The Highway 527 study site instrumentation was not operational until the fall of 2007. Air temperature recording equipment was installed in the fall of 2007, therefore all on site air temperature data were available for any calibration conducted after the fall of 2007. Thermistor data at the site however, were not available until January 10, 2008. For this reason only the thaw season of 2008 and the 2008/2009 full season were available for analysis.

An examination of the thermistor readings during the 2008/2009 study period at the Highway 527 site indicates that all of the thermistors appeared to be working properly. However, for unknown reasons the datalogger did not record the thermistor readings between February 10, 2009 and March 30, 2009. After this problem was detected the datalogger was reset and all of the thermistor readings were again recorded properly. Furthermore, after March 30, 2009 the thermistor data indicates that the frost depth exceeded the depth of the lowest thermistor (2.55 m). For this reason no observed frost depth in known between March 30, 2009 and the date of complete subsurface thaw (May 24, 2009). Figure 3.15 indicates the air temperatures recorded and the interpolated frost and thaw depths at the Highway 527 study site during the 2008/2009 period, while Table 3.5 indicates the available data for this site.

Table 3.1 Highway 569 Probe Hole (PH#5) Information

PH#5	
0 - 25 mm	Asphalt Surface Treatment (AST)
25 - 210 mm	Granular A, Brown, Moist
210 - 250 mm	AST or Asphalt Concrete (AC)
250 - 490 mm	Silty fine sand, Brown, Moist
490 - 1030 mm	Sand and gravel, Grey turning brown, Very moist to wet
1030 - 1230 mm	Silt, Grey, Moist
1230 - 1690 mm	Clayey silt, Brown, Very moist and partially frozen

Table 3.2 Highway 569 Probe Hole (PH#6) Information

PH#6	
0 - 35 mm	Asphalt Surface Treatment (AST)
35 - 110 mm	Granular A, Brown, Very moist
110 - 175 mm	AST or Asphalt Concrete (AC)
175 - 300 mm	Sand and gravel, brown, Very moist
300 - 710 mm	Silty fine sand, Occasional gravel, Brown, Very moist
710 - 1320 mm	Silt, Grey, Moist
1320 - 1850 mm	Clayey silt, Brown, Very moist and partially frozen

Table 3.3 Material Layer Thicknesses for the Highway 569 Study Site

Material	Depth (m)
Asphalt Concrete	0 – 0.025
Granular A Sub-base	0.025 – 0.21
Asphalt Concrete	0.21 – 0.25
Silty Fine Sand	0.25 – 0.49
Sand and Gravel	0.49 – 1.03
Silt	1.03 – 1.23
Clayey Silt	1.23 – 2.55

Table 3.4 Highway 569 Data Available for Analysis

Highway 569 Available Data	
Air Temperatures	Thermistor Readings
October 15, 2005 - May 18, 2006	December 5, 2005 - May 29, 2006
October 31, 2007 – December 31, 2008	October 31, 2007 - July 2, 2008
January 1, 2009 – December 31, 2009	November 14, 2008 - July 2, 2009
January 1, 2010 - April 22, 2010	December 8, 2009 – April 22, 2010

-Note that lightweight deflectometer data availability will be presented in Chapter 5

Table 3.5 Highway 527 Data Available for Analysis

Highway 527 Available Data	
Air Temperatures	Thermistor Readings
January 10, 2008 – February 10, 2009	January 10, 2008 - February 10, 2009
March 30, 2009 – April 22, 2010	March 30, 2009 – April 22, 2010

-Note that lightweight deflectometer data availability will be presented in Chapter 5

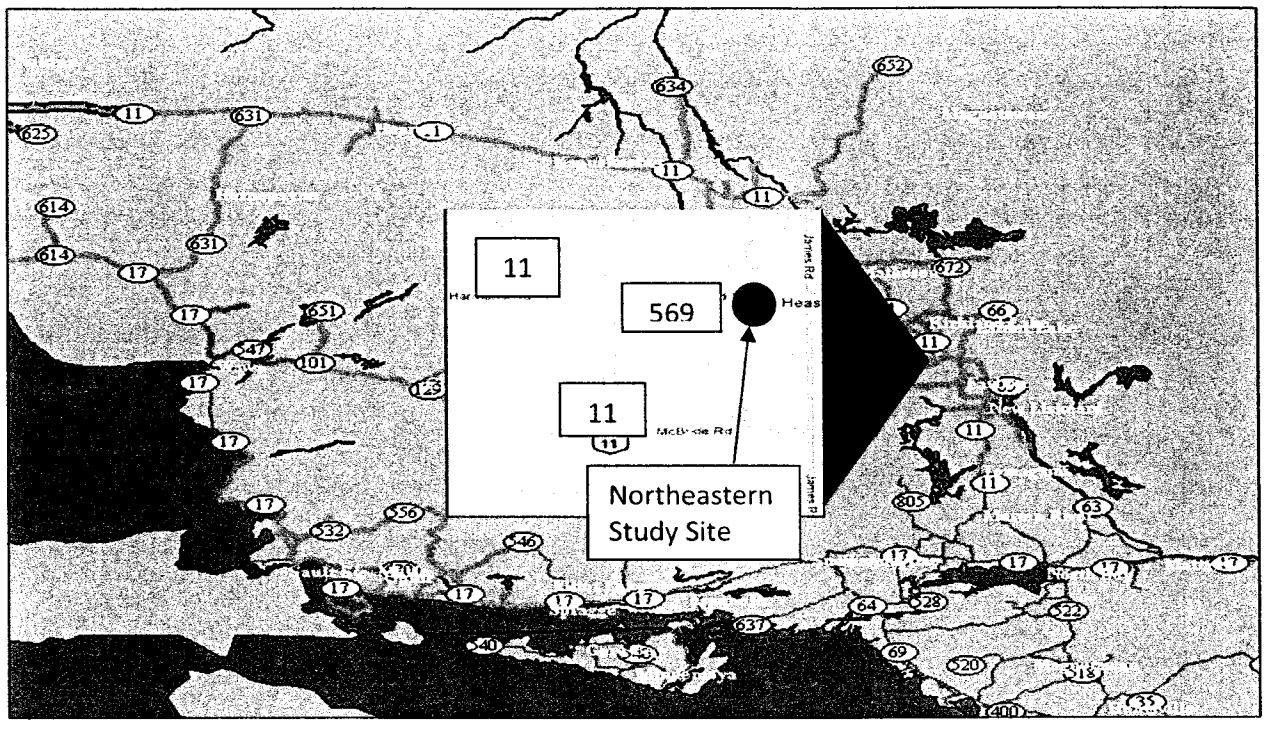

Figure 3.1 Highway 569 Study Site Location, Northeastern Ontario (https://customers.twncs.com/Roads/common)

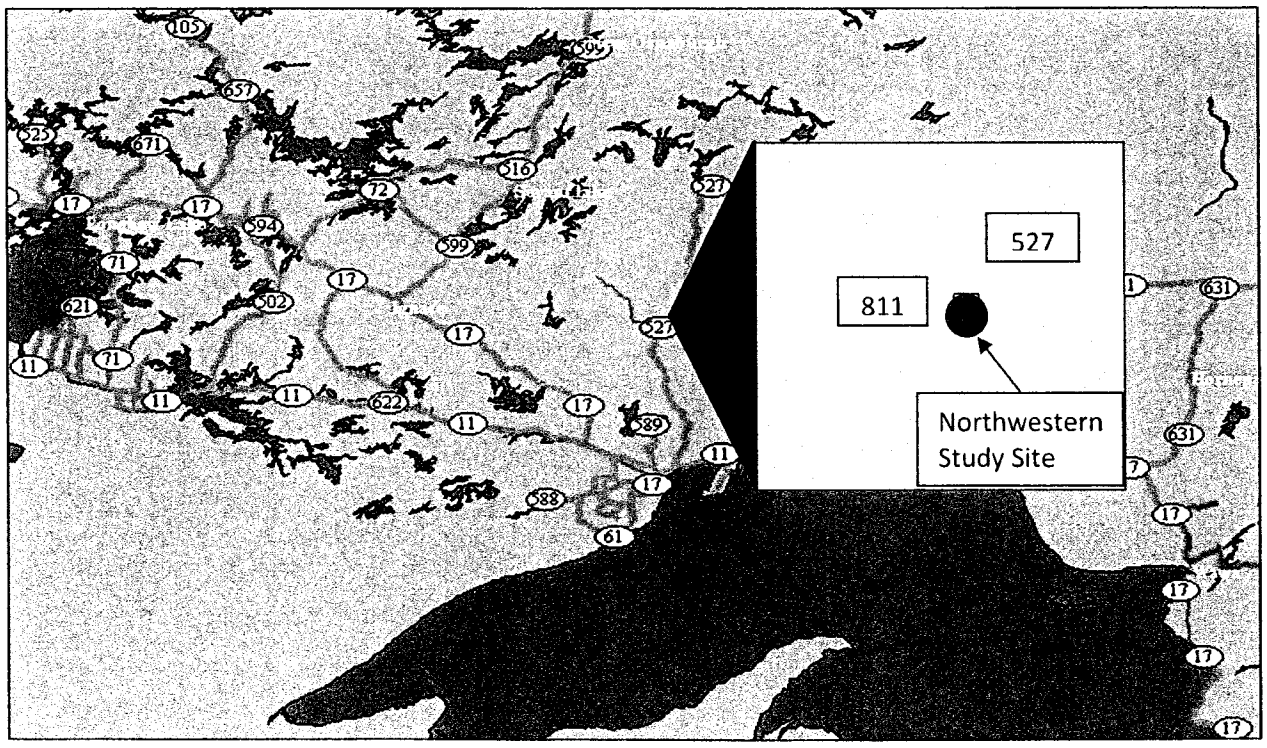

Figure 3.2 Highway 527 Study Site Location, Northwestern Ontario (https://customers.twncs.com/Roads/common)

Figure 3.3 Thermistor Installation at Northeastern Study Site

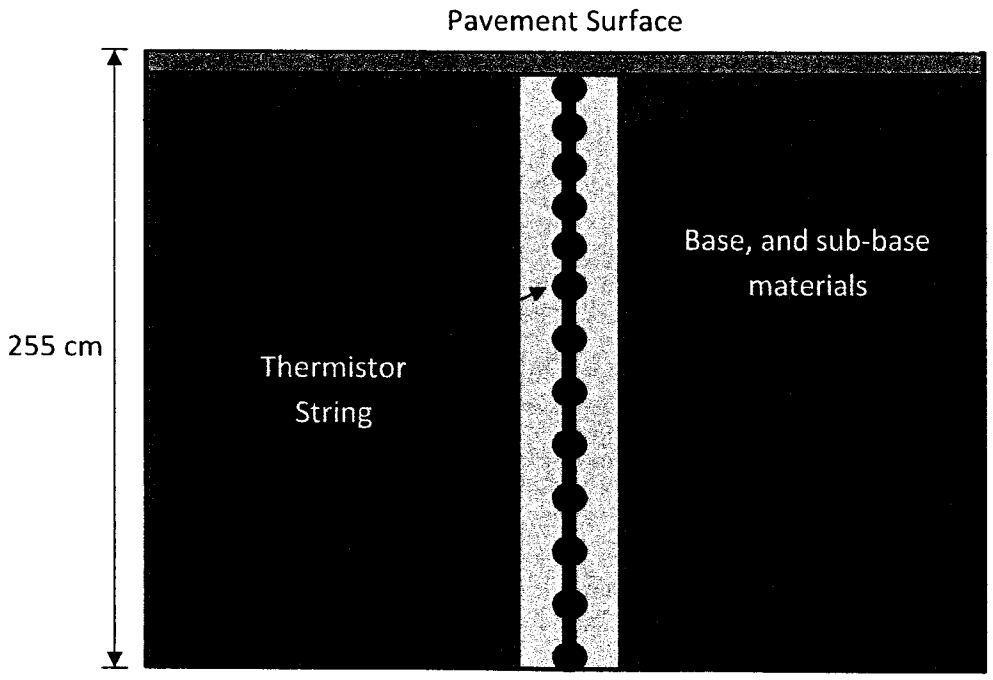

Figure 3.4 Thermistor String Profile

Figure 3.5 Burying Thermistor Cables (Highway 527 Study Site)

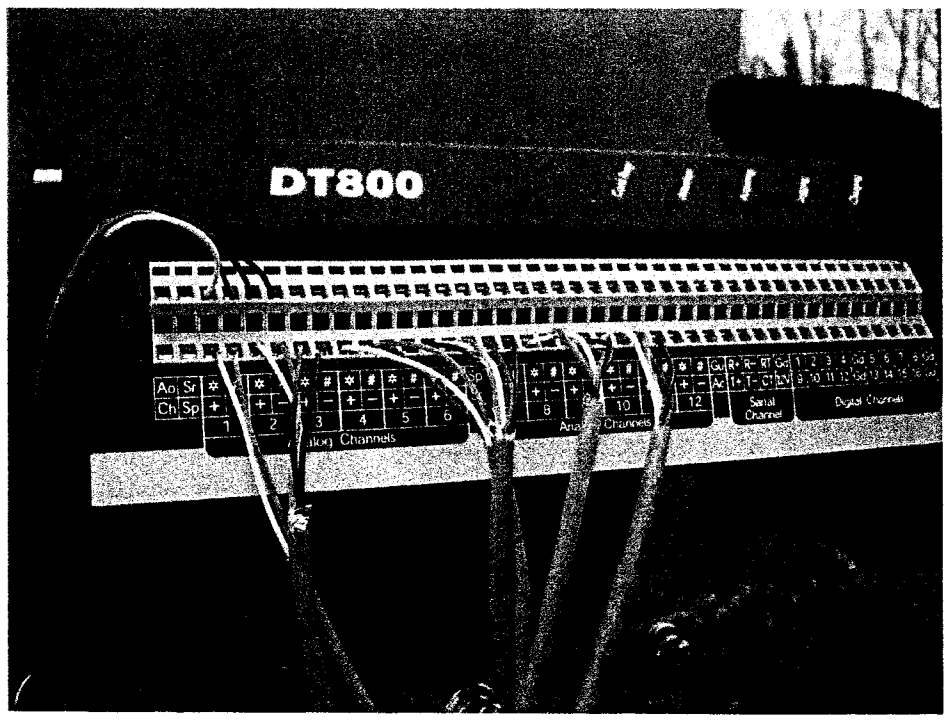

Figure 3.6 Dataloggers Installed at Northern Ontario Study Sites

Figure 3.7 Highway 569 Study Site

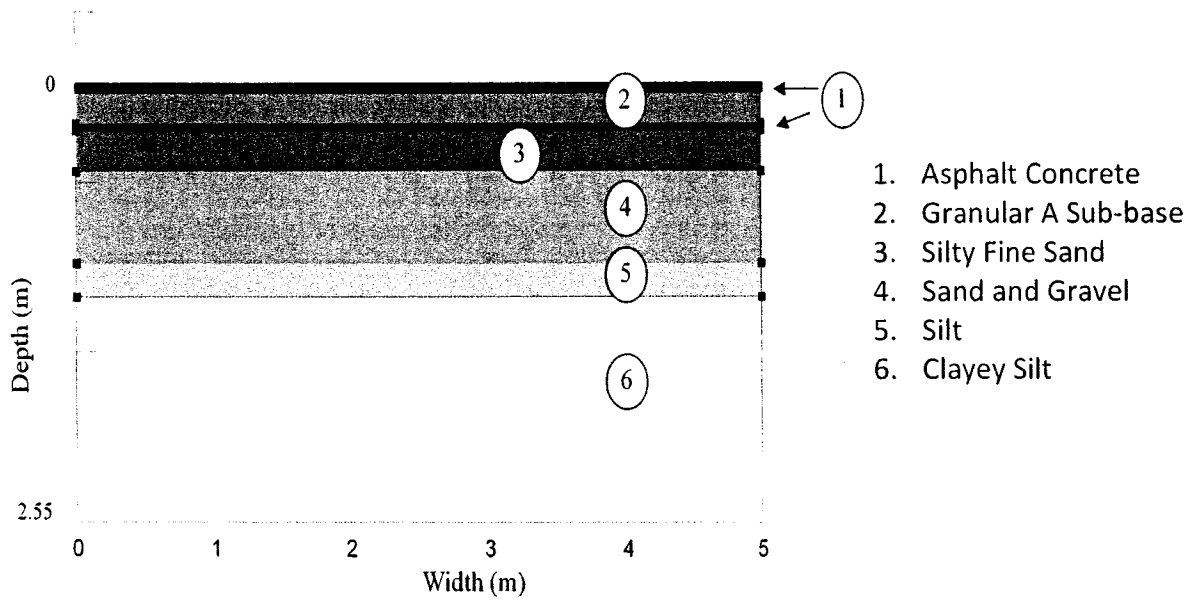

Figure 3.8 Highway 569 Study Site Roadway Cross Section

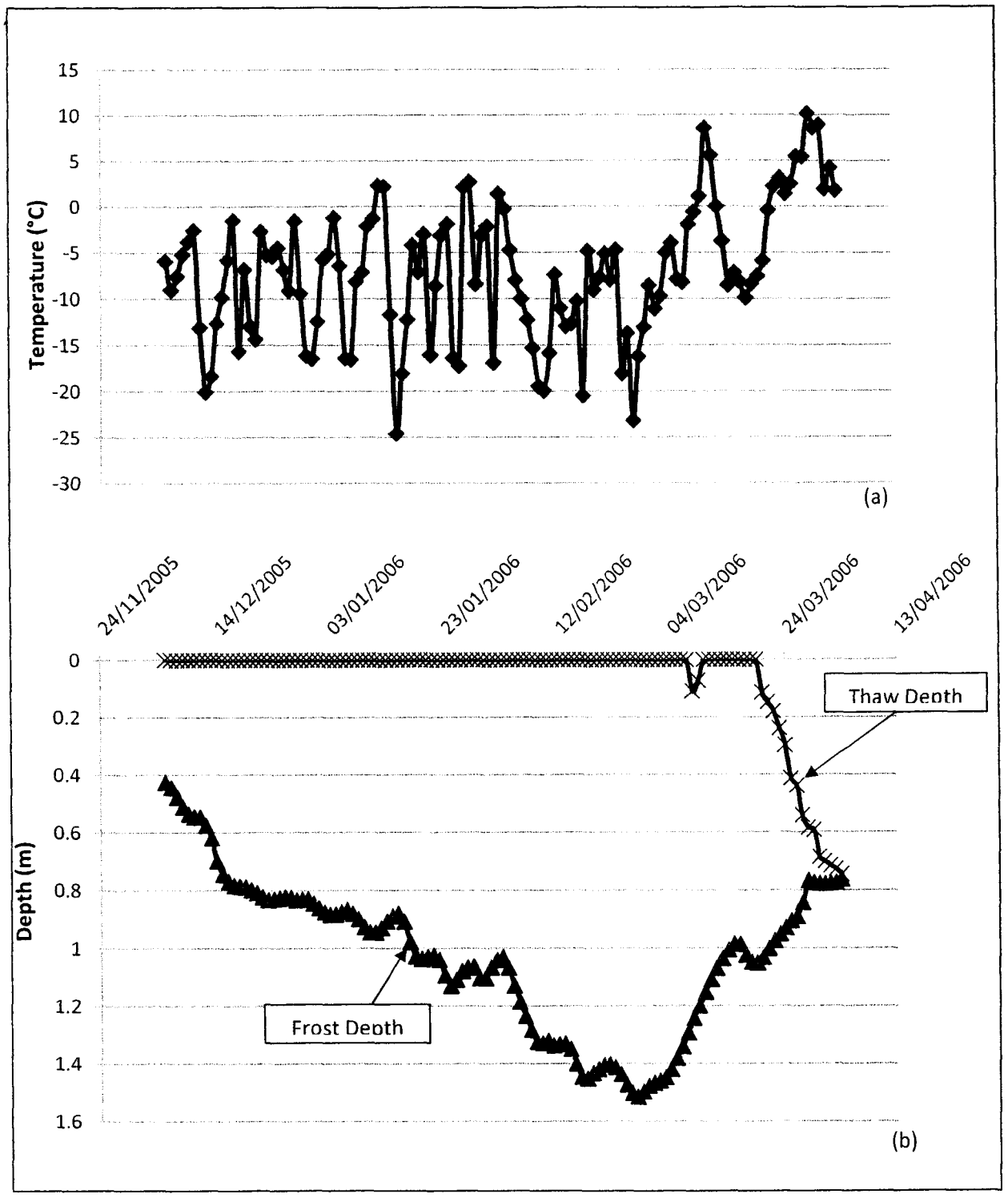

Figure 3.9 (a) Air Temperatures (b) and Measured Frost/Thaw Depths for Highway 569, 2005/2006

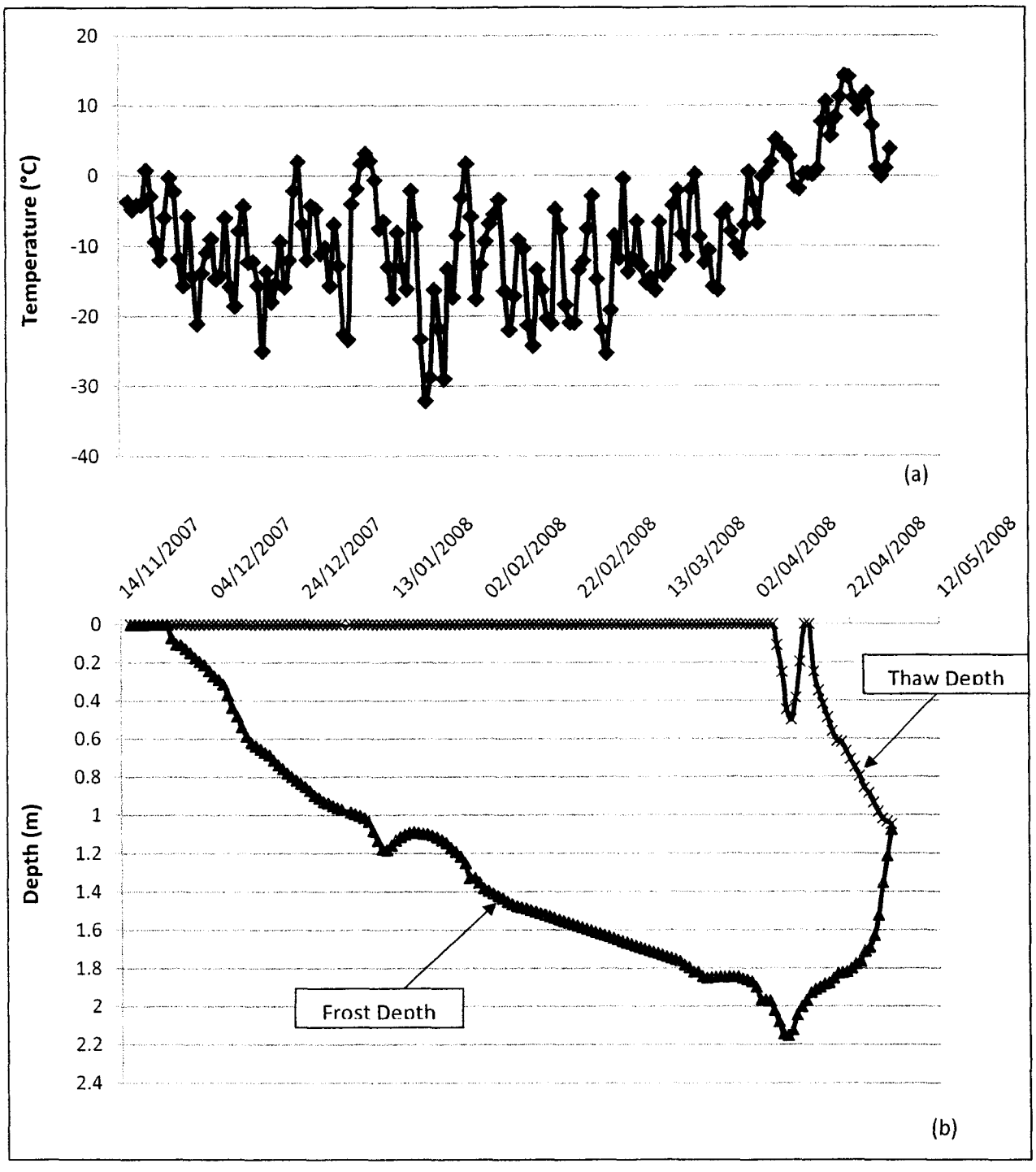

Figure 3.10 (a) Air Temperatures (b) and Measured Frost/Thaw Depths for Highway 569, 2007/2008

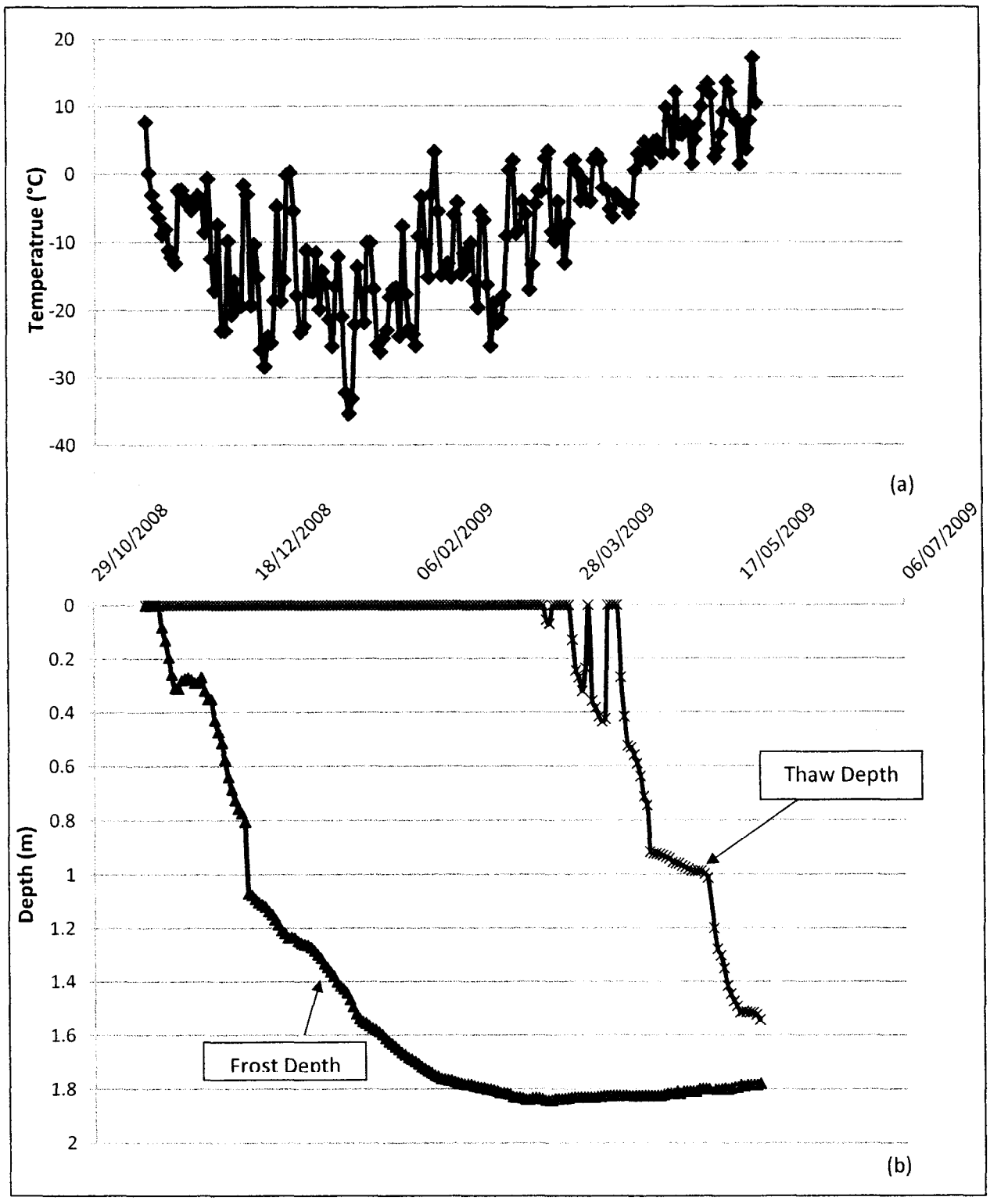

Figure 3.11 (a) Air Temperatures (b) and Measured Frost/Thaw Depths for Highway 569, 2008/2009

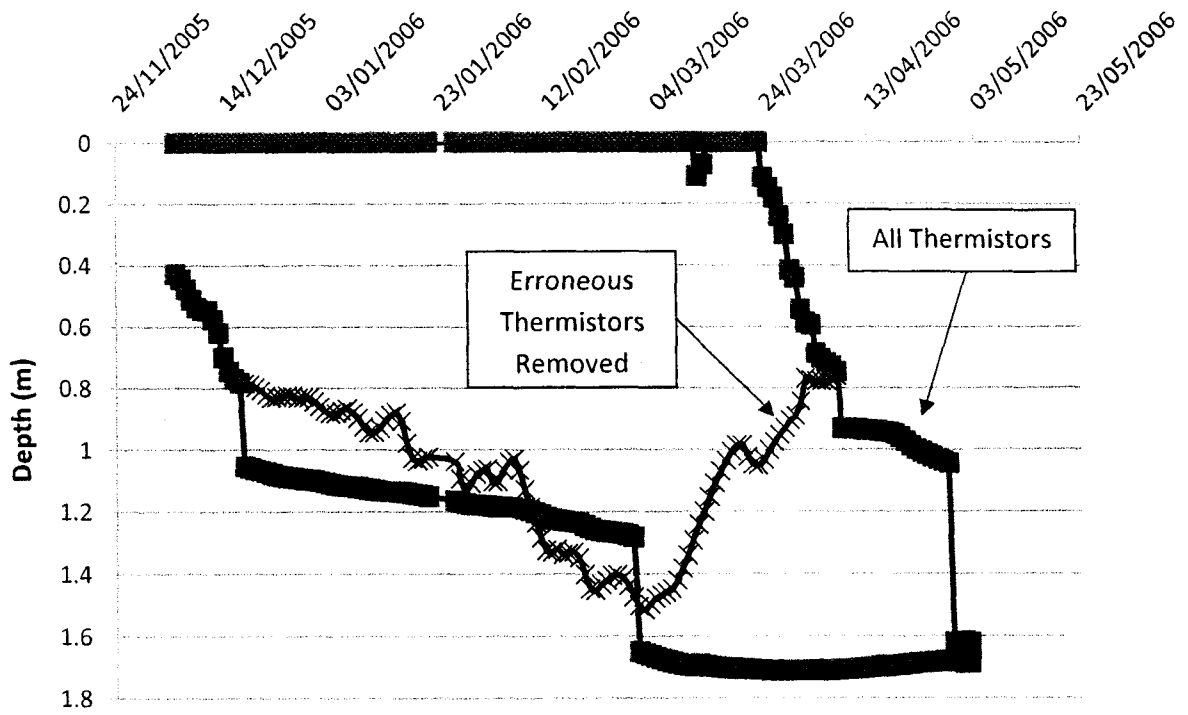

Figure 3.12 Removal of Erroneous Thermistors at the Highway 569 Study Site (2005/2006)

Figure 3.13 Highway 527 Study Site

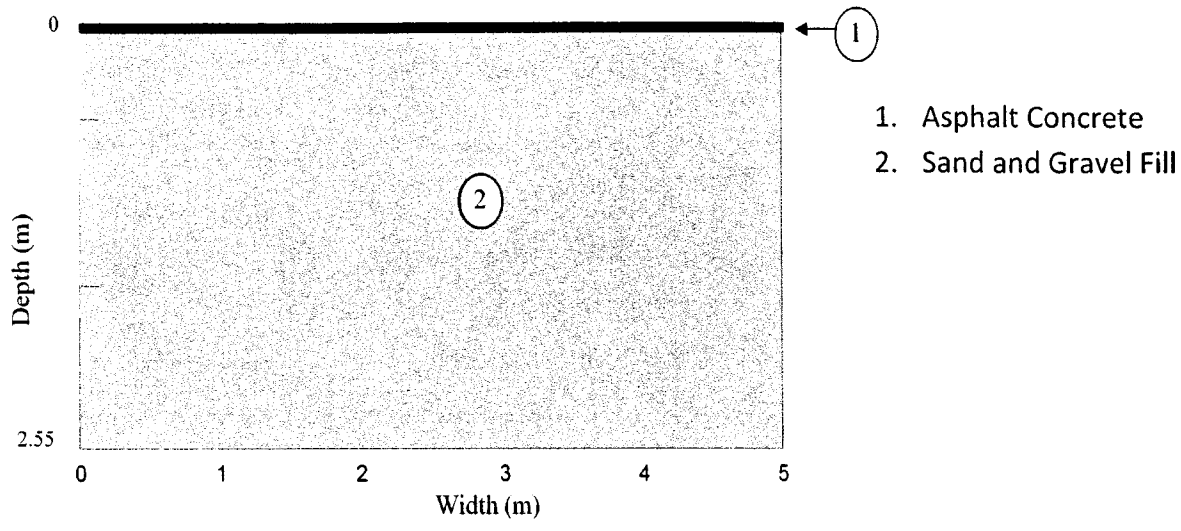

Figure 3.14 Highway 527 Study Site Roadway Cross Section

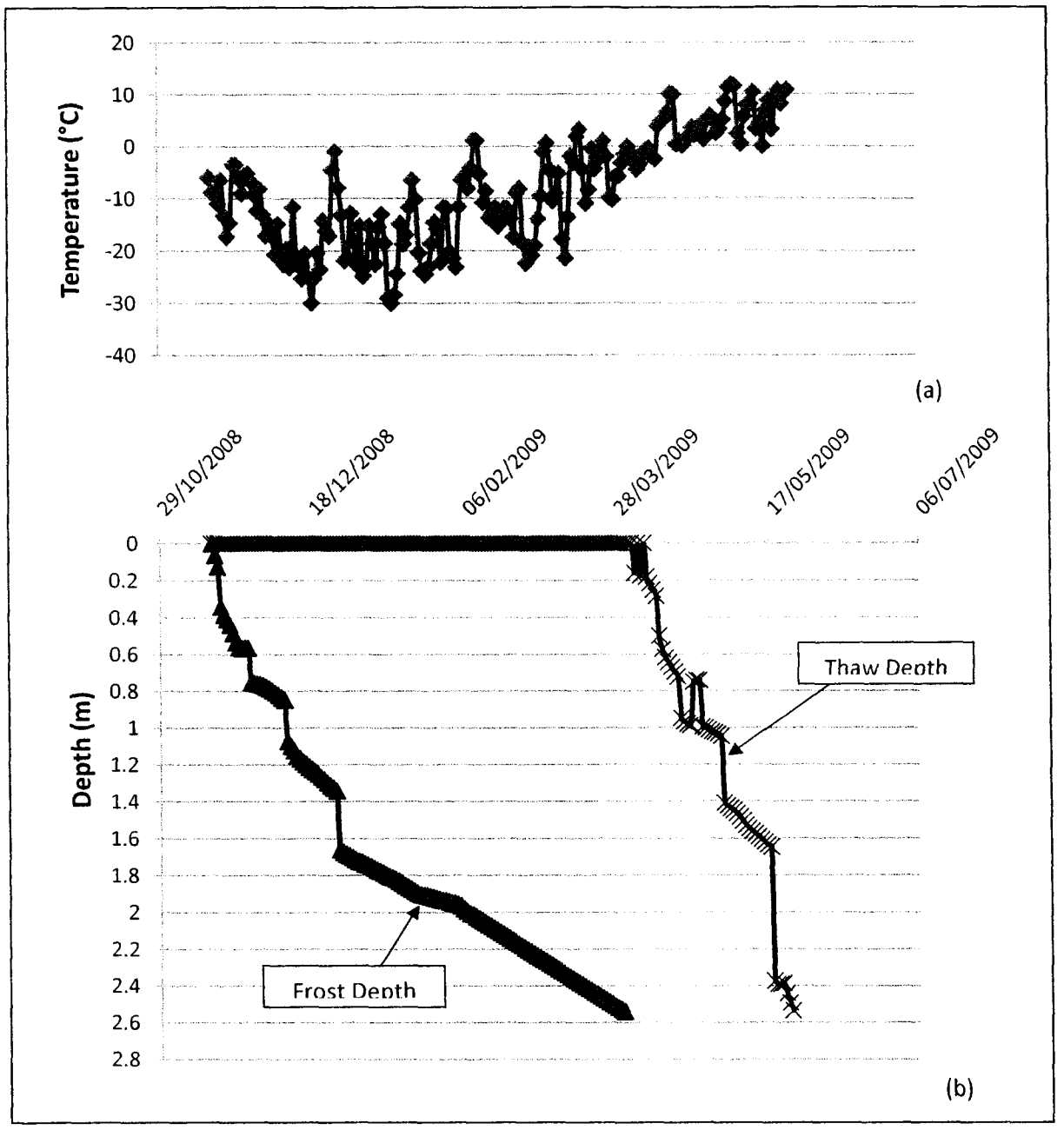

Figure 3.15 (a) Air Temperatures and (b) Measured Frost/Thaw Depths for Highway 527, 2008/2009

4.0 Development and Calibration of SLR Methods for Northern Ontario Conditions

4.1 SLR Method Development and Calibration Procedure

The empirical Mn/DOT method, the semi-empirical Waterloo method and the thermal numerical modelling based TEMP/W method were selected for further development and calibration, as described in Section 2.4.1.7. Air temperatures and interpreted freezing front and thawing front depths with time for the 2005/2006, 2007/2008, and 2008/2009 winter/spring seasons for the Highway 569 site and 2008/2009 winter/spring season for the Highway 527 site, provided in Sections 3.4.2 and 3.5.2, respectively, were used for calibration. Coefficients and parameters required for the methods to carry out the SLR predictions for winter/spring 2009/2010 were developed from these calibrations.

4.2 Threshold Thawing Depth for SLR Application

As indicated in Section 2.4, SLRs should commence when the thawing front migration exceeds a depth which results in significant pavement structure weakening. The literature presented in Section 2.4 suggests that a thawing front depth between the onset of pavement surface thawing to a depth of 600 mm will result in significant pavement structure weakening. For the purposes of this research a thawing depth of 300 mm has been selected as the threshold or triggering thawing depth for applying SLRs. This depth was selected for the following two reasons:

1. The Mn/DOT approach was developed through calibrating a 12 inch (300 mm) thawing depth with a specified CTI (www.mrr.dot.state.mn.us). Maintaining this criterion and comparing it with the frost and thaw depth simulation methods (Waterloo method

and TEMP/W method) it is possible to obtain a more representative comparison of the three methods.

2. Steinert et al. (2005) indicated that in general the pavement structure moduli were high when the pavement section was completely frozen and during the early part of the thawing period when the pavement structure is partially thawed.

When dealing with refreeze periods during the spring thaw, the Mn/DOT has determined that refreeze periods are too unstable and do not add a significant amount of strength to the roadway to consider removing the SLRs once they have been placed (www.dot.state.mn.us). For this reason, any refreeze period occurring after SLRs have been implemented are disregarded.

4.3 Mn/DOT Method Calibration

Calibration of the Mn/DOT method required historical air temperature data which were used to develop a threshold CTI for each of the calibration years. At each location during each study period the interpreted thaw depths were plotted versus time and the date at which the thawing front exceeded the SLR implementation depth of 300 mm for at least three successive days, was noted. These dates were then compared with corresponding CTI values.

At the Highway 569 location calibration was conducted for the three winter/spring seasons as described in Section 4.1. Figures 4.1 and 4.2 show the date at which the thawing depth exceeded the 300 mm threshold and the corresponding CTI, respectively, during the 2005/2006 season. Equation (2.23) and the reference temperatures given in Table 2.5 were used to calculate the CTI values. Figures 4.3 and 4.4 show the 2007/2008 calibration, while Figures 4.5 and 4.6 indicate the 2008/2009 calibration. Figures 4.3 and 4.5 show that significant thawing, followed by refreezing, occurred in spring 2008 and spring 2009. The initial thawing in fact exceeded the 300 mm threshold. In both of these cases, a three-day forecast indicated that the thawing depth would still have exceeded the 300 mm threshold and as a result triggered the application of SLRs. Following the Mn/DOT procedures under these circumstances the subsequent refreeze periods were disregarded

The CTI values for the three study periods when the 300 mm thaw depth was exceeded (26.4 °C-days, 50.3 °C-days and 43.6 °C-days for 2005/2006, 2007/2008 and 2008/2009, respectively) were averaged to yield a CTI value of 40.1 °C-days for the Highway 569 location.

The Highway 527 study site calibration was conducted using the 2008/2009 data. Figures 4.7 and 4.8 show the date at which the 300 mm thawing depth occured and the corresponding CTI. The CTI for the Highway 527 study site was found to be 64.3 °C-days.

Calibration of the SLR removal using the Mn/DOT method was based on thawing duration averages. For the Highway 569 study site the time required from the onset of SLRs (i.e. 300 mm thawing depth) to the complete thawing of the pavement structure was observed and recorded for each calibration period. The thawing duration was found to be 10 days in 2006, 24 days in 2008 and 55 days in 2009. Furthermore, following Berg (2010) an additional 7 days was added to each thawing duration period. This is required to allow for complete drainage of the subsurface melt water. Once the subsurface has drained, the stiffness of the pavement structure will be restored which allows for safe removal of the SLRs. The average of the three thawing seasons plus the additional 7 days was found to be 37 days, which was taken as the calibrated thawing duration for the northeastern study site.

A similar SLR removal calibration was used at the Highway 527 study site. Again, with only one year of calibration data available the thawing duration calibration was only based on the 2008/2009 thawing season. The thawing season duration (44 days) plus the additional 7 days resulted in a calibrated thawing duration of 51 days.

Using the calibrated SLR implementation TI value and removal based on thawing duration, a prediction for each study site was developed for the 2009/2010 season. This prediction will be used to assess the ability of the Mn/DOT method to accurately predict a 300 mm thawing depth and the subsequent need for SLR placement. Furthermore, thawing season durations will be examined to observe if SLRs are removed at an appropriate time.

4.4 The University of Waterloo Method Calibration

As with the Mn/DOT method, the Waterloo method was calibrated using three winter/spring seasons of data for the Highway 569 study site and only one winter/spring season of data for

the Highway 527 study site. For each calibration year, daily average air and pavement surface temperatures and average daily thermistor measurements are available as shown in Tables 3.4 and 3.5. The average daily air and corresponding pavement surface temperatures were plotted month by month and the intercept of the best fit line for these values were the monthly reference temperatures. The reference temperature plot for November 10 to December 10 for the Highway 569 site for the 2005/2006 season is shown in Figure 2.4. This procedure was reproduced monthly yielding a monthly set of reference temperature values. These reference temperatures account for the differences between air and pavement surface temperatures due to solar energy. The reference temperatures are then used along with measured air temperatures to determine a FI and a TI as indicated in Equations 4.1 and 4.2 (Baiz et al., 2007):

$$\begin{cases} FI_0 = -T_0 \\ FI_{i+1} = FI_i - T_{i+1} \\ FI_i < 0 \Rightarrow FI_i \equiv 0 \end{cases} \quad (4.1)$$

Where:

i = Number of days after the day indexed as day (i = 0)

(i = 0) = Day on which T_{air} first falls below 0°C

FI_0 = Freezing Index value on day i = 0 (in °C-days)

FI_i = Freezing Index value on day i (in °C-days)

T_0 = Average daily air temperature on day i = 0 (in °C)

$$\begin{cases} TI_0 = -T_{ref} \\ TI_{i+1} = T_{i+1} + TI_i - T_{ref} \\ TI_i < 0 \Rightarrow TI_i \equiv 0 \end{cases} \quad (4.2)$$

Where:

i = Number of days after the day indexed as day (i = 0)

(i = 0) = Day on which T_{air} first falls below 0°C

TI_0 = Thawing index value on day i = 0 (in °C-days)

TI_i = Thawing Index value on day i (in °C-days)

T_{ref} = Monthly reference temperature (in °C) (see Section 2.4.1.2)

Linear regressions and the least squares estimation method as described in Section 2.4.1.2 were used to calculate the calibration coefficients used in the Waterloo method (Equation 4.3):

$$\text{Calibration coefficients} = [\mathrm{X'X}] \times [\mathrm{X'Y}] \tag{4.3}$$

Where:

$$[X'X] = \begin{bmatrix} 1 \\ \sqrt{FI} \\ \sqrt{TI} \end{bmatrix} \times \left[1, \sqrt{FI}, \sqrt{TI}\right]$$

$$[X'Y] = \begin{bmatrix} 1 \\ \sqrt{FI} \\ \sqrt{TI} \end{bmatrix} \times [(\mathrm{A}, \mathrm{B}, \mathrm{C} \text{ or } \mathrm{D})]$$

A = Matrix of measured frost depths during freezing season (to calculate coefficients a, b and c)

B = Matrix of measured thaw depths during freezing season (to calculate coefficients d, e, and f)

C = Matrix of measured frost depths during thawing season (to calculate coefficients g, h and i)

D = Matrix of measured thaw depths during thawing season (to calculate coefficients j, k and l)

This procedure was followed for both the Highway 569 and 527 study sites for all of the available study periods.

4.4.1 Highway 569 Waterloo Method Calibration

Plotting the FI and the TI for the Highway 569 study site during the 2005/2006 season (Figure 4.9) and selecting the date in which the FI begins to continuously decrease while the TI begins to continually increase corresponds to an i_0 day of March 20, 2006. Using this i_0 day to separate the freezing and thawing season, calibration coefficients "a" through "k" were established using the procedures described in Section 4.4 (Table 4.1). These coefficients were placed into the Waterloo method algorithm (Equations 2.24 and 2.25) and a plot of the measured and the estimated (i.e. calculated) frost and thaw depths (Figure 4.10) was created to observe the accuracy of the model estimation for the given study period. The calibrated algorithm reproduces the frost and thawing front depths with time quite accurately, as shown in Figure 4.10.

This same approach was followed to determine the calibration coefficients for the 2007/2008 and 2008/2009 seasons. A plot of the 2007/2008 FI and TI values (Figure 4.11) indicates that the start of the thawing season (day i_0) occurred on April 7th, 2008. Using this i_0 day and the measured frost and thaw depths, the calibration coefficients for this study period were determined (Table 4.1). Again, the measured and estimated values were plotted; the calculated results compare quite well with the measured results (Figure 4.12).

This calibration procedure was followed for a third time for the 2008/2009 study period. An examination of the TI and FI values indicated that day i_0 occurs on April 15th, 2009 (Figure 4.13). This date was again used to determine the calibration coefficients for this study period (Table 4.1). A plot of the 2008/2009 measured and estimated frost and thaw depths (Figure 4.14) indicates that the Waterloo method provides good accuracy in reproducing the measured frost and thaw depths in a back analysis or history matching mode.

Reference temperatures and calibration coefficients were developed using an average of the three calibration years (Table 4.1). These coefficients will be used for the prediction for the 2009/2010 freeze/thaw period. A 5-day forecast will be used to plot forecasted FI and TI values, which in turn will be used to select day i_0.

4.4.2 Development of the Predictive Capability of the Waterloo Method

Using the coefficients determined from the 2005/2006 and 2007/2008 Highway 569 data, a preliminary prediction of the 2008/2009 season was conducted to assess this method in a predictive manner. Preliminary predictions were conducted using the 2005/2006 calibration coefficients (Figure 4.15(a)), the 2007/2008 calibration coefficients (Figure 4.15(b)) and an average of the two study periods calibration coefficients (Figure 4.15(c)). The 2005/2006 and 2007/2008 calibration coefficients are given in Table 4.1. It can be seen from these figures that direct use of the Waterloo coefficients from one year to the next results in erratic trends of both the freezing and thawing fronts when thawing begins. The use of this method without modification to the coefficients can result in unrealistic results, such as the presence of a thawing front more than 3 metres above the surface of the pavement structure (Figure 4.15(a)).

An examination of the algorithm developed for the Waterloo method (Equations 2.24 and 2.25) indicates that coefficients "g" and "j" are related to the calculation of initial depths of the frost and thaw, respectively, immediately after day i_0 (i.e. start of the thawing season). In order for the Waterloo method to be used effectively in a predictive manner the "g" and "j" coefficients must be adjusted to coincide with the depths of the estimated (i.e. calculated) frost and thaw just prior to day i_0 (i.e. the end of the freezing season).

The amount of adjustment made to the variables "g" and "j" was determined by initially plotting the frost and thaw depths during the freezing season using Equation 2.24. This was continued until day i_0 had been reached. Then, Equation 2.25 was used to determine the thawing season frost and thaw depth for day i_0. This provided two sets of frost and thaw depths for day i_0, one for the freezing season and another for the thawing season. As variables "g" and "j" are not linked with either the FI or TI in Equation 2.25 they can be adjusted to match the thawing season frost and thaw depths with the freezing season frost and thaw depths on day i_0. Table 4.2 lists the adjusted calibration coefficients that were used in this preliminary prediction.

It can been seen in Figure 4.16 that adjusting coefficient "g", which contributes to the initial depth of the frost during the thawing season, from 791.3 to 990 and coefficient "j", which contributes to the initial depth of the thaw during the thawing season, from -861.8 to -1175 for the 2008/2009 Highway 569 prediction using 2005/2006 calibration coefficients, results in a far closer match to the measured results. For each set of coefficients it can be seen that there is a significant difference between the calculated (Table 4.1) and the adjusted (Table 4.2) calibration coefficients "g" and "j" for 2005/2006 and 2007/2008. For this reason, any predictions using the Waterloo method must have the coefficients "g" and "j" adjusted using this procedure at the onset of day i_0. This procedure is described in Section 6.1.2.

4.4.3 Highway 527 Waterloo Method Calibration

The Highway 527 site was calibrated in the same manner as the Highway 569 site, but only the 2008/2009 data were available for use. A plot of the FI and TI values at the Highway 527 site (Figure 4.17) indicates that day i_0 falls on April 3, 2009. Reference temperatures and calibration

coefficients were determined in the same manner as for the Highway 569 site (Table 4.3). Comparison of Table 4.1 and Table 4.3 shows that the calibration coefficients for the Highway 569 and Highway 527 sites are quite different, and the coefficients for the three years for Highway 569 vary quite significantly. Figure 4.18 shows that the estimated (i.e. calculated) frost and thaw depth from the calibrated model closely match the observed results, as with the Highway 569 analysis. The calibration coefficients from this model along with forecasted air temperatures will be used to conduct a prediction of the 2009/2010 freeze/thaw season at the Highway 527 study site.

4.5 TEMP/W Method Calibration

As with the previous two methods the TEMP/W method will be calibrated using three seasons of data for the Highway 569 study site and only the 2008/2009 data set for the Highway 527 study site. Calibration of the TEMP/W method requires defining representative pavement structure material and thermal properties and appropriate lower and upper boundary conditions.

4.5.1 Mesh Properties

The mesh region properties in the TEMP/W model represent the various pavement structure materials present at each study site. The thermal model mesh is assigned both thermal and material properties. For the Highway 569 study site, these properties were estimated from probehole descriptions and observations. The probehole results indicate the nature of the subsurface materials, but did not clearly indicate the presence of a groundwater table. At the Highway 527 study site, detailed borehole logging information was not recorded during the installation of the thermistors and as a result the pavement structure material properties were estimated from observations of materials excavated from the borehole.

For each of the subsurface layers appropriate dry unit weight, degree of saturation and specific gravity values were estimated. Table 4.4 and Table 4.5 indicate the estimated material properties for each subsurface layer at the Highway 569 site and the Highway 527 site, respectively. Furthermore, published values (TEMP/W, 2007) of the thermal conductivity of soil

particles, water and ice and the specific heat capacity of solids, water and ice, were used to determine the thermal conductivity, heat capacity and unfrozen water content of each subsurface layer. The volumetric water content of each layer is also required and was determined by first converting the dry unit weight (γ_d) into a dry density (ρ_d) using Equation 4.4.

$$\rho_d \left(\frac{kg}{m^3}\right) = \gamma_d \left(\frac{kN}{m^3}\right) \times \left(\frac{1000}{9.81}\right) \tag{4.4}$$

Secondly, the void ratio (e) for the material was calculated using Equation 4.5:

$$e = \frac{G_s \times \rho_w}{\rho_d} - 1 \tag{4.5}$$

Where:

G_s = Specific Gravity of soil solids

ρ_w = Density of water (1000 kg / m^3)

Then, the gravimetric water content (w) is determined using the void ratio (e) and the degree of saturation (S) as outlined in Equation 4.6.

$$w\ (\%) = \frac{S \times e}{G_s} \tag{4.6}$$

Finally, a conversion (Equation 4.7) from gravimetric water content(w) to volumetric water content (θ) was determined.

$$\theta\ (\%) = \frac{\gamma_d}{\gamma_w} \times w \tag{4.7}$$

The frozen and unfrozen thermal conductivity values for each pavement structure material were determined using Cotê and Konrad's (2006) (outlined in Section 2.3.2.3), while

the frozen and unfrozen volumetric heat capacities of each material layer were determined using Equation (2.20). Tables 4.6 and 4.7 indicate the baseline thermal properties at Highway 569 and Highway 527, respectively that were determined using these methods.

Conversion from Watts to Kilojoules is achieved through the following equation.

$$\text{Wattsecond} = 0.001 \text{ Kilojoules} \tag{4.8}$$

The thermal conductivity values used in the TEMP/WI model were calculated using the normalized thermal conductivity relationship develop by Cotê and Konrad (2006) (Equation 4.9) and applying the conversion from Wattsecond to Kilojoules indicated in Equation 4.8.

$$k_r = \frac{K S_r}{1 + (K - 1) - S_r} \tag{4.9}$$

Where:

kr = Normalized thermal conductivity

S_r = Degree of Saturation

K = Empirical parameter used to account for different soil types in the frozen and unfrozen state

4.5.2 Lower Thermal Boundary Condition

Two possible lower boundary condition options were assessed for the TEMP/W method. The first approach involved determining a depth at which seasonal air temperature variations have no effect on the subsurface temperatures. This approach (constant temperature approach) involved examining the maximum and minimum temperatures obtained at each thermistor throughout 2007/2008 and extrapolating to a depth and temperature at which these values would remain constant (Figure 4.19). The second approach was to use the temperatures recorded by the lowest thermistor in the pavement structure thermistor string (lowest thermistor approach). Both of these approaches were applied to a model of the Highway 569 study site for the 2007/2008 season (Figure 4.20). In each case the baseline mesh properties outlined in Table 4.6 and n-factored air temperature upper boundary condition only were

maintained while only the lower boundary condition was changed. As the pavement structure below the depth of 2.25 m is unknown, the pavement structure material of the deepest layer was used (clayey silt), when extending the lower boundary condition from 2.25 m to 5 m. It can be observed in Figure 4.20 that the use of the lowest thermistor approach results in simulated data matching more closely to the measured data than the constant temperature approach. Based on this result all further calibrations for both the Highway 569 and Highway 527 study sites were done using the lowest thermistor approach as the lower boundary condition.

Another factor to consider when examining the lower boundary condition is the potential impact from the geothermal gradient which would provide heat flow to the pavement structure from below. If the additional heat from the geothermal gradient is not accounted for in the model simulations the models may indicate frost leaving the subsurface after the measured data would indicate. The use of the lowest thermistor method should capture the increased heat from the geothermal gradient; however a comprehensive study of the effects that the geothermal gradient had on the lower boundary condition was not conducted.

In order to use the lowest thermistor approach as a lower boundary condition in a predictive model for the Highway 569 study site, an average of the 2005/2006, 2007/2008 and 2008/2009 daily lowest thermistor temperature values had to be determined. This process had to not only account for the daily temperature differences between the three calibration periods but also represent the differences in thawing rate that were present from year to year. Figure 4.21 indicates the daily lowest thermistor values for each of the study periods individually and the average of the temperature values and thawing rate that is to be used in the predictive models. It must be noted that the lowest thermistor (255 cm) for the 2007/2008 and 2008/2009 seasons was displaying erroneous values which were not used in analysis. For this reason the 225 cm thermistor data were used to develop the predictive lower thermistor boundary condition. The lowest thermistor values that are used in the predictions for Highway 569 are listed in Appendix D.

With only one year of data from which to develop the lowest thermistor values (for the thermistor at a depth of 255cm) for predictions at the Highway 527 study, the prediction values

will be the same as the 2008/2009 Highway 527 values (Figure 4.22). The lowest thermistor values that are used in the predictions for Highway 527 are listed in Appendix E.

4.5.3 Upper Thermal Boundary Condition

Three different approaches were examined as potential upper boundary condition options. The first two approaches utilize TEMP/W boundary condition input options, while the third involves adjusting air temperature values prior to inputting them into the thermal model.

The first approach (climate approach) utilizes the climate boundary condition input option available in TEMP/W. This approach requires numerous variables including daily maximum and minimum temperatures, daily maximum and minimum relative humidity values, and average daily wind speed and precipitation data. Furthermore, three options for including the amount of solar radiation applied to the upper boundary are available. The first option is to estimate the amount of net radiation in $MJ/m^2/day$. This is done by providing the latitude of the study site and allowing the TEMP/W program to generate an amount of radiation based the site location. The second option is to directly input the net amount of solar radiation recorded at the site (if available) on a daily basis using the "User Net Radiation" option available in the climate boundary condition input menu. The amount of net radiation is determined by measuring the amount of incoming solar radiation and subtracting the amount of radiation being emitted from the earth. This option further increases the amount of measured input data required but is the most accurate in representing the solar radiation conditions at the site. The third option is to input the potential amount of evaporation and transpiration that would occur on a daily basis. From these values the TEMP/W model will estimate the amount of solar radiation required to achieve the allotted amount of evaporation and transpiration at the site. Considering all of the variables that are accounted for using the climate input boundary condition it has the potential to be the most representative of the actual conditions. However, collecting and compiling all the available data are difficult and time consuming. Further to this, numerous inputs including wind speed, precipitation, evaporation and transpiration values at the site are not currently measured and have to be estimated, which results in a decrease in the accuracy of the model in simulating measured results.

The second approach (n-factor approach) requires the input of average daily air temperature values. These air temperatures are then multiplied by a modification factor (n-factor) which accounts for the effects of solar radiation and pavement surface conditions. They in effect provide estimates of pavement surface temperatures from corresponding air temperatures. TEMP/W allows the creation of a function that applies specified n-factors based on daily air temperatures. Following Andersland and Ladanyi (2004) when air temperatures above 0°C an n-factor of one or greater is applied, depending on the type of surface material present at the site. When air temperatures are below 0°C an n-factor of less than one is applied, thereby increasing the temperatures. An issue with this option is that the n-factor does not significantly affect temperatures that are close to 0°C. For example, if the air temperature in the summer months is 30°C then applying an n-factor of 1.5 would yield a surface temperature of 45°C, whereas if the air temperature in the spring was 1°C, then the corresponding air temperature would only be 1.5°C.

The third approach (reference temperature approach) involves manually increasing the measured air temperatures by a weekly floating reference temperature, for example as outlined by the Mn/DOT (2004) (Table 2.3). The modified air temperatures can then be input into the thermal model as the upper boundary condition. These increases in temperature are intended to account for the increased solar radiation during the spring thaw period. This approach has the potential to be more effective than the n-factor approach in adjusting air temperatures close to 0°C as air temperatures slightly below 0°C will be adjusted to represent pavement surface temperatures that are likely above 0°C, which the n-factor approach could not accomplish.

A series of simulations for the Highway 569 study site for the 2007/2008 season were conducted to examine the accuracy of simulating measured freezing and thawing results when each of three upper boundary condition approaches is applied to the model. For these simulations the baseline thermal properties listed in Table 4.6 were used and the measured lowest thermistor temperature data were used as the lower boundary condition.

A comparison of the n-factor approach and the climate approach (Figure 4.23) indicates that the n-factor approach (applying an n-factor of 2.3 for temperatures above 0°C and 0.6 for

temperatures below 0°C) is more accurate at simulating the depth of freezing, the initiation and rate of thawing and the time of complete subsurface thawing than the climate approach. Figure 4.24 illustrates the changes in air temperature resulting from the application of the n-factor. For this reason it was decided that the n-factor approach is more accurate and easier to implement than the climate approach for use as an upper boundary condition.

A second simulation was conducted to compare the n-factor approach with the reference temperature approach (Figure 4.25). The difference between the measured air temperatures and the measured air temperatures with the addition of the reference temperature is shown in Figure 4.26. It can be seen that both upper boundary conditions are reasonably accurate in predicting the onset, rate and duration of the thawing period. However, both options inaccurately simulate the upward migration of the frost front during the spring thaw period. It can also be observed that the n-factor approach is slightly more accurate at determining the duration of thawing and equally as accurate as the reference temperature approach in simulating the thawing and refreeze period prior to the onset of the general thaw (March 8, 2006 – March 15, 2006).

The comparison of the three upper boundary condition approaches in simulating the measured freezing and thawing trends at the Highway 569 study site, indicates that the n-factor approach is the most accurate. Because of this, the TEMP/W model calibrations at both study sites were conducted using the n-factor approach as the upper boundary condition.

4.5.4 Sensitivity Analysis of the Pavement Structure Material Properties

A sensitivity analysis was performed using the Highway 569 study site for the 2007/2008 study period to examine the effects that systematic changes in the calculated thermal properties resulting from increases and decreases in the subsurface moisture conditions have on the simulated frost and thaw depths. Two simulations using the TEMP/W program were conducted as part of the sensitivity analysis. For both of the simulations the lowest thermistor readings were used as the lower boundary condition (explained in Section 4.5.2) and n-factored air temperatures were used as the upper boundary conditions (explained in Section 4.5.3).

The first analysis examined the effects of increasing the degree of saturation (S) from the baseline value of 50% to 100% in all of the pavement structure soil material layers, on the simulated frost and thaw depths. Table 4.8 lists the pavement structure layer material and thermal properties that result from the increase in the degree of saturation. This model will be compared with both the measured frost and thaw depths as well as a TEMP/W model created using the baseline thermal properties in Table 4.6. This comparison will provide insight into the model's response to maximizing the subsurface moisture conditions.

In the second analysis, the degree of saturation is reduced to 15% in all of the pavement structure soil materials. This reduction to 15% simulates the residual degree of saturation for unsaturated soils (Fredlund and Rahardio, 1993). Table 4.9 indicates the baseline and material and thermal properties of the pavement structure material layers when the degree of saturation is set at 15%. As with the fully saturated model, this model will be compared with the measured frost and thaw depths and a model constructed using the baseline thermal properties.

The model simulation conducted under fully saturated conditions indicates that an increase in subsurface moisture will have an impact on both the freezing front depth and the duration needed for full subsurface thawing (Figure 4.27). This increase in moisture and subsequent changes to the material thermal properties increases the depth of penetration of the frost front, thereby increasing the overall amount of frost thickness within the subsurface. The increased frost thickness substantially increases the amount of time required to achieve full subsurface thawing. This is in good accordance with TEMP/W (2007) which states:

> *"adjusting the water content affects the length of time the temperature profile "hovers" around the freezing point before it starts to drop off rapidly again. This length of time is directly related to the latent heat that is released so the more water there is, the more latent heat, and the longer it takes to be removed."*

The model created with the degree of saturation set at 15% for all pavement structure soil materials, indicates expedited frost removal from the pavement structure when compared

with the baseline model created with the degree of saturation set at 50% (Figure 4.28). This model as with the fully saturated model reacts as expected and is in accordance with the TEMP/W (2007) statement.

The depth of frost and thaw are strongly tied to changes in the thermal properties and moisture conditions of the pavement structure materials as indicated in Figures 4.19 and 4.20. Determining more precise thermal properties for each site however, would require more data, extensive sample collection and laboratory testing. For this reason all of the calibrations and predictions will be conducted using the baseline thermal properties outlined in Tables 4.6 and 4.7.

4.5.4 TEMP/W Highway 569 Calibration

Calibrations for the 2005/2006, 2007/2008 and 2008/2009 seasons were conducted using the available lowest thermistor temperature values as the bottom boundary condition and the baseline thermal properties outlined in Table 4.6. For each season numerous simulations were conducted varying the n-factor for both the air temperatures above and below 0°C.

For the 2005/2006 season the n-factor values of 2.3 and 0.5 resulted in the closest match to measured data (Figure 4.29). The initial frost depth estimation for the 2005/2006 season is significantly deeper than the measured data indicates. This inaccurate frost depth estimation is a result of the TEMP/W program interpolating between the temperatures set at the top and bottom boundary conditions after the freezing season had already commenced. This interpolation does not accurately represent the temperature profile of the pavement structure as a whole. Furthermore, subsequent frost depths are based on the initial conditions resulting in inaccurate frost depths throughout the entire freezing period.

As indicated in Section 4.5.3 the use of an n-factor of 2.3 for air temperatures above 0°C and 0.6 for air temperatures below 0°C results in the closest fit between the simulated and measured results for the 2007/2008 season. It can also been seen in Figure 4.30 that the use of 2.3 and 0.6 n-factor values for temperatures above and below 0°C, respectively, closely simulates the thawing and refreeze period that occurs between April 3, 2008 and April 12, 2008.

For the 2008/2009 season n-factor values of 2.3 and 0.6 result in the closest fit between simulated and measured results (Figure 4.31). The TEMP/W simulations for the 2008/2009 season do not accurately match the periods of thawing and refreezing that occur between March 23, 2009 and April 7, 2009 and the initiation of thawing is overestimated by 5 days. These n-factor values, however, resulted in a simulation that most closely matched the overall thawing trend and gave the closest approximation to the time of complete subsurface thawing. The simulations indicate that the complete subsurface thawing would occur well before the measured data suggest. It should be noted however, that the temperatures of the remaining frozen zone between the simulated complete thawing and measured complete thawing are only slightly below 0°C.

Predictions of the 2009/2010 freeze/thaw period will be conducted using the lowest thermistor values listed in Appendix D and the baseline thermal properties provided in Table 4.6. Furthermore, the average of the n-factor values for the three calibration periods (2.3 for temperatures above 0°C and 0.57 for temperatures below 0°C) will be used as the upper boundary condition in the prediction.

4.5.5 TEMP/W Highway 527 Calibration

The same TEMP/W calibration procedure that was used for the Highway 569 study site was repeated for the Highway 527 study site, with the exception that only 2008/2009 winter/spring season data are used. Numerous simulations of the Highway 527 study site indicate that n-factor values of 2.3 for air temperatures above 0°C and 0.8 for air temperatures below 0°C provide the best match between simulated and measured data (Figure 4.32). As these values are the only ones available they will be used in the 2009/2010 predictions. The predictions at the Highway 527 study site will be conducted using the lowest thermistor values listed in Appendix E and the baseline thermal properties indicated in Table 4.7.

Table 4.1 Calculated Waterloo Reference Temperatures and Calibration Coefficients for the Highway 569 Study Site

Monthly Reference Temperature (°C)		2005/2006	2007/2008	2008/2009	Average
November		0.03	-3.35	-4.93	-2.75
December		-4.15	-1.30	-2.94	-2.79
January		-2.21	0.79	-0.90	-0.77
February		-2.79	-0.06	-2.15	-1.67
March		-7.61	-2.05	-5.22	-4.96
April		-4.45	-5.42	-2.53	-4.14
May		-1.30	-3.68	8.58	1.20
	Calibration Coefficients				
Freezing Season Coefficients (Eq. 2.24)	a	-3.63	34.28	-31.39	-0.25
	b	-4.71	-5.80	-3.96	-4.82
	c	5.14	-1.41	2.92	2.22
	d	0.19	1.93	31.74	11.29
	e	-0.01	-0.07	-0.98	-0.35
	f	-0.23	-0.85	-2.11	-1.06
Thawing Season Coefficients (Eq. 2.25)	g	791.31	53.12	-145.33	233.03
	h	-28.66	-7.43	-0.92	-12.34
	i	-0.14	4.60	0.14	1.53
	j	-861.83	-1525.79	-1425.31	-1271
	k	28.96	38.59	32.05	33.20
	l	-5.66	-0.72	1.19	-1.73
	Day i_0	3/20/06	4/7/08	4/15/09	-

Table 4.2 Adjusted Waterloo Calibration Coefficients used in 2008/2009 Preliminary Prediction (Highway 569)

Adjusted Calibration Coefficients		2005/2006	2007/2008	Average
Freezing Season Coefficients (Eq. 2.24)	a	-3.63	34.28	15.33
	b	-4.71	-5.80	-5.25
	c	5.14	-1.41	1.86
	d	0.19	1.93	1.06
	e	-0.01	-0.07	-0.04
	f	-0.23	-0.85	-0.54
Thawing Season Coefficients (Eq. 2.25)	g	990.00	80.00	540.00
	h	-28.66	-7.43	-18.04
	i	-0.14	4.60	2.23
	j	-1175.00	-1610.00	-1385.00
	k	28.96	38.59	33.78
	l	-5.66	-0.72	-3.19

Table 4.3 Waterloo Reference Temperatures and Calibration Coefficients for the Highway 527 Study Site

Monthly Reference Temperature (°C)		2008/2009
November		-4.20
December		-4.73
January		1.14
February		1.37
March		-3.67
April		-3.67
May		-3.00
	Calibration Coefficients	
Freezing Season Coefficients (Eq. 2.24)	a	-6.17
	b	-5.52
	c	0.97
	d	1.15
	e	-0.04
	f	-0.09
Thawing Season Coefficients (Eq. 2.25)	g	-255.00
	h	5.46E-11
	i	1.05E-11
	j	-1572.26
	k	36.64
	l	-6.54
	Day i_0	4/3/09

Table 4.4 Estimated Material Properties for the Highway 569 Study Site

Material	Estimated Properties and Assumptions
Asphalt Surface Treatment (AST)	- AST has typical asphalt thermal and material properties
	- Assumed to hold no water in microfissures or cracks
Granular A	- Dry unit weight = 17 kN/m^3
	- Degree of Saturation = 50%
	- Specific Gravity = 2.65
Asphalt Concrete (AC)	- Same assumptions as AST above
Silty-Fine Sand	- Dry unit weight = 17 kN/m^3
	- Degree of Saturation = 50%
	- Specific Gravity = 2.70
Sand and Gavel	- Dry unit weight = 20 kN/m^3
	- Degree of Saturation = 50%
	- Specific Gravity = 2.65
Silt	- Same assumptions as silty fine sand above
Clayey Silt	- Dry unit weight = 18 kN/m^3
	- Degree of Saturation = 50%
	- Specific Gravity = 2.75

Table 4.5 Estimated Material Properties for the Highway 527 Study Site

Material	Estimated Properties and Assumptions
Asphalt Surface Treatment (AST)	- AST has typical asphalt thermal and material properties
	- Assumed to hold no water in microfissures or cracks
Sand and Gravel Fill	- Dry unit weight = 17 kN/m^3
	- Degree of Saturation = 50%
	- Specific Gravity = 2.65

Table 4.6 Baseline Thermal Properties Used at the Highway 569 Study Site

AST	0 - 25mm	
Unfrozen Thermal Conductivity	108	kJ/(day*m*°C)
Frozen Thermal Conductivity	108	kJ/(day*m*°C)
Water Content	0	m^3/m^3
Unfrozen Volumetric Heat Capacity	2520	kJ/(kg*°C)
Frozen Volumetric Heat Capacity	2520	kJ/(kg*°C)
Granular A	25 - 210mm	
Unfrozen Thermal Conductivity	108	kJ/(day*m*°C)
Frozen Thermal Conductivity	144.5	kJ/(day*m*°C)
Water Content	0.173	m^3/m^3
Unfrozen Volumetric Heat Capacity	1955	kJ/(kg*°C)
Frozen Volumetric Heat Capacity	1628	kJ/(kg*°C)
AC	210 - 250mm	
Unfrozen Thermal Conductivity	108	kJ/(day*m*°C)
Frozen Thermal Conductivity	108	kJ/(day*m*°C)
Water Content	0	m^3/m^3
Unfrozen Volumetric Heat Capacity	2520	kJ/(kg*°C)
Frozen Volumetric Heat Capacity	2520	kJ/(kg*°C)
Silty Fine Sand	250 - 490mm	
Unfrozen Thermal Conductivity	106.2	kJ/(day*m*°C)
Frozen Thermal Conductivity	144.2	kJ/(day*m*°C)
Water Content	0.179	m^3/m^3
Unfrozen Volumetric Heat Capacity	1980	kJ/(kg*°C)
Frozen Volumetric Heat Capacity	1641	kJ/(kg*°C)
Sand and Gravel	490 - 1030mm	
Unfrozen Thermal Conductivity	127	kJ/(day*m*°C)
Frozen Thermal Conductivity	147.6	kJ/(day*m*°C)
Water Content	0.115	m^3/m^3
Unfrozen Volumetric Heat Capacity	1930	kJ/(kg*°C)
Frozen Volumetric Heat Capacity	1731	kJ/(kg*°C)
Silt	1030 - 1230mm	
Unfrozen Thermal Conductivity	106.2	kJ/(day*m*°C)
Frozen Thermal Conductivity	144.2	kJ/(day*m*°C)
Water Content	0.179	m^3/m^3
Unfrozen Volumetric Heat Capacity	1980	kJ/(kg*°C)
Frozen Volumetric Heat Capacity	1641	kJ/(kg*°C)
Clayey Silt	1230 - 1690mm	
Unfrozen Thermal Conductivity	110.0	kJ/(day*m*°C)
Frozen Thermal Conductivity	144.8	kJ/(day*m*°C)
Water Content	0.166	m^3/m^3
Unfrozen Volumetric Heat Capacity	1999	kJ/(kg*°C)
Frozen Volumetric Heat Capacity	1689	kJ/(kg*°C)

Table 4.7 Baseline Thermal Properties Used at the Highway 527 Study Site

AST	0 - 25mm	
Unfrozen Thermal Conductivity	108	kJ/(day*m*°C)
Frozen Thermal Conductivity	108	kJ/(day*m*°C)
Water Content	0	m^3/m^3
Unfrozen Volumetric Heat Capacity	2520	kJ/(kg*°C)
Frozen Volumetric Heat Capacity	2520	kJ/(kg*°C)
Sand and Gravel Fill	**25 - 255mm**	
Unfrozen Thermal Conductivity	108	kJ/(day*m*°C)
Frozen Thermal Conductivity	144.5	kJ/(day*m*°C)
Water Content	0.173	m^3/m^3
Unfrozen Volumetric Heat Capacity	1955	kJ/(kg*°C)
Frozen Volumetric Heat Capacity	1628	kJ/(kg*°C)

Table 4.8 Material and Thermal Properties with Baseline and Fully Saturated Conditions (Highway 569 site)

	Baseline	S = 100%	
AST	**0 - 25mm**	**0 - 25mm**	
Unfrozen Thermal Conductivity	108	108	kJ/(day*m*°C)
Frozen Thermal Conductivity	108	108	kJ/(day*m*°C)
Water Content	0	0	m^3/m^3
Unfrozen Volumetric Heat Capacity	2520	2520	kJ/(kg*°C)
Frozen Volumetric Heat Capacity	2520	2520	kJ/(kg*°C)
Granular A	**25 - 210mm**	**25 - 210mm**	
Unfrozen Thermal Conductivity	108	200.6	kJ/(day*m*°C)
Frozen Thermal Conductivity	144.5	125.7	kJ/(day*m*°C)
Water Content	0.173	0.346	m^3/m^3
Unfrozen Volumetric Heat Capacity	1955	2679	kJ/(kg*°C)
Frozen Volumetric Heat Capacity	1628	1991	kJ/(kg*°C)
AC	**210 - 250mm**	**210 - 250mm**	
Unfrozen Thermal Conductivity	108	108	kJ/(day*m*°C)
Frozen Thermal Conductivity	108	108	kJ/(day*m*°C)
Water Content	0	0	m^3/m^3
Unfrozen Volumetric Heat Capacity	2520	2520	kJ/(kg*°C)
Frozen Volumetric Heat Capacity	2520	2520	kJ/(kg*°C)
Silty Fine Sand	**250 - 490mm**	**250 - 490mm**	
Unfrozen Thermal Conductivity	106.2	123.7	kJ/(day*m*°C)
Frozen Thermal Conductivity	144.2	200.6	kJ/(day*m*°C)
Water Content	0.179	0.358	m^3/m^3
Unfrozen Volumetric Heat Capacity	1980	2730	kJ/(kg*°C)
Frozen Volumetric Heat Capacity	1641	2016	kJ/(kg*°C)
Sand and Gravel	**490 - 1030mm**	**490 - 1030mm**	
Unfrozen Thermal Conductivity	127	146.8	kJ/(day*m*°C)
Frozen Thermal Conductivity	147.6	200.8	kJ/(day*m*°C)
Water Content	0.115	0.231	m^3/m^3
Unfrozen Volumetric Heat Capacity	1930	2413	kJ/(kg*°C)
Frozen Volumetric Heat Capacity	1731	1972	kJ/(kg*°C)
Silt	**1030 - 1230mm**	**1030 - 1230mm**	
Unfrozen Thermal Conductivity	106.2	123.7	kJ/(day*m*°C)
Frozen Thermal Conductivity	144.2	200.6	kJ/(day*m*°C)
Water Content	0.179	0.358	m^3/m^3
Unfrozen Volumetric Heat Capacity	1980	2730	kJ/(kg*°C)
Frozen Volumetric Heat Capacity	1641	2016	kJ/(kg*°C)
Clayey Silt	**1230 - 1690mm**	**1230 - 1690mm**	
Unfrozen Thermal Conductivity	110.0	128.0	kJ/(day*m*°C)
Frozen Thermal Conductivity	144.8	200.6	kJ/(day*m*°C)
Water Content	0.166	0.333	m^3/m^3
Unfrozen Volumetric Heat Capacity	1999	2696	kJ/(kg*°C)
Frozen Volumetric Heat Capacity	1689	2037	kJ/(kg*°C)

Table 4.9 Material and Thermal Properties with Baseline Conditions and Degree of Saturation = 15% (Highway 569 Site)

	Baseline	S = 15%	
AST	**0 - 25mm**	**0 - 25mm**	
Unfrozen Thermal Conductivity	108	108	kJ/(day*m*°C)
Frozen Thermal Conductivity	108	108	kJ/(day*m*°C)
Water Content	0	0	m^3/m^3
Unfrozen Volumetric Heat Capacity	2520	2520	kJ/(kg*°C)
Frozen Volumetric Heat Capacity	2520	2520	kJ/(kg*°C)
Granular A	**25 - 210mm**	**25 - 210mm**	
Unfrozen Thermal Conductivity	108	70.6	kJ/(day*m*°C)
Frozen Thermal Conductivity	144.5	70.1	kJ/(day*m*°C)
Water Content	0.173	0.052	m^3/m^3
Unfrozen Volumetric Heat Capacity	1955	1448	kJ/(kg*°C)
Frozen Volumetric Heat Capacity	1628	1375	kJ/(kg*°C)
AC	**210 - 250mm**	**210 - 250mm**	
Unfrozen Thermal Conductivity	108	108	kJ/(day*m*°C)
Frozen Thermal Conductivity	108	108	kJ/(day*m*°C)
Water Content	0	0	m^3/m^3
Unfrozen Volumetric Heat Capacity	2520	2520	kJ/(kg*°C)
Frozen Volumetric Heat Capacity	2520	2520	kJ/(kg*°C)
Silty Fine Sand	**250 - 490mm**	**250 - 490mm**	
Unfrozen Thermal Conductivity	106.2	69.2	kJ/(day*m*°C)
Frozen Thermal Conductivity	144.2	69.5	kJ/(day*m*°C)
Water Content	0.179	0.054	m^3/m^3
Unfrozen Volumetric Heat Capacity	1980	1455	kJ/(kg*°C)
Frozen Volumetric Heat Capacity	1641	1379	kJ/(kg*°C)
Sand and Gravel	**490 - 1030mm**	**490 - 1030mm**	
Unfrozen Thermal Conductivity	127	85.3	kJ/(day*m*°C)
Frozen Thermal Conductivity	147.6	77.1	kJ/(day*m*°C)
Water Content	0.115	0.035	m^3/m^3
Unfrozen Volumetric Heat Capacity	1930	1592	kJ/(kg*°C)
Frozen Volumetric Heat Capacity	1731	1562	kJ/(kg*°C)
Silt	**1030 - 1230mm**	**1030 - 1230mm**	
Unfrozen Thermal Conductivity	106.2	69.2	kJ/(day*m*°C)
Frozen Thermal Conductivity	144.2	69.5	kJ/(day*m*°C)
Water Content	0.179	0.054	m^3/m^3
Unfrozen Volumetric Heat Capacity	1980	1455	kJ/(kg*°C)
Frozen Volumetric Heat Capacity	1641	1379	kJ/(kg*°C)
Clayey Silt	**1230 - 1690mm**	**1230 - 1690mm**	
Unfrozen Thermal Conductivity	110.0	72.1	kJ/(day*m*°C)
Frozen Thermal Conductivity	144.8	70.8	kJ/(day*m*°C)
Water Content	0.166	0.05	m^3/m^3
Unfrozen Volumetric Heat Capacity	1999	1512	kJ/(kg*°C)
Frozen Volumetric Heat Capacity	1689	1445	kJ/(kg*°C)

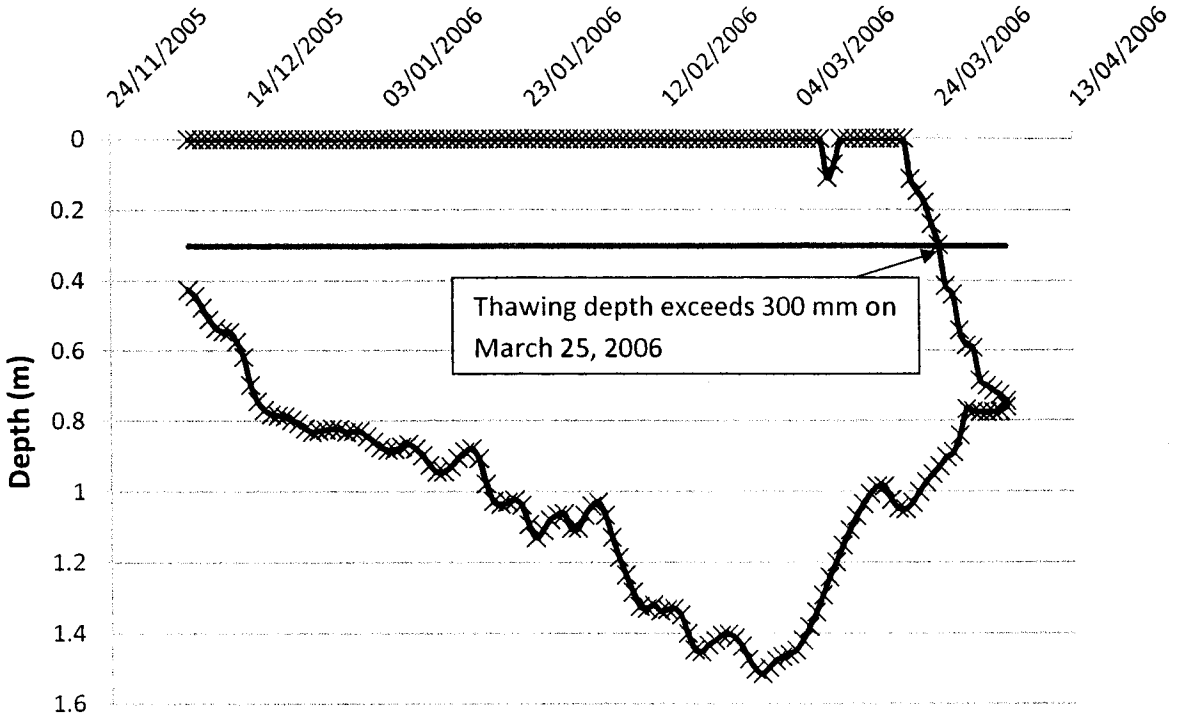

Figure 4.1 Frost/Thaw Depths for Highway 569, 2005/2006 Season

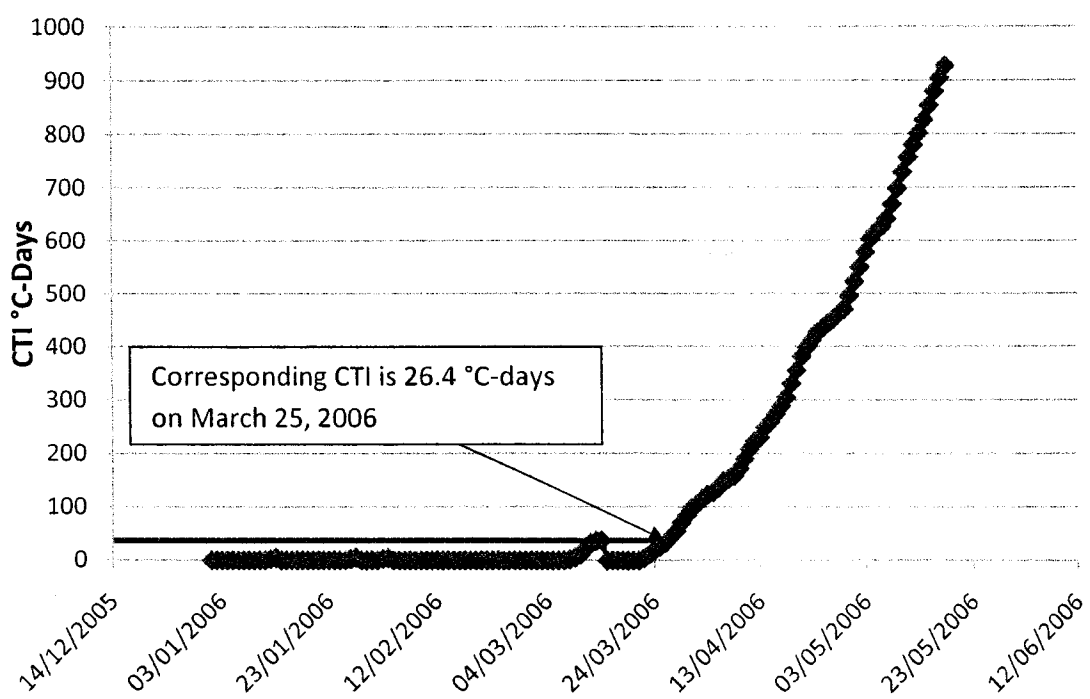

Figure 4.2 Corresponding Cumulative Thawing Index (CTI) for Highway 569, 2005/2006 Season

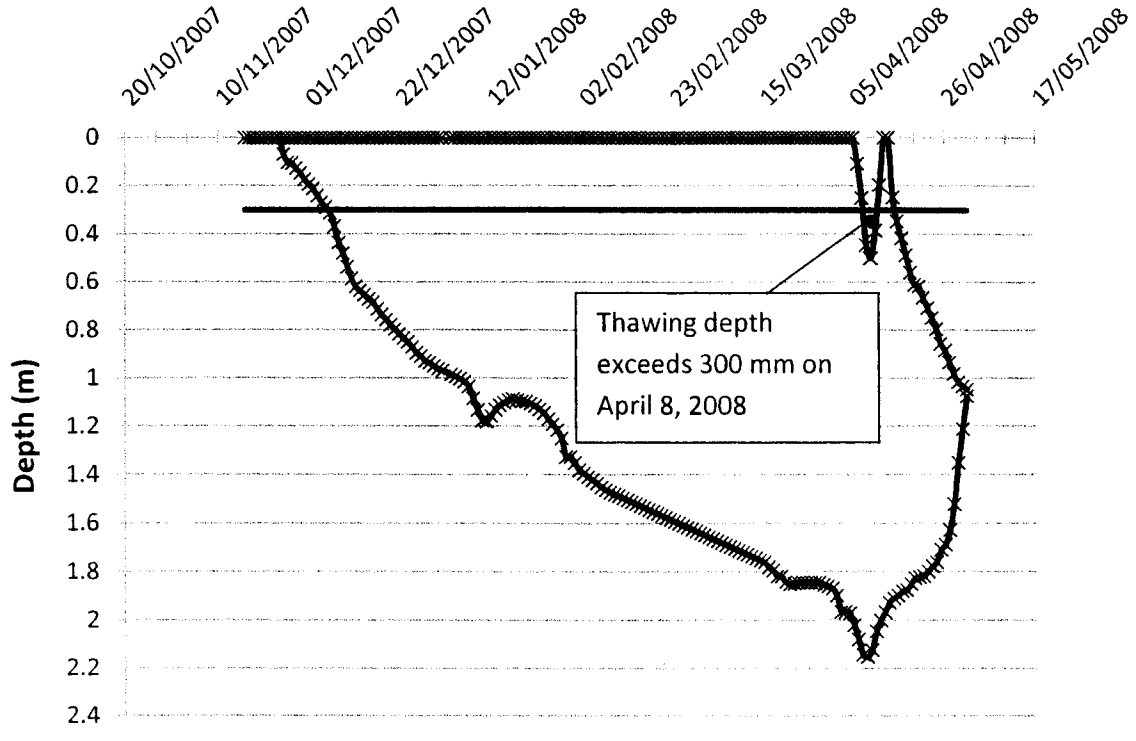

Figure 4.3 Frost/Thaw Depths for Highway 569, 2007/2008 Season

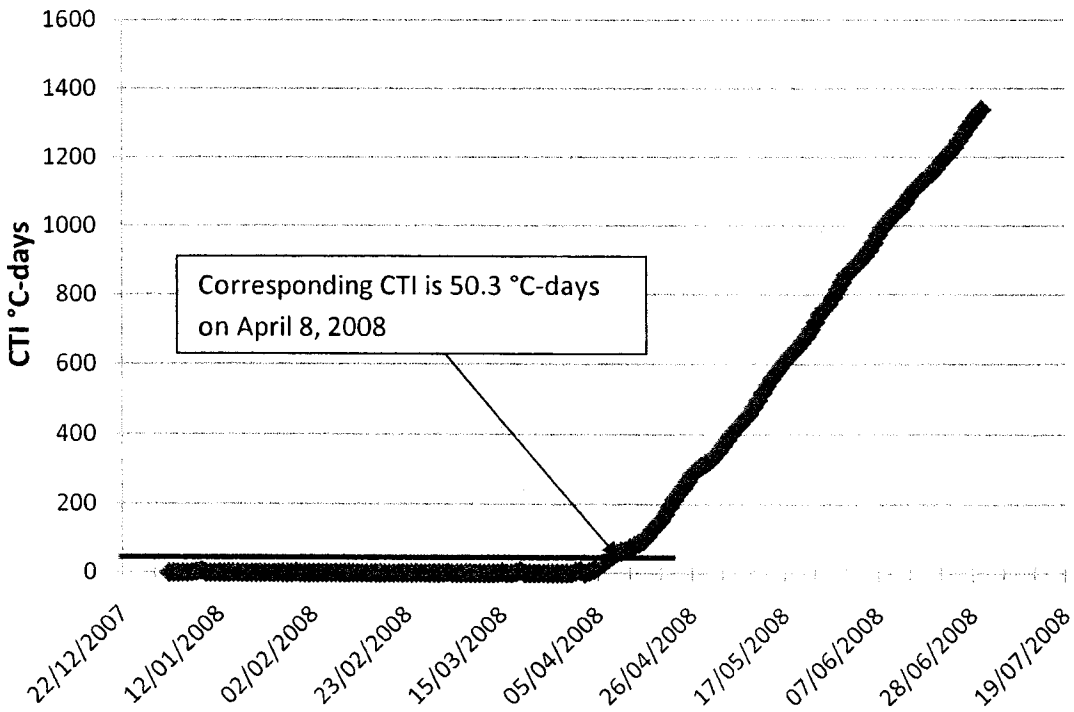

Figure 4.4 Corresponding Cumulative Thawing Index (CTI) for Highway 569, 2007/2008 Season

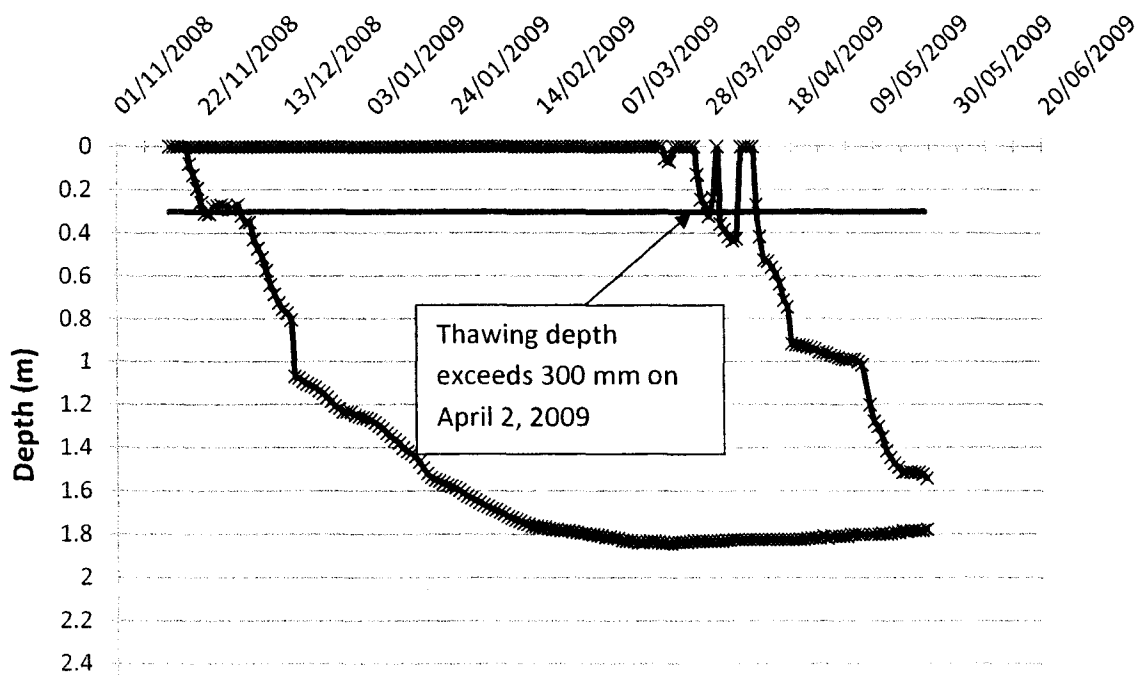

Figure 4.5 Frost/Thaw Depths for Highway 569, 2008/2009 Season

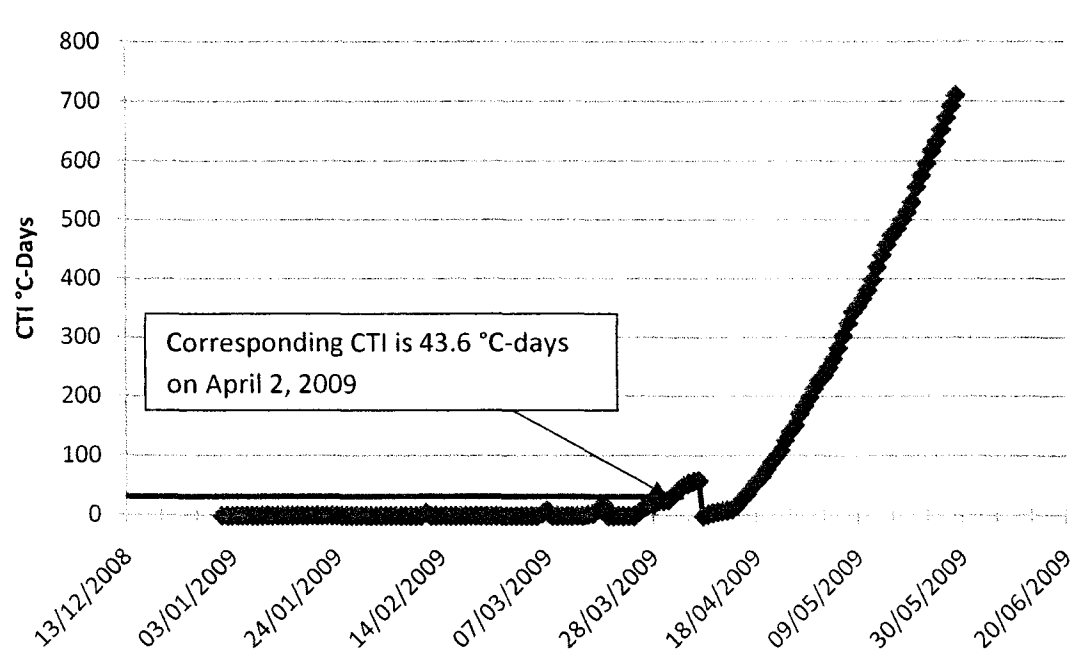

Figure 4.6 Corresponding Cumulative Thawing Index (CTI) for Highway 569, 2008/2009 Season

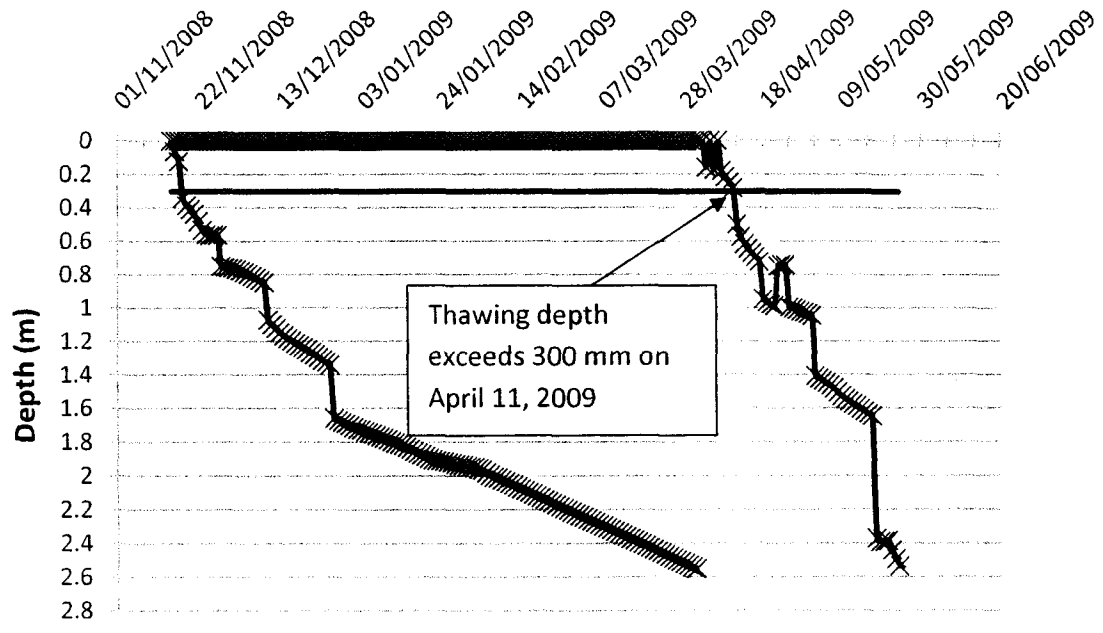

Figure 4.7 Frost/Thaw Depths for Highway 527, 2008/2009 Season

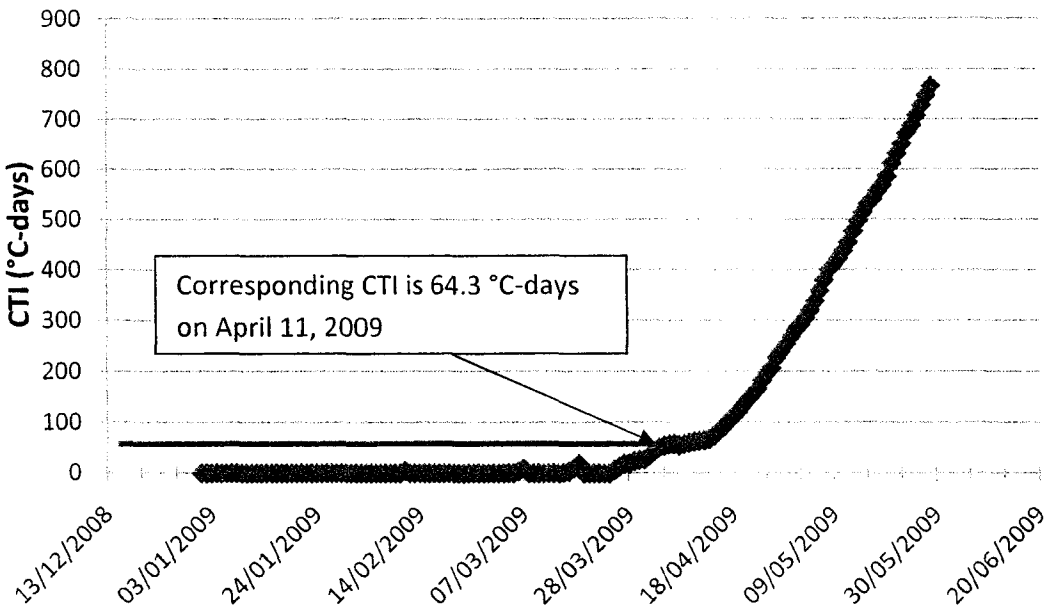

Figure 4.8 Corresponding CTI for Highway 527, 2008/2009 Season

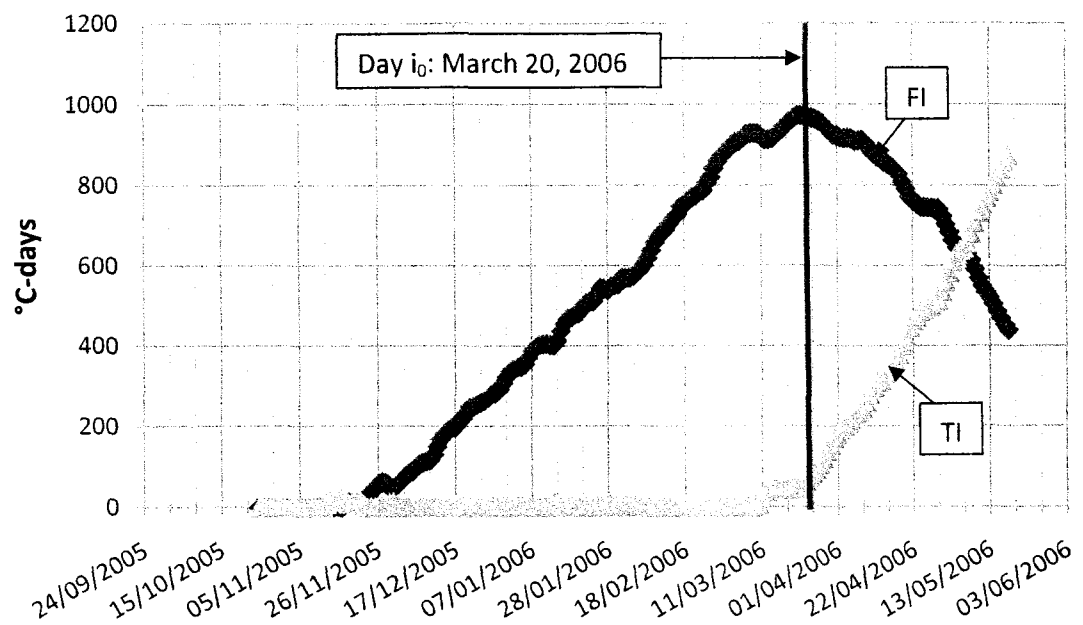

Figure 4.9 FI and TI values for Highway 569, 2005/2006 Season

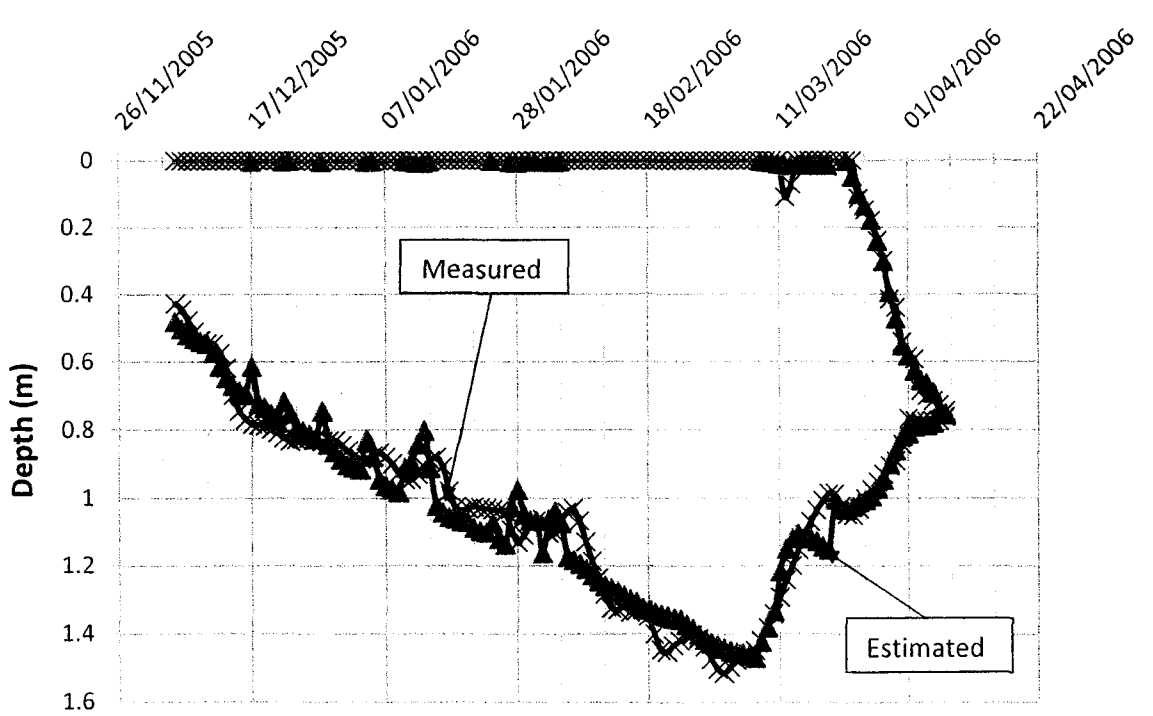

Figure 4.10 Waterloo Frost and Thaw Estimation for Highway 569, 2005/2006 Season

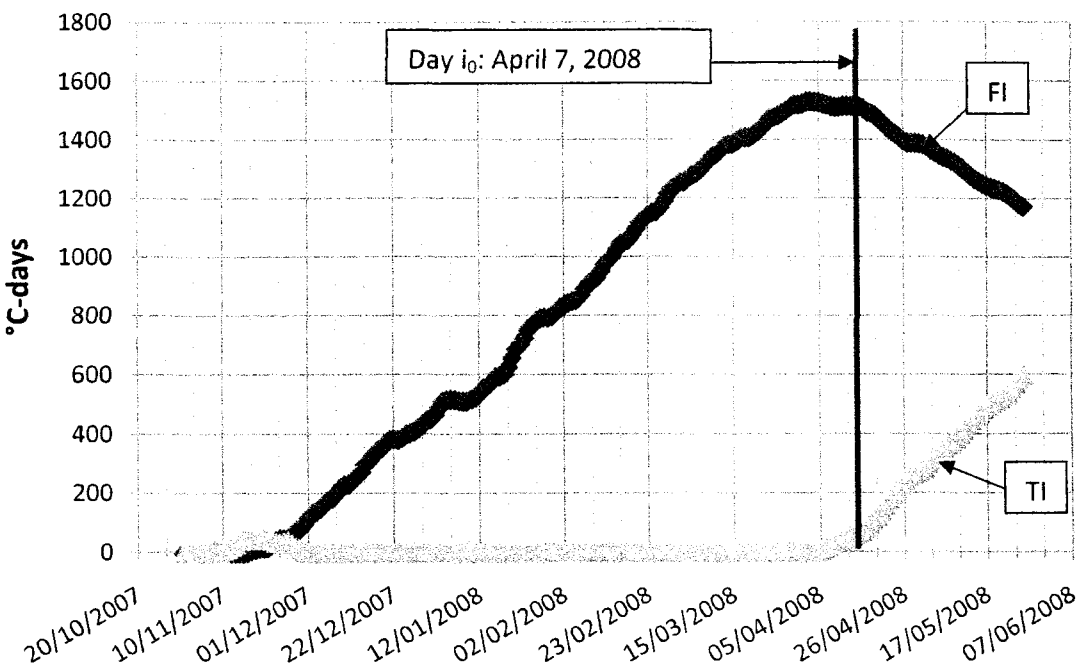

Figure 4.11 FI and TI Values for Highway 569, 2007/2008 Season

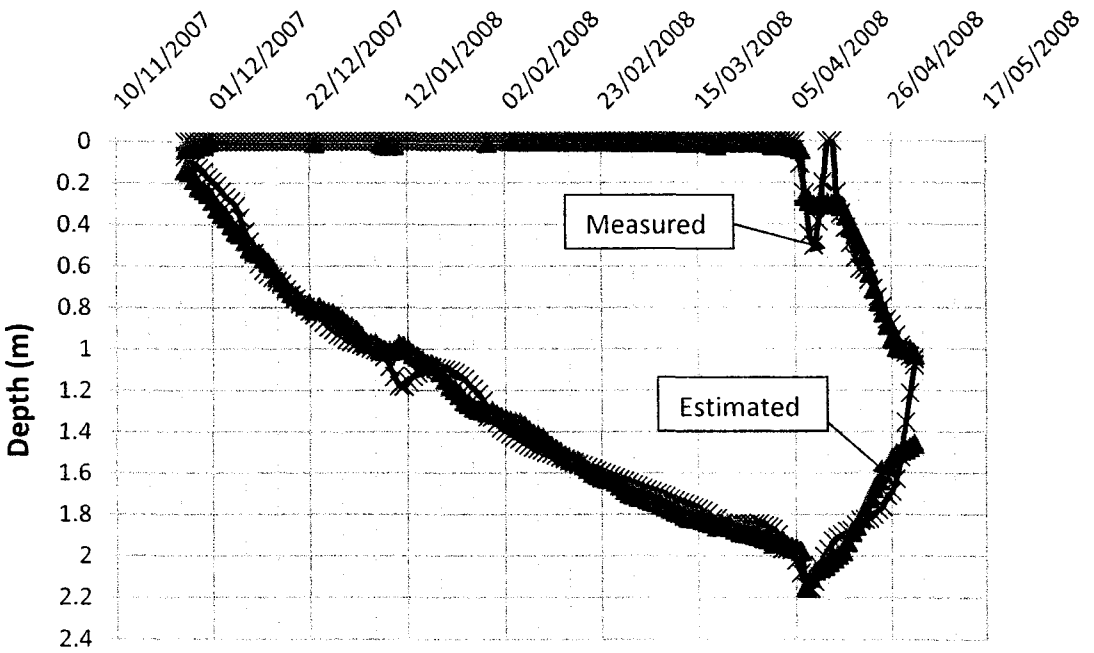

Figure 4.12 Waterloo Frost and Thaw Estimation for Highway 569, 2007/2008 Season

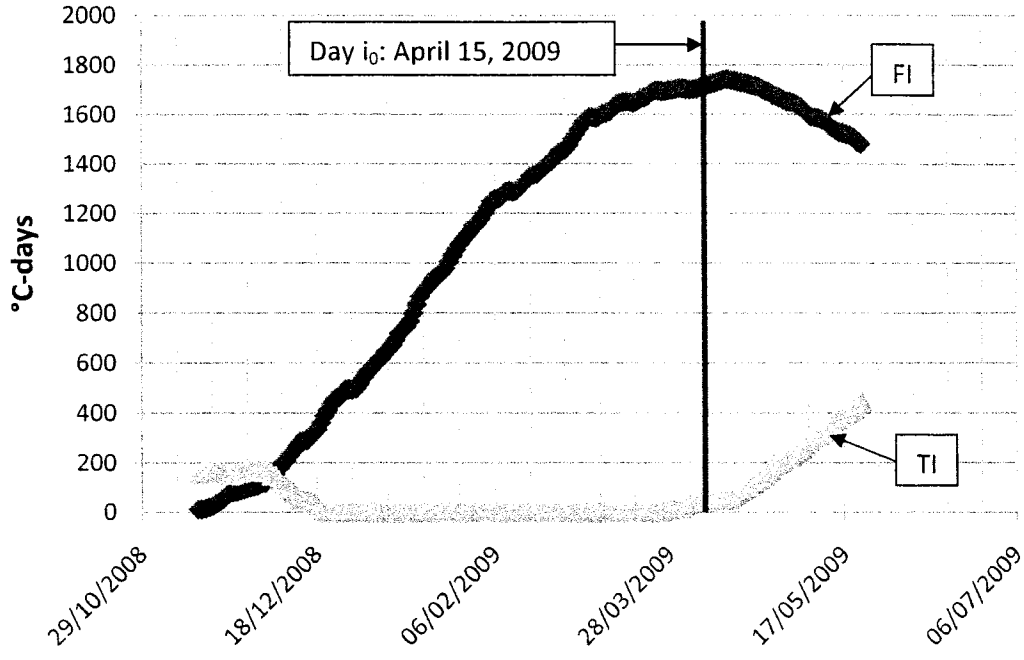

Figure 4.13 FI and TI Values for Highway 569, 2008/2009 Season

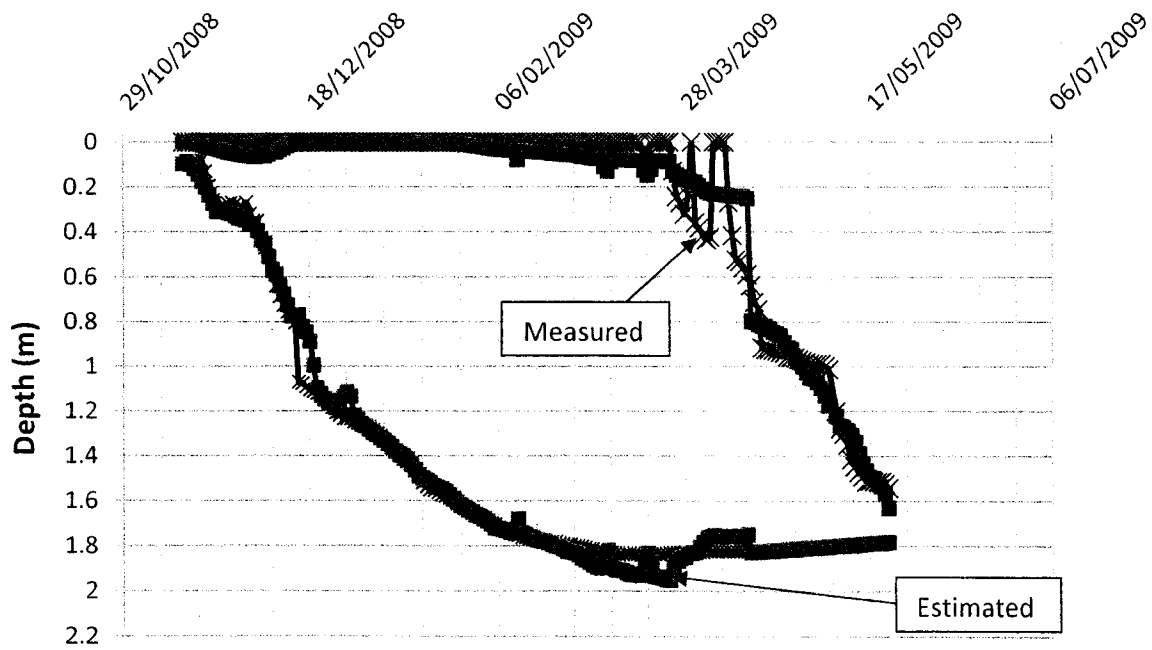

Figure 4.14 Waterloo Frost and Thaw Estimation for Highway 569, 2008/2009 Season

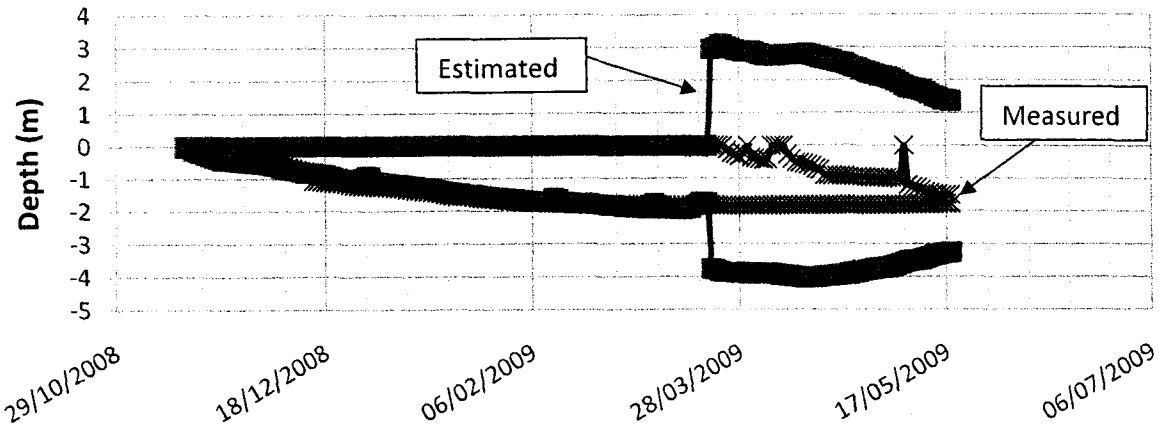

Figure 4.15(a) 2008/2009 Waterloo Prediction of frost and thaw depths using 2005/2006 Calibration Values (Highway 569)

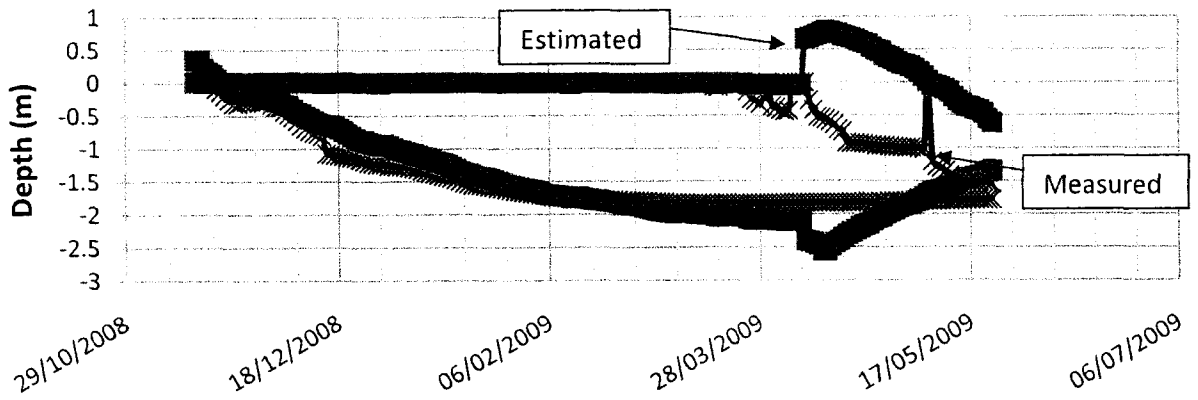

Figure 4.15(b) 2008/2009 Waterloo Prediction frost and thaw depths using 2007/2008 Calibration Values (Highway 569)

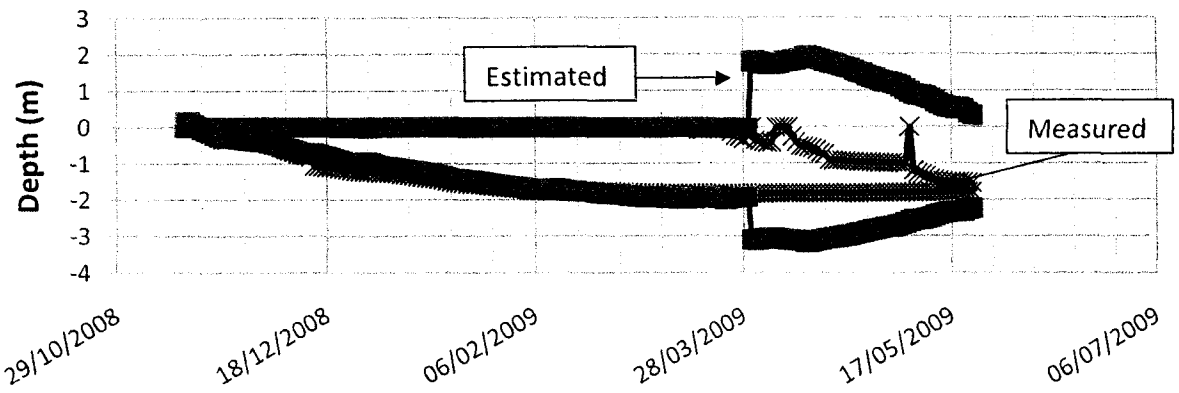

Figure 4.15(c) 2008/2009 Waterloo Prediction of frost and thaw depths using Average Calibration Values (Highway 569)

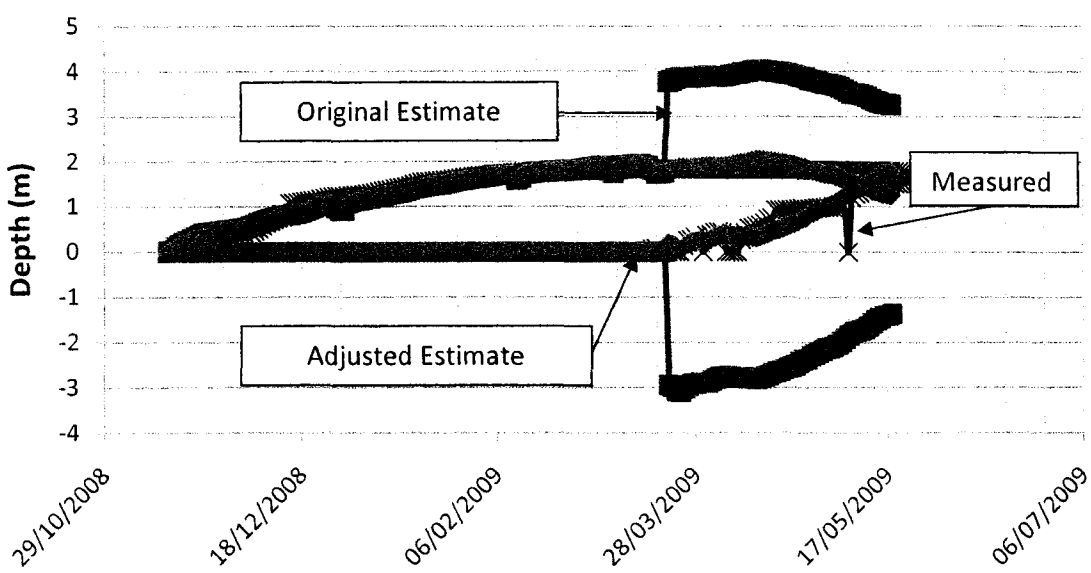

Figure 4.16 Waterloo Method Prediction for 2008/2009 at Highway 569 using Original and 2005/2006 Calibration Coefficients

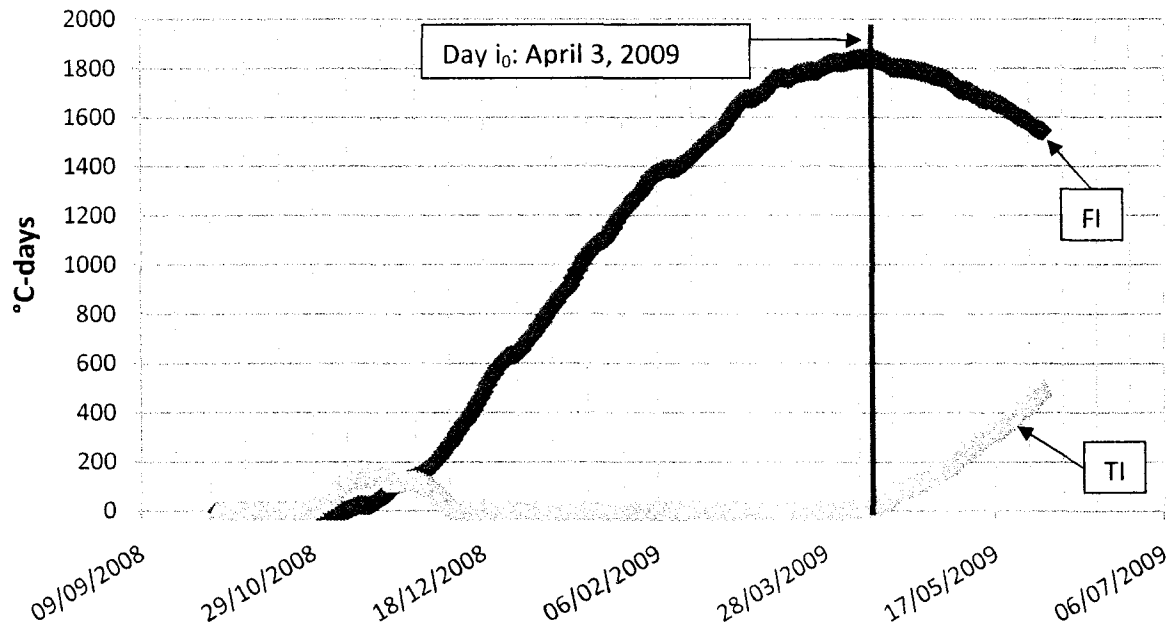

Figure 4.17 Freezing Index (FI) and Thawing Index (TI) Values for Highway 527, 2008/2009 Season

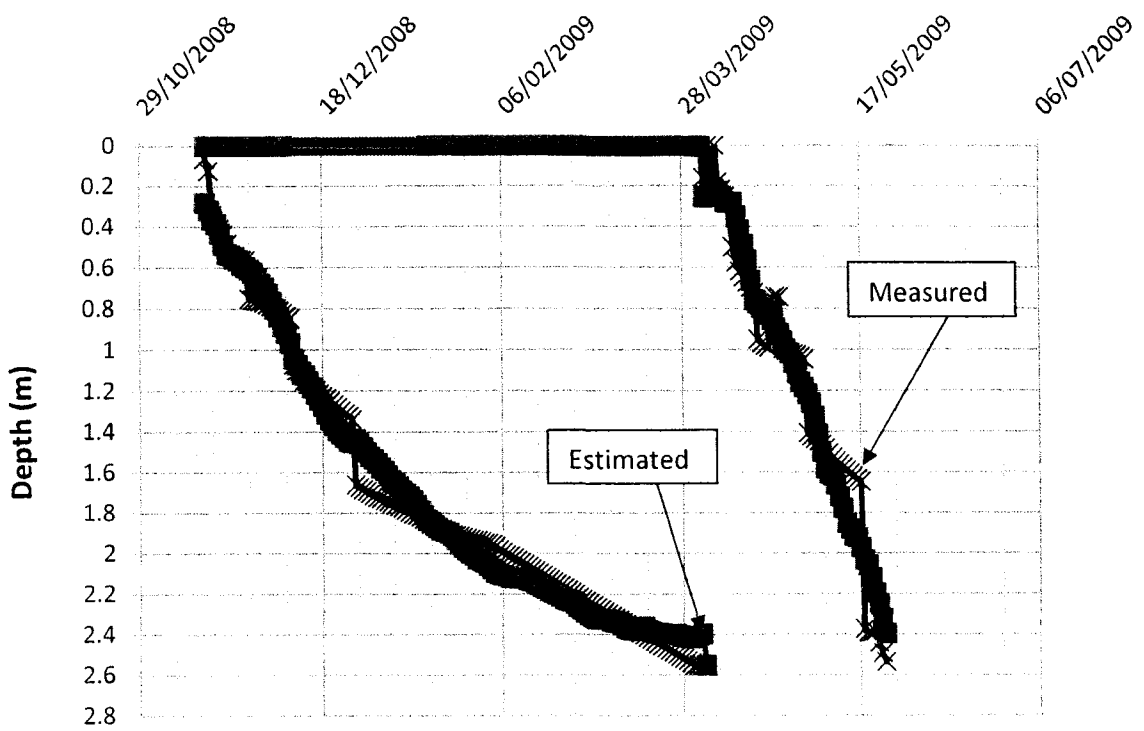

Figure 4.18 Waterloo Frost and Thaw Estimation for Highway 527, 2008/2009 Season

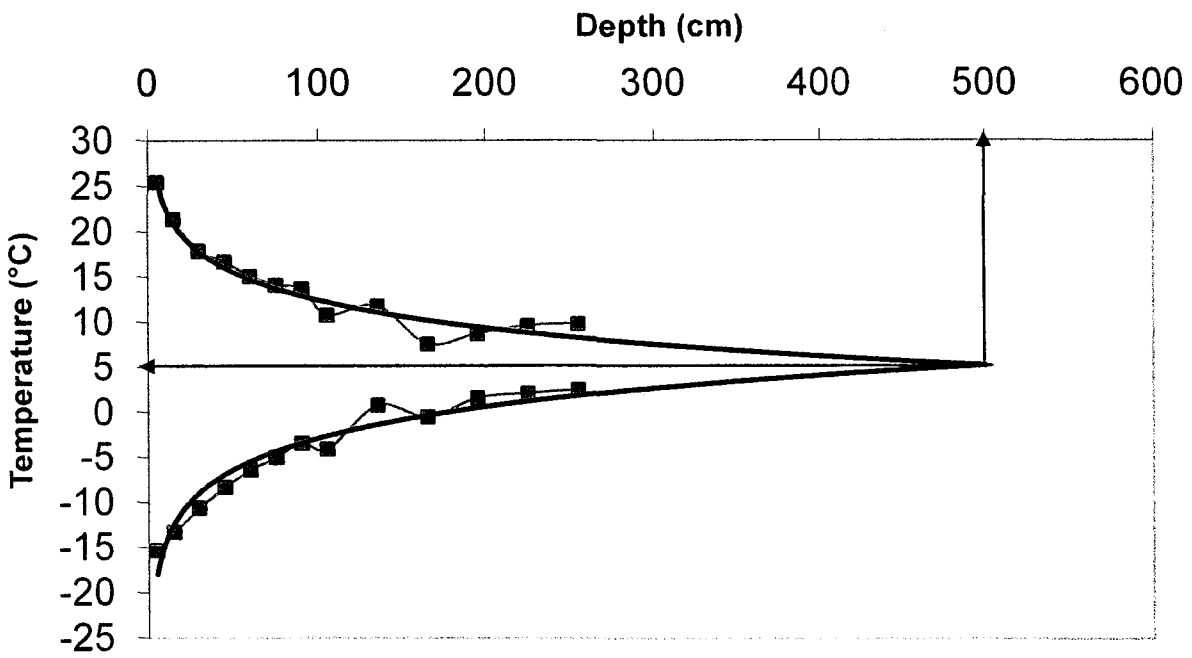

Figure 4.19 Maximum and Minimum Temperature Values Recorded at Each Thermistor and their Use in Determination of the Constant Bottom Temperature Boundary Condition at the Highway 569 Study Site

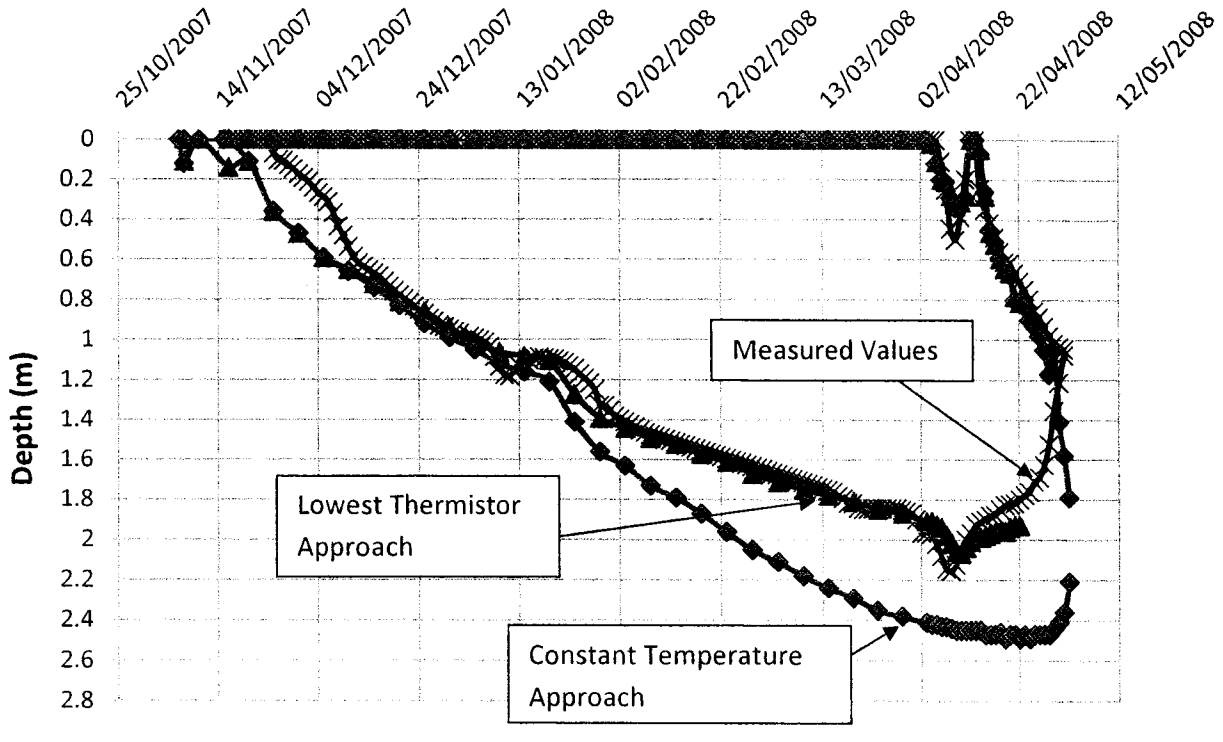

Figure 4.20 Lower Boundary Condition Examination for Highway 569, 2007/2008 Season

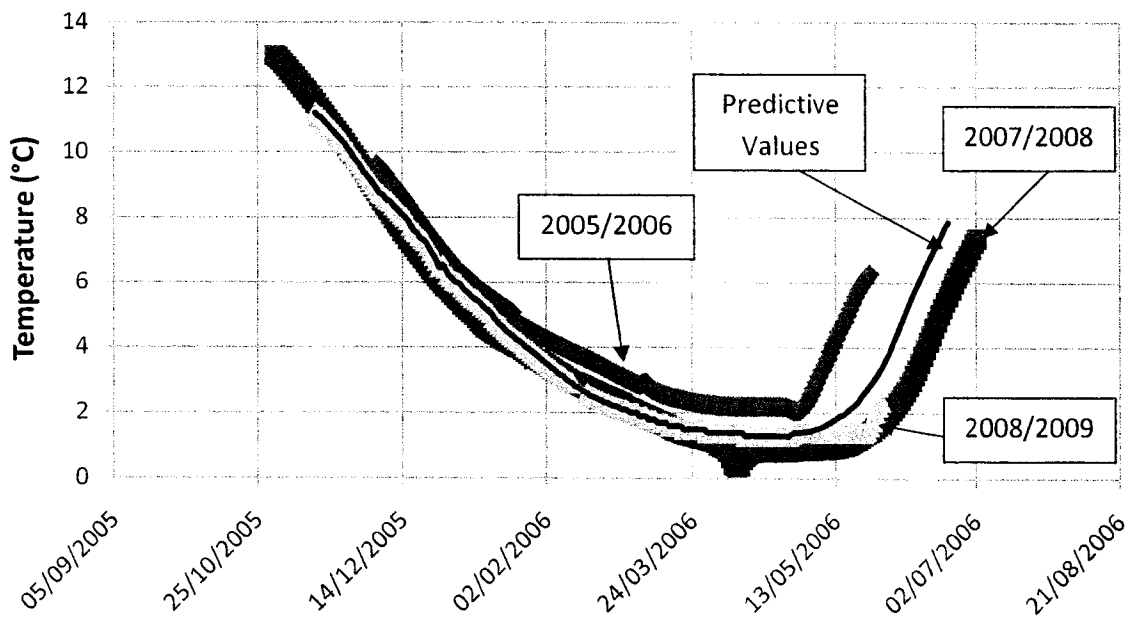

Figure 4.21 Lowest Thermistor Predictive Value Determination for the Highway 569 Study Site

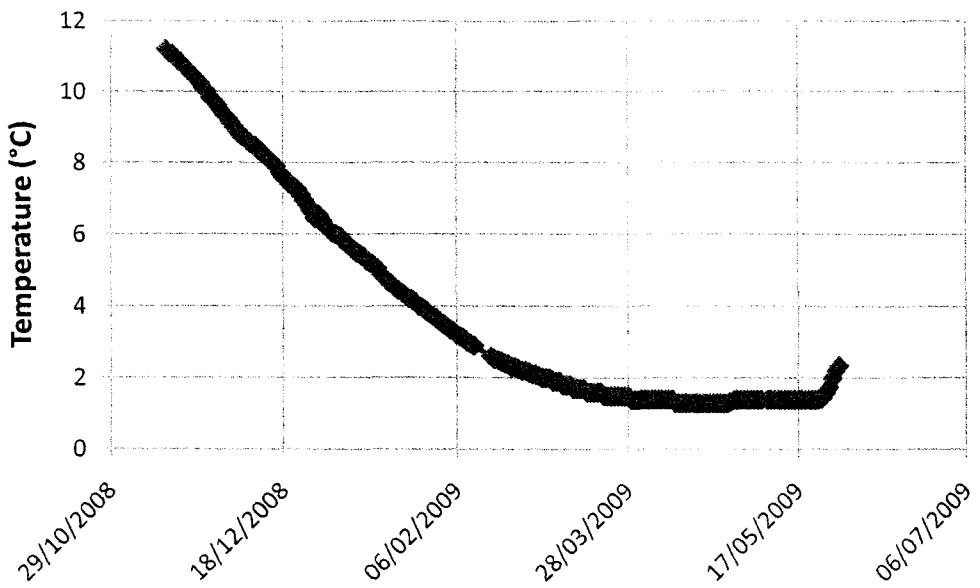

Figure 4.22 Lowest Thermistor Predictive Value Determination for the Highway 527 Study Site

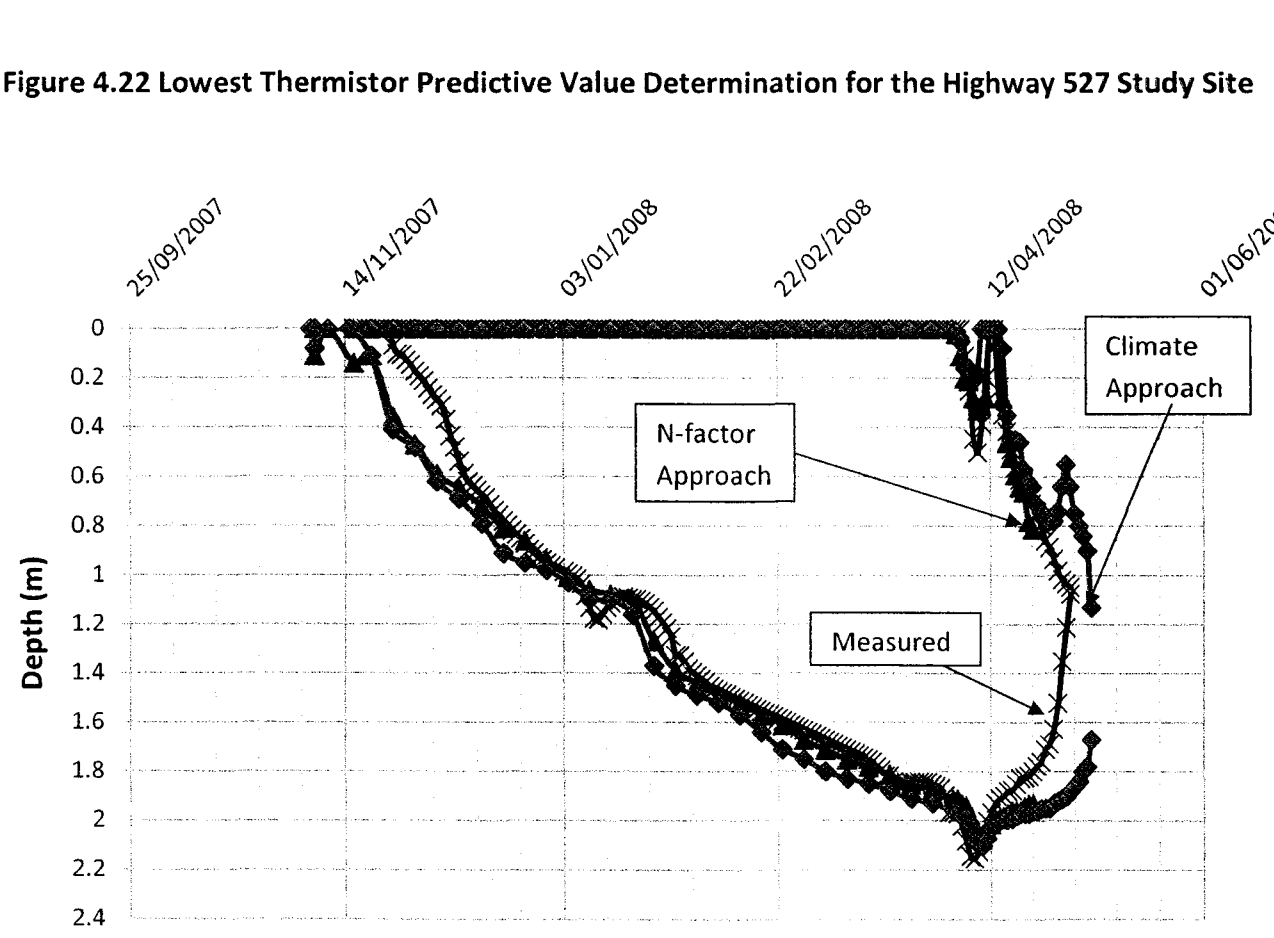

Figure 4.23 Examination of the N-factor and Climate Approach Upper Boundary Conditions for Highway 569 During the 2007/2008 Season

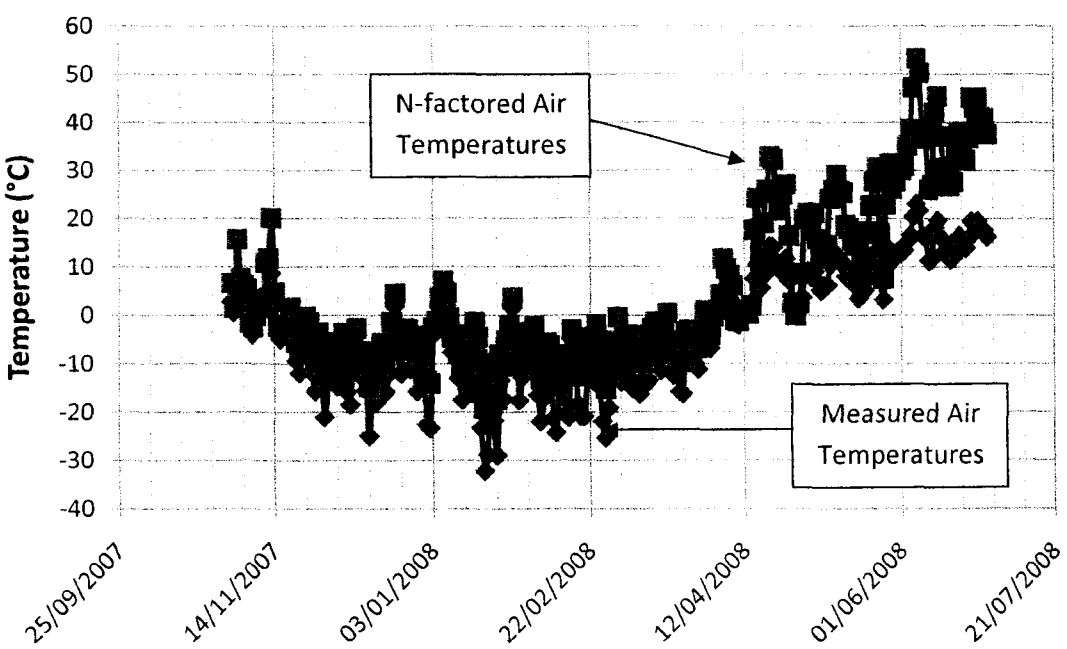

Figure 4.24 Air and N-factored Air Temperatures at the Highway 569 Study Site (2007/2008)

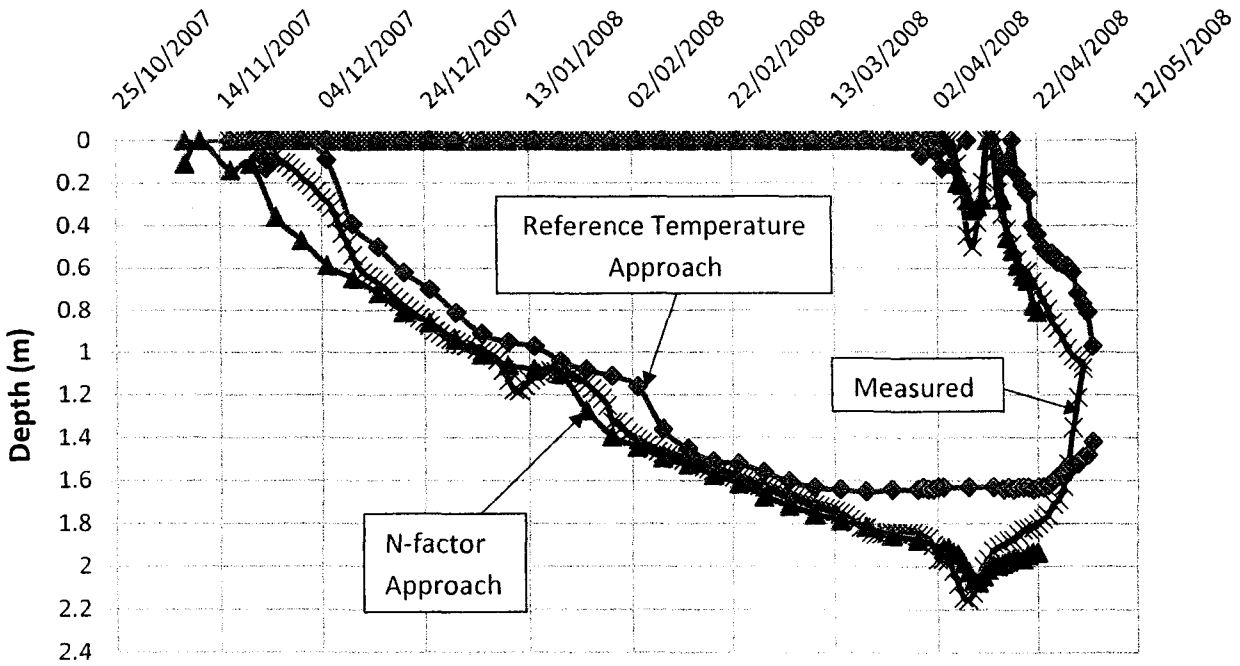

Figure 4.25 Examination of the N-factor and Reference Temperature Approach Upper Boundary Conditions for Highway 569 During the 2007/2008 Season

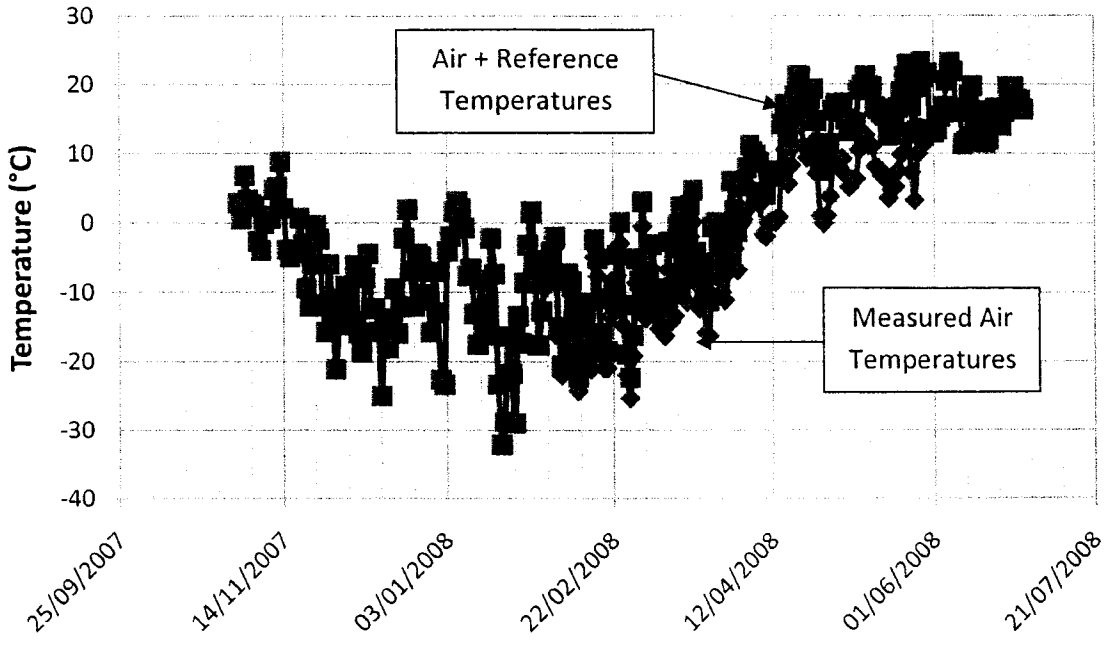

Figure 4.26 Air and Air with Additional Reference Temperatures at the Highway 569 Study Site (2007/2008)

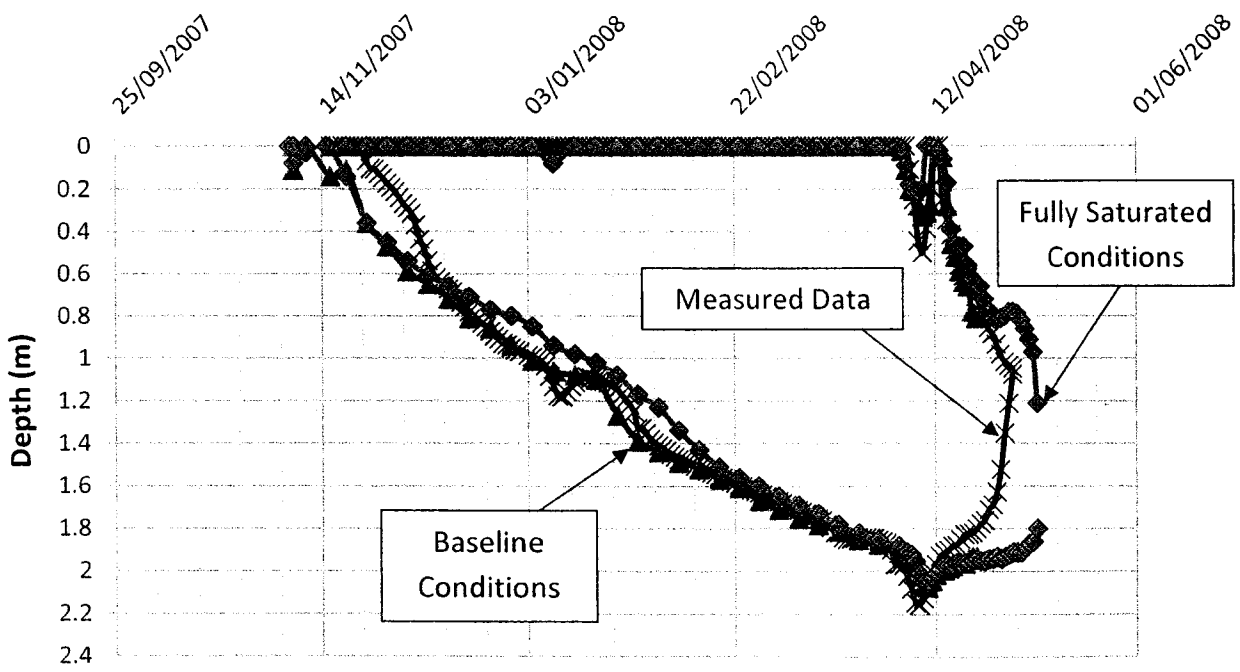

Figure 4.27 Sensitivity of the Thermal Model Under Fully Saturated Pavement Structure Materials Condition at the Highway 569 Study Site (2007/2008)

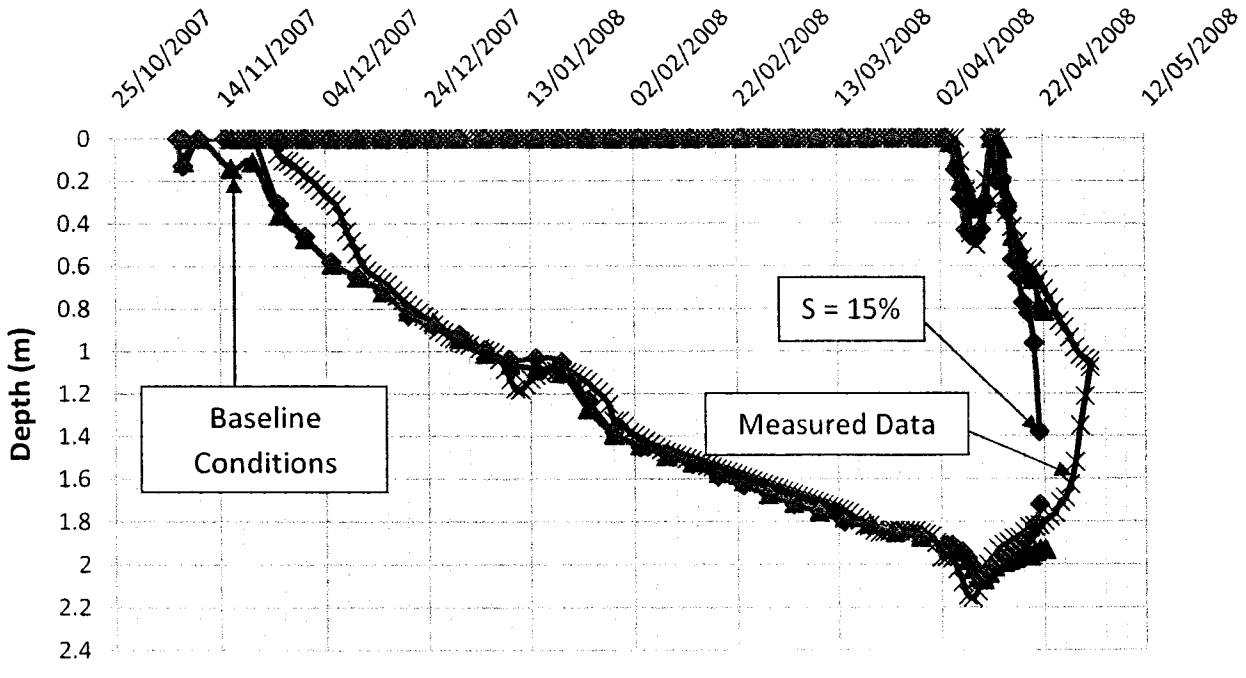

Figure 4.28 Sensitivity of the Thermal Model to Residual Degree of Saturation (15%) Conditions at the Highway 569 Study Site (2007/2008)

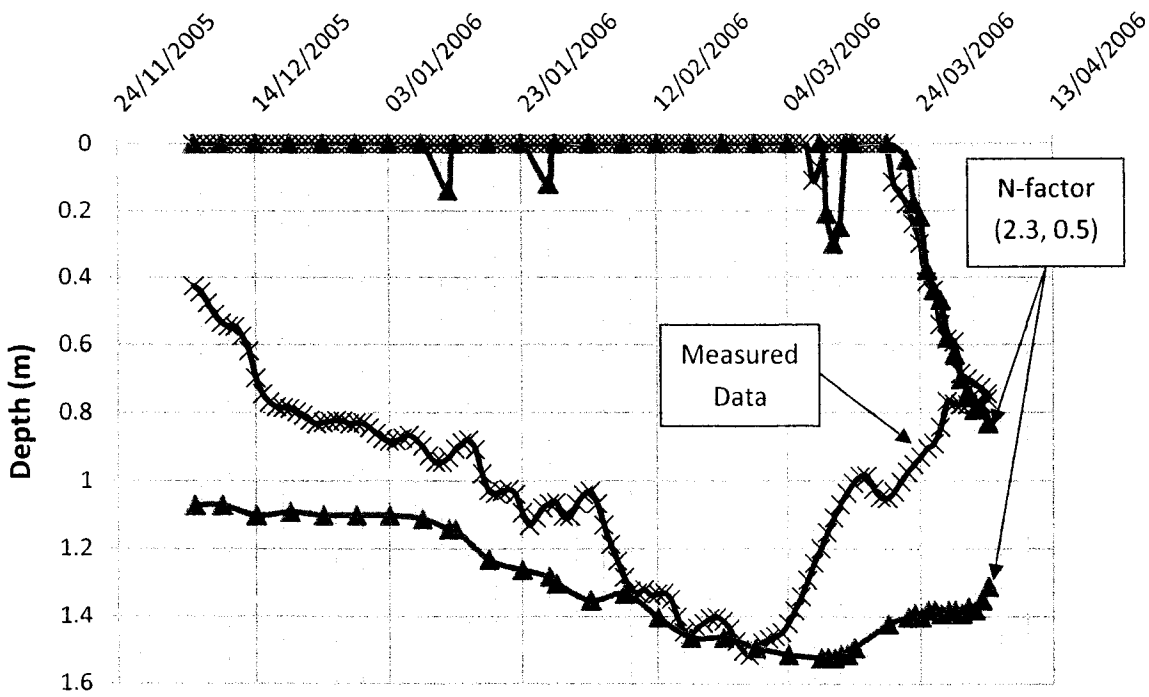

Figure 4.29 TEMP/W Calibration of the Frost and Thaw Depth Simulations for Highway 569 for the 2005/2006 Season

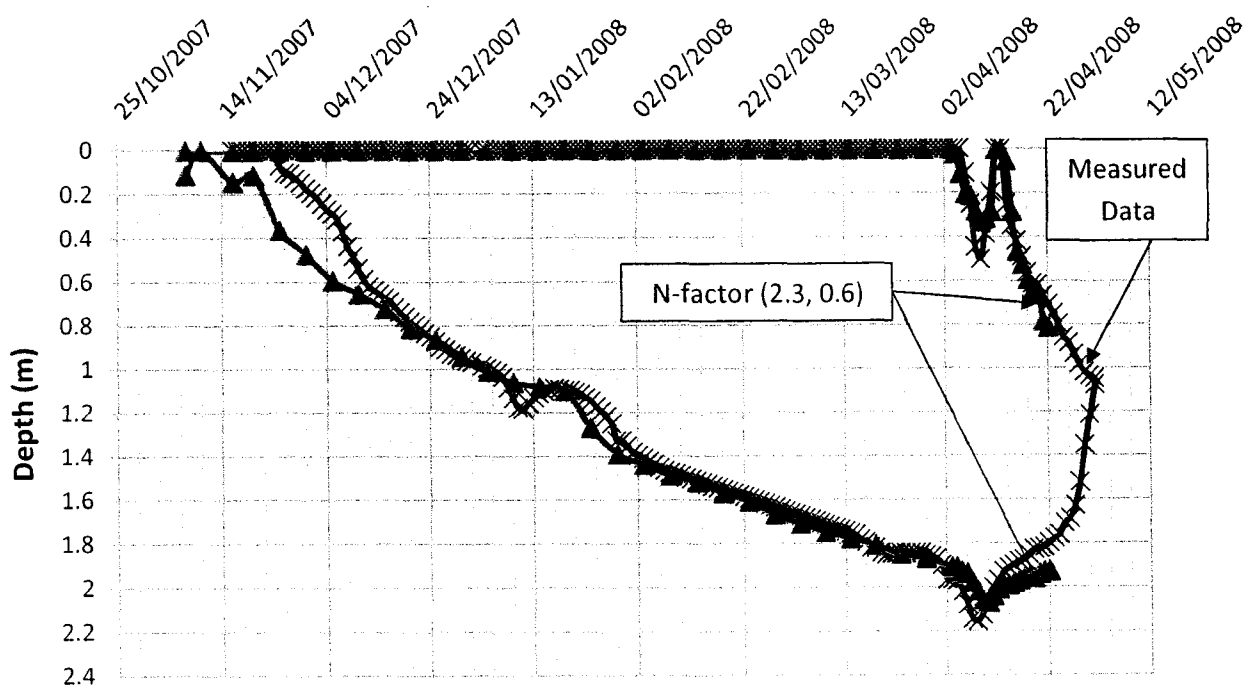

Figure 4.30 TEMP/W Calibration of the Frost and Thaw Depth Simulations for Highway 569 for the 2007/2008 Season

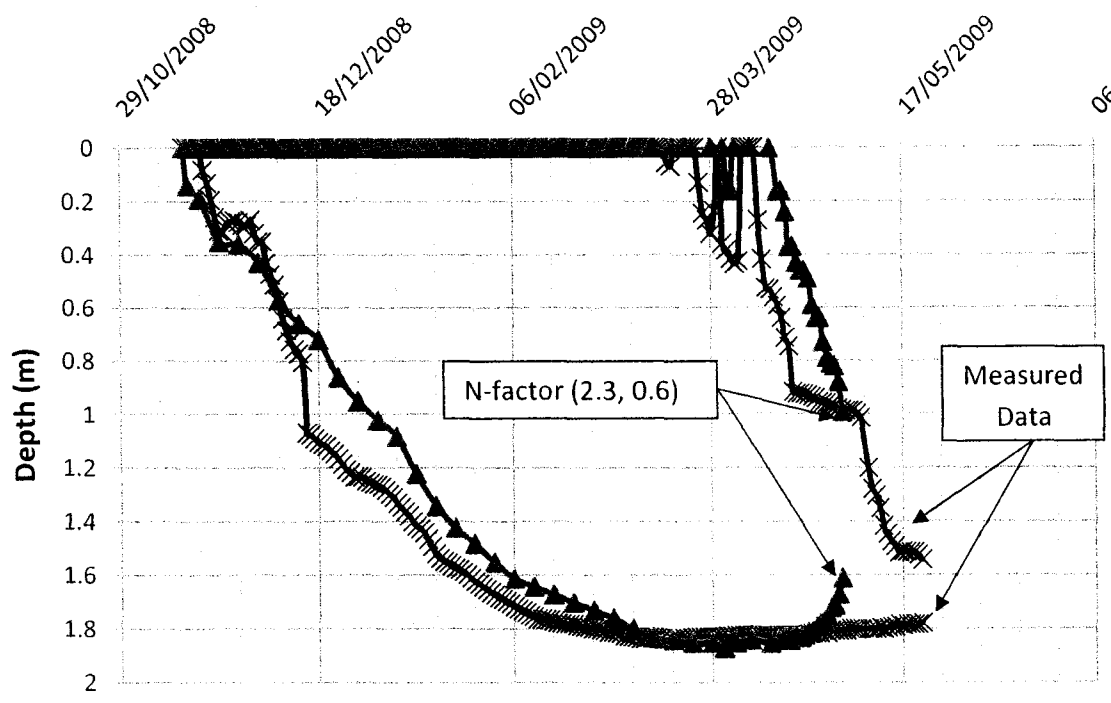

Figure 4.31 TEMP/W Calibration of the Frost and Thaw Depth Simulations for Highway 569 for the 2008/2009 Season

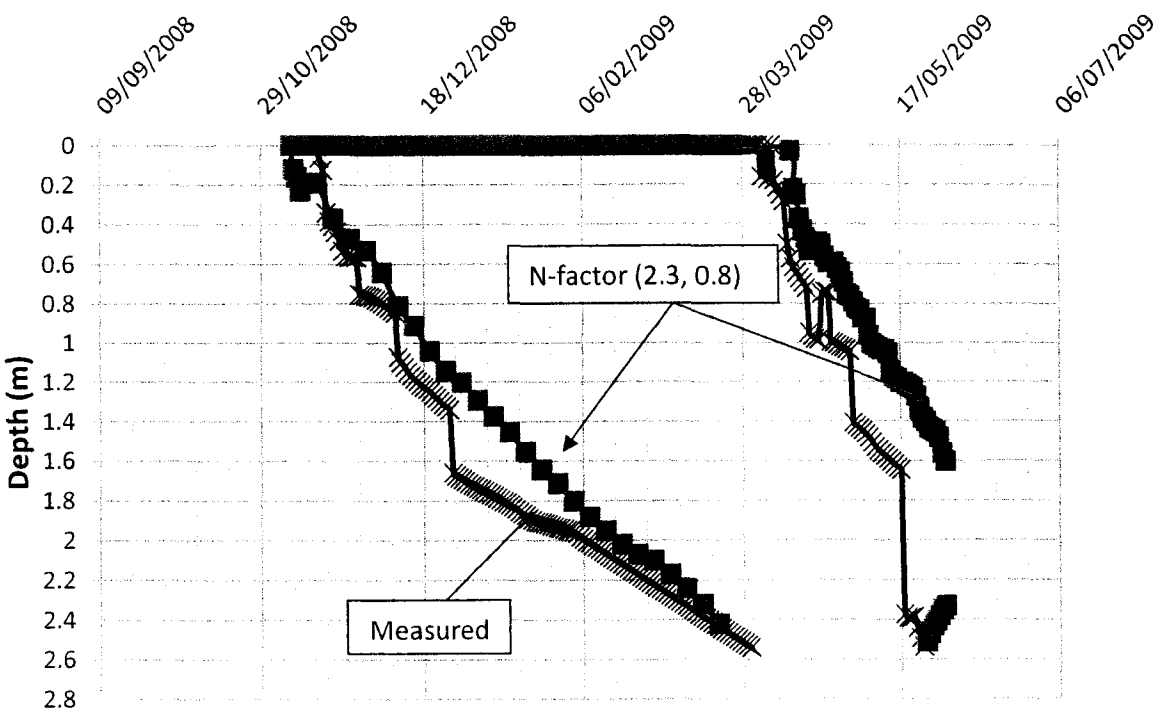

Figure 4.32 TEMP/W Calibration of the Frost and Thaw Depth Simulations for Highway 527 for the 2008/2009 Season

5.0 Pavement Deflection Data Collection and Analysis for Northern Ontario Study Sites

5.1 Data Collection Procedures

Pavement stiffness testing was conducted using an LWD at both the Highway 569 and Highway 527 study sites. This testing was conducted beginning at the start of the freezing season, until the pavement stiffness exceeded the limits of the LWD and again at the onset of the thawing season, until deflections had reduced to summer baseline deflection or surface deflection modulus measurements. Tables 5.1 and 5.2 indicate the dates when LWD testing was conducted at the Highway 569 and 527 locations, respectively.

At both the Highway 569 and 527 study sites 30 LWD test points were established following the procedures outlined in Appendix F, and shown in Figure 5.1. At the Highway 569 study site fifteen of the test points were located along the centerline of the eastbound lane and fifteen were located along the centerline of the westbound bound lane (Figure 5.2). At the Highway 527 study site fifteen of the LWD test points were located in the northbound lane while the other fifteen were located in the southbound lane (Figure 5.3).

Following the LWD testing procedure outlined by Steinert et al. (2005), 6 drops of the maximum weight (20 kg) from the maximum drop height (approximately 850 mm) were used to generate the greatest force on the pavement surface (Figure 5.4). A bottom plate diameter of 300 mm was used in all testing. In some cases additional geophones were connected to the LWD to measure deflections at specified distances from the center of the LWD, however, these results provided little additional, useful data for the overall analysis of the pavement stiffness and were therefore not used. The exclusion of the additional geophone data is also in agreement with the Steinert et al. (2005) LWD procedure.

At each location the first drop was omitted from analysis as it was used to set the LWD. Subsequent drops were monitored on a Personal Data Assistant (PDA) and any abnormal drops were omitted and additional drops were conducted in order to maintain the required 5 useable drops per test location. The drop statistics were collected in the PDA and at the cessation of testing were transferred to a lap top computer where further analysis using the LWDmod software could be conducted.

Surface deflections were examined and the corresponding surface deflection moduli were calculated with the LWDmod software. These data were compared with measured frost and thaw depths to establish a correlation between pavement stiffness, measured as increases or decreases in deflection and surface deflection modulus, and the frozen and thawed pavement structure conditions.

In addition, side-by-side testing of the LWD with a FWD was conducted at the Highway 569 study site for 5 testing periods between March 17, 2008 and May 5, 2008 (Table 5.1). Analysis will be conducted to assess the correspondence between LWD measured parameters and FWD measured parameters.

5.2 Pavement Stiffness Data Collected at Northern Ontario Low Volume Roads by the MTO and LU

As described in Section 5.1, LWD testing was carried out at the Highway 527 site during the 2008 spring thawing period and the 2008/2009 and 2009/2010 winter/spring seasons. Lakehead University performed the LWD testing during 2008/2009 winter/spring season at the Highway 527 study site, while the Ministry of Transportation of Ontario (MTO) conducted the spring 2008 and the 2009/2010 winter/spring season testing. Furthermore, the MTO performed all of the testing at the Highway 569 study site during the 2008/2009 season. Although the testing was performed by two parties, the same testing procedures and guidelines were maintained at both locations during all testing events. These tests provided both freezing season and thawing season surface deflection measurements and surface modulus values at the test sites. The LWD data were formatted for analysis and compared with the observed frost and thaw depths at their respective sites. This comparison was conducted to observe the

effects that freezing and thawing of the pavement structure have on pavement stiffness. Data collection guidelines and procedures are described in Section 5.1. The surface modulus results were determined by taking the average of all the LWD surface modulus measurements from all of the testing locations described in Appendix F (i.e. the average of 150 drops per study site per testing day).

5.2.1 Pavement Deflection Testing Comparison with Measured Frost and Thaw Depth for the Highway 569 Site

The results of LWD testing at the Highway 569 study site during the spring of 2008 (Figure 5.5) provide little useable data during the thawing period, as the testing was conducted either before the initiation of the spring thaw or after the pavement structure had fully thawed (see Table 5.1 for Highway 569 testing dates). An examination of the data does indicate, however, that the pavement stiffness was inexplicably reduced prior to any thawing in the pavement structure. Furthermore, it can be seen in Figure 5.5 that an increase in surface modulus occurs after complete subsurface thawing, at some time between May 2, 2008 and May 15, 2008. This is in accordance with Berg (2010) who noted that pavement stiffness would be restored approximately 7 days after complete subsurface thawing.

Only three sets of LWD tests were performed at the Highway 569 study site during the spring thaw period in 2009, limiting the analysis for this time period. Figure 5.6 does however provide evidence that the surface modulus of the pavement structure was reduced after the initiation of thawing. The results of this testing also indicate that the pavement stiffness began to slightly recover prior to complete subsurface thawing.

5.2.2 Pavement Deflection Testing Comparison with Measured Frost and Thaw Depths for the Highway 527 Site

During the spring 2008 season the MTO performed a series of four LWD tests at the Highway 527 study site (see Table 5.2 for testing dates). Figure 5.7 indicates the surface modulus values from the results of these tests and the corresponding frost and thaw depths. It can be seen in

Figure 5.7 that after the thawing depth at the Highway 527 study site exceeds 0.3 m, the pavement stiffness as represented by the surface modulus is reduced by more than half from.

LWD testing was carried out for five weeks at the Highway 527 study site during the 2008 freezing season beginning on October 24, 2008 and ending on December 10, 2008 (see Table 5.2 for Highway 527 testing dates). These test results are used to assess changes in pavement stiffness as the pavement structure froze. Figure 5.8 shows the surface deflection modulus values obtained from the LWD results and the corresponding frost depths. It can be seen in Figure 5.8 that for the three weeks of testing prior to the presence of subsurface frost the measured pavement surface modulus was on average 261 MPa. Shortly after frost penetrated the subsurface (to a depth of approximately 0.4 m) the measured pavement surface modulus, from a test on November 21, 2008, increased to 8690 MPa, 33 times larger than the modulus values of the previous test. Further to this, an additional test was carried out on December 17, 2008. This test indicated that the pavement structure was too stiff for the small force exerted by the LWD to create a surface deflection, therefore no pavement surface modus value could be calculated.

Further LWD testing was performed at both the Highway 527 site (Table 5.2) during the 2009 spring season. A comparison of the frost and thaw depths with surface modulus values for the 2009 thawing season at the Highway 527 site are provided in Figure 5.9. As with the values for the 2008 spring thaw period at Highway 527 (Figure 5.7), the 2009 spring thaw surface modulus values are significantly reduced as a result of pavement structure thawing. The surface modulus values prior to the onset of pavement structure thawing however, indicate an inexplicable increase from around 700 MPa to 1900 MPa. During the spring of 2009 after this increase, the surface modulus values are reduced when the pavement structure thaws to a depth of 0.3 m (Figure 5.9) compared with a 0.4 m thaw depth in the spring of 2008.

LWD testing was continued at the Highway 527 study site during the spring of 2010. The results of these tests indicate again that during the initial thawing period, the pavement surface modulus values are significantly reduced (Figure 5.10). For the 2010 spring thawing period, a thawing depth of 0.2 m resulted in a significant surface deflection modulus reduction. Further

to this, the refreeze period between May 25, 2010 and May 29, 2010 appeared to have no effect on the surface modulus.

5.2.3 LWD and FWD Comparison for Northeastern Ontario Study Sites

During the 2008 spring thawing season side-by-side testing of the LWD and a FWD were conducted at the Highway 569, Highway 66 and Highway 624 low volume road test sites in northeastern Ontario. Pavement structure profile information for the Highway 66 and Highway 624 study sites is provided in Tables 5.3 and 5.4, respectively.

When examining the modulus values, research suggests that LWD composite modulus values should be modified by a specified factor to obtain corresponding FWD composite modulus values. This modification factor is to account for the smaller drop weights and variances in the testing procedures. Research by Steinert et. al (2005) found that when pavement layers are thin, as they are at the Highway 569 and Highway 624 study sites, a comparison of composite modulus values indicates that a LWD modulus = 1.33 FWD modulus correlation provides the highest coefficient of determination (R^2) values (0.87). They also found that when pavement layers are thick, as is the case at the Highway 66 site, a LWD modulus = 0.75 FWD modulus correlation gives the best R^2 value (0.56) under these conditions. Steinert et.al (2005) concluded that "in general terms, correlation coefficients tended to increase as pavement thickness decreased".

The LWDmod software requires the input of estimated seed values (subgrade modulus and exponent on non-linearity) to calculate the composite modulus. This estimation of these values reduces the accuracy of the calculated composite modulus values. As a result of the inaccuracy in determining representative composite modulus values from the LWD surface modulus values obtained from the test results of pavement surface modulus values determined with the LWD will be compared with composite modulus values determined from FWD.

FWD composite modulus values were plotted against corresponding LWD surface modulus values obtained through side-by-side testing (Figure 5.11). The low coefficient of determination (R^2) of 0.52 indicates that the data do not correspondence well. It is also apparent that data scatter becomes higher with higher modulus values. For this reason, values

with FWD composite modulus values greater than 4000 MPa and LWD surface modulus values greater than 2000 MPa were removed from analysis (Figure 5.12). The removal of the FWD composite modulus data is in accordance with Steinert et al. (2005), who note that when composite modulus values exceed 4000 MPa correlation irregularities begin to appear and therefore these data should not be considered. When excluding data that have FWD composite modulus values greater than 4000 MPa and LWD surface modulus values greater than 2000 MPa (Figure 5.12), it can be seen that the R^2 value increases to 0.60 and the number of outliers has been reduced. These findings reinforce the exclusion of FWD composite modulus values above 4000 MPa and LWD surface modulus values greater than 2000 MPa to provide a better statistical fit.

As mentioned previously, Steinert et al. (2005) indicate that as pavement thickness increases the correlation coefficient between LWD and FWD composite modulus values decreases. For this reason, the comparative results from the Highway 569 and Highway 624 study sites, each with a pavement thickness of 25 mm, were separated from data from Highway 66, where the pavement thickness is 270 mm, to observe if this same correlation exists between FWD composite modulus values and LWD surface modulus values. Figure 5.13 indicates the FWD composite modulus and corresponding surface modulus results for the Highway 569 and Highway 624 data, while Figure 5.14 provides the Highway 66 comparison. It can be seen from Figures 5.13 and 5.14 that based on the limited data collected at the three sites, the pavement thickness has little effect on the correlation between the FWD composite modulus values and the corresponding LWD surface modulus as the R^2 value for the thicker pavement layer at Highway 66 (0.65) is the same as the R^2 value for the thinner pavement layer at Highways 569 and 624 (0.65).

A good correlation between the LWD and FWD values would provide increased confidence in using the LWD to determine quantitative pavement structure properties such as elastic modulus values, during freezing and thawing periods. Based on the comparison of the FWD composite modulus values with the LWD surface modulus values however, little support is provided for using the LWD to predict FWD values, based on the low R^2 value in all of the comparisons.

Table 5.1 LWD and FWD Testing Dates at the Highway 569 Study Site

Light Weight Deflectometer (LWD)	Falling Weight Deflectometer (FWD)
April 3, 2006	March 17, 2008
December 6, 2007	April 3, 2008
March 17, 2008	April 16, 2008
April 3, 2008	May 2, 2008
April 16, 2008	May 5, 2008
May 2, 2008	
May 15, 2008	
May 27, 2008	
March 17, 2009	
April 2, 2009	
May 6, 2009	
May 21, 2009	
December 8, 2009	
December 16, 2009	
March 11, 2010	

Table 5.2 LWD Testing Dates at the Highway 527 Study Site

Light Weight Deflectometer (LWD)	Light Weight Deflectometer (LWD) Cont'd.
March 27,2008	March 4, 2010
April 9, 2008	March 11, 2010
April 21, 2008	March 17, 2010
June 3, 2008	March 24, 2010
October 24, 2008	March 30, 2010
October 31, 2008	April 8, 2010
November 14, 2008	April 15, 2010
November 21, 2008	
December 10, 2008	
March 9, 2009	
March 16,2009	
March 23, 2009	
March 30, 2009	
April 9, 2009	
April 16, 2009	

Table 5.3 Highway 66 Pavement Structure Profile

Highway 66	
Depth	Pavement Structure Material
0 - 270 mm	Asphalt Concrete
270 - 430 mm	Granular A
430 - 1005 mm	Silt Fine Sand
1005 - 1450 mm	Silty Clay
1450 - 1900 mm	Silty Fine Sand

Table 5.4 Highway 624 Pavement Structure Profile

Highway 624	
Depth	Pavement Structure Material
0 - 25 mm	Asphalt Surface Treatment
25 - 305 mm	Granular A
305 - 1000 mm	Sand and Gravel
1000 - 1500 mm	Clayey Silt
1500 - 2000 mm	Clayey Silt / Silty Clay

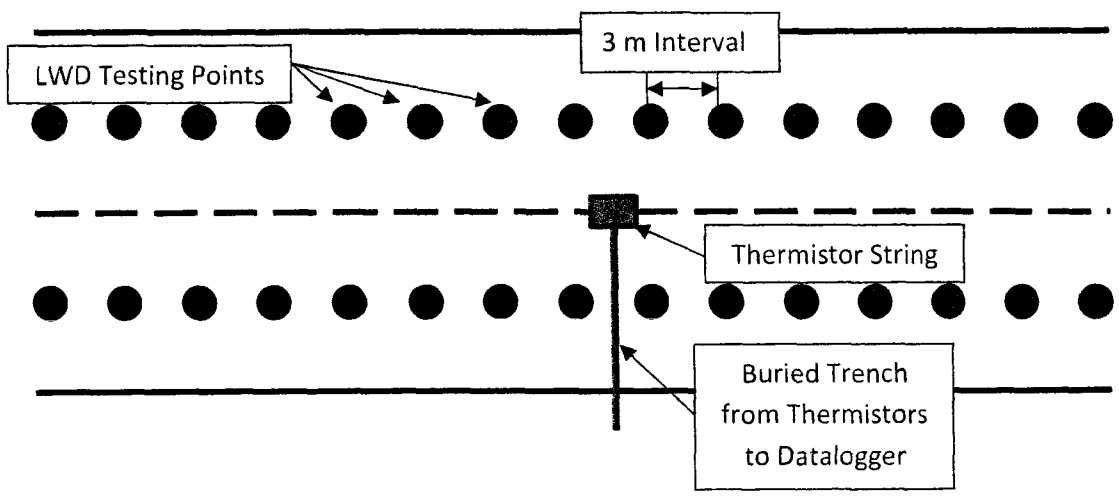

Figure 5.1 LWD Data Collection Site Schematic

Figure 5.2 Placement of the LWD Testing Points at the Highway 569 Study Site

Figure 5.3 Placement of the LWD Testing Points at the Highway 527 Study Site

Figure 5.4 LWD Testing at the Highway 527 Study Site

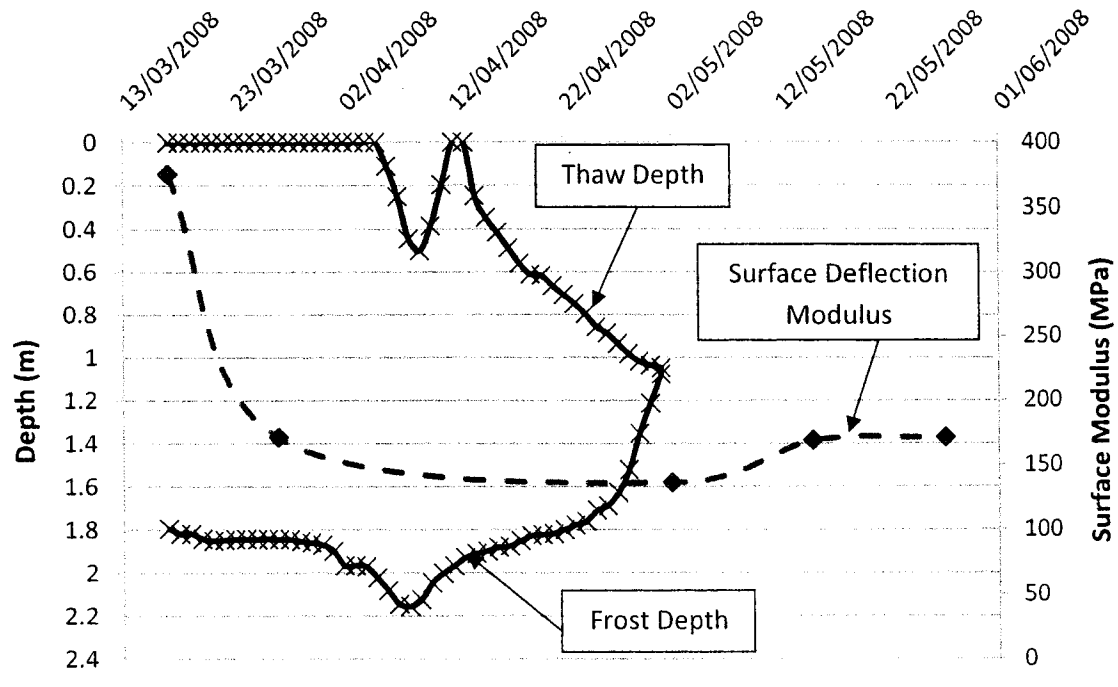

Figure 5.5 Surface Modulus and Observed Frost and Thaw Depths Versus Time at the Highway 569 Study Site, Thawing Season 2008

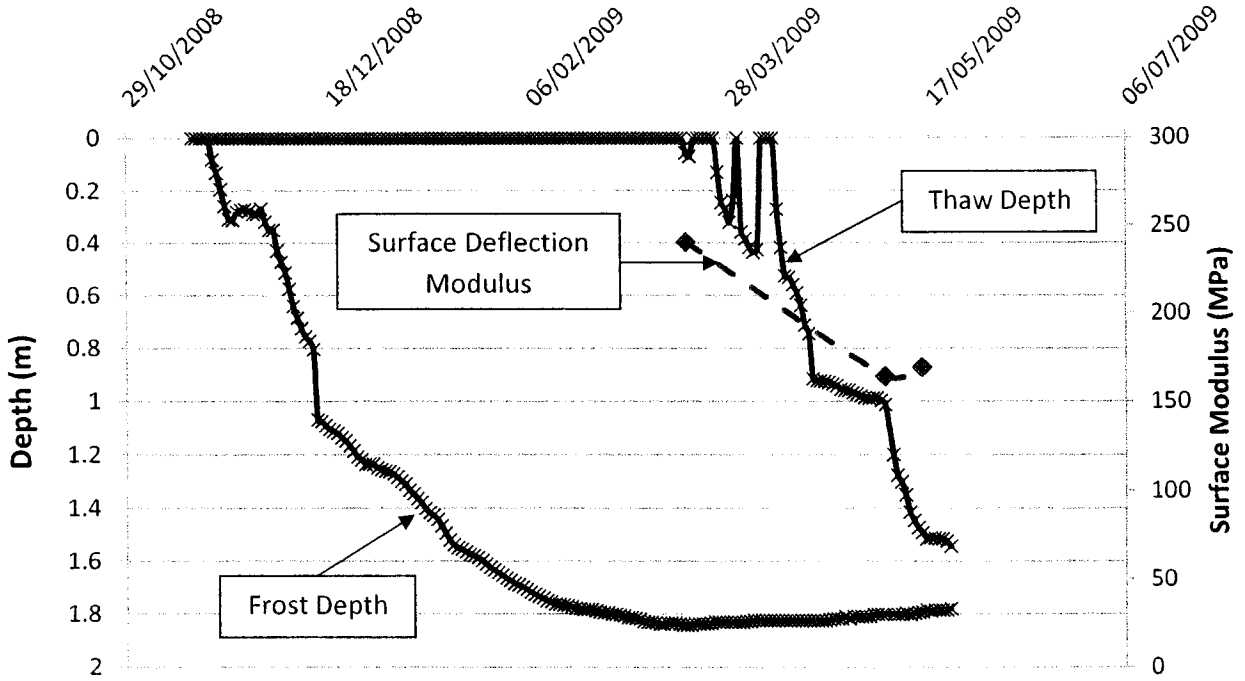

Figure 5.6 Surface Modulus and Observed Frost and Thaw Depths Versus Time at the Highway 569 Study Site, Thawing Season 2009

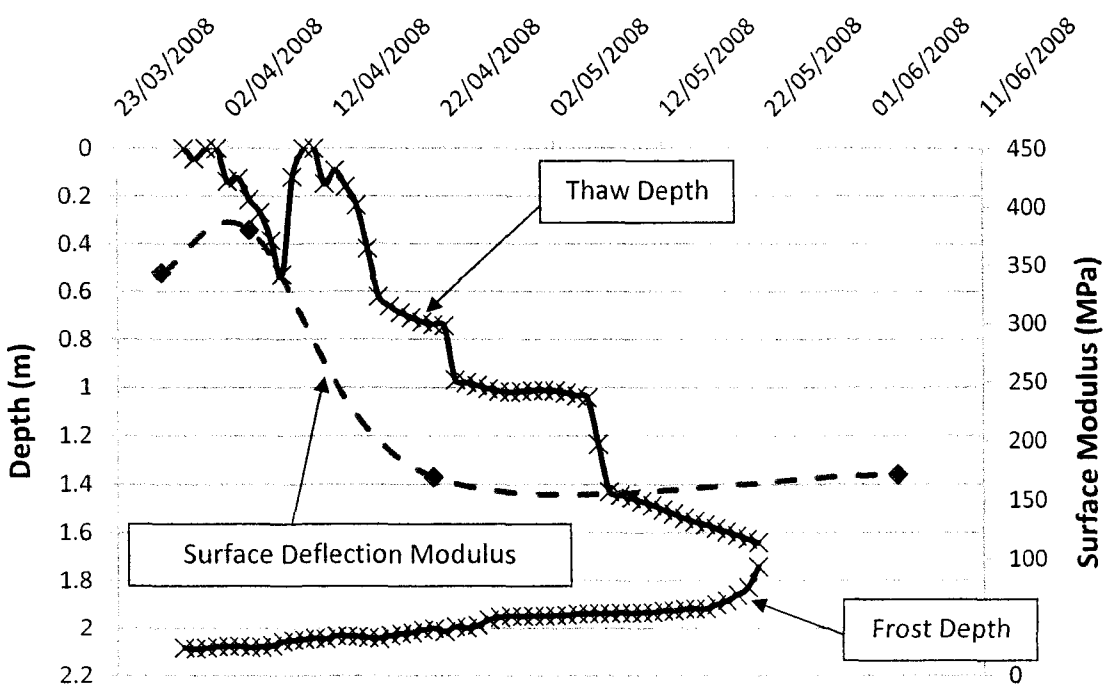

Figure 5.7 Surface Modulus and Observed Frost and Thaw Depths Versus Time at the Highway 527 Study Site, Thawing Season 2008

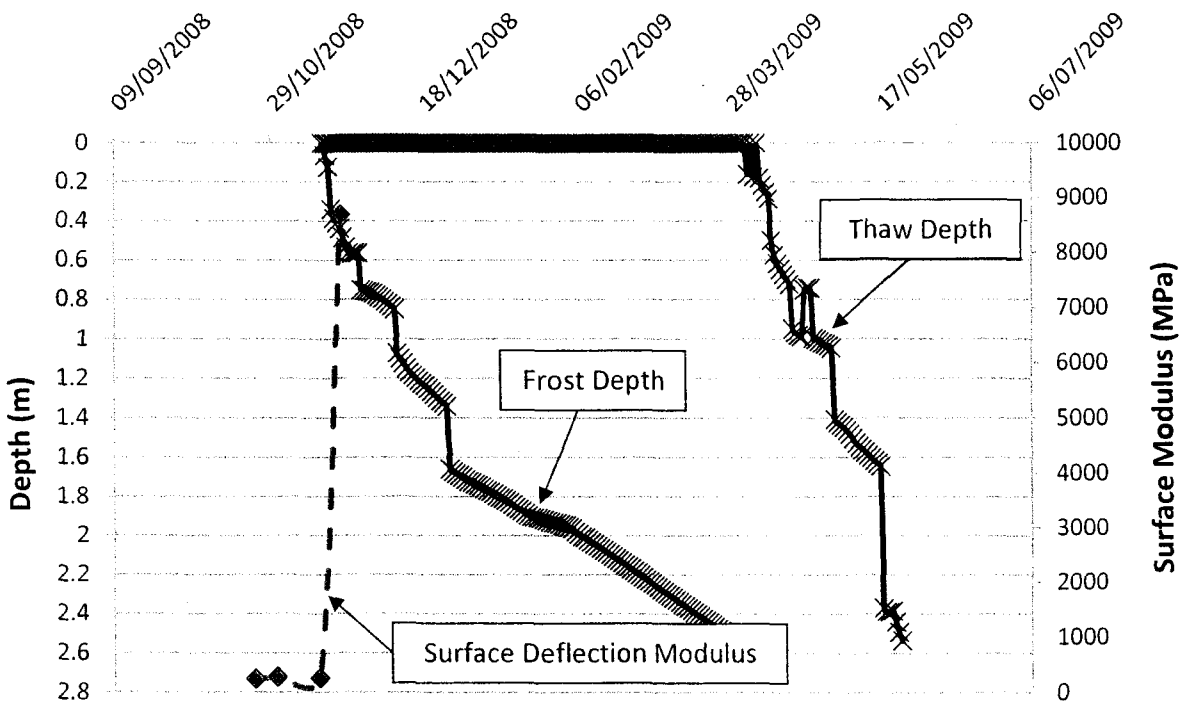

Figure 5.8 Surface Modulus and Observed Frost and Thaw Depths Versus Time at the Highway 527 Study Site, Freezing Season 2008

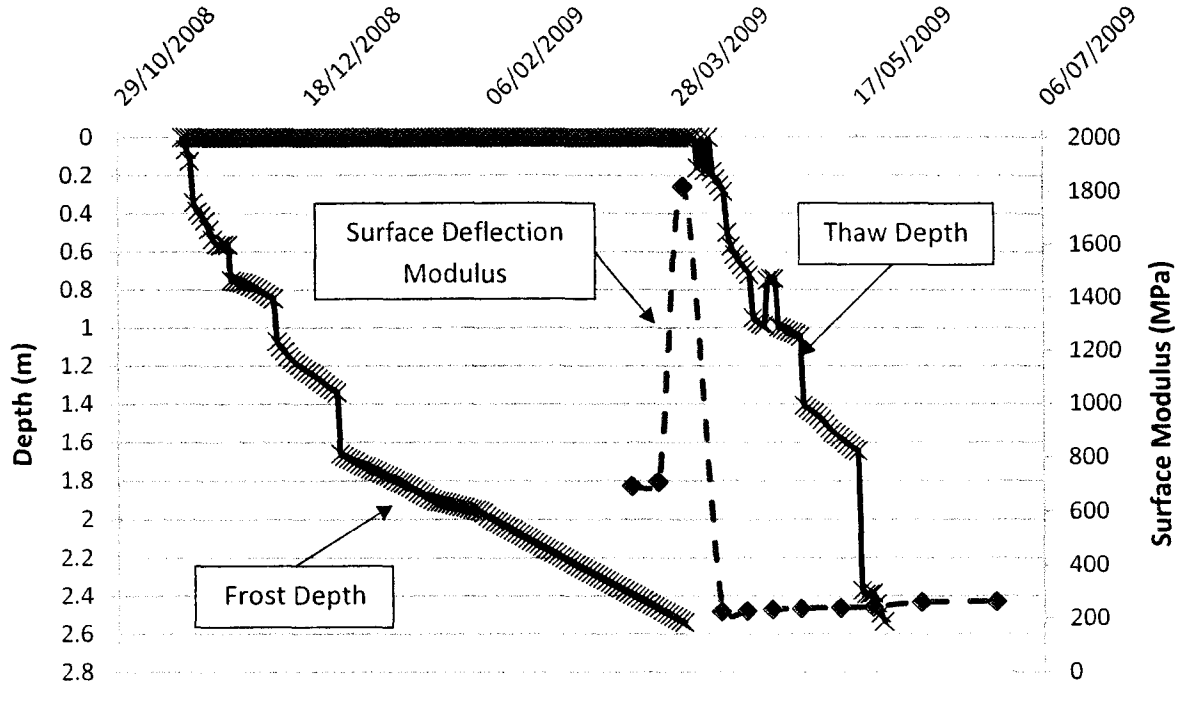

Figure 5.9 Surface Modulus and Observed Frost and Thaw Depths Versus Time at the Highway 527 Study Site, Thawing Season 2009

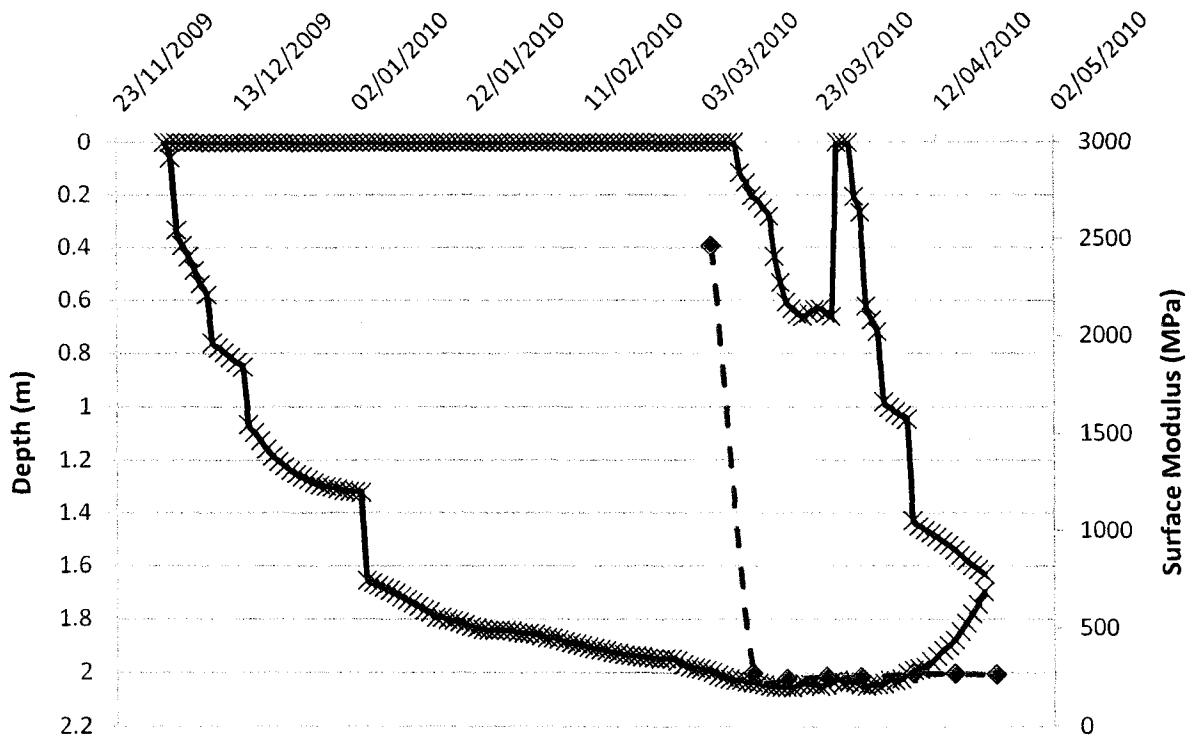

Figure 5.10 Surface Modulus and Observed Frost and Thaw Depths Versus Time at the Highway 527 Study Site, Thawing Season 2010

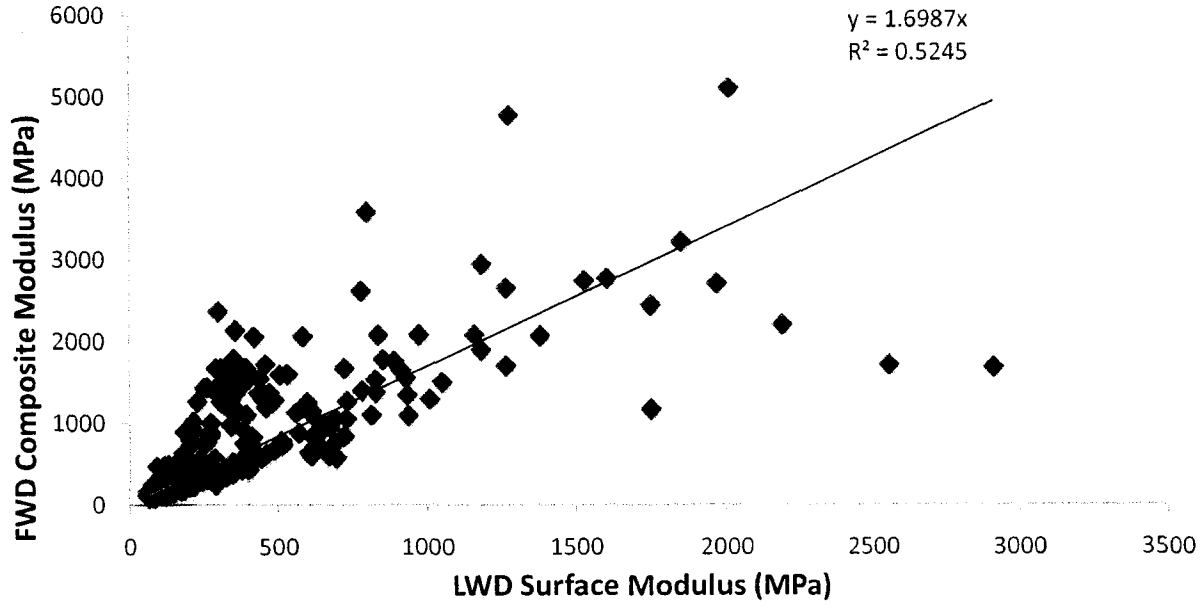

Figure 5.11 Comparison of All LWD Surface Modulus Values and FWD Composite Modulus Values for Side-by-Side Testing at the Northeastern Ontario Testing Sites (Spring 2008)

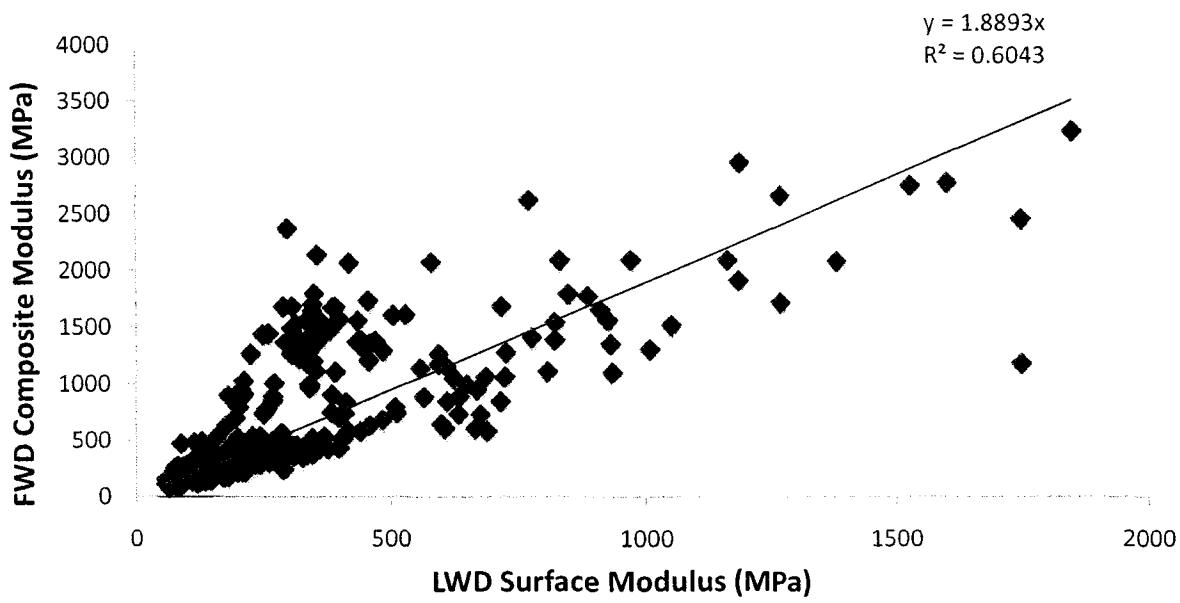

Figure 5.12 Comparison of LWD Surface Modulus Values and FWD Composite Modulus Values (Excluding FWD Composite Modulus Values Greater than 4000 MPa and LWD Surface Modulus Values Greater than 2000 MPa) for Side-by-Side Testing at the Northeastern Ontario Testing Sites (Spring 2008)

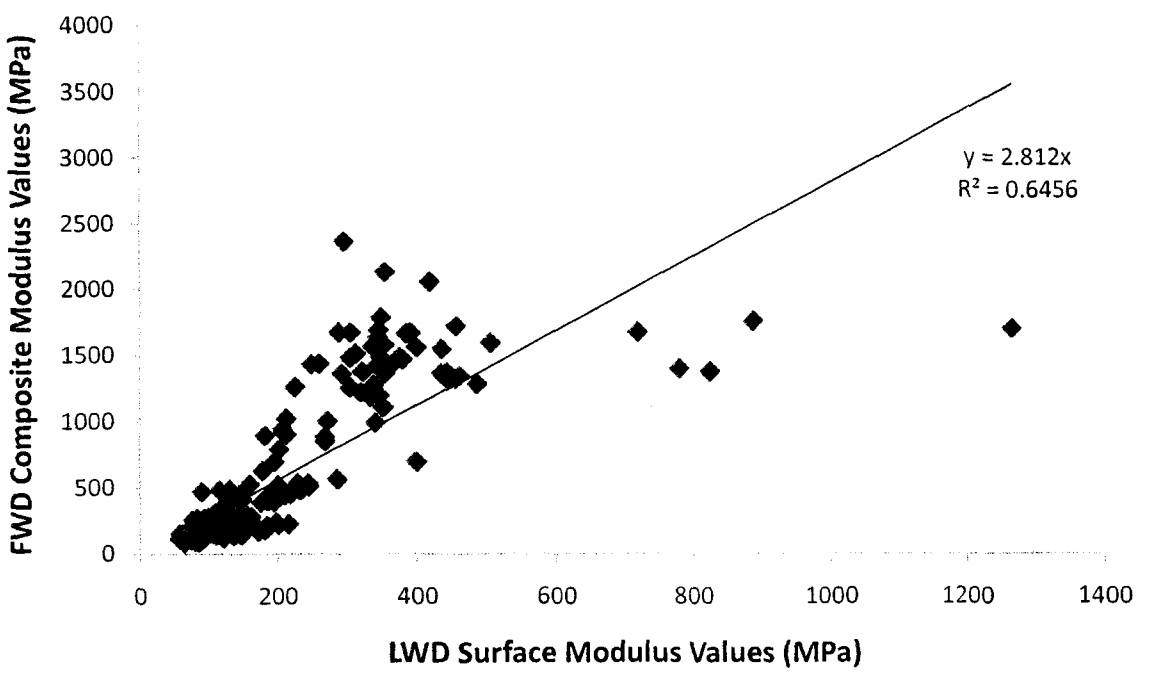

Figure 5.13 FWD Composite Modulus Values and Corresponding LWD Surface Modulus Values at the Highway 569 and 624 Sites, Spring 2008

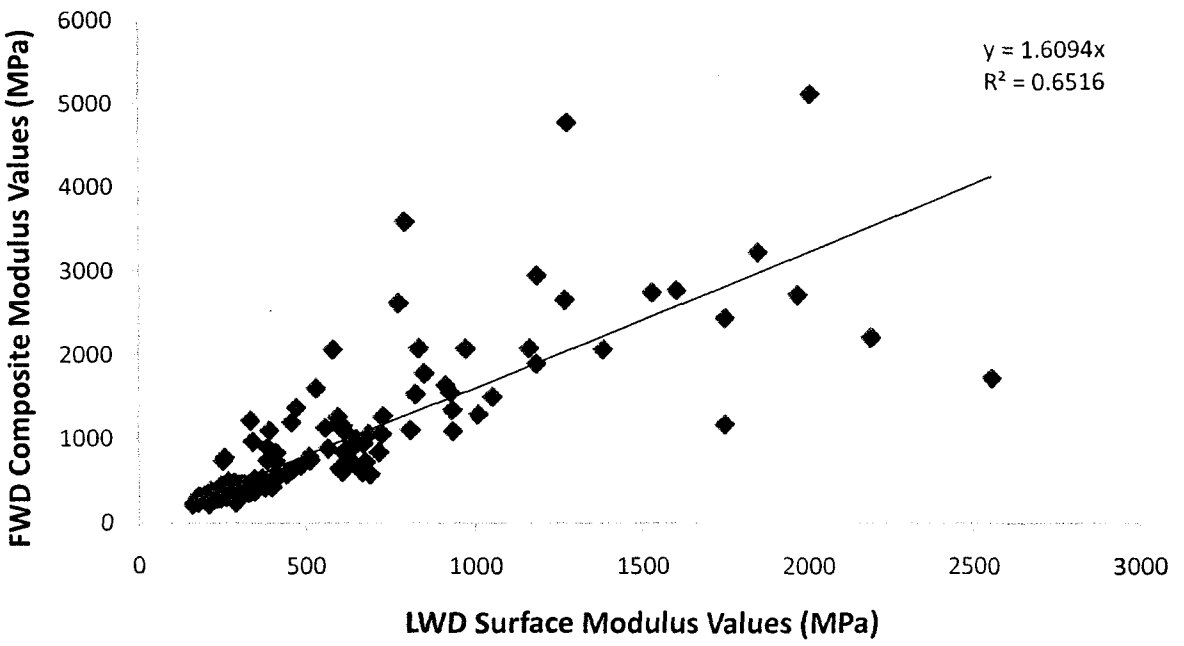

Figure 5.14 FWD Composite Modulus Values and Corresponding LWD Surface Modulus Values at the Highway 66 Site, Spring 2008

6.0 Predictions of SLR Methods for Winter/Spring 2009/2010 and Comparison with Observed Conditions

6.1 Highway 569 Predictions

The Mn/DOT, the Waterloo and the TEMP/W methods for SLR application and removal were tested in a predictive manner for the 2009/2010 winter/spring season at the Highway 569 study site. These predictions use the calibrated values for each method that were determined as described in Section 4 and outlined in Appendix G. The predictions from these methods are compared with observed conditions for 2009/2010 (Figure 6.1) obtained and interpreted from thermistors installed at the site to assess their accuracy in a predictive manner.

6.1.1 Highway 569 Mn/DOT Method Prediction

The Mn/DOT method was calibrated for the Highway 569 study site following the procedures outlined in Section 4.3. From this calibration it was determined that a CTI in excess of 40.1 °C-days would trigger the implementation of SLRs at the Highway 569 site. It was also established that a duration of 37 days after the implementation of SLRs would be used to trigger removal of the SLRs.

The CTI for the 2009/2010 season was calculated using the average daily air temperatures recorded at the site. In order to avoid the lag period between SLR requirement and SLR implementation described in Section 2.4.1, a 5-day forecast from New Liskeard, Ontario, the closest municipality to the site, was used to forecast the CTI five days ahead (Figure 6.2). Once the forecasted CTI value exceeded 40.1 °C-days, notification of the impending SLRs could be provided to the transportation industry.

As with the calibration of this method, the reference temperatures listed in Table 2.5 were subtracted from the measured and forecasted air temperatures to calculate the CTI. Figure 6.3 indicates the average daily air temperatures and the average daily air temperatures adjusted by the reference temperatures that were used in the CTI calculation for the beginning of the 2009/2010 thawing season.

The CTI calculations began on February 22, 2010, which was identified as the start of the thaw period, based on average daily air temperatures being below 0°C. Figure 6.4 shows that the CTI exceeded the threshold value of 40.1 °C-days on March 13, 2010. Using the 37 day SLR placement duration developed by using the average of the 2005/2006, 2007/2008 and 2008/2009 thawing durations which includes the additional 7 days required for pavement stiffness restoration, indicates that the SLRs should be removed on April 19, 2010.

6.1.2 Highway 569 Waterloo Method Prediction

For the Waterloo method prediction for the Highway 569 study site, the average of the 2005/2006, 2007/2008 and 2008/2009 monthly reference temperatures and calibration coefficients (Table 6.1) were used. As with the Mn/DOT method average daily air temperatures recorded at the site along with the 5-day forecast from New Liskeard, Ontario were used in the FI and TI calculations.

As described in Section 4.4.1 adjustments after day i_0 to the coefficients "g" and "j" had to be made. In order to accomplish this, the Waterloo algorithm (Equation 2.24) was used with the freezing season coefficients (a through f from Table 6.1) until the FI and TI values calculated using the 5-day forecast temperature values indicate a change from the freezing season to the thawing season (day i_0) (Figure 6.5). A plot of the estimated frost and thaw depth during the freezing season (using Equation 2.24 and the coefficients in Table 6.1) until day i_0 indicates the initial depths for the frost and thaw for the thawing season (Figure 6.6). The frost and thaw depths were then estimated using Equation 2.25 for day i_0 with the calibration coefficients for the thawing season (g through l in Table 6.1) (Figure 6.7). Then, the coefficients "g" and "j" were adjusted to match the depth of the frost and thaw at the end of the freezing season to the depth of the frost and thaw at the start of the thawing season. Table 6.1 provides the adjusted

calibration coefficients that were used in this prediction. Adjustment of "g" as described in Section 4.4.2 from 233 to -264 and "j" from -1271 to -1045 (Table 6.1) were found to provide the closest match between the freezing and thawing season depth on day i_0. During this adjustment stage, any thawing depth estimated to be above the pavement surface throughout the freezing season was constrained to the top of the pavement surface.

Next, the frost and thaw depths during the thawing season were estimated using the average values for the coefficients "h", "l", "k", and "l" described in Section 4.4.2, and the adjusted coefficients "g" and "j" (Table 6.1), until the model indicates complete subsurface thawing.

The Waterloo method 2009/2010 season prediction indicates that the thawing depth would exceed the 300 mm threshold described in Section 4.2 on April 14, 2010 indicated on Figure 6.8. As a result of the late thawing initiation date predicted by the Waterloo method, the time required to reach full subsurface thawing is not estimated to occur until far beyond what was observed at the study site.

6.1.3 Highway 569 TEMP/W Method Prediction

As with the Waterloo method, the TEMP/W method was used to predict the frost and thaw depths for the Highway 569 site for the 2009/2010 season. As outlined in Section 4.5 the predictive model was run using the baseline thermal properties listed in Table 4.6, the lowest thermistor values shown in Figure 4.23 as the lower boundary condition and an average of the 2005/2006, 2007/2008 and 2008/2009 calibration n-factor values (2.3 and 0.57 for temperatures above and below 0°C, respectively) that were applied to the average daily air temperatures as the upper boundary condition.

The average daily air temperatures that were input into the predictive model were collected in the same manner as for the Mn/DOT and Waterloo methods (i.e. daily averages were collected at the site and 5-day forecasts were provided from New Liskeard, Ontario). The effect that the application of the n-factor has on the average daily air temperatures can be seen in Figure 6.9.

Figure 6.10 shows that the estimated thaw depth exceeds the 300 mm threshold depth on March 14, 2010, indicating the implementation of SLRs. The model does indicate a significant refreeze period between March 20, 2010 and March 30, 2010. Following the procedures outlined in Section 4.2, once the thawing depth exceeds the 300 mm threshold and SLRs have been implemented, refreeze periods are not considered in the implementation and removal decision. It can also been seen in Figure 6.10 that the model predicts complete pavement structure thawing on April 4, 2010.

6.1.4 Comparison of the SLR Method Predictions with Observed Conditions for the Highway 569 Site

All three SLR method predictions were compared with frost and thaw depths interpreted from the thermistor values at the Highway 569 test site (Figure 6.1). This comparison was performed to assess each model's ability to accurately determine when SLRs should be implemented and removed at the Highway 569 study site. It can be seen in Figure 6.1 that the observed thawing depth exceeds 300 mm on March 11, 2010 and that the frost has not completely left the pavement structure until April 21, 2010, at which time the pavement structure is fully thawed.

Comparing the SLR implementation date of March 13, 2010 predicted by the Mn/DOT method with the observed conditions (300 mm depth exceeded on March 11, 2010) indicates that the Mn/DOT method accurately estimated the SLR implementation date for this site. Furthermore, the 37 day SLR placement duration used in the Mn/DOT prediction indicates removal of SLRs on April 19, 2010. Comparing this date for SLR removal with the observed date for complete subsurface thawing (April 21, 2010) plus the additional 7 days required for pavement stiffness restoration (April 28, 2010) indicates that the Mn/DOT method predicts removing the SLRs 9 days earlier.

When comparing the Waterloo method with the observed frost and thaw depths for the Highway 569 study site (Figure 6.11) it can be seen that this method significantly overestimates the time required for the pavement structure to thaw to a depth of 300 mm (April 14, 2010 for the Waterloo method compared to March 11, 2010 for the observed). As a result of the overestimated SLR implementation date, the date of complete subsurface thawing was also

overestimated. In addition to this, the Waterloo method did not accurately represent the significant thawing event between March 25, 2010 and March 30, 2010 and the refreeze period indicated by the observed frost and thaw depths.

Figure 6.11 indicates that the Waterloo method prediction of the frost depth during the freezing season closely matches that of the observed data. After the day i_0 however, the accuracy of the frost depth estimation is reduced.

Comparing the TEMP/W method with the observed data (Figure 6.12) indicates that the model can accurately estimate the initiation and rate of thawing of the pavement structure, resulting in a close match between the estimated SLR implementation date (March 14, 2010) and the date obtained from the observed data (March 11, 2010). The TEMP/W method also captures the refreeze period indicated by the observed data, however, the TEMP/W method indicates a shallower thawing depth than the observed data prior to the refreeze period. Furthermore, the TEMP/W method estimates that the pavement structure will be completely thawed on April 4, 2010, 17 days sooner than the observed data indicate (April 21, 2010).

The TEMP/W method can closely estimate the initiation of subsurface freezing, as well as the maximum depth of frost (Figure 6.12) however, this method indicates earlier complete pavement structure thawing, than the observed data does.

6.2 Highway 527 Predictions

As with the Highway 569 predictions, the three SLR methods described in Section 4 were used in a predictive manner for the Highway 527 study site for the 2009/2010 season. The methods were then compared with the observed frost and thaw depths interpreted obtained from the thermistor values (Figure 6.13) at the site to assess their accuracy.

6.2.1 Highway 527 Mn/DOT Method Prediction

The Mn/DOT prediction for the Highway 527 study site required average daily air temperatures for calculation of the CTI. These values were obtained from the site. The 5-day forecast average daily air temperature values required to avoid an implementation lag time were determined from an average of the values for Armstrong, Ontario and Thunder Bay, Ontario.

The average of Armstrong and Thunder Bay were used because the Highway 527 study site lies approximately halfway between the two locations (Figure 6.14). Following the Mn/DOT method guideline, the weekly reference temperatures provided in Table 2.5 were subtracted from the average daily air temperatures (Figure 6.15). From the beginning of the 2009/2010 thawing season, the CTI was calculated following Equation 2.23. Once the CTI exceeded the threshold value of 64.3 °C-days, SLRs were implemented.

Following this procedure the CTI was observed to exceed 64.3 °C-days on March 14, 2010 (Figure 6.16). Using the 2008/2009 thawing duration plus an additional seven days required for pavement stiffness restoration, giving a duration of 51 days, SLRs were predicted to be removed on May 4, 2010.

6.2.2 Highway 527 Waterloo Method Prediction

The calibrated Waterloo method was used to predict frost and thaw depths for the Highway 527 site. As with the Mn/DOT method, the average daily air temperatures were obtained from the site, while the 5-day forecasted temperatures were obtained by taking an average of the Armstrong and Thunder Bay, Ontario average daily air temperatures.

The average daily air temperatures and the monthly reference temperatures provided in Table 6.2 were input into Equations 3.1 and 3.2 to calculate the FI and TI values for the freezing season. A plot of the FI and TI values (Figure 6.17) was constructed to determine the date at which the freezing season changed to the thawing season (day i_0)

Following the same procedures outlined for the adjustment of variables "g" and "j" described in Section 4.4.2 and used for the Highway 569 site, it was found that adjusting variable "g" from -255 to -193 and "j" from -1572 to -1240, resulted in the closest match between the freezing season frost and thaw depths and the thawing season frost and thaw depths on day i_0. Using the adjusted coefficients listed in Table 6.2 the Waterloo method indicates initial thawing to exceed the 300 mm threshold depth on March 13, 2010 (Figure 6.18). It can also be seen in Figure 6.18 that full pavement structure thawing was estimated to occur on April 25, 2010

6.2.3 Highway 527 TEMP/W Method Prediction

The predictive TEMP/W model was run using the baseline thermal properties listed in Table 4.7, the lowest thermistor temperature values shown in Figure 4.22 as the lower boundary condition and n-factored average daily air temperatures as the upper boundary condition. At the Highway 527 study site, n-factor values of 2.3 for temperatures above 0°C and 0.8 for temperatures below 0°C were used. Figure 6.19 indicates the changes in the average daily air temperatures used in the 2009/2010 model when the n-factor modifications were applied. As with the Mn/DOT and Waterloo methods, the average daily air temperatures were obtained from the site and any temperatures used for a 5-day prediction were obtained by averaging the average daily air temperature forecasts from Armstrong and Thunder Bay, Ontario.

Figure 6.20 shows that the TEMP/W method predicts that the thawing depth exceeds the 300 mm thawing depth threshold on March 12, 2010. Further to this, the TEMP/W method indicates two periods of refreezing, the first being between March 20 and March 23, 2010 and the second being between March 26 and March 29, 2010.

An examination of the operation of the TEMP/W program is required to assess when the pavement structure would be completely thawed at the Highway 527 study site for the 2009/2010 prediction. The TEMP/W program computes the temperature at any point within the pavement structure using the upper and lower boundary condition values as limits. During the 2008/2009 calibration season the frost front progressed to a depth below the 2.55 m thermistor on March 26, 2009, as indicated in Section 3.5.2. Examining the lowest thermistor values used in the Highway 527 prediction (Figure 4.22 and Appendix E) which are the values from the 2008/2009 winter/spring calibration season, it is evident that the lowest thermistor values were below 0°C between March 26, 2009 and May 24, 2009. These values were then used as the lower boundary condition in the predictive model. As a result, the TEMP/W model will continue to indicate the presence of a 0°C isotherm at some depth between the pavement surface (with temperatures above 0°C) and the lowest thermistor at a depth of 2.55 m (with input temperatures below 0°C) until May 24, 2010, the date when the lowest thermistor value exceeds 0°C. Due to the use of this boundary condition in the prediction, the Highway 527 TEMP/W prediction (Figure 6.20) indicates an anomalous lower frost depth trend during the

period of pavement surface thawing. During the thawing season the frozen subsurface soils will typically thaw from the bottom up due to the effects of the geothermal gradient. For the 2009/2010 prediction it is evident that during the pavement structure thawing, the lower frost front continues to migrate deeper into the pavement structure. This illustrates a problem with using the lowest thermistor temperatures as a bottom boundary condition in a TEMP/W predictive model.

6.2.4 Comparison of the SLR Method Predictions with Observed Conditions for the Highway 527 Site

All three of the SLR methods are compared with the observed frost and thaw depths interpreted from the thermistor data for the Highway 527 study site. Figure 6.13 shows that the pavement structure thawing exceeds the 300 mm threshold depth on March 15, 2010. Furthermore, the observed data shows that the pavement structure is completely thawed on April 21, 2010.

The Mn/DOT method predictions show that the CTI would exceed the 64.3 °C-day threshold on March 14, 2010. This date closely matches the March 15, 2010 date that the observed data indicate for SLR implementation. Furthermore, the SLR removal date of May 4, 2010, based on a 51 day SLR duration described in Section 6.2.1, is only 5 days later than the observed pavement structure complete thawing plus the additional 7 days required for pavement stiffness restoration (April 28, 2010).

The Waterloo method prediction for the frost and thaw depths for the 2009/2010 season indicates that the thawing depth would exceed 300 mm on March 13, 2010 (Figure 6.21). This date is in good accordance with the observed data, which indicates that the thawing depth would reach 300 mm on March 15, 2010. The Waterloo method also captures the refreeze period between March 24, 2010 and March 30, 2010 however, it does not fully represent the magnitude of the refreeze indicated by the observed data. Figure 6.21 indicates that the Waterloo method closely predicts both the freezing and thawing front penetration rates and durations of the observed data, and as a result, closely predicts the date of complete

pavement structure thawing (April 25, 2010 compared with April 21, 2010 for the observed data).

Comparing the TEMP/W method prediction with the observed conditions indicates that the thawing depth would exceed 300 mm on March 12, 2010, 3 days prior to the observed date of March 15, 2010 (Figure 6.22). The TEMP/W method gives two periods of refreeze (April 21, 2010 – April 23, 2010 and April 26, 2010 – April 30, 2010) compared to only one refreeze period shown by the observed data. Figure 6.22 indicates that during the initial thawing period the TEMP/W method closely represents the rate of thawing. As a result of the lowest thermistor boundary condition issues described in Section 6.2.3, however, this method does not accurately represent the frost front migration into the pavement structure or the time to complete subsurface thawing.

6.3 History Matching for the Measured 2009/2010 Frost and Thaw Depths at Highway 569 and Highway 527

The predictions using the Waterloo method for the Highway 569 study site and the TEMP/W method at the Highway 527 site for the 2009/2010 season were the most inaccurate. Further to this, the Highway 527 site Waterloo method prediction using only one calibration year was more accurate in estimating the frost and thaw depths than the Highway 569 site having three years of calibration data. The predictive accuracy of the Waterloo and TEMP/W methods are strongly associated with the accuracy of the input parameters and boundary conditions, respectively, as described in Sections 4.4.1 and 4.5.5. History matching using measured 2009/2010 season data from both sites was conducted to investigate the relationship between the use of accurate inputs in these methods and developing accurate predictions.

Using the Waterloo method calibration methods described in Section 4.4 with the measured frost and thaw depths observed at the Highway 569 site, a new set of reference temperatures and calibration coefficients that represent the conditions at the site during the 2009/2010 season have been developed. Comparing the new set of coefficients with the average set of coefficients used in the predictions indicates significant differences (Table 6.3). When plotting the estimated frost and thaw depths using the history matched set of

coefficients and reference temperatures, along with the original predicted and measured frost and thaw depths it can be seen that, as with the Waterloo method calibration seasons, using the coefficients evaluated from measured data provides a much better match between frost and thaw depths and the observed conditions (Figure 6.23).

Even though use of the Waterloo method gave good predictions for the application and removal of SLRs for the Highway 527 study site for the 2009/2010 season, history matching using the measured frost and thaw depths was conducted to compare the history matched calibration coefficients with those used for the prediction. Table 6.4 lists the reference temperatures and calibration coefficients determined from history matching for the Highway 527 study site. While Figure 6.24 shows a good match between the frost and thaw depths from history matching and those observed, a comparison of the history matching and prediction calibration coefficients (Table 6.4) shows little similarity between the two sets of values. Based on this comparison and the inaccuracy of the Waterloo method to predict the Highway 569 site conditions, it is very difficult to develop a set of coefficients for the Waterloo method that can be used for reliable predictions for SLR implementation, even when multiple calibration years of data are available. Further research, particularly focusing on a method to develop coefficients that give more reliable frost and thaw depth predictions would need to be conducted for the Waterloo method.

Use of the 2008/2009 lower boundary condition in the Highway 527 2009/2010 TEMP/W prediction resulted in a poor simulation of the frost depth and trend during the thawing season. When the thermistor values measured at the site for the 2009/2010 season were used as the lower boundary condition the SLR removal date accuracy was greatly improved, indicating full pavement structure thawing on April 25, 2010 instead of May 24, 2010 (Figure 6.25). Comparing these dates with the date of observed pavement structure thawing (April 21, 2010) indicates the improvement in prediction accuracy that can be made from the use of accurate and representative boundary conditions. It can also be seen in Figure 6.25 that adjustment of the lower boundary condition has little effect on the thawing patterns near the surface of the pavement structure.

6.4 Summary and Assessment of SLR Methods

Comparing the prediction results of all three SLR methods with observed frost and thaw depths indicates that the methods display varying levels of predictive ability, however, all are limited to some degree. Table 6.5 provides a summary of predictive accuracy of the three methods tested.

The Mn/DOT method requires the least amount of inputs and can be easily implemented. At both the Highway 569 and 527 locations the Mn/DOT method closely predicted the date when SLRs should be applied compared with the date of the observed 0.3 m thawing depth. The use of the average SLR placement duration for the Mn/DOT method reasonably predicted the removal of SLRs at both the Highway 569 and 527 locations (9 days soon and 6 days late, respectively) (see Table 6.3). The use of additional sites and additional study years to obtain a more representative average thawing duration could improve the accuracy of these predictions. In addition, the potential of correlating weather condition indices from the current season, such as frost depth or cumulative freezing index, with historical thawing durations correlated with the same historical indices should be investigated. This might provide a more reliable, accurate thawing duration than using an average duration value, as the experience with the Highway 569 site prediction has indicated. A limitation of the Mn/DOT method is the inability of the method to predict the actual amount of frozen pavement structure.

The Waterloo method prediction closely matched the observed frost and thaw depths for the Highway 527 study site. The prediction of frost and thaw depths however, was highly inaccurate for predicting SLR application and removal dates for the the Highway 569 site. This is a result of the method's reliance on accurate and representative calibration coefficients. Furthermore, this method requires an adjustment to the "g" and "j" coefficients when transitioning from the freezing to the thawing season, making it more difficult to implement. Further calibration using more study periods should be considered to potentially increase the accuracy of the calibration coefficients to represent the conditions at the study sites and increase the overall accuracy of the method.

The TEMP/W model prediction closely matched the date when an observed thawing depth of 0.3 m was reached at both the Highway 569 and Highway 527 study sites. Comparing the Highway 569 prediction which used a three year average data set for the lower boundary condition with the Highway 527 prediction which used only a one year data set for the lower boundary condition illustrates the reliance of this method on the ability to define representative boundary conditions. Further examination of additional study periods at the Highway 527 study site to obtain a more representative lower boundary condition should increase the predictive abilities of the model at this site. While this method requires the most inputs, it has the ability to represent numerous pavement structure conditions and climate conditions, making it the easiest of the methods to transfer to and represent multiple sites.

Table 6.1 Monthly Reference Temperatures and Adjusted Calibration Coefficients Used for the 2009/2010 Waterloo Prediction for the Highway 569 Study Site

Monthly Reference Temperature (°C)		Unadjusted Coefficients	Adjusted Coefficients 2009/2010
November		-2.75	-2.75
December		-2.79	-2.79
January		-0.77	-0.77
February		-1.67	-1.67
March		-4.96	-4.96
April		-4.14	-4.14
May		1.2	1.2
Calibration Coefficients			
Freezing Season Coefficients (Eq. 2.24)	a	-0.25	-0.25
	b	-4.82	-4.82
	c	2.22	2.22
	d	11.29	11.29
	e	-0.35	-0.35
	f	-1.06	-1.06
Thawing Season Coefficients (Eq. 2.25)	g	233	-264
	h	-12.34	-12.34
	i	-1.53	-1.53
	j	-1271	-1045
	k	33.20	33.20
	l	-1.73	-1.73
Day i_0		15/3/10	15/3/10

Table 6.2 Monthly Reference Temperatures and Adjusted Calibration Coefficients Used for the 2009/2010 Waterloo Method Prediction for the Highway 527 Study Site

Monthly Reference Temperature (°C)		Unadjusted Coefficients	Adjusted Coefficients 2009/2010
November		-4.20	-4.20
December		-4.73	-4.73
January		1.14	1.14
February		1.37	1.37
March		-3.67	-3.67
April		-3.67	-3.67
May		-3	-3.00
	Calibration Coefficients		
Freezing Season Coefficients (Eq. 2.24)	a	-6.17	-6.17
	b	-5.52	-5.52
	c	0.97	0.97
	d	1.15	1.15
	e	-0.04	-0.04
	f	-0.09	-0.09
Thawing Season Coefficients (Eq. 2.25)	g	-255	-193
	h	5.5×10^{-11}	5.5×10^{-11}
	i	1.1×10^{-11}	1.1×10^{-11}
	j	-1572	-1240
	k	36.64	36.64
	l	-6.54	-6.54
	Day i_0	10/3/10	10/3/10

Table 6.3 Average Prediction and History Matched Waterloo Method Coefficients used for the Highway 569 Study Site during the 2009/2010 Season

Monthly Reference Temperature (°C)		Average Values used in Predictions	History Matching Values
November		-2.75	-4.33
December		-2.79	-3.32
January		-0.77	-1.61
February		-1.67	-0.65
March		-4.96	-3.79
April		-4.14	-3.98
May		1.2	-
Calibration Coefficients			
Freezing Season Coefficients (Eq. 2.24)	a	-0.25	40.72
	b	-4.82	-6.85
	c	2.22	-0.40
	d	11.29	2.32
	e	-0.35	-0.07
	f	-1.06	-4.99
Thawing Season Coefficients (Eq. 2.25)	g	-264	-136
	h	-12.34	-0.95
	i	-1.53	-0.10
	j	-1045	-4.00
	k	33.20	0.12
	l	-1.73	-6.56
Day I_0		15/3/10	13/3/10

Table 6.4 Average Prediction and History Matched Waterloo Method Coefficients used for the Highway 527 Study Site during the 2009/2010 season

Monthly Reference Temperature (°C)		Average Values Used in Predictions	History Matching Values
November		-4.20	1.07
December		-4.73	-3.72
January		1.14	0.13
February		1.37	-0.77
March		-3.67	-0.42
April		-3.67	-0.42
May		-3.00	-
	Adjusted Coefficients		
Freezing Season Coefficients (Eq. 2.24)	a	-6.17	-8.59
	b	-5.52	-5.84
	c	0.97	3.02
	d	1.15	-0.28
	e	-0.04	-0.02
	f	-0.09	-3.75
Thawing Season Coefficients (Eq. 2.25)	g	-193	449
	h	5.5×10^{-11}	-18.47
	i	1.1×10^{-11}	-1.76
	j	-1240	19.62
	k	36.64	2.27
	l	-6.54	-20.81
	$Day\ I_0$	10/3/10	14/3/10

Table 6.5 Summary of SLR Method Prediction Results (2009/2010)

Highway	SLR Method	SLR Implementation	Represents Refreeze Period	Pavement Structure Completely Thawed	SLR Removal
569	Mn/DOT	March 13, 2010	No	Unknown	April 19, 2010
569	Waterloo	April 14, 2010	Yes	Unknown	Unknown
569	TEMP/W	March 14, 2010	Yes	April 4, 2010	April 11, 2010
569	**Observed**	**March 11, 2010**	-	**April 21, 2010**	**April 28, 2010**
527	Mn/DOT	March 14, 2010	No	Unknown	May 4, 2010
527	Waterloo	March 13, 2010	Yes	April 25, 2010	May 2, 2010
527	TEMP/W	March 12, 2010	Yes	May 24, 2010	May 31, 2010
527	**Observed**	**March 15, 2010**	-	**April 21, 2010**	**April 28, 2010**

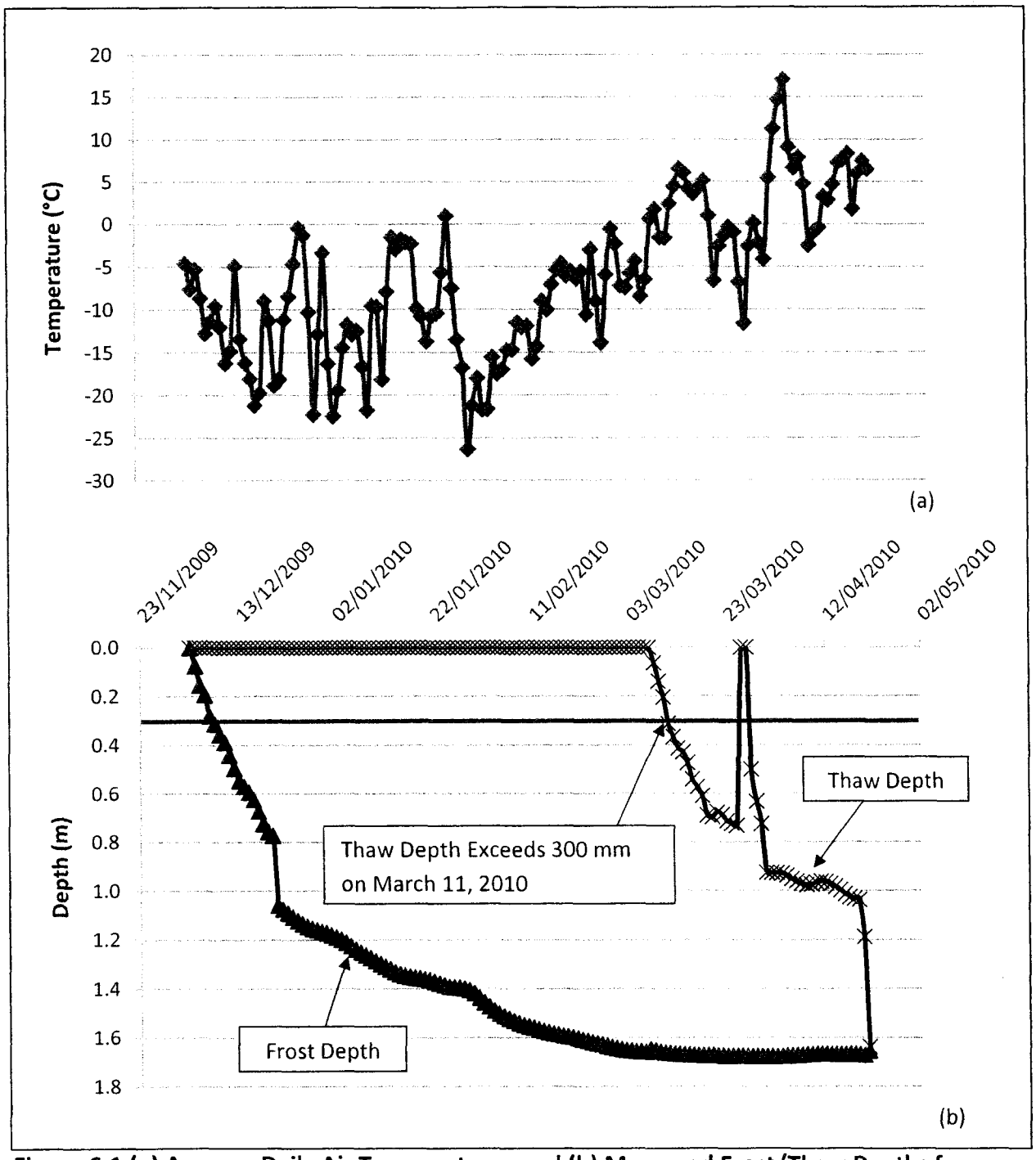

Figure 6.1 (a) Average Daily Air Temperatures and (b) Measured Frost/Thaw Depths for Highway 569, 2009/2010

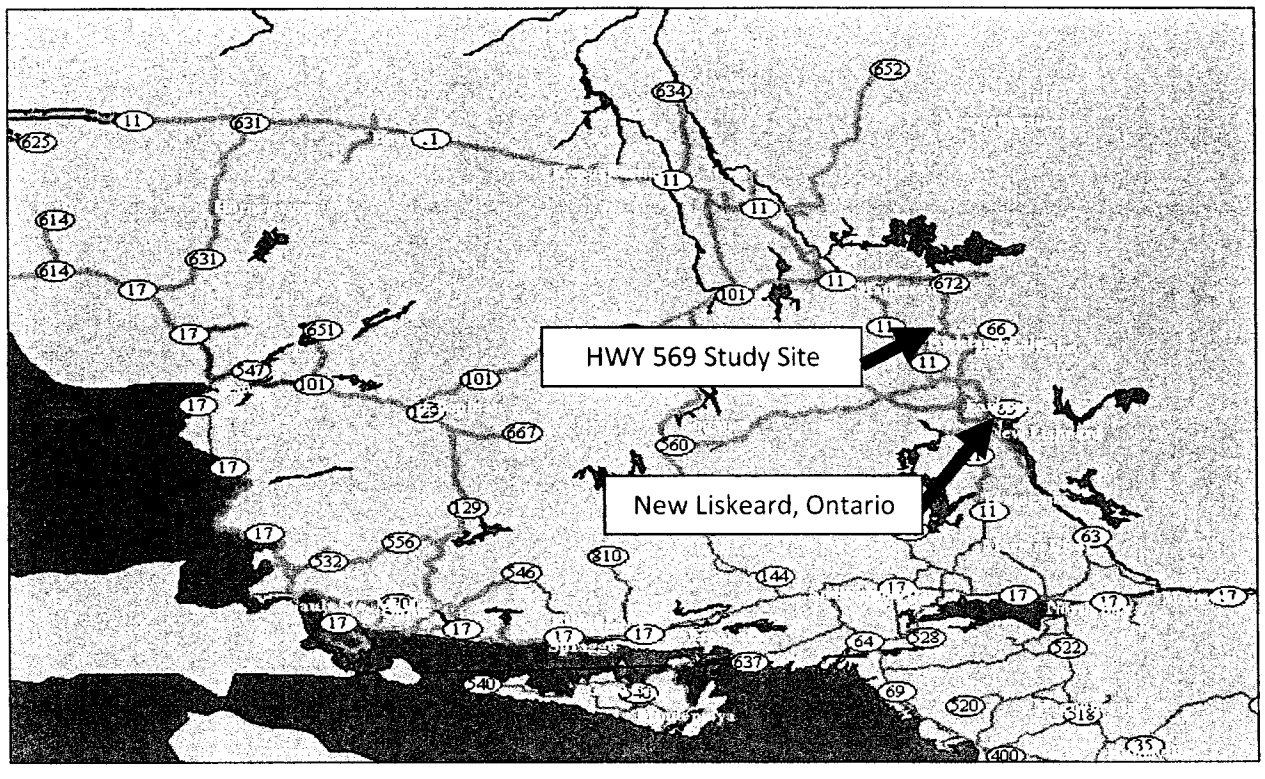

Figure 6.2 Highway 569 Study Site Location Compared to 5-day Forecast Municipality

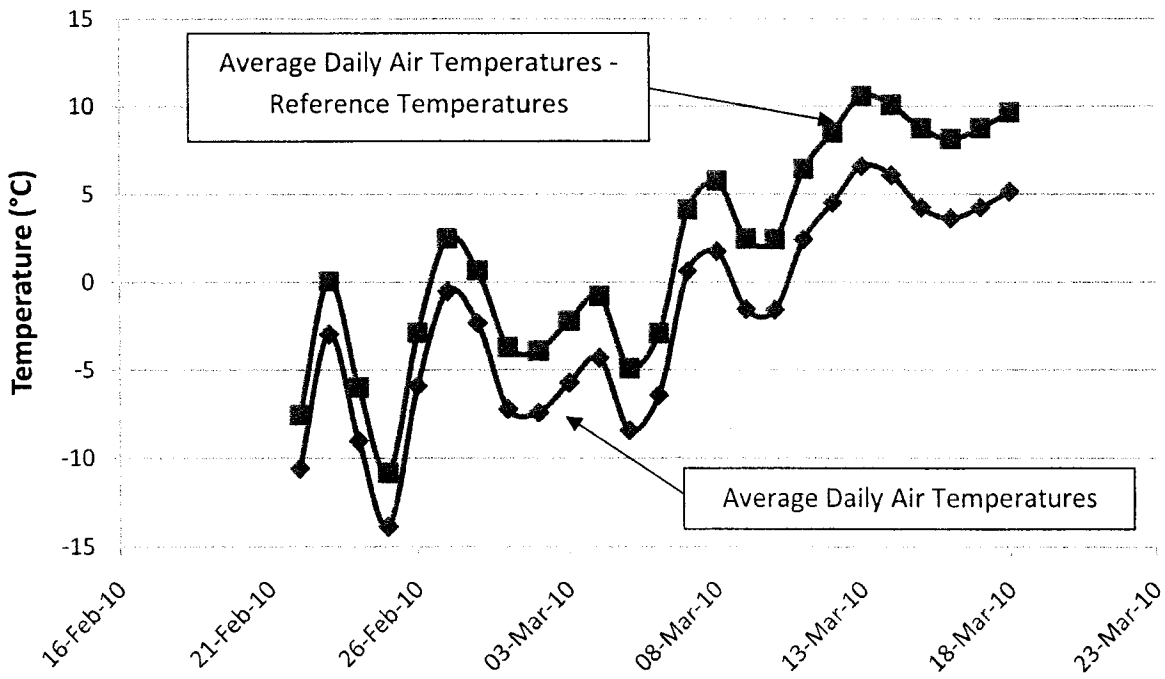

Figure 6.3 Air Temperature Modifications by the Mn/DOT Weekly Reference Temperatures used in 2009/2010 Mn/DOT Prediction for the Highway 569 Study Site

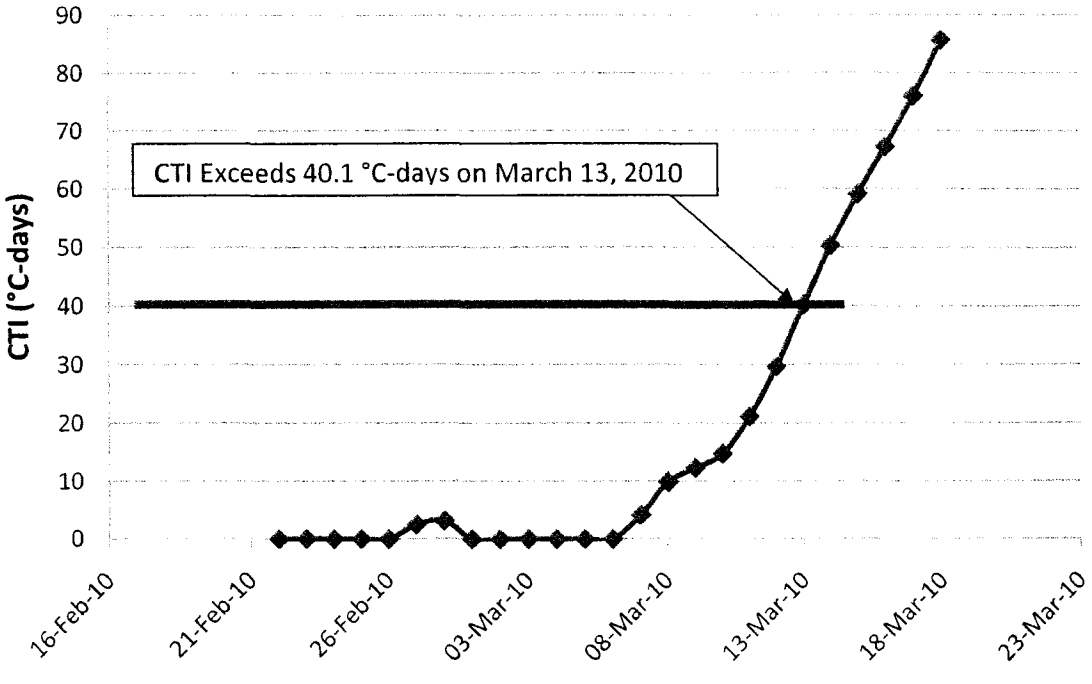

Figure 6.4 Mn/DOT Method Cumulative Thawing Index (CTI) Calculation for the 2009/2010 Season for the Highway 569 Study Site

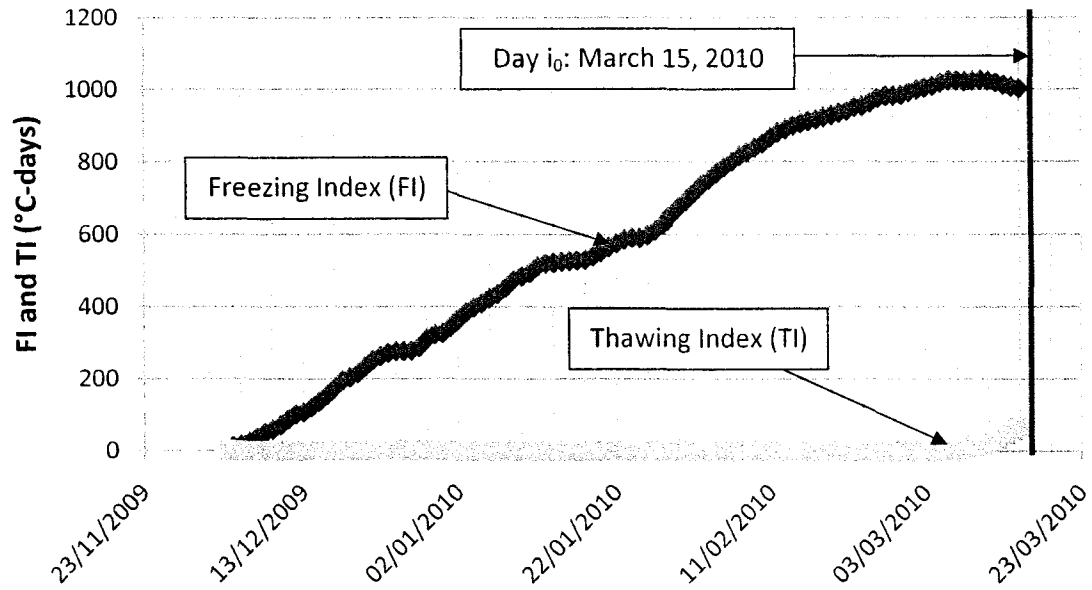

Figure 6.5 Determination of Waterloo Method Day i_0 for the 2009/2010 Prediction for the Highway 569 Study Site

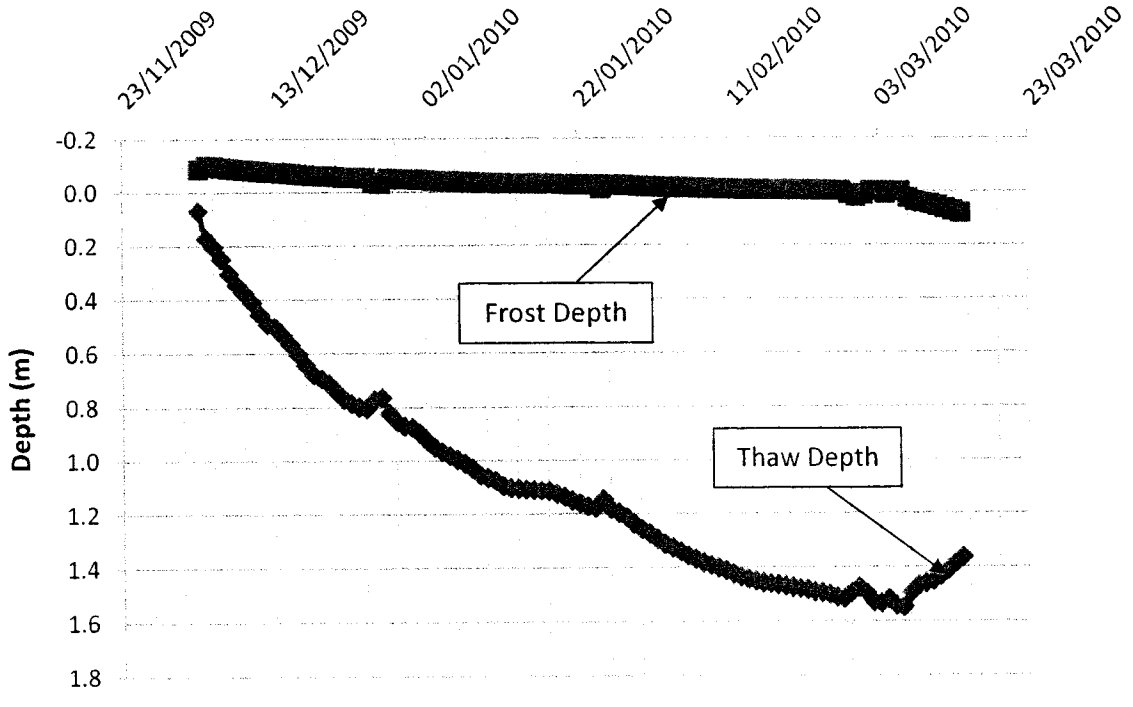

Figure 6.6 Estimated Freezing Season Frost and Thaw Depth for the Waterloo Method during the 2009/2010 Season for the Highway 569 Study Site

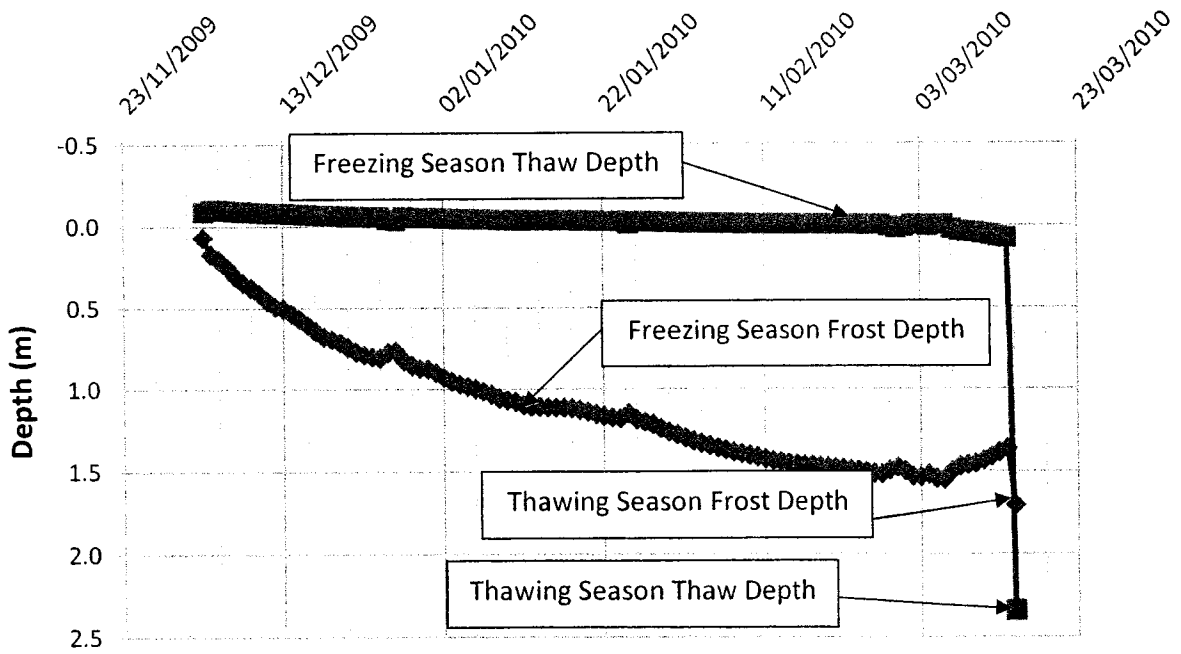

Figure 6.7 Estimated Thawing Season Frost and Thaw Depths on Day i_0 using Unadjusted Calibration Coefficients for the Highway 569 Study Site for the 2009/2010 Prediction

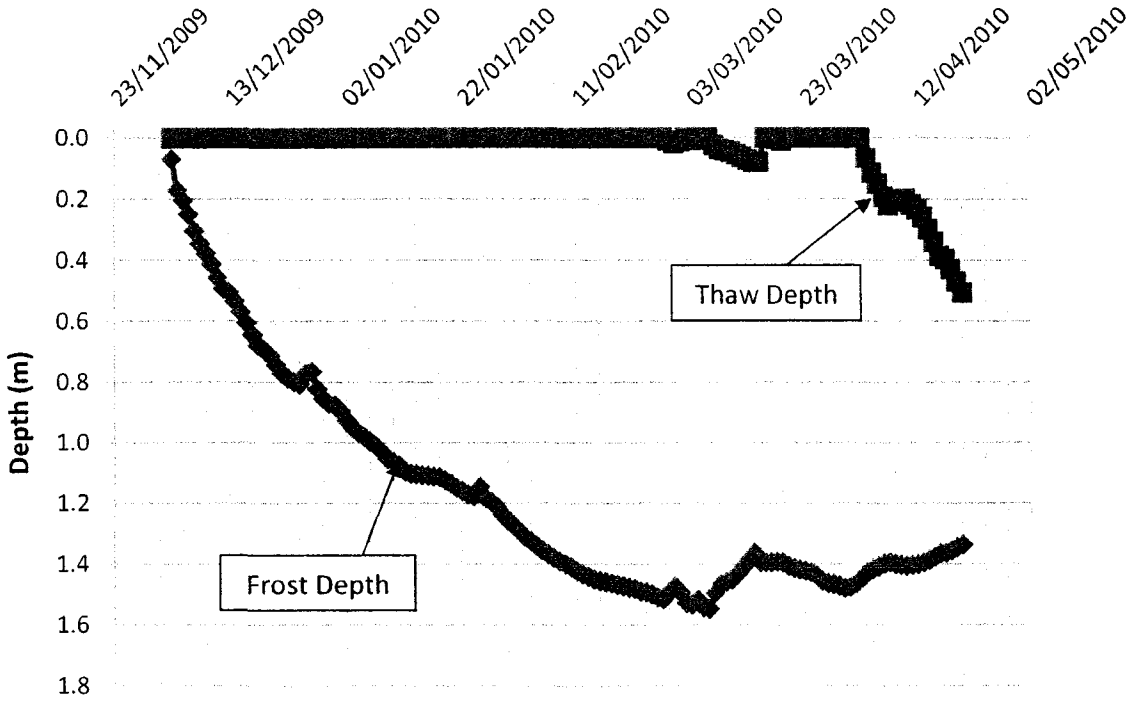

Figure 6.8 Estimated Frost and Thaw Depths for the Highway 569 Study Site using the Adjusted Calibration Coefficients for the 2009/2010 Waterloo Method Prediction

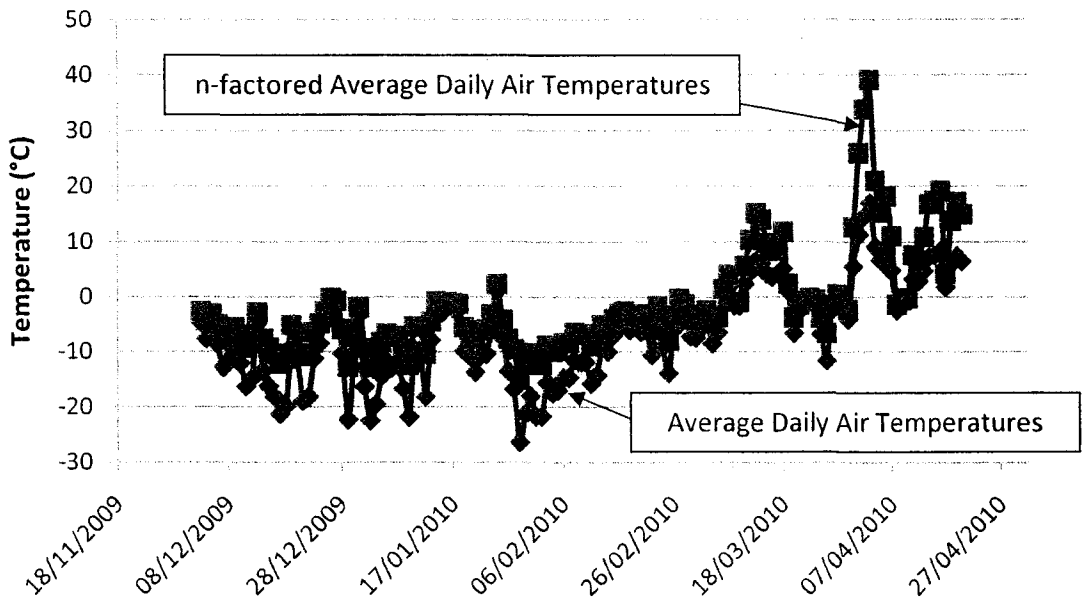

Figure 6.9 Air and N-factored Air Temperatures for Highway 569 for the 2009/2010 TEMP/W Prediction

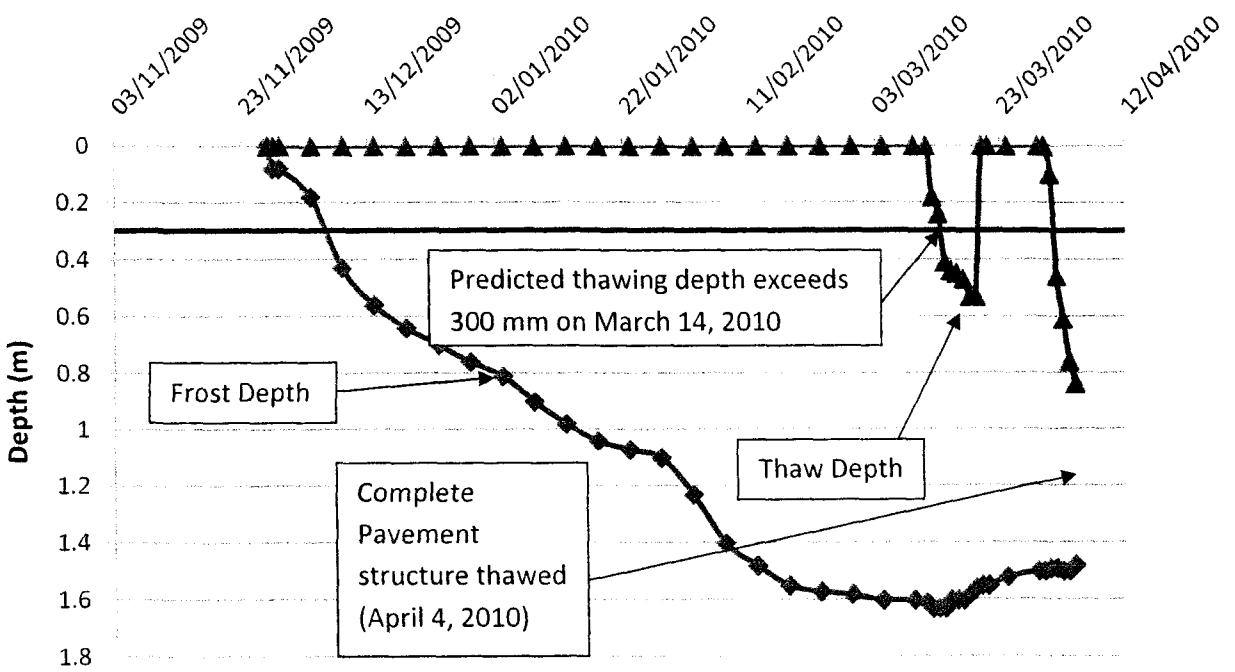

Figure 6.10 TEMP/W 2009/2010 Prediction for the Highway 569 Study Site

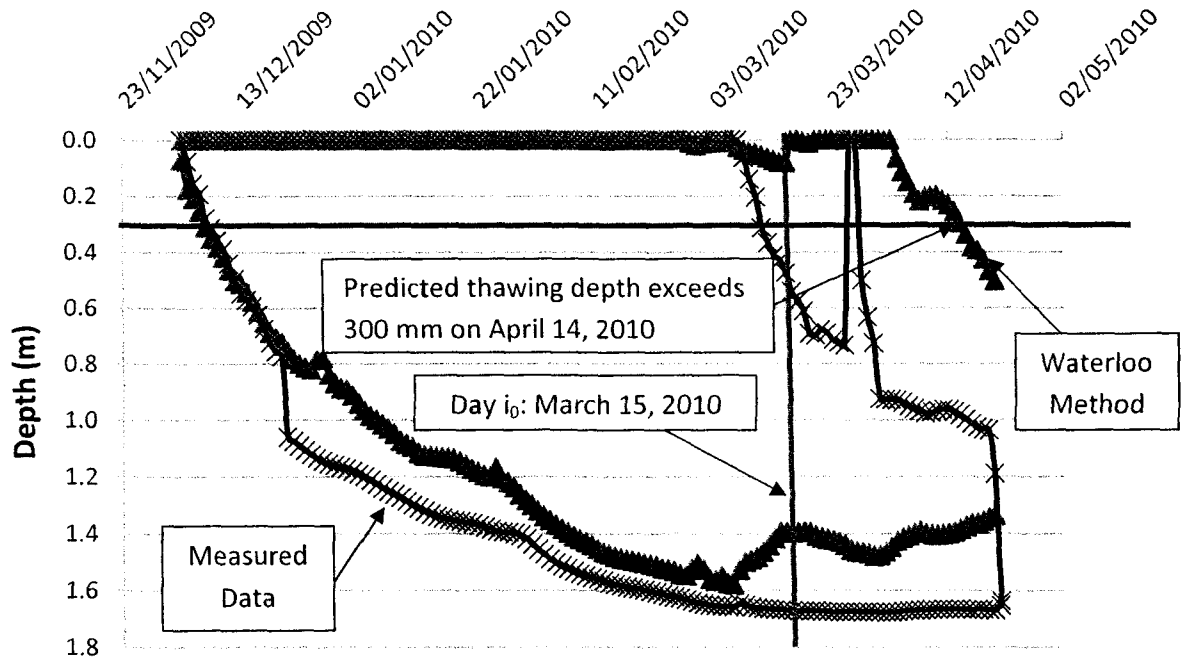

Figure 6.11 Waterloo Prediction and Observed Conditions for the Highway 569 Study Site during 2009/2010

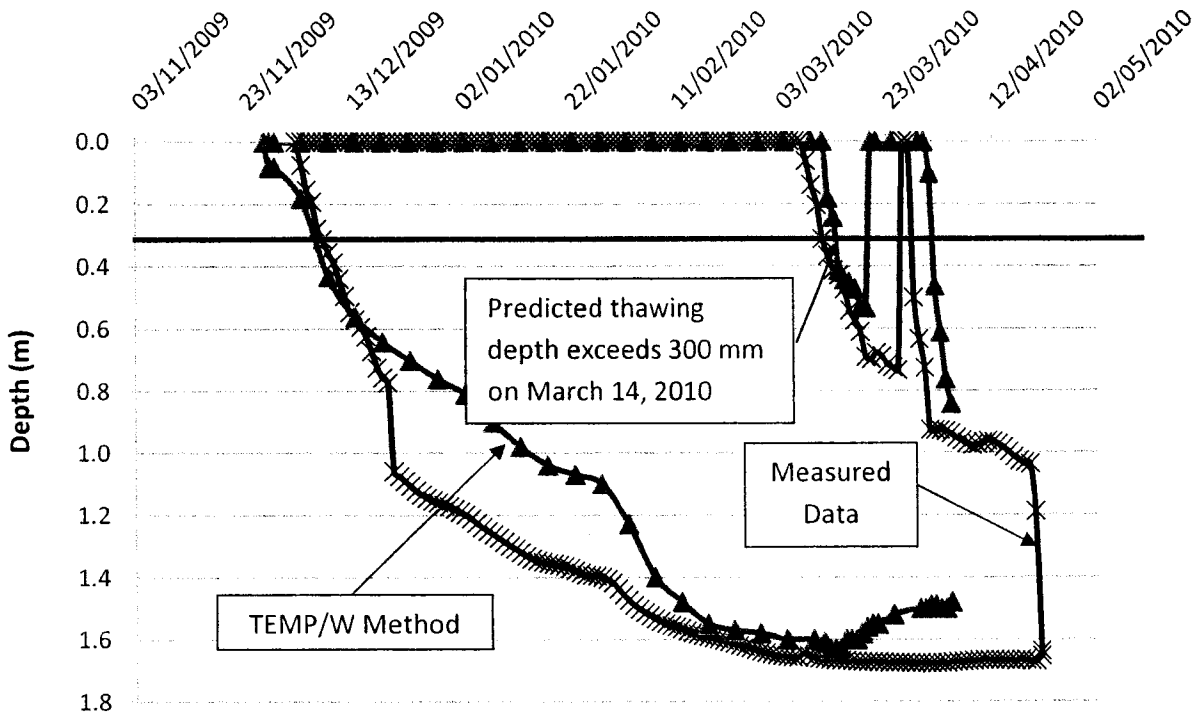

Figure 6.12 TEMP/W Prediction and Observed Conditions for the Highway 569 Study Site during 2009/2010

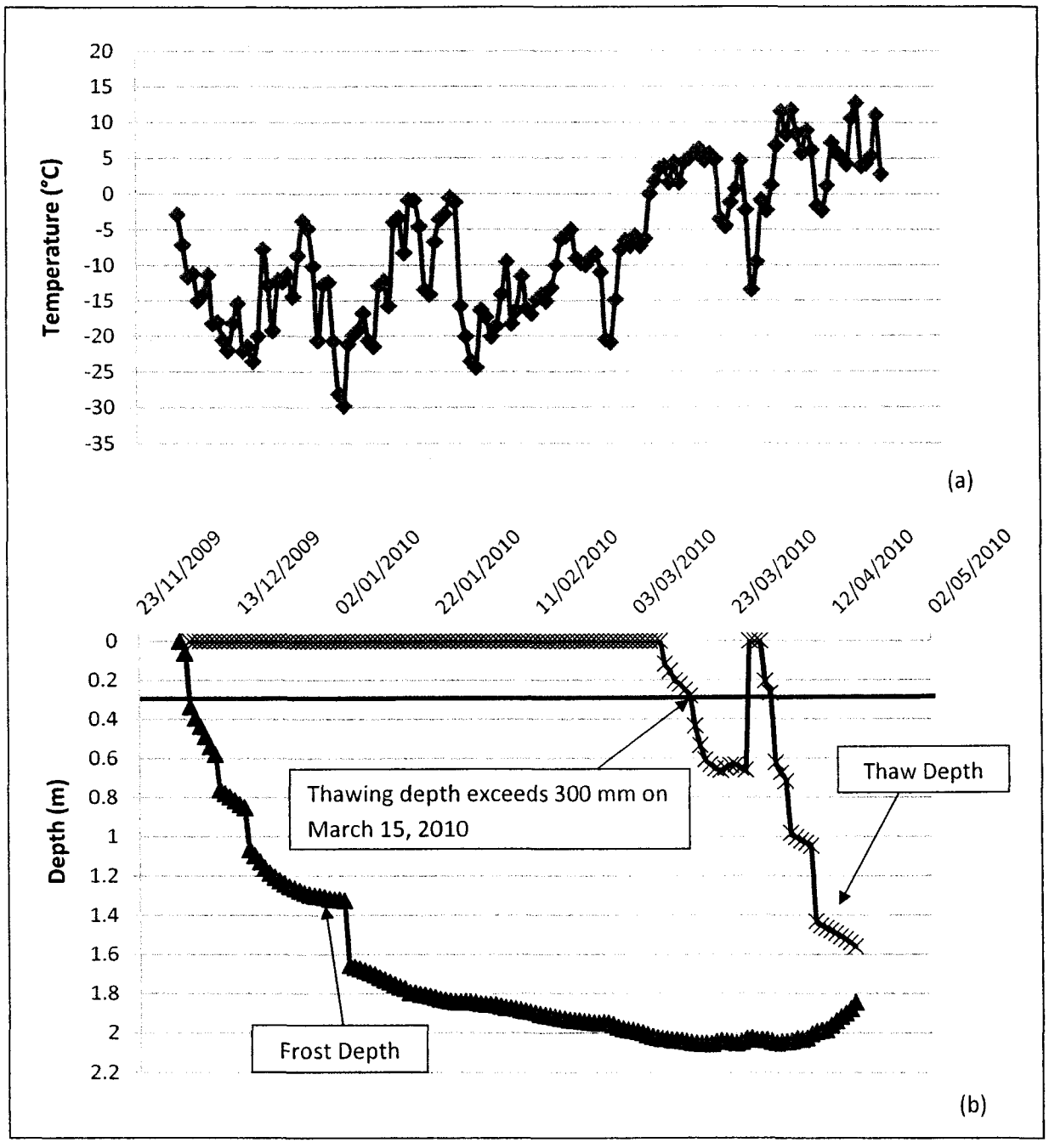

Figure 6.13 Average Daily Air Temperatures and Measured Frost/Thaw Depths for Highway 527, 2009/2010

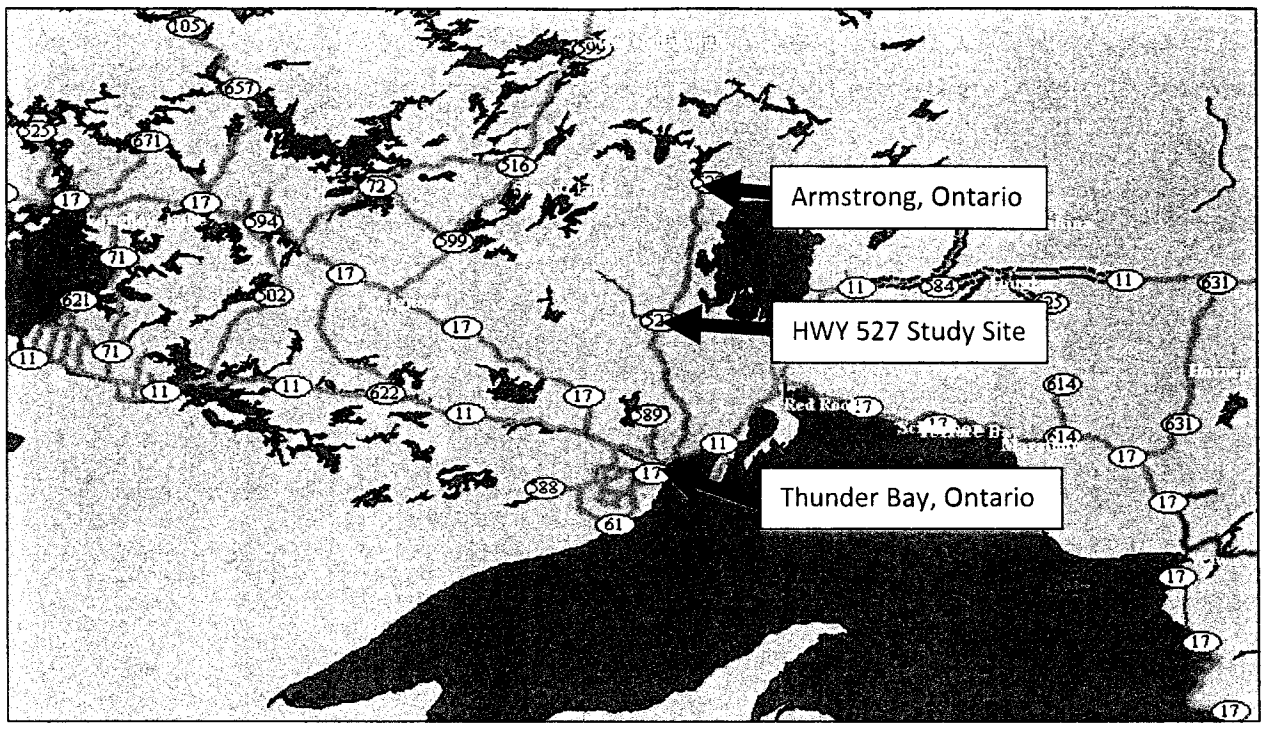

Figure 6.14 Highway 527 Study Site Location Compared to 5-day Forecast Municipalities

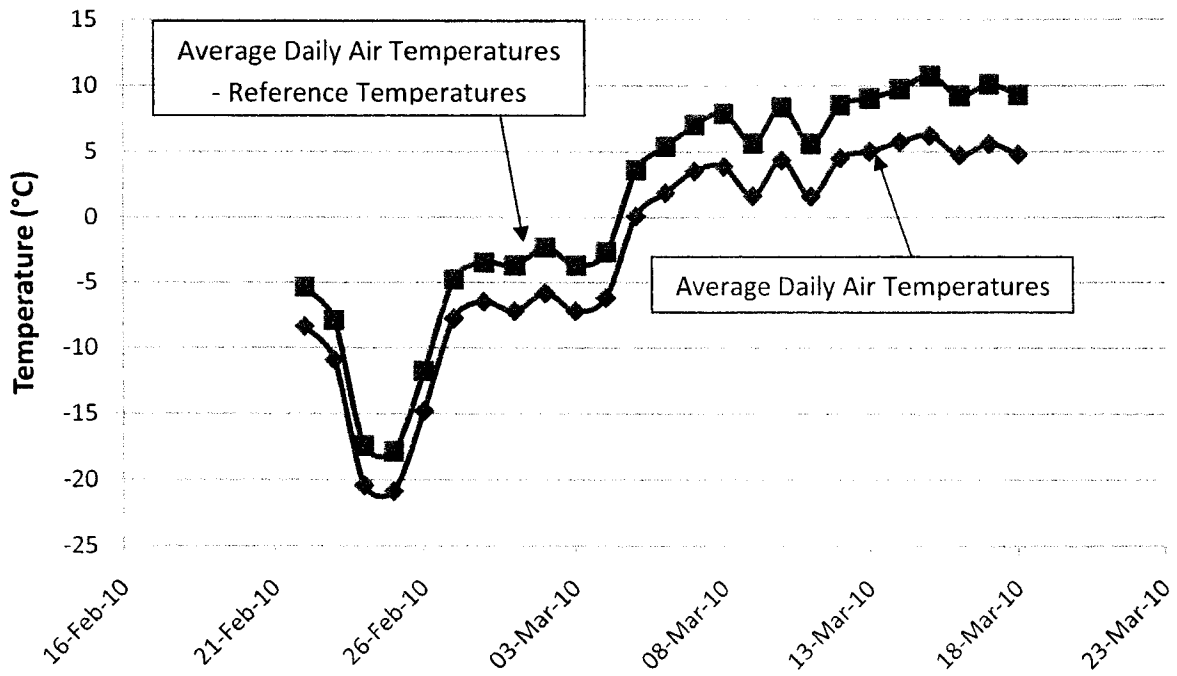

Figure 6.15 Air Temperature Modifications by the Reference Temperatures used in 2009/2010 Mn/DOT Prediction for the Highway 527 Study Site

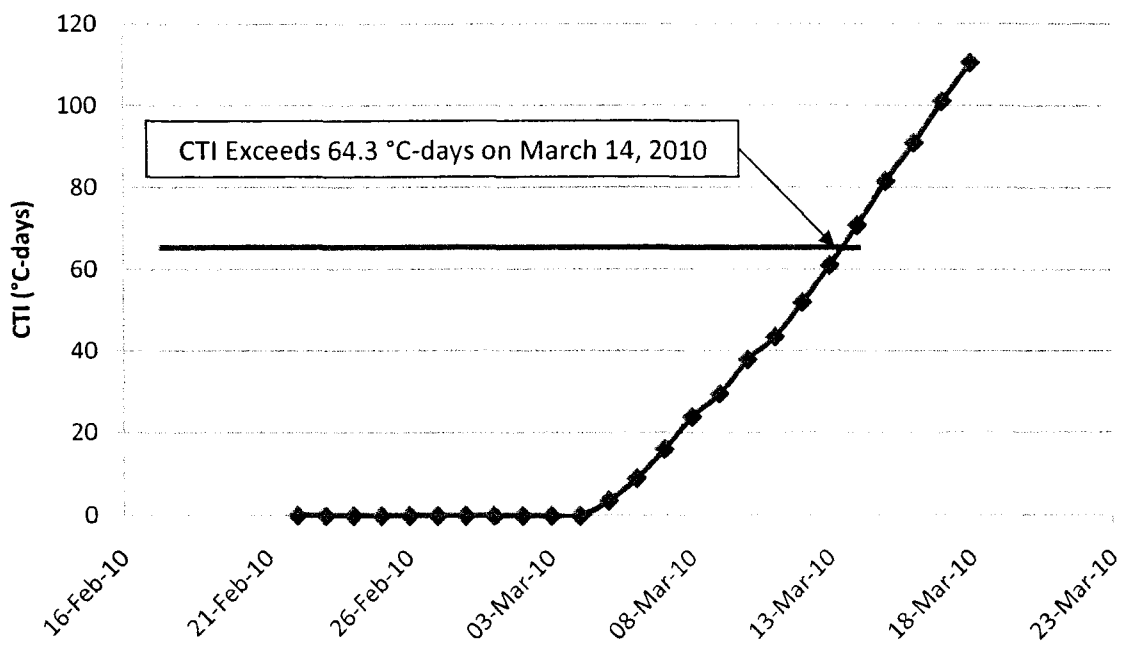

Figure 6.16 Mn/DOT Method CTI Calculation for the 2009/2010 Season for the Highway 527 Study Site

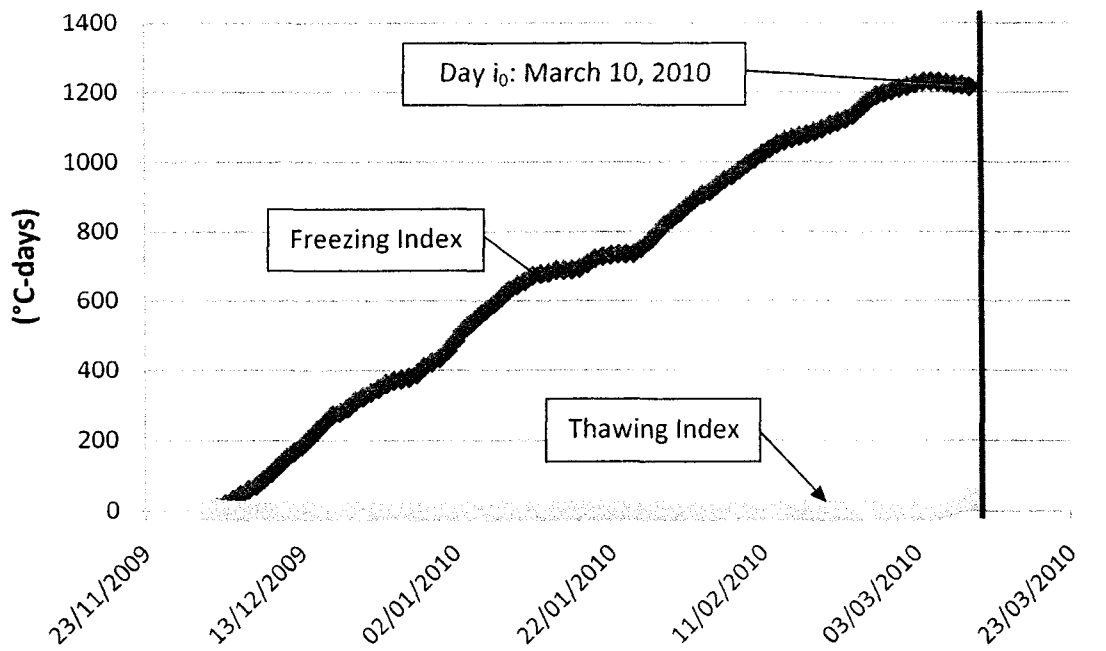

Figure 6.17 Day i_0 Determination at Highway 527 during the 2009/2010 Prediction

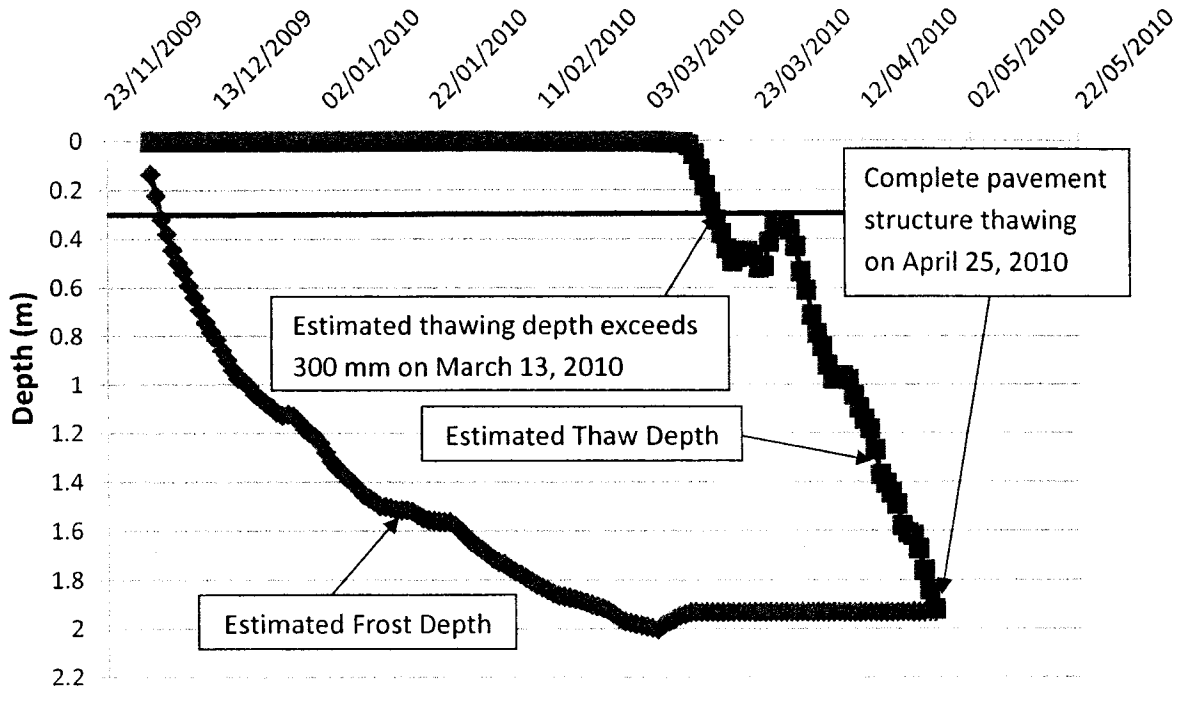

Figure 6.18 Estimated Frost and Thaw Depths for the Highway 527 Study Site using the Adjusted Calibration Coefficients for the 2009/2010 Waterloo Method Prediction

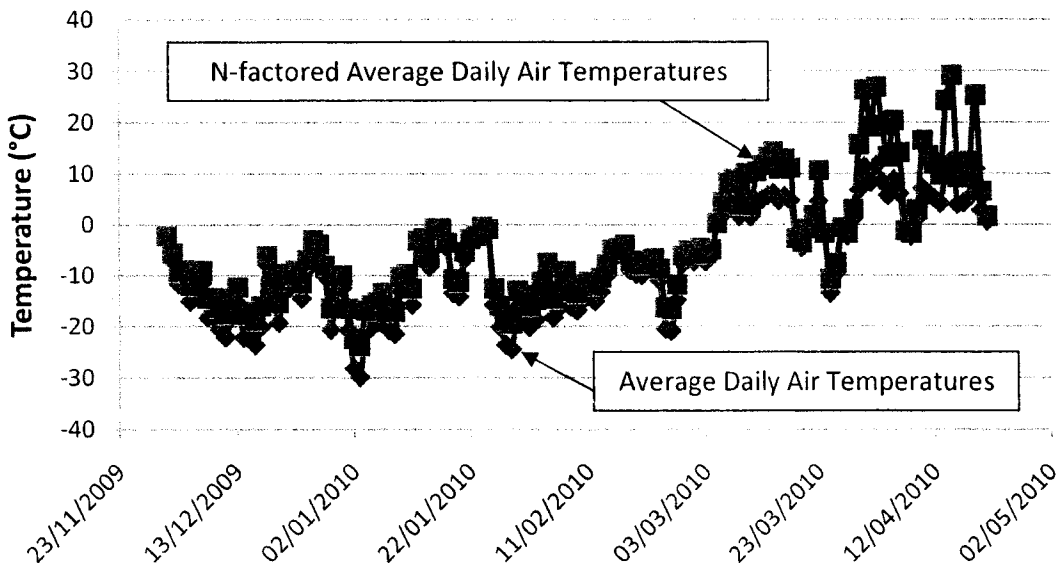

Figure 6.19 Air and N-factored Air Temperatures for Highway 527 for the 2009/2010 TEMP/W Prediction

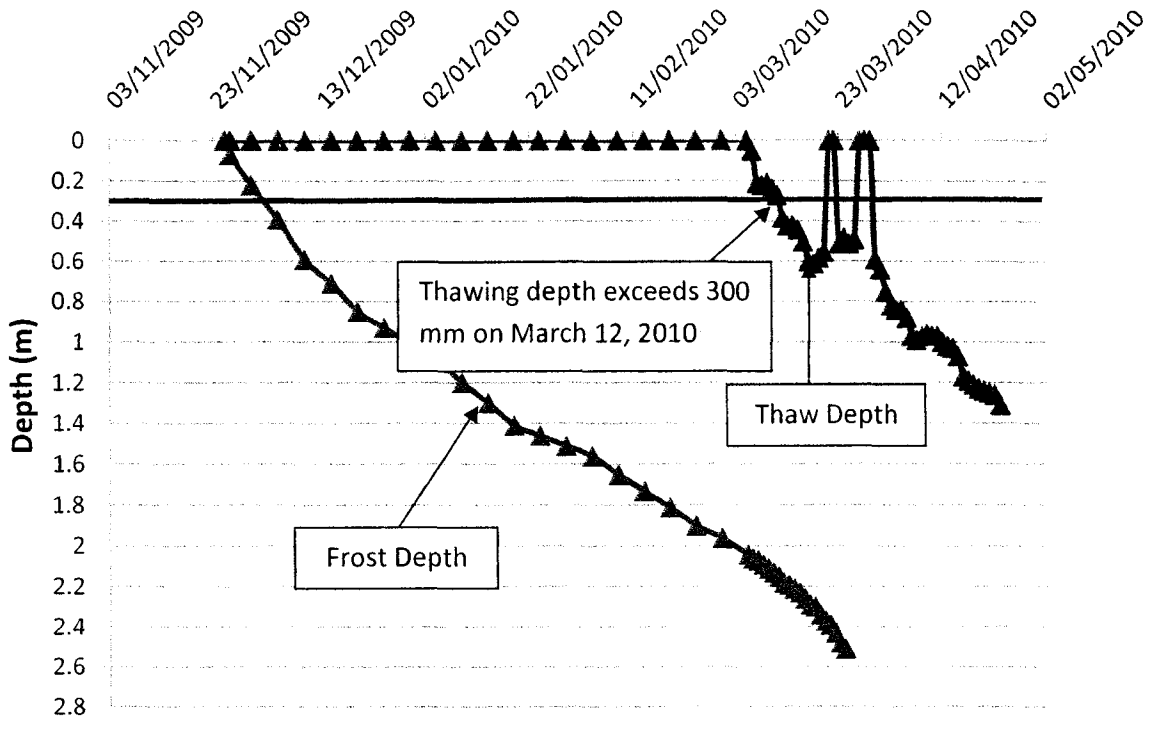

Figure 6.20 TEMP/W 2009/2010 Prediction for the Highway 527 Study Site

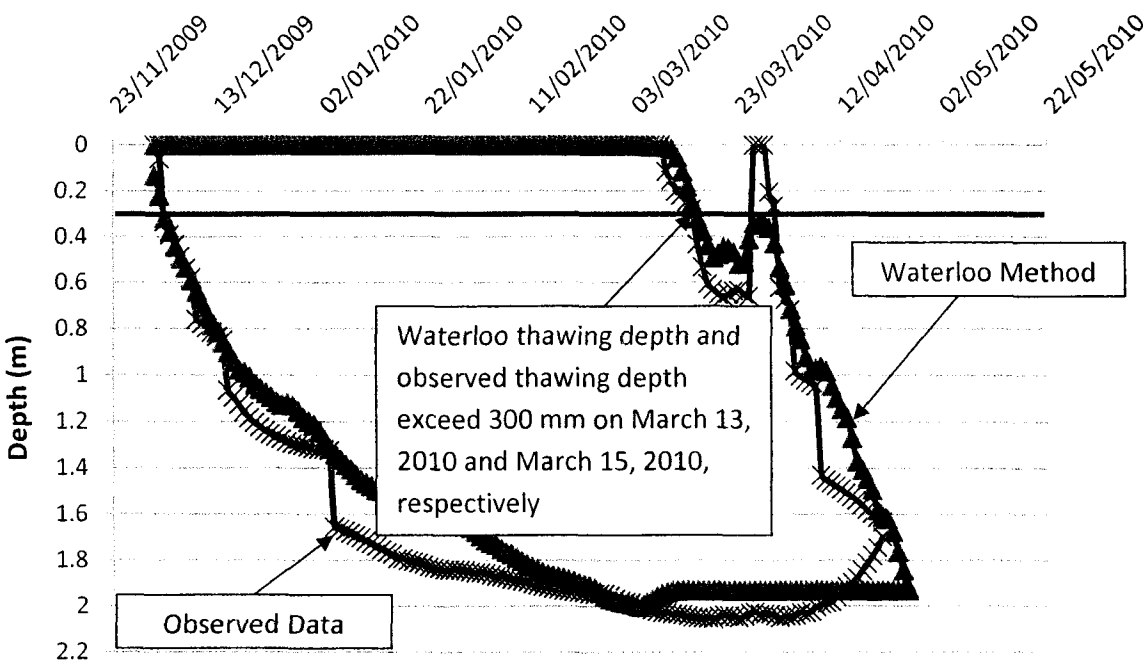

Figure 6.21 Waterloo Prediction and Observed Conditions for the Highway 527 Study Site for 2009/2010

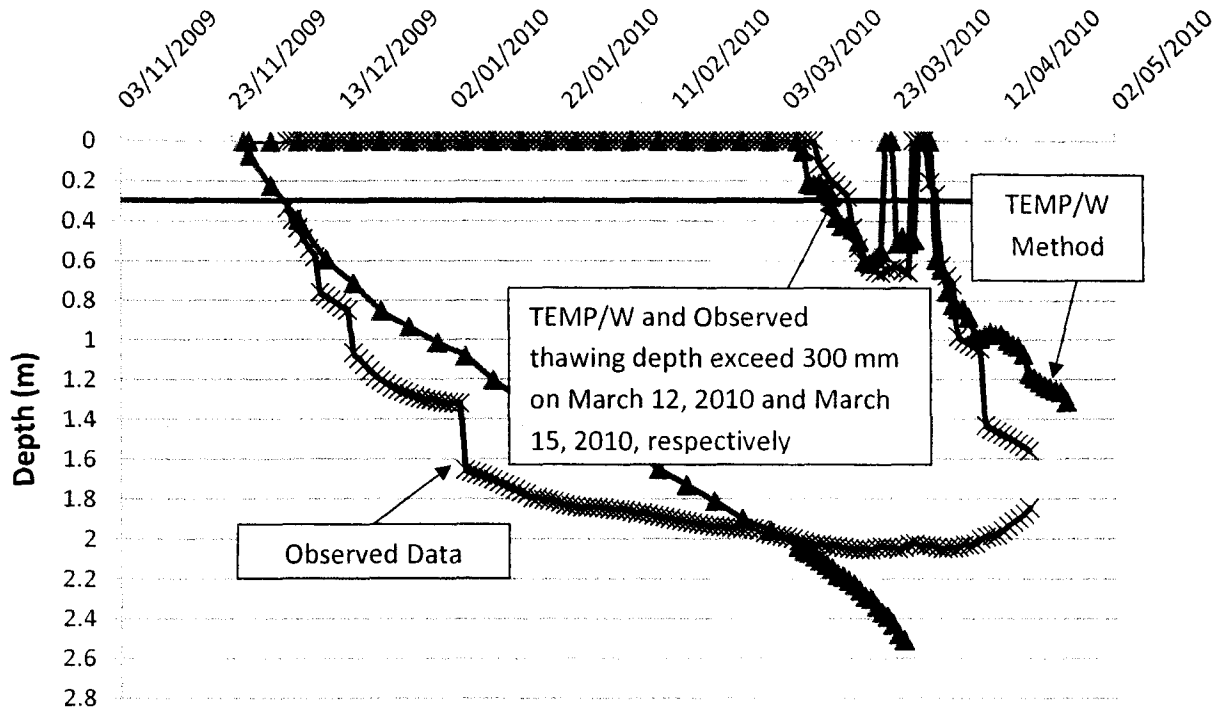

Figure 6.22 TEMP/W Prediction and Observed Conditions for Highway 527 Study Site for 2009/2010

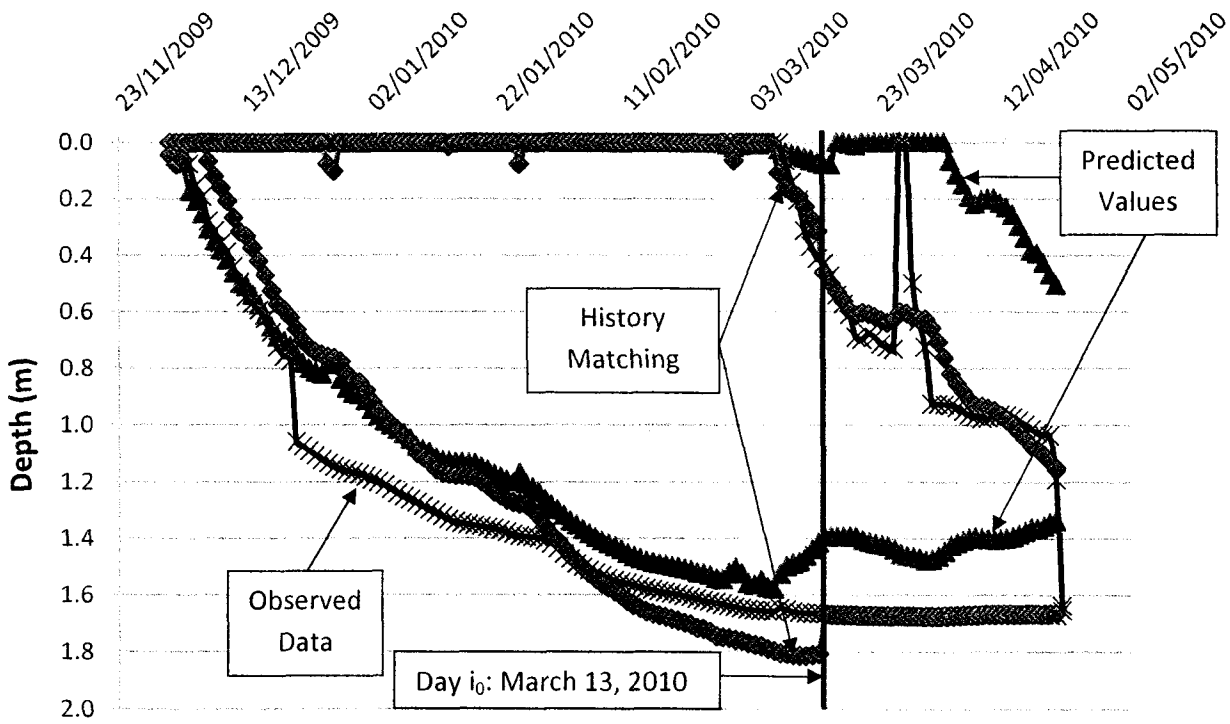

Figure 6.23 Waterloo Method Prediction and History Matching Results for the Highway 569 Study Site (2009/2010)

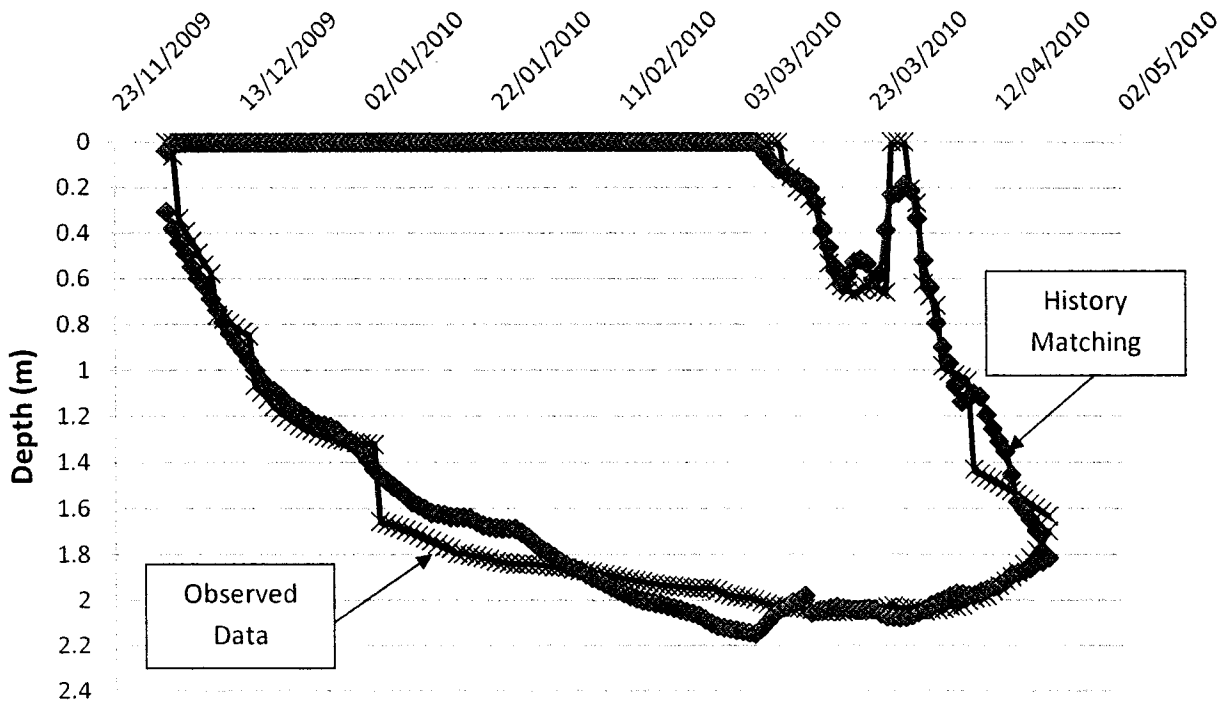

Figure 6.24 Waterloo Method Prediction and History Matching for the Highway 527 Study Site (2009/2010)

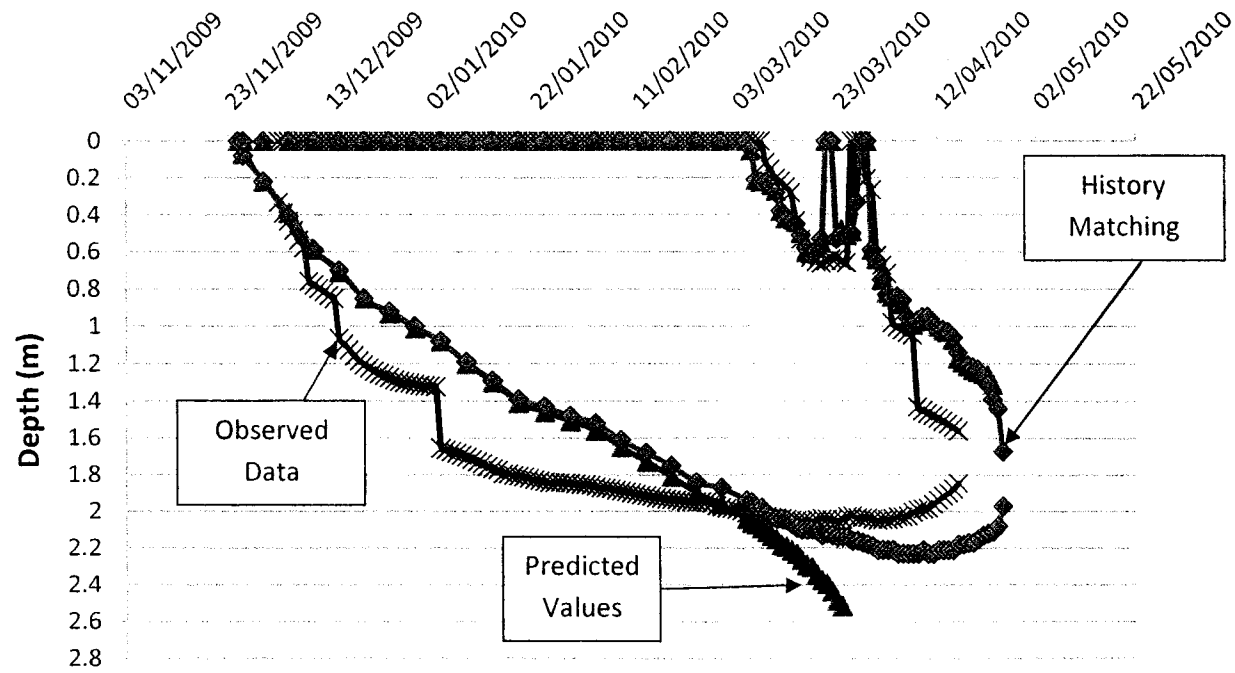

Figure 6.25 TEMP/W Method Prediction and History Matching Results for the Highway 527 Study Site (2009/2010)

7.0 Development of the Lakehead University SLR Method

7.1 Overall Pavement Stiffness Assessment for Application in the Lakehead University SLR Method

After examining the deflection and stiffness data collected by the MTO and LU (Section 5.2), it was concluded that there is a significant decrease in pavement stiffness at the Highway 527 and 569 study sites when progressing from frozen to thawed conditions. The extent of the thawing depth at the time of pavement stiffness reduction ranges from approximately 0.2 m to 0.6 m. These depths are in accordance with the values presented by Ovik et al. (2000). Therefore, based on these results the assumed threshold thawing depth of 300 mm is acceptable. Further testing at these sites and additional sets on a more frequent basis would be required to refine the threshold thawing depth. Furthermore, the results of the LWD testing by the MTO and LU indicate that the pavement stiffness is typically recovered at some time after the pavement structure is completely thawed. Combining these findings with the comments by Berg (2010) reinforces the inclusion of 7 additional days after complete subsurface thawing as a criterion for the removal of SLRs. This allows pavement stiffness to be recovered. Furthermore, because the LWD results typically indicate a decrease in pavement stiffness during pavement structure thawing and a slight increase in pavement stiffness after complete pavement structure thawing, the LWD could be used to aid in SLR implementation and removal.

When comparing LWD surface modulus values with FWD composite modulus values, Steinert et al.'s (2005) recommendation that composite modulus values greater than 4000 MPa be excluded from analysis along with the removal of LWD surface modulus values greater than 2000 MPa, provide a closer correlation between the northern Ontario measured surface modulus values and the corresponding FWD composite modulus values. The correlation of these values however remains low, with the R^2 value only increasing from 0.52 to 0.60. Based

on these results, further testing and analysis is required to increase confidence in the use of the surface modulus values obtained from the LWD to determine corresponding FWD composite modulus values. Research by Steinert et al. (2005) indicates a close correspondence between LWD and FWD composite modulus values. Determining the accurate seed values required to convert surface modulus values into composite modulus values using LWDmod may provided a better correlation between the LWD and FWD measurements at the northern Ontario study sites. Increasing the strength of the correlation between the LWD and FWD values would increase the confidence in the use of an LWD to estimate quantitative pavement structure stiffness values. Determining specific stiffness values could allow for the development of SLR triggering and removal threshold modulus values.

7.2 Lakehead University SLR Method

The Lakehead University (LU) SLR method was developed using the results of the Mn/DOT, Waterloo and TEMP/W SLR method assessment (Section 6.3). In addition to the assessment results, the LU method incorporates the pavement stiffness results (Section 5.2) into the SLR implementation and removal criteria.

The LU method was developed in a stepwise manner following the method development flow chart depicted in Figure 1.2. The first step in the method development was to assess three potential SLR methods that varied from empirically based (Mn/DOT method) to semi-empirically based (Waterloo method) to analytically based (TEMP/W method) with respect to the prediction accuracy of the methods and the ease of implementation of each method.

The Mn/DOT method was calibrated to trigger application of SLRs with a threshold CTI value that corresponds to a thawing front depth of 0.3 m at each site. This method only requires average daily air temperatures and the use of previously determined weekly reference temperatures. The results of this method provided in Section 6.3 indicate that this method will closely predict the implementation of SLRs. The Mn/DOT method, however, did not give accurate removal dates, missing on average by approximately 7 days. Furthermore, this method does not provide an indication of the location of the frost and thaw fronts.

The Waterloo method requires the greatest amount of adjustments throughout the thawing season and as indicated in Section 6.3, is highly dependent on how well the calibration coefficients based on historical data represent a given site and a current thawing event. When based on limited data sets to calibrate the Waterloo coefficients the accuracy of the method in a predictive manner is diminished. As a result of the lack of representative calibration coefficients for future predictions, the LU method will not use the Waterloo method.

The TEMP/W method requires the greatest amount of inputs, many of which are estimated based on limited probehole information and typical soil properties. The sensitivity analysis (Section 4.5.1.2) indicates that the accuracy of the model is depends on material and thermal property inputs. Furthermore, the TEMP/W predictions described in Section 6.2.4 illustrate the dependency of the method on accurate boundary conditions. A benefit of the TEMP/W method, however, is its ability to represent numerous pavement structure profiles under numerous climatic conditions.

Based on the amount of inputs required for each method and the performance of each method during the predictive analysis, the Mn/DOT method provides the best combination of SLR application and removal applications and the fewest number of inputs required. For this reason the Lakehead University (LU) SLR method is based on the Mn/DOT method, as modified to represent northern Ontario conditions. Future applications of this method require only a 5-day forecast of the average daily air temperatures and the average daily air temperature values provided by the RWIS stations as the only inputs. Further developmental work should include additional pavement deflection testing and correlation with thawing depths for additional sites to refine the threshold thawing depth, correlation of the CTI with the threshold thawing depth for additional sites, further work to better refine prediction of the thawing duration and the SLR removal date and a closer examination of the reference temperatures to be used for northern Ontario conditions. In addition to this, the TEMP/W program can be used as a tool to continuously refine the LU method through analysis of potential pavement structures and environmental conditions to represent locations besides those tested and calibrated.

The analysis of the LWD results provided in Section 7.1 indicates the use of a 0.3 m thawing depth as the threshold value for triggering SLR application at the sites studied in this

research. In addition, the LWD surface modulus results can be used to identify the onset of pavement structure thawing due to a reduction in the measured pavement stiffness during the thawing period. Furthermore, the pavement stiffness results presented in Section 7.1 indicate a slight rebound of the surface modulus within a maximum of two weeks of full pavement structure thawing, therefore, the LWD surface modulus values can be used to aid in SLR removal decisions.

In summary, the LU method can be implemented as follows (Figure 7.1):

1. Regions within the province of Ontario will be established by grouping areas that share similar climate conditions and geographical characteristics.
2. Average daily air temperatures from the RWIS stations and 5 day forecasts from the closest locations of interest will be collected for input into the method. The average daily air temperatures will be adjusted by reference temperatures. The set of equations listed as Equation 2.23 will be used to calculate the CTI. The values given in Table 2.5 can be used until further work is conducted to refine these values for northern Ontario conditions.
3. The adjusted daily air temperatures will be used to calculate the CTI and the CTI will be compared with a threshold or triggering value that represents the conditions in each of the established regions. This method will be used to predict the date for which SLRs should be applied. Initial calibration of this model indicates that a CTI of 40 °C-days for the Highway 569 study site and 64 °C-days for the Highway 527 site results in a close match between predicted and observed SLR placement dates. SLRs will be removed when the date corresponding to the predicted thawing duration plus an additional seven days (required for pavement stiffness restoration) is reached. The average thawing duration plus 7 days has been found to equal 37 days at the Highway 569 study site (Average of the 2005/2006, 2007/2008 and 2009/2010 seasons) and 51 days at the Highway 527 study site (2008/2009 season).
4. LWD surface modulus data will be collected to observe changes in pavement stiffness during the predicted spring thawing period; these data can be used to refine the SLR application prediction. The surface modulus values can also be monitored to observe

surface modulus increases which indicate pavement stiffness recovery; these values can aid in the refinement of the SLR removal decision.

5. The TEMP/W program will be used to assess variation in the climate condition at these two study sites and others so that the threshold CTI, reference temperatures and the thawing duration used for SLR placement and removal can be further refined. The TEMP/W program can also be used to simulate numerous pavement structures under varying climate conditions to develop potential CTI values for locations outside of the two study sites.
6. Continuous refinement of the method parameters on a yearly basis in response to the observed frost and thaw depth should be conducted. Further refinement of the LU method using TEMP/W simulations and other RWIS instrumented sites would assist with developing CTI values that accurately represent the established regions.

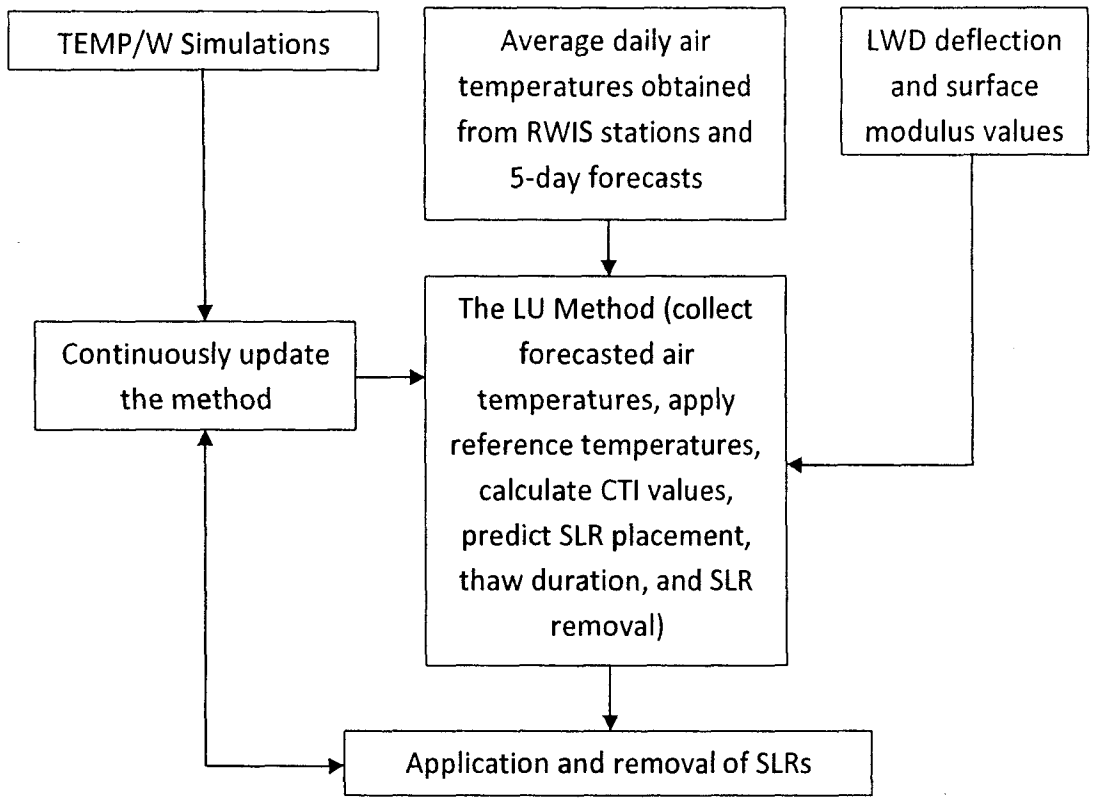

Figure 7.1 LU Method Implementation Flow Chart

8.0 Conclusions and Recommendations

8.1 Research Summary and Conclusions

The purpose of this research was to develop an effective SLR application and removal method that could be applied to low volume roads in northern Ontario. The development of the northern Ontario SLR method began with a detailed review and assessment of other SLR methods currently being developed or used in Canada and the northern United States.

Many jurisdictions throughout Canada and the northern United States currently use engineering judgment, prescheduled dates, visual observations, pavement deflection testing, and empirical methods alone or in combination, to apply and remove SLRs. A limitation to the use of engineering judgment, prescheduled dates and pavement deflection testing is the lag time between the need and the placement of SLRs, where significant pavement structure damage can occur. This lag time is required to notify the transportation industry of impending SLRs (typically 3–5 days).

Empirically based methods currently in use, such as the Mn/DOT method which uses a threshold CTI to trigger the application of SLRs, require the least amount of inputs and can easily be implemented. Furthermore, forecasted air temperatures can be used to project the application of SLRs in advance. This allows notice to be provided to the transportation industry of impending SLRs, thereby avoiding the lag time issue. Limitations to the emprirical methods, however, include the inability to estimate pavement structure frost and thaw front depths and account for site specific conditions such as pavement structure properties.

Semi-empirical methods have been developed to predict the frost and thaw depths within the pavement structure. Using these predictions, SLRs can be placed during the estimated period of spring thawing. As with the empirical methods, forecasted temperatures can be used in the method to predict the depth of the frost and thaw fronts in advance,

allowing notification of impending SLRs to the transportation industry. These methods are limited, however, in that they require a database of reference temperatures and frost and thaw depth algorithm coefficients in order to be used in a predictive manner. These methods, as with the empirical methods, do not directly account for site specific conditions such as the pavement structure properties.

Analytical/numerical based methods can easily be applied to any pavement structure and climate condition for which an analysis can be conducted. As with the other approaches, forecasted temperatures can be used to avoid the notification lag time. These methods however, require the greatest amount of inputs and require specific pavement structure information and definition of representative boundary conditions.

From this detailed review and assessment three methods were selected for further analysis and assessment. These methods cover a range from empirically based methods to analytical/ numerically based methods. The first method is an empirical method developed by the Mn/DOT which utilizes air and reference temperatures to calculate a CTI. Once the CTI exceeds a triggering value, SLRs are applied. SLR removal using this method is based on historical data and observed field conditions. The second method examined is a semi-empirical method developed by the University of Waterloo. This method uses air and reference temperatures in the calculation of FI and TI values. Measured frost and thaw depths are used in conjunction with the FI and TI values to develop model calibration coefficients. The calibration coefficients and the FI and TI values are input into an algorithm that estimates frost and thaw depths, which are used to determine SLR placement and removal. The third SLR method uses thermal numerical modelling to predict the frost and thaw depths which, as with the Waterloo method, can be used to determine SLR implementation and removal dates. TEMP/W from GEO-SLOPE International Ltd. was selected as the thermal numerical analysis code for use in this project.

Pavement deflection testing using an LWD was conducted at two sites instrumented by the MTO, one in northwestern Ontario (Highway 527) and one in northeastern Ontario (Highway 569). The purpose of this testing was to determine pavement stiffness response to

changes in the observed frost and thaw depths during the winter/spring seasons. LWD surface modulus values were used to assess the pavement stiffness for this testing.

The results of the LWD testing at the onset of the freezing season for the northwestern Ontario site show that the surface modulus values increased significantly, from an average value of 261 MPa for the three weeks before the presence of subsurface frost, to 8690 MPa after the frost had penetrated to a depth of approximately 0.4 m. Only one day of testing at the northeastern Ontario site was conducted during the freezing season indicating a surface modulus of 1743 MPa corresponding to an observed frost depth of 0.6 m.

LWD tests performed throughout the 2008, 2009 and 2010 thawing seasons at the northwestern Ontario site indicate that surface modulus values are significantly reduced when the pavement structure has thawed to depths of about 0.4 m, 0.3 m and 0.2 m, respectively. For this reason a thaw depth of 0.3 m is used in this project as the trigger value for SLR application. This 0.3 m triggering value is in accordance with Ovik et al. (2000) who found that pavement deflections significantly increase when the pavement structure has thawed between 300 mm and 600 mm. Further to this, all of the LWD test results at both the northwestern and northeastern locations during the spring seasons show slight increases in pavement stiffness for up to two weeks after the pavement structure has completely thawed. This is in accordance with (Berg, 2010) who noted that pavement stiffness would be restored approximately 7 days after complete subsurface thawing. As a result of these findings, SLR removal 7 days after complete pavement structure thawing is used for this project in the assessment of the three SLR methods.

Side-by-side LWD/FWD tests were conducted during the 2008 spring season at three northeastern Ontario instrumented sites. The results of these tests were analyzed to observe any potential correlation between the two devices. Using the LWDmod program to convert surface modulus values into corresponding composite modulus values requires the estimation of unknown seed values (subsurface modulus and coefficient of non-linearity values). For this reason LWD surface modulus values were correlated with FWD composite modulus values. The correlation between these values was found to be poor ($R^2 = 0.52$). Following Steinert et al. (2005), FWD composite modulus values greater than 4000 MPa were removed from analysis. In

addition to this, LWD surface modulus values greater than 2000 MPa were also removed from analysis. The removal of these values only slightly increased the R^2 value to 0.60. As a result of the poor correlation between the LWD and FWD testing, the LWD test results will only be used to qualify changes in pavement stiffness during the spring thaw season and not provide a quantifiable number to trigger the application or removal of SLRs.

Using the SLR application and removal criteria determined from the pavement deflection testing and correlations with pavement structure thawing depths, the three SLR methods were assessed through a program of calibration and prediction using measured frost and thaw depths at both the northeastern and northwestern Ontario sites. Each of the methods used three winter/spring seasons of data (2005/2006, 2007/2008, 2008/2009) available for calibration at the northeastern Ontario site and one winter/spring season of data (2008/2009) available for calibration at the northwestern Ontario site.

For the Mn/DOT method calibration for the northeastern study site, the CTI value that corresponded to the threshold thawing depth of 0.3 m ranged from 26.4 °C-days to 50.3 °C-days over the three calibration seasons. At the northwestern site the CTI value for the threshold thawing depth was calculated to be 64.3 °C-days. Based on a comparison of these CTI values, the thawing front depth at the northeastern study site appears to be more sensitive to increases in air temperature than the northwestern study site, as the pavement structure at that northeastern site thaws to a depth of 0.3 m, at least 14 °C-days sooner, than it does at the northwestern site.

Calibration of the Mn/DOT method for SLR removal used the average pavement structure thawing duration. The observed frost and thaw depths at the northeastern site indicated thawing durations of 10, 24 and 55 days, for the 2005/2006, 2007/2008 and 2008/2009 seasons, respectively. Significant fluctuations in the thawing duration (i.e. 45 days when comparing the 2005/2006 and 2007/2008) on a yearly basis limit the ability of this method to accurately predict the SLR removal date.

During the calibration of the Waterloo method, it was observed that the method was highly sensitive to the algorithm calibration coefficients. The calibration coefficients were also found to be highly inconsistent on a yearly basis at the northeastern study site. This made it

difficult to determine calibration coefficients that could reliably represent the pavement structure freezing and thawing conditions at the study sites. During a preliminary prediction of the 2008/2009 season using the 2005/2006 and 2007/2008 calibration coefficients, it was discovered that significant adjustments had to be made to two coefficients ("g" and "j") on day i_0 to match the estimated freezing season frost and thaw depths with the estimated thawing season frost and thaw depths.

Calibration of TEMP/W for simulations of pavement structure frost and thaw depths at the two sites indicate that using n-factored air temperatures as the upper boundary condition result in the best match between simulated and measured values, compared to the reference temperature and climate approaches. Furthermore, using the lowest thermistor values as the lower boundary condition for the model improved the match between simulated results and measured results when compared with using a constant temperature at a constant depth as the lower boundary condition.

A sensitivity analysis was conducted with TEMP/W to examine the effects that changes in the subsurface moisture condition have on model simulations. The sensitivity analysis results indicate that the TEMP/W model is sensitive to changes in the material and thermal properties that result from changes in the subsurface moisture content. Increasing the degree of saturation will increase the time that is required for the pavement structure to fully thaw. Conversely, reducing the degree of saturation will reduce the thawing time required. The TEMP/W method requires the most number of inputs and an understanding of the pavement structure profile, making it the most difficult of the methods assessed to implement.

Three calibrated SLR methods were assessed in a predictive manner for both the northeastern and northwestern Ontario sites for the 2009/2010 season. Using the calibrated Mn/DOT method to predict the SLR application and removal dates for the 2009/2010 season at the northeastern Ontario study site provided an accurate SLR application date (March 13, 2010) when compared to the measured data (March 11, 2010). This method however, was less accurate when predicting the removal of SLRs (April 19, 2010 for the prediction compared to April 28, 2010 for the observed).

When the Mn/DOT method was calibrated for the northwestern Ontario study site and used to predict the SLR application and removal dates for the 2009/2010 season, it was again accurate in predicting the SLR application date (March 14, 2010) compared with the observed conditions (March 15, 2010). The northwestern site SLR removal date prediction was more accurate than the northeastern Ontario site date, indicating SLR removal 6 days after the observed conditions indicated (May 4, 2010 for the prediction compared to April 28, 2010 for the observed). The results of these predictions show that use of the Mn/DOT method is quite accurate in predicting the SLR application date (within 1 – 2 days). SLR removal was predicted to be removed 9 days too soon at the northeastern study site and 5 days late at the northwestern study site. The inaccuracy of the SLR removal dates can be attributed to the large differences in the thawing duration on a yearly basis noted in the Mn/DOT method calibrations. The use of further study sites and study seasons could increase the accuracy of the average pavement structure thawing duration. In addition, the potential of correlating weather condition indices from the current season such as frost depth or cumulative freezing index, with historical thawing durations correlated with the same historical indices should be investigated. This might provide a more reliable, accurate thawing duration than using an average duration value, as the experience with the Highway 569 site prediction has indicated.

Using the calibrated Waterloo method in a predictive manner for the 2009/2010 season at the northeastern Ontario study site indicated that the thawing depth would exceed 0.3 m on April 14, 2010, long after the date indicated by the observed conditions (March 11, 2010). As a result of the inaccurate thawing depth prediction, the predicted time of the complete pavement structure thawing at the Highway 569 site was also significantly offset.

When the calibrated Waterloo method was used to predict the frost and thaw depths at the northwestern Ontario study site, the accuracy was significantly better than at the northeastern Ontario site. The Waterloo method predicted that the thawing would exceed 0.3 m on March 13, 2010, two days sooner than indicated by the observed data (March 15, 2010). This method also closely predicted the date in which the pavement structure would be completely thawed (April 25, 2010) when compared to the observed data (April 21, 2010).

Furthermore, results of the predicted frost and thaw depth correspond well with observed depths at all times throughout the freezing and thawing season.

Based on the results of these predictions, the Waterloo method can be used to accurately predict the frost depths during the freezing season at both sites. During the thawing season, however, the average calibration coefficients do not accurately represent the conditions at the northeastern Ontario site. This results in significant errors in the Waterloo prediction. This research shows that it is very difficult to develop a set of coefficients for the Waterloo method that can be used for reliable predictions for SLR implementation, even when multiple calibration years of data are available. Further research, particularly focusing on a method to develop coefficients that gave more reliable frost and thaw depth predictions would need to be conducted for the Waterloo method.

For the northeastern study site, the calibrated TEMP/W method closely predicted the date that thawing exceeded 0.3 m (March 14, 2010) when compared to the observed date (March 11, 2010) for the 2009/2010 prediction. However this method was inaccurate in predicting the date in which complete pavement structure thawing would occur (April 4, 2010 for the prediction compared to April 21, 2010 for the observed).

For the northwestern Ontario study site, the TEMP/W method again provided a good prediction of the 0.3 m thawing depth date (March 12, 2010 for the prediction compared with March 15, 2010 for the observed). Using the lowest thermistor values from the 2008/2009 season as the lower boundary condition for the prediction however, resulted in significant inaccuracy of the frost depth prediction, resulting in a much later date (May 24, 2010 for complete pavement structure thawing) when compared with the observed date (April 21, 2010).

The results of these TEMP/W predictions highlight the need for accurate boundary conditions. Based on both the calibration and predictive exercises it can be seen that the thawing depth during the spring is closely associated with the upper boundary condition, while the frost front migration is strongly tied to both the upper and the lower boundary conditions. It is therefore necessary to accurately define both boundary conditions to maximize the accuracy of the predictive model.

History matching of the 2009/2010 season data using the Waterloo method predictions further indicates that the calibration coefficients are not consistent. The Highway 527 calibration coefficients from the 2008/2009 season show little similarity to the history matched calibration coefficients for the 2009/2010 season, even though both sets of coefficients provide a good fit to the observed frost and thaw depths. History matching of the 2009/2010 season data using the TEMP/W method indicates that the use of a representative lower boundary condition will result in a far better estimate of the frost and thaw depth within the pavement structure.

The LU method for implementation of SLRs in northern Ontario was developed based on the results of the three SLR method calibrations and predictions and the LWD pavement deflection results. The results from the LWD testing indicate that a thawing depth of approximately 0.3 m results in a significant pavement stiffness reduction. For this reason a thawing depth of 0.3 m is used as the trigger for SLR application for the LU method. The LWD results also indicate that there is a slight increase in pavement stiffness within 2 weeks of complete pavement structure thawing. As a result of this, a date corresponding to 7 days after complete pavement structure thawing is used for SLR removal for the LU method.

The results of the SLR calibrations and predictions indicate that the use of a CTI method, similar to the one developed by the Mn/DOT, but calibrated to represent northern Ontario conditions, results in the closest prediction of observed frost and thaw depths. The set of equations listed as Equation 2.23 should be used to calculate the CTI. Furthermore, the CTI-based LU method requires the least amount of inputs and is the easiest of the methods assessed to implement.

The CTI-based LU method, however, is site specific. To overcome this issue, multiple locations consisting of various pavement structures and climate conditions in northern Ontario must be monitored and SLR placement and removal dates correlated with CTI values and observed frost and thaw depths. In addition, the TEMP/W program can be used to simulate numerous pavement structures under varying climate conditions to develop further correlations of SLR placement and removal dates with threshold CTI values and simulated frost and thaw depths.

LWD pavement deflection results obtained from future testing can be used to aid in the refinement of the SLR application threshold thawing depth and the SLR removal date through an examination of pavement stiffness responses to changes in observed frost and thaw depths at the instrumented sites in northern Ontario. The LWD results can be used to further develop CTI values that account for both threshold thawing depths and corresponding pavement stiffness and to further investigate the time required for restoration of pavement structure stiffness after complete thawing.

In order for the LU SLR method to be implemented across Ontario, specific regions will have to be identified. For representative CTI values for application of SLRs and thaw durations/removal dates to be developed for a specific region, numerous factors will have to be considered, including geographical characteristics and climate conditions.

8.3 Recommendations for Future Work

The following are recommendations for further research based on the work conducted in this thesis:

1. Perform a detailed and comprehensive geotechnical characterization of the instrumented sites in northern Ontario and of any future instrumented sites.
2. Utilize the data available from all of the instrumented sites in northern Ontario to expand the LU SLR method to accurately represent larger areas instead of just the two study sites.
3. Develop regions throughout the province of Ontario that have similar geographical characteristics and undergo similar climate conditions. Develop CTI values and average thawing durations for each of the regions so that SLRs can be applied and removed appropriately for each region. The issue of climate change should also be considered in these activities.
4. Examine a more accurate approach in determining SLR removal. This may include examining freezing season patterns using a cumulative freezing index to provide insight into the following thawing season trends.
5. Conduct more trial predictions in order to further assess and refine the LU SLR method

6. Develop a more accurate method in dealing with the lower boundary condition in the TEMP/W models at the instrumented sites and develop a comprehensive method of performing TEMP/W simulations for uninstrumented sites.
7. Continue to correlate the LWD values with both frost and thaw depths and measured FWD values in order to establish a quantifiable LWD surface modulus value for SLR application and removal. The SLR application and removal CTI values and LWD surface modulus values could then be compared.
8. Examine potential options for increasing the force applied to the pavement surface when conducting deflection testing, perhaps through the development of an intermediately weighted deflectometer.
9. Use the pavement surface and air temperatures recorded at the RWIS stations to develop northern Ontario weekly reference temperatures that could be used in the LU method. Compare these reference temperatures with those developed by the Mn/DOT to observe the differences that result from more northern climate conditions.
10. Examine the effects that loading patterns including cyclic loading have on structurally weakened pavement structures either through the use of stress-strain modelling or full scale testing.
11. Examine the effect that the inclusion of road salts within the pavement structure has on the soil freezing and thawing patterns.

References

Ahmed, Z., Maher, M., Marshall, P.C. (2006), "Context Sensitive Pavement Design for Low Volume Road Applications", 2006 Annual Conference of the Transportation Association of Canada, Charlottetown, Prince Edward Island

Alaska Department of Transportation and Public Facilities (ADOT&PF) (2007), Implementation of Seasonal Highway Weight Restrictions, Policy No. 07.05.030

Amos, D. (2006),"Pavement Smoothness and Fuel Efficiency: An Analysis of the Economic Dimensions of the Missouri Smooth Road Initiative", Missouri Department of Transportation Organizational Results, Report No. OR07-005

Andersland, O., Ladanyi, B. (1994), "An Introduction to Frozen Ground Engineering", Chapman and Hall, New York

Andersland, O., Ladanyi, B. (2004), "Frozen Ground Engineering", The American Society of Civil Engineers and John Wiley and Sons

Anderson, D.M., Morgenstern, N.R, (1973) "Physics, chemistry and mechanics of frozen ground: a review. 2nd International Conference on Permafrost, Yakutsk U.S.S.R, North American Contribution, US National Academy of Sciences, pp. 257-288

Baiz, S., Tighe, S.L., Mills, B., Haas, C.T. (2007), "*Using Road Weather Information Systems (RWIS) to Control Load Restrictions on Gravel and Surface-Treated Highways*" Ministry of Transportation Engineering Standards Branch Report

Berg, R. (2010), Personal communication

Buchanan, F., Gwartz, S.E. (2005), "*Road Weather Information Systems at the Ministry of Transportation, Ontario*", 2005 Annual Conference of the Transportation Association of Canada, Calgary, Alberta

Canadian Strategic Highway Research Program (C-SHRP) (2002), "*Seasonal Load Restrictions in Canada and Around the World*", C-SHRP Technical Brief #21

Cote, J., Konrad, J-M. (2006), "*Estimating Thermal Conductivity of Pavement Granular Materials and Subgrade Soils*", Transportation Research Record No. 1967, pp 10-19

Dynatest (2006), "*DYNATEST 3031 LWD Light Weight Deflectometer, Owner's Manual Version 10.0*", Dynatest International

Eaton, R.A., Berg, R.L., Hall, A., Miller, H.J., Kestler, M.A. (2009), "*Initial Analysis of the New Hampshire Shire Spring Load Restriction Procedure*" 14th Annual Conference on Cold Regions Engineering, pp 532-545

Farouki, O.T. (1982), "*Evaluation of Methods for Calculating Soil Thermal Conductivity*" U.S. Cold Regions Research and Engineering Laboratory, CRREL Report 82-8

Fredlund, D.G., Rahardio, H. (2003), Soil Mechanics for Unsaturated Soils, Wiley-Interscience

Hein, D.D., Cole, R.M. (2002), "*Establishment and Monitoring of Pavement Load Restrictions in the Province of British Columbia*" 2002 Annual Conference of the Transportation Association of Canada, Winnipeg, Manitoba

Johansen, O. (1975), Thermal Conductivity of Soils, Ph.D. dissertation, Norwegian Technical University, U.S. Army Cold Regions Research Engineering Lab, Translation 637, July 1977

Kersten, M.S. (1949), "*Laboratory research for the determination of the thermal properties of soils*", Arctic Construction and Frost Effects Laboratory Technical Report 23

Kestler M.A., Hanek, G., Truebe,M., Bolander, P. (1999), "Removing Spring Thaw Load Restrictions from Low-Volume Roads, Development of a Reliable, Cost-Effective Method" Transportation Research Record No. 1652, pp. 188-197

Johansen, O. (1975), "*Thermal conductivity of soils*" Ph.D. thesis, Norway, Trondheim University (CRREL Draft Translation 637, 1977)

Johnston, G.H., (ED.) (1981), "Permafrost Engineering Design and Construction", Wiley, Toronto

Ladanyi, B. (1989), "Effect of Salinity and Temperature on the Behavior of Frozen Soils", Workshop on impact of saline permafrost, Winnipeg, Dept of Civil Engineering

Mabood, F., Tighe, S.L., Klement, T., Kazmierowski, T., Mercier, S. (2008), "*Evaluating Tire Pressure Control Systems (TPCS)to Improve Productivity and Mitigate Pavement Damage*" Poster Session 2008 Annual Conference of the Transportation Association of Canada, Toronto, Ontario

Minnesota Department of Transportation (Mn/DOT) (2004), Engineering Services Division Technical Memorandum No. 04-20-MAT-03

Ningyuan, L., Kazmierowski, T., Lane, B. (2006), "*Long-Term Monitoring of Low-Volume Road Performance in Ontario*", 2006 Annual Conference of the Transportation Association of Canada, Charlottetown, Prince Edward Island

Petryna, D. (2010), Personal communication

Ontario Provincial Standard Specification (OPSS) (2004), Material Specification for Aggregates-Base, Subbase, Select Subgrade, and Backfill Material

Ovik, J.M., Siekmeier, J.A, Van Duesen, D.A. (2000), *Improved Spring Load Restriction Guidelines Using Mechanistic Analysis*, Minnesota Department of Transportation, Report No. MN/RC-2000-18

Rutherford, M.S. (1989), "*Pavement Response and Load Restrictions on Spring Thaw-Weakened Flexible Pavements*", Transportation Research Record No. 1252, pp. 1-11

Sanger, F.J. (1963), "*Degree-days and heat conduction in soils*" Proceedings, Permafrost International Conference, National Academy of Science – National Research Council

Steinert, B.C., Humphrey, D.N., Kestler, M.A. (2005), "Portable Falling Weight Deflectometer Study", New England Transportation Consortium, Report No. NETCR52

Stewart, R.B., (2003), "*Climate Change: Implications for Forest Ecosystems and Forest Management in Eastern Ontario*", East Central Woodlot Conference, Lindsay, Ontario

Technology for Alaskan Transport (TAT) (2006), DOT Statewide Research & Technology Transfer Local Technical Assistance Program, Volume 31, No.3

TEMP/W (2007), "*Thermal Modeling with TEMP/W An Engineering Methodology Third Edition*", GEO-SLOPE International Ltd.

The Weather Network Commercial Services (TWNCS) (2009),"RWIS Site Summary Page" https://rwis.pelmorex.com/scanweb/SWFrame.asp?pgid=7664533268913, Accessed (18/08/2009)

Tice, A.R., Anderson, D.M., Banin, A. (1976), "*The prediction of Unfrozen Water Contents in Frozen Soils from Liquid Limit Determinations*", U.S. Army Cold Regions Research Engineering Lab, CRREL Rep. 76-8

Transportation Association of Canada, TAC (1997), "Pavement Design and Management Guide", Ottawa, Ontario

U.S.S.R., (1969), "Handbook for the design of bases and foundations of buildings and other structures on permafrost", S.S. Vyalov, and G.V. Porkhaev (Editors), National Research Council Canada, Canada Institute for Scientific and Technical Information, Ottawa, Technical Translation TT-1865, 1976

Van Deusen, D. (1998), "*Improved Spring Load Restriction Guidelines Using Mechanistic Analysis*", Cold Regions Impact of Civil Works, Ninth International Conference on Cold Regions Engineering, pp 188-199

WEBSITES

www.climate.weatheroffice.ec.gc.ca, accessed on September 17, 2009

www.Educationcanada.com, accessed on September 17, 2009

www.mrr.dot.state.mn.us, accessed on April 14, 2010

www.omega.ca, accessed on April 13, 2010

Appendix A – Thermistor Removal Criteria

The removal of thermistor readings from the data series will be conducted when one or more of the following occurs:

1. No data are recorded from the thermistor.

2. Obvious errors exist (e.g. a subsurface thermistor reading of 180°C).

3. An anomalous significant difference between one thermistor reading and the shallower and deeper thermistor readings exists (4°C or greater) on the same day.

Example

Thermistor Depth	Temperature Measurement	Date
45 cm	-2°C	January 5, 2008
60 cm	+9°C	January 5, 2008
75 cm	-1.5°C	January 5, 2008

- 60 cm thermistor reading would be removed

4. If thermistor reading trends do not correspond to air temperature trends (e.g. consistent air temperature trends well above 0°C with thermistor reading trends at the thermistors near the pavement surface indicating a further decrease in temperatures below 0°C)

5. Unfounded and illogical jumps between thermistor readings above 0°C and thermistor readings below 0°C

Example

Thermistor Depth	Temperature Measurement	Date
90 cm	-0.5°C	January 5, 2008
105 cm	1.9°C	January 5, 2008
135 cm	3.1°C	January 5, 2008
165 cm	-0.6°C	January 5, 2008
195 cm	3.3°C	January 5, 2008

- 165 cm thermistor reading would be removed

Appendix B – Frost and Thaw Depth Determination Excel Macros

(Courtesy Baiz et al., 2007)

```
Function LowerFrostFringe(ThresholdTemp, T01, T02, T03, T04, T05, T06, T07, T08, T09, T10, T11, T12,
T13)
D01 = 5
D02 = 15
D03 = 30
D04 = 45
D05 = 60
D06 = 75
D07 = 90
D08 = 105
D09 = 135
D10 = 165
D11 = 195
D12 = 225
D13 = 255
If T13 < ThresholdTemp Then
   Depth = D13
ElseIf T12 < ThresholdTemp And T13 > ThresholdTemp Then
   Depth = ((D13 - D12) / (T13 - T12)) * (ThresholdTemp - T12) + D12
ElseIf T11 < ThresholdTemp And T12 > ThresholdTemp Then
   Depth = ((D12 - D11) / (T12 - T11)) * (ThresholdTemp - T11) + D11
ElseIf T10 < ThresholdTemp And T11 > ThresholdTemp Then
   Depth = ((D11 - D10) / (T11 - T10)) * (ThresholdTemp - T10) + D10
ElseIf T09 < ThresholdTemp And T10 > ThresholdTemp Then
   Depth = ((D10 - D09) / (T10 - T09)) * (ThresholdTemp - T09) + D09
ElseIf T08 < ThresholdTemp And T09 > ThresholdTemp Then
   Depth = ((D09 - D08) / (T09 - T08)) * (ThresholdTemp - T08) + D08
ElseIf T07 < ThresholdTemp And T08 > ThresholdTemp Then
   Depth = ((D08 - D07) / (T08 - T07)) * (ThresholdTemp - T07) + D07
ElseIf T06 < ThresholdTemp And T07 > ThresholdTemp Then
   Depth = ((D07 - D06) / (T07 - T06)) * (ThresholdTemp - T06) + D06
ElseIf T05 < ThresholdTemp And T06 > ThresholdTemp Then
   Depth = ((D06 - D05) / (T06 - T05)) * (ThresholdTemp - T05) + D05
ElseIf T04 < ThresholdTemp And T05 > ThresholdTemp Then
   Depth = ((D05 - D04) / (T05 - T04)) * (ThresholdTemp - T04) + D04
ElseIf T03 < ThresholdTemp And T04 > ThresholdTemp Then
   Depth = ((D04 - D03) / (T04 - T03)) * (ThresholdTemp - T03) + D03
ElseIf T02 < ThresholdTemp And T03 > ThresholdTemp Then
   Depth = ((D03 - D02) / (T03 - T02)) * (ThresholdTemp - T02) + D02
ElseIf T01 < ThresholdTemp And T02 > ThresholdTemp Then
   Depth = ((D02 - D01) / (T02 - T01)) * (ThresholdTemp - T01) + D01
End If
LowerFrostFringe = -Depth
End Function
```

```
Function UpperFrostFringe(ThresholdTemp, T01, T02, T03, T04, T05, T06, T07, T08, T09, T10, T11, T12,
T13)
D01 = 5
D02 = 15
D03 = 30
D04 = 45
D05 = 60
D06 = 75
D07 = 90
D08 = 105
D09 = 135
D10 = 165
D11 = 195
D12 = 225
D13 = 255
If T01 < ThresholdTemp Then
   Depth = 0
ElseIf T02 < ThresholdTemp And T01 > ThresholdTemp Then
   Depth = ((D02 - D01) / (T02 - T01)) * (ThresholdTemp - T01) + D01
ElseIf T03 < ThresholdTemp And T02 > ThresholdTemp Then
   Depth = ((D03 - D02) / (T03 - T02)) * (ThresholdTemp - T02) + D02
ElseIf T04 < ThresholdTemp And T03 > ThresholdTemp Then
   Depth = ((D04 - D03) / (T04 - T03)) * (ThresholdTemp - T03) + D03
ElseIf T05 < ThresholdTemp And T04 > ThresholdTemp Then
   Depth = ((D05 - D04) / (T05 - T04)) * (ThresholdTemp - T04) + D04
ElseIf T06 < ThresholdTemp And T05 > ThresholdTemp Then
   Depth = ((D06 - D05) / (T06 - T05)) * (ThresholdTemp - T05) + D05
ElseIf T07 < ThresholdTemp And T06 > ThresholdTemp Then
   Depth = ((D07 - D06) / (T07 - T06)) * (ThresholdTemp - T06) + D06
ElseIf T08 < ThresholdTemp And T07 > ThresholdTemp Then
   Depth = ((D08 - D07) / (T08 - T07)) * (ThresholdTemp - T07) + D07
ElseIf T09 < ThresholdTemp And T08 > ThresholdTemp Then
   Depth = ((D09 - D08) / (T09 - T08)) * (ThresholdTemp - T08) + D08
ElseIf T10 < ThresholdTemp And T09 > ThresholdTemp Then
   Depth = ((D10 - D09) / (T10 - T09)) * (ThresholdTemp - T09) + D09
ElseIf T11 < ThresholdTemp And T10 > ThresholdTemp Then
   Depth = ((D11 - D10) / (T11 - T10)) * (ThresholdTemp - T10) + D10
ElseIf T12 < ThresholdTemp And T11 > ThresholdTemp Then
   Depth = ((D12 - D11) / (T12 - T11)) * (ThresholdTemp - T11) + D11
ElseIf T13 < ThresholdTemp And T12 > ThresholdTemp Then
   Depth = ((D13 - D12) / (T13 - T12)) * (ThresholdTemp - T12) + D12
Else
   Depth = 0
End If
UpperFrostFringe = -Depth
End Function
```

Appendix C – Granular A Specifications

(OPSS, 2004)

Granular A – A set of requirements for dense graded aggregates intended for use as granular base within the pavement structure, granular shouldering, and backfill

Granular A may be produced by crushing one or more of the following:

1. Quarried bedrock
2. Naturally formed deposits of sand, gravel and cobbles
3. RAP up to 30% by mass
4. RCM
5. Air cooled blasé-furnace slag or nickel slag
6. Glass or ceramic material up to 15% by mass combined

Table 1
Physical Property Requirements

Laboratory Test	MTO Test Number	Granular O	Granular A	Granular S	Granular B Type I and Type II	Granular M	Select Subgrade Material
Coarse Aggregate Petrographic Requirement	LS-609	(Note 2)	(Note 1) (Note 2)	(Note 2)	(Note 1) (Note 2)	(Note 1) (Note 2)	(Note 2)
Freeze-Thaw Loss, % maximum	LS-614	15	N/A	N/A	N/A	N/A	N/A
Fine Aggregate Petrographic Requirement	LS-616 LS-709	(Note 3)					
Micro-Deval Abrasion Coarse Aggregate loss, % maximum	LS-618	21	25	25	30 (Note 4)	25	30 (Note 4)
Micro-Deval Abrasion Fine Aggregate loss, % maximum	LS-619	25	30	30	35	30	N/A
Plasticity Index	LS-704	0	0	0	0	0	0
Percent crushed, minimum	LS-607	100	50	50	N/A	50	N/A
2 or more crushed faces, % minimum	LS-617	85	N/A	N/A	N/A	N/A	N/A
Asphalt Coated Particles, % maximum	LS-621	N/A	30	30	(Note 5)	30	N/A

Notes:

1. Granular A, B Type I, or M may contain up to 15% by mass of crushed glass and ceramic material combined.
2. Granular A, B Type I, M, and S shall not contain more than 1% by mass of deleterious material. Granular O, Granular B Type II, and SSM shall not contain more than 0.1% by mass of wood. Petrographic classification of rock type need not be reported. This requirement is only to be reported when such material is present.
3. Test required for materials north of the French and Mattawa Rivers only. For materials with greater than 5.0% passing the 75 µm sieve, the amount of mica passing the 150 µm sieve and retained on the 75 µm sieve, shall not exceed 10% of the material in that sieve fraction unless either testing according to LS-709 determines permeability values to be greater than 1.0×10^{-4} cm/s or field experience show satisfactory performance. Prior data demonstrating compliance with this requirement will be acceptable provided such testing has been done within the past five years and that field performance of these materials has been satisfactory.
4. The coarse aggregate Micro-Deval abrasion loss test requirements will be waived if the material has more than 80% passing the 4.75 mm sieve.
5. Granular B Type I may contain up to 30% asphalt coated particles. Granular B Type II shall not contain RAP or asphalt coated products.

Table 2
Gradation Requirements - Percent Passing

MTO Test Number	Sieve	Granular						Select Subgrade Material
		O	A	S	B (Note 1)		M	
					Type I (Note 2)	Type II		
LS-602	150 mm	N/A	N/A	N/A	100	N/A	N/A	100
	106 mm	N/A	N/A	N/A	N/A	100	N/A	N/A
	37.5 mm	100	N/A	N/A	N/A	N/A	N/A	N/A
	26.5 mm	95-100	100	100	50-100	50-100	N/A	50-100
	19.0 mm	80-95	85-100 (87-100*)	90-100	N/A	N/A	100	N/A
	13.2 mm	60-80	65-90 (75-95*)	75-100	N/A	N/A	75-95	N/A
	9.5 mm	50-70	50-73 (60-83*)	60-85	N/A	N/A	55-80	N/A
	4.75 mm	20-45	35-55 (40-60*)	40-60	20-100	20-55	35-55	20-100
	1.18 mm	0-15	15-40	20-40	10-100	10-40	15-40	10-100
	300 µm	N/A	5-22	11-25	2-65	5-22	5-22	5-95
	150 µm	N/A	N/A	N/A	N/A	N/A	N/A	2.0-65.0
	75 µm	0-5.0	2.0-8.0 (2.0-10.0**)	9.0-15.0 (9.0-17.0**)	0-8.0 (0-10.0**)	0-10.0	2.0-8.0 (2.0-10.0**)	0-25.0

Notes:

1. Where Granular B is used for granular backfill for pipe subdrains, 100% of the material shall pass the 37.5 mm sieve.
2. Where RAP is included in Granular B Type I, 100% of the RAP shall pass the 75 mm sieve. Conditions in Note 1 supersede this requirement.

* Where the aggregate is obtained from an air-cooled blast furnace slag source.

** Where the aggregate is obtained from a quarry or an air-cooled blast furnace slag or nickel slag source.

Appendix D –Lowest Thermistor Values During Predictions for Highway 569

Date	Temp (°C)
November 14, 2009	11.20
November 15, 2009	11.10
November 16, 2009	11.05
November 17, 2009	10.95
November 18, 2009	10.85
November 19, 2009	10.75
November 20, 2009	10.65
November 21, 2009	10.55
November 22, 2009	10.45
November 23, 2009	10.35
November 24, 2009	10.25
November 25, 2009	10.10
November 26, 2009	10.00
November 27, 2009	9.83
November 28, 2009	9.73
November 29, 2009	9.63
November 30, 2009	9.48
December 1, 2009	9.35
December 2, 2009	9.25
December 3, 2009	9.13
December 4, 2009	9.00
December 5, 2009	8.88
December 6, 2009	8.75
December 7, 2009	8.70
December 8, 2009	8.60
December 9, 2009	8.52
December 10, 2009	8.48
December 11, 2009	8.35
December 12, 2009	8.28
December 13, 2009	8.18
December 14, 2009	8.08
December 15, 2009	8.00
December 16, 2009	7.90
December 17, 2009	7.73
December 18, 2009	7.60

Date	Temp (°C)
December 19, 2009	7.53
December 20, 2009	7.40
December 21, 2009	7.33
December 22, 2009	7.25
December 23, 2009	7.10
December 24, 2009	6.95
December 25, 2009	6.80
December 26, 2009	6.65
December 27, 2009	6.45
December 28, 2009	6.55
December 29, 2009	6.40
December 30, 2009	6.23
December 31, 2009	6.15
January 1, 2010	6.05
January 2, 2010	6.00
January 3, 2010	5.97
January 4, 2010	5.83
January 5, 2010	5.75
January 6, 2010	5.68
January 7, 2010	5.58
January 8, 2010	5.50
January 9, 2010	5.45
January 10, 2010	5.38
January 11, 2010	5.28
January 12, 2010	5.20
January 13, 2010	5.13
January 14, 2010	5.05
January 15, 2010	4.90
January 16, 2010	4.80
January 17, 2010	4.70
January 18, 2010	4.63
January 19, 2010	4.53
January 20, 2010	4.45
January 21, 2010	4.38
January 22, 2010	4.30

Date	Temp (°C)
January 23, 2010	4.23
January 24, 2010	4.18
January 25, 2010	4.10
January 26, 2010	4.00
January 27, 2010	3.95
January 28, 2010	3.88
January 29, 2010	3.80
January 30, 2010	3.73
January 31, 2010	3.65
February 1, 2010	3.58
February 2, 2010	3.50
February 3, 2010	3.43
February 4, 2010	3.35
February 5, 2010	3.30
February 6, 2010	3.20
February 7, 2010	3.15
February 8, 2010	3.10
February 9, 2010	3.00
February 10, 2010	2.95
February 11, 2010	2.90
February 12, 2010	2.80
February 13, 2010	2.78
February 14, 2010	2.70
February 15, 2010	2.65
February 16, 2010	2.60
February 17, 2010	2.53
February 18, 2010	2.50
February 19, 2010	2.45
February 20, 2010	2.40
February 21, 2010	2.38
February 22, 2010	2.30
February 23, 2010	2.30
February 24, 2010	2.25
February 25, 2010	2.20
February 26, 2010	2.20

Date	Temp (°C)	Date	Temp (°C)	Date	Temp (°C)
February 27, 2010	2.15	April 8, 2010	1.40	May 18, 2010	1.40
February 28, 2010	2.10	April 9, 2010	1.40	May 19, 2010	1.40
March 1, 2010	2.10	April 10, 2010	1.40	May 20, 2010	1.40
March 2, 2010	2.05	April 11, 2010	1.30	May 21, 2010	1.40
March 3, 2010	2.00	April 12, 2010	1.30	May 22, 2010	1.40
March 4, 2010	2.00	April 13, 2010	1.30	May 23, 2010	1.41
March 5, 2010	2.00	April 14, 2010	1.30	May 24, 2010	1.40
March 6, 2010	1.90	April 15, 2010	1.30	May 25, 2010	1.41
March 7, 2010	1.90	April 16, 2010	1.30	May 26, 2010	1.42
March 8, 2010	1.90	April 17, 2010	1.30	May 27, 2010	1.43
March 9, 2010	1.80	April 18, 2010	1.30	May 28, 2010	1.44
March 10, 2010	1.80	April 19, 2010	1.30	May 29, 2010	1.45
March 11, 2010	1.80	April 20, 2010	1.30	May 30, 2010	1.49
March 12, 2010	1.70	April 21, 2010	1.30	May 31, 2010	1.50
March 13, 2010	1.70	April 22, 2010	1.30	June 1, 2010	1.53
March 14, 2010	1.70	April 23, 2010	1.30	June 2, 2010	1.57
March 15, 2010	1.70	April 24, 2010	1.30	June 3, 2010	1.62
March 16, 2010	1.60	April 25, 2010	1.30	June 4, 2010	1.66
March 17, 2010	1.60	April 26, 2010	1.30	June 5, 2010	1.71
March 18, 2010	1.60	April 27, 2010	1.35	June 6, 2010	1.77
March 19, 2010	1.60	April 28, 2010	1.40	June 7, 2010	1.82
March 20, 2010	1.60	April 29, 2010	1.40	June 8, 2010	1.88
March 21, 2010	1.50	April 30, 2010	1.40	June 9, 2010	1.93
March 22, 2010	1.50	May 1, 2010	1.40	June 10, 2010	1.97
March 23, 2010	1.50	May 2, 2010	1.40	June 11, 2010	2.06
March 24, 2010	1.50	May 3, 2010	1.40	June 12, 2010	2.13
March 25, 2010	1.50	May 4, 2010	1.40	June 13, 2010	2.19
March 26, 2010	1.50	May 5, 2010	1.40	June 14, 2010	2.27
March 27, 2010	1.50	May 6, 2010	1.40	June 15, 2010	2.35
March 28, 2010	1.50	May 7, 2010	1.40	June 16, 2010	2.48
March 29, 2010	1.40	May 8, 2010	1.40	June 17, 2010	2.60
March 30, 2010	1.40	May 9, 2010	1.40	June 18, 2010	2.69
March 31, 2010	1.40	May 10, 2010	1.40	June 19, 2010	2.82
April 1, 2010	1.40	May 11, 2010	1.40	June 20, 2010	2.92
April 2, 2010	1.40	May 12, 2010	1.40	June 21, 2010	3.06
April 3, 2010	1.40	May 13, 2010	1.40	June 22, 2010	3.19
April 4, 2010	1.40	May 14, 2010	1.40	June 23, 2010	3.33
April 5, 2010	1.40	May 15, 2010	1.40	June 24, 2010	3.49
April 6, 2010	1.40	May 16, 2010	1.40	June 25, 2010	3.67
April 7, 2010	1.40	May 17, 2010	1.40	June 26, 2010	3.84

Date	Temp (°C)
June 27, 2010	4.05
June 28, 2010	4.26
June 29, 2010	4.46
June 30, 2010	4.69
July 1, 2010	4.89
July 2, 2010	5.12
July 3, 2010	5.32
July 4, 2010	5.53
July 5, 2010	5.72
July 6, 2010	5.92
July 7, 2010	6.09
July 8, 2010	6.29
July 9, 2010	6.49
July 10, 2010	6.67
July 11, 2010	6.83
July 12, 2010	7.02
July 13, 2010	7.18
July 14, 2010	7.36
July 15, 2010	7.54
July 16, 2010	7.73
July 17, 2010	7.87

Appendix E –Lowest Thermistor Values During Predictions for Highway 527

Date	Temp (°C)	Date	Temp (°C)	Date	Temp (°C)
October 1, 2009	10.34	November 7, 2009	8.48	December 14, 2009	5.32
October 2, 2009	10.31	November 8, 2009	8.42	December 15, 2009	5.23
October 3, 2009	10.29	November 9, 2009	8.36	December 16, 2009	5.14
October 4, 2009	10.27	November 10, 2009	8.30	December 17, 2009	5.00
October 5, 2009	10.23	November 11, 2009	8.23	December 18, 2009	4.91
October 6, 2009	10.20	November 12, 2009	8.16	December 19, 2009	4.83
October 7, 2009	10.15	November 13, 2009	8.08	December 20, 2009	4.71
October 8, 2009	10.11	November 14, 2009	8.03	December 21, 2009	4.58
October 9, 2009	10.07	November 15, 2009	7.97	December 22, 2009	4.50
October 10, 2009	10.03	November 16, 2009	7.92	December 23, 2009	4.37
October 11, 2009	9.98	November 17, 2009	7.85	December 24, 2009	4.26
October 12, 2009	9.91	November 18, 2009	7.78	December 25, 2009	4.18
October 13, 2009	9.84	November 19, 2009	7.69	December 26, 2009	4.05
October 14, 2009	9.82	November 20, 2009	7.62	December 27, 2009	3.93
October 15, 2009	9.77	November 21, 2009	7.55	December 28, 2009	3.85
October 16, 2009	9.73	November 22, 2009	7.48	December 29, 2009	3.78
October 17, 2009	9.67	November 23, 2009	7.35	December 30, 2009	3.72
October 18, 2009	9.63	November 24, 2009	7.25	December 31, 2009	3.64
October 19, 2009	9.57	November 25, 2009	7.17	January 1, 2010	3.53
October 20, 2009	9.54	November 26, 2009	7.08	January 2, 2010	3.43
October 21, 2009	9.50	November 27, 2009	6.98	January 3, 2010	3.38
October 22, 2009	9.45	November 28, 2009	6.87	January 4, 2010	3.28
October 23, 2009	9.39	November 29, 2009	6.77	January 5, 2010	3.22
October 24, 2009	9.35	November 30, 2009	6.67	January 6, 2010	3.15
October 25, 2009	9.30	December 1, 2009	6.58	January 7, 2010	3.05
October 26, 2009	9.25	December 2, 2009	6.48	January 8, 2010	2.98
October 27, 2009	9.21	December 3, 2009	6.36	January 9, 2010	2.92
October 28, 2009	9.16	December 4, 2009	6.29	January 10, 2010	2.84
October 29, 2009	9.11	December 5, 2009	6.19	January 11, 2010	2.76
October 30, 2009	9.01	December 6, 2009	6.09	January 12, 2010	2.70
October 31, 2009	8.94	December 7, 2009	6.02	January 13, 2010	2.67
November 1, 2009	8.91	December 8, 2009	5.90	January 14, 2010	2.62
November 2, 2009	8.84	December 9, 2009	5.81	January 15, 2010	2.55
November 3, 2009	8.76	December 10, 2009	5.73	January 16, 2010	2.48
November 4, 2009	8.66	December 11, 2009	5.62	January 17, 2010	2.38
November 5, 2009	8.59	December 12, 2009	5.54	January 18, 2010	2.31
November 6, 2009	8.54	December 13, 2009	5.41	January 19, 2010	2.25

Date	Temp (°C)	Date	Temp (°C)	Date	Temp (°C)
January 20, 2010	2.16	March 1, 2010	0.65	April 10, 2010	-0.20
January 21, 2010	2.08	March 2, 2010	0.62	April 11, 2010	-0.20
January 22, 2010	2.01	March 3, 2010	0.59	April 12, 2010	-0.21
January 23, 2010	1.98	March 4, 2010	0.57	April 13, 2010	-0.22
January 24, 2010	1.95	March 5, 2010	0.54	April 14, 2010	-0.23
January 25, 2010	1.89	March 6, 2010	0.51	April 15, 2010	-0.23
January 26, 2010	1.83	March 7, 2010	0.48	April 16, 2010	-0.24
January 27, 2010	1.77	March 8, 2010	0.46	April 17, 2010	-0.24
January 28, 2010	1.70	March 9, 2010	0.43	April 18, 2010	-0.19
January 29, 2010	1.64	March 10, 2010	0.40	April 19, 2010	-0.17
January 30, 2010	1.63	March 11, 2010	0.38	April 20, 2010	-0.16
January 31, 2010	1.56	March 12, 2010	0.35	April 21, 2010	-0.15
February 1, 2010	1.51	March 13, 2010	0.32	April 22, 2010	-0.16
February 2, 2010	1.49	March 14, 2010	0.29	April 23, 2010	-0.16
February 3, 2010	1.46	March 15, 2010	0.27	April 24, 2010	-0.16
February 4, 2010	1.43	March 16, 2010	0.24	April 25, 2010	-0.16
February 5, 2010	1.36	March 17, 2010	0.21	April 26, 2010	-0.16
February 6, 2010	1.30	March 18, 2010	0.19	April 27, 2010	-0.15
February 7, 2010	1.25	March 19, 2010	0.16	April 28, 2010	-0.14
February 8, 2010	1.23	March 20, 2010	0.13	April 29, 2010	-0.14
February 9, 2010	1.19	March 21, 2010	0.11	April 30, 2010	-0.13
February 10, 2010	1.16	March 22, 2010	0.08	May 1, 2010	-0.12
February 11, 2010	1.13	March 23, 2010	0.05	May 2, 2010	-0.12
February 12, 2010	1.11	March 24, 2010	0.02	May 3, 2010	-0.14
February 13, 2010	1.08	March 25, 2010	0.00	May 4, 2010	-0.17
February 14, 2010	1.05	March 26, 2010	-0.03	May 5, 2010	-0.20
February 15, 2010	1.02	March 27, 2010	-0.06	May 6, 2010	-0.21
February 16, 2010	1.00	March 28, 2010	-0.08	May 7, 2010	-0.22
February 17, 2010	0.97	March 29, 2010	-0.11	May 8, 2010	-0.20
February 18, 2010	0.94	March 30, 2010	-0.14	May 9, 2010	-0.18
February 19, 2010	0.92	March 31, 2010	-0.16	May 10, 2010	-0.21
February 20, 2010	0.89	April 1, 2010	-0.17	May 11, 2010	-0.22
February 21, 2010	0.86	April 2, 2010	-0.18	May 12, 2010	-0.23
February 22, 2010	0.84	April 3, 2010	-0.18	May 13, 2010	-0.23
February 23, 2010	0.81	April 4, 2010	-0.19	May 14, 2010	-0.22
February 24, 2010	0.78	April 5, 2010	-0.18	May 15, 2010	-0.21
February 25, 2010	0.75	April 6, 2010	-0.19	May 16, 2010	-0.19
February 26, 2010	0.73	April 7, 2010	-0.19	May 17, 2010	-0.20
February 27, 2010	0.70	April 8, 2010	-0.20	May 18, 2010	-0.21
February 28, 2010	0.67	April 9, 2010	-0.20	May 19, 2010	-0.18

Date	Temp (°C)
May 20, 2010	-0.17
May 21, 2010	-0.17
May 22, 2010	-0.12
May 23, 2010	-0.08
May 24, 2010	-0.02
May 25, 2010	0.06
May 26, 2010	0.15
May 27, 2010	0.22
May 28, 2010	0.30
May 29, 2010	0.41
May 30, 2010	0.54
May 31, 2010	0.65
June 1, 2010	0.79
June 2, 2010	0.93
June 3, 2010	1.12

Appendix F – LWD Testing Guideline

SLA Testing Procedures

The following are the exact coordinates of the test site on Highway 527:
N 49.35982° W 089.37746°

- Upon arriving to the site there should be noticeable paint markings on the road surface as well as RWIS equipment station nearby. The following is a schematic of a typical site.

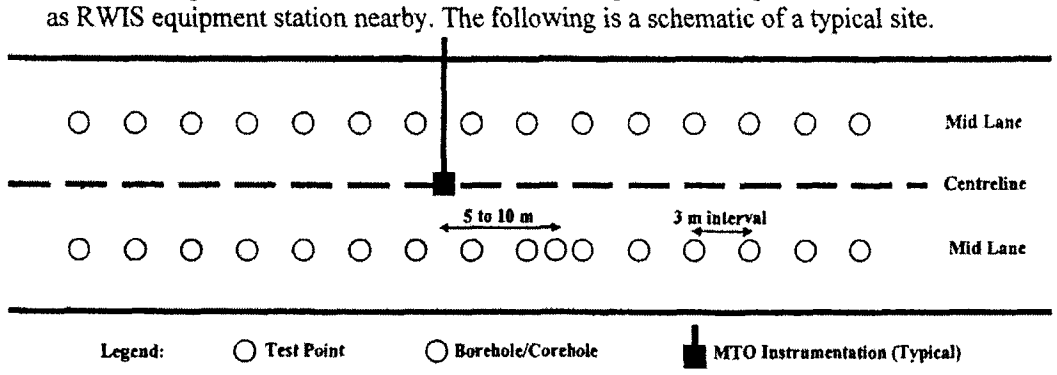

- On the first day of testing, please bring a can of paint to refresh the paint marks if required.
- Using your traffic control, close one of the lanes to begin testing. Traffic control should comply with OTM book 7. A TL-20A lane closure will be required.
- Assemble the LWD using the 20kg assembly and a height close to the maximum height to maximize the load. It is not crucial to maintain the same height for each test but it is desirable.
- Each test spot requires 6 drops of the 20kg weight before moving to the next spot. When moving to the next spot, change the location number on the software, LWD 3031.
- Once spots 1-15 are completed, move the lane closure to the other lane and test spots 16-30.
- If additional geophones are used, they are to be place in the direction of vehicle traffic.
- The attached LWD data field sheet should be filled out during each test. Pictures and documentation of the quality of the road surface should also be made.
- If it begins to snow, shovelling the snow away from the test spots will be required.
- As instructed in the manual, when analyzing the data using LWDmod, the first drop at each location is to be deleted as well as any other drops with defected graphs.

Testing is to be performed once a week from the week of Oct.20/08 to the week of Dec. 1/08. Testing resume for the thaw season and is again required once a week from the week of Mar. 30/09 to the week of May 18/09.

Appendix G – SLR Method Prediction Criteria

Mn/DOT

- Air temperatures will be obtained using 5 day forecast provided at theweathernetwork.com
    - Northwestern section of the province will be represented by air temperature forecasts averaged (50/50) for Thunder Bay and Armstrong, Ontario.
    - Northeastern section of the province will be represented by air temperature forecasts provided for New Liskeard, Ontario.
- The Freezing Index (FI), the Thawing Index (TI) and the Cumulative Thawing Index (CTI) will be calculated daily, using the forecasted temperatures
- SLRs will be implemented when the forecasted CTI exceeds the calibrated threshold CTI for at least 3 consecutive days
    - Northwestern Threshold CTI = 64.3°C-days
    - Northeastern Threshold CTI = 40.1°C-days
- SLRs will be removed at specified durations after the implementation of SLRs which corresponds to the calibrated length of the thawing season plus an additional week.
    - Northwestern SLR Duration = 51 days
    - Northeastern SLR Duration = 37 days

Waterloo

- Air temperatures will be obtained using 5 day forecast provided at theweathernetwork.com
    - Northwestern section of the province will be represented by air temperature forecasts averaged (50/50) for Thunder Bay and Armstrong, Ontario.
    - Northeastern section of the province will be represented by air temperature forecasts provided for New Liskeard, Ontario.
- The following calibrated monthly reference temperatures will be used to convert air temperatures into corresponding surface temperatures

Northeastern

Tref Oct. 1 to Oct. 27	-6.9
Tref Oct. 28 to Nov. 27	-2.74
Tref Nov. 28 to Dec. 27	-2.78
Tref Dec. 28 to Jan. 27	-0.77
Tref Jan. 28 to Feb. 27	-1.67
Tref Feb. 28 to Mar. 27	-4.96
Tref Mar. 28 to April 27	-4.13
Tref April 28 to May 27	3.6

Northwestern

Tref Oct. 1 to Oct. 27	-6.90
Tref Oct. 27 to Nov. 27	-4.20
Tref Nov. 27 to Dec. 27	-4.73
Tref Dec. 27 to Jan. 27	1.14
Tref Jan. 27 to Feb. 27	1.37
Tref Feb. 27 to Mar. 27	-3.67
Tref Mar. 27 to April 27	-3.67
Tref April 27 to May 27	-3.00

- Model freezing and thawing coefficients will be determined using the average values determined in calibrations

<u>Northeastern</u>

- a = -0.25
- b = -4.82
- c = 2.22
- d = 11.29
- e = -0.35
- f = -1.06
- g = 233
- h = -12.34
- i = -1.53
- j = -1271
- k = 33.2
- l = -1.73

<u>Northwestern</u>

- a = -6.17
- b = -5.52
- c = 0.97
- d = 1.15
- e = -0.04
- f = -0.09
- g = -255
- h = 5.46E-11
- h = 1.05E-11
- j = -1572
- k = 36.64
- l = -6.54

- Day i_o will be predicted by calculating the Thawing Index (TI) using the 5 day forecast. At this point coefficients "g" and "j" will be adjusted to match freezing season data.
- SLRs will be implemented when the initial thawing depth exceeds 300 mm and remains below 300 mm for 3 successive predicted days.
- SLRs will be removed one week after complete subsurface thawing has been predicted using the 5 day forecast.

<u>TEMP/W</u>

- Material properties will remain the same as in the calibration methods.

- Upper boundary conditions will use the 5 day forecast provided at theweathernetwork.com
    - Northwestern section of the province will be represented by air temperature forecasts averaged (50/50) for Thunder Bay and Armstrong, Ontario.
    - Northeastern section of the province will be represented by air temperature forecasts provided for New Liskeard, Ontario.
- Two models will be constructed using the temperature modification function approach. The n-factor values for each region are as follows:
    - Northwestern modification functions
        - Freezing = 2.3
        - Thawing = 0.8
    - Northeastern modification functions
        - Freezing = 2.3
        - Thawing = 0.57
- The bottom boundary condition will be determined through a combination of average freezing and thawing trends, depths and durations. See file "Bottom Boundary Condition Predictions.xls" for the bottom boundary condition temperatures used.
- SLRs will be implemented when the initial thawing depth exceeds 300 mm and remains below 300 mm for 3 successive predicted days.
- SLRs will be removed one week after complete subsurface thawing has been predicted using the 5 day forecast.